INVESTIGATION OF INJECTION MOULDING FOR

NOVEL DRUG DELIVERY SYSTEMS

VOLUME I OF II

S.S. DESHMUKH

PhD

2015

INVESTIGATION OF INJECTION MOULDING FOR NOVEL DRUG DELIVERY SYSTEMS

An investigation into the use of injection moulding to produce pharmaceutical dosage forms and to understand the relationship between materials, processing conditions and performance, in particular drug release and stability

Volume I of II

Shivprasad Shahajirao DESHMUKH

Submitted for the Degree of

Doctor of Philosophy

School of Life Sciences

University of Bradford

2015

Abstract

Shivprasad Shahajirao Deshmukh

Investigation of injection moulding for novel drug delivery systems

An investigation into the use of injection moulding to produce pharmaceutical dosage forms and to understand the relationship between materials, processing conditions and performance, in particular drug release and stability

Key words: Hot melt extrusion, injection moulding, solid dispersion, crystallisation, Ibuprofen, felodipine, HPMCAS, Soluplus®, controlled release

The feasibility of the injection moulding (IM) was explored for the development of novel drug delivery systems. Controlled release formulations were developed using a substituted cellulose derivative, hydroxypropyl methyl cellulose acetate succinate (HPMCAS) and a graft co-polymer (Soluplus®). BCS class II drugs ibuprofen and the felodipine were selected based on their physicochemical properties.

In the present work, a homogenous dispersion of drugs in the polymer matrices was achieved using Hot Melt Extrusion (HME) and extruded pellets obtained were used for the development of the injection moulded systems. Four systems were developed using the IM consisting of ibuprofen-HPMCAS, ibuprofen-Soluplus®, felodipine-PEO-HPMCAS and felodipine-Soluplus®.

The ibuprofen acts as a good plasticiser compared to felodipine therefore, felodipine containing IM systems required a plasticiser (PEO) when processed with HPMCAS. The analysis of extruded pellets and injection moulded systems using modulated DSC (MDSC) and Raman spectroscopy confirmed the formation of an amorphous molecular dispersion (i.e solid

solution) in the case of all four systems. The phase separation behaviour and the amorphous stability of the systems was studied at various stress conditions. This revealed the "surface crystallisation" behaviour of the ibuprofen-HPMCAS systems. Temperature-composition phase diagram constructed based on the melting point depression and the Flory-Huggins lattice solution theory provided the explanation for the phase separation and crystallisation behaviour of ibuprofen-HPMCAS systems. The advanced characterisation techniques like DMA, 2D XRD and 3D laser microscopy provided the detailed understanding of crystal habits, phase seperation and surface crystallisation. The significant effect of the stress conditions on the rate of shrinkage was observed where, higher shrinkage tendency of a HPMCAS IM system was observed compared to Soluplus® IM systems.

The extruded pellets provided the faster drug release compared to the moulded tablets suggests the effect of particle size as well as the densification during IM on the dissolution rate of the dosage form. The nature of the polymer and processing history were the contributing factors for the dissolution of the dosage forms.

Dedicated To My Beloved

Mother

& all The Deshmukh family members

Acknowledgements

I would like to express my special appreciation and thanks to my supervisors Dr.Adrian Kelly and Prof.Anant Paradkar, they both have been a tremendous mentor for me. I would like to thank them for encouraging my research and for allowing me to grow as a research scientist. Their advice on both research as well as on my career has been invaluable. Due to interdisciplinary research initiation I got a chance to work across two unique research centres, Centre for Pharmaceutical Engineering Sciences (CPES) and Polymer IRC. I would like to specially thank Prof. Anant Paradkar for giving me this opportunity and guidance throughout this research.

I am very grateful to Dr. Adrian Kelly for his invaluable guidance and moral support throughout this work. He helped me a lot to get trained on polymer processing techniques like hot melt extrusion and injection moulding. With his constant support, advice during technical discussions and proof reading my reports, I would say I have certainly improved my understanding, scientific writing and presentation skills to a great extent.

I would especially like to thank technicians in polymer IRC, Mr. John Wyborn and Mr.Glen Thomson and the man with great heart Mr.Keith Norris. All of you have been there to support me when I worked in a lab and collected data for my Ph.D. thesis.

My special thanks to my friends and colleagues at CPES. Your support made the stay in Bradford very pleasant and a memorable one. During PhD work

Table of Contents

List of Figures

List of Tables

Abbreviations

ANDA	:	Abbreviated New Drug Application ANOVA
ANOVA	:	Analysis Of Variance
API	:	Active Pharmaceutical Ingredient
BCS	:	Biopharmaceutical Classification System
DMA:	:	Dynamic Mechanical Analysis
DSC	:	Differential Scanning Calorimetry
FDA	:	Food and Drug Administration
FTIR	:	Fourier Transform Infrared
GMP	:	Good Manufacturing Practice
HME	:	Hot Melt Etrusion
HPMCAS	:	Hydroxypropyl Methyl Cellulose Acetate Succinate
IM	:	Injection Moulding
IP	:	Intellectual Property
NIR	:	Near Infra-Red
PAT	:	Process Analytical Technique
PEO	:	Polyethylene Oxide
PVP	:	Polyvinylpyrrolidone
PXRD	:	Powder X-ray Diffraction
QbD	:	Quality by Design
RH	:	Relative Humidity
RT:	:	Room Temperature
SEM	:	Scanning Electron Microscopy
SLS	:	Sodium Lauryl Sulphate
USP	:	United State Pharmacopoeia
UV	:	Ultra-Violet

Symbols

G_{mix}	:	Free energy of mixing
ɣ	:	Shear rate
r2	:	Coefficient of determination
Tg	:	Glass transition temperature
β	:	Regression coefficients
δ	:	Solubility parameter
φ	:	Volume fraction
χ		Interaction parameter
$τ_w$	:	Shear stress
η	:	Shear viscosity

Chapter 1

Introduction

Hot melt extrusion (HME) is a widely applied technique in the plastics industry, which has recently become viable for the processing of pharmaceuticals. In a short time, this technique has become a part of pharmaceutical product development. It offers several advantages such as solvent free continuous processing, homogenous particulate dispersion (i.e. solid dispersion) or molecular dispersion (i.e. solid solution) of actives in a polymer matrix. Moreover, acceptance in the pharmaceutical development relies on its flexibility to process complex mixtures of drugs with a wide range of excipients and to produce various dimensions of dosage forms. However, the end products of melt extrusion are generally obtained in the form of intermediate products such as pellets or granules which need further processing to develop into the finished products or dosage forms.

Injection moulding (IM) is another commonly used manufacturing process for the fabrication of intricate polymeric parts with excellent dimensional accuracy. A wide variety of products are manufactured using injection moulding, which vary greatly in their size, complexity and application. Hence, application of this process for development of moulded drug delivery systems for pharmaceuticals could expand applications of existing melt processes. This process has been widely used for the manufacturing of pharmaceutical packaging materials and more recently for production of biomedical devices such

as scaffolds, microneedles and microfluidic devices (Gomes et al., 2001) (Haugen et al., 2006). In the context of scalability, the unique features of IM are that it consists of a single unit operation, has a higher speed, greater product range and higher throughput.

Although the IM process has great potential to process material, it has limitations in terms of the suitability of materials. Not all polymeric systems are suitable for injection moulding due to the high temperatures and pressures encountered. Polymers are highly sensitive to temperatures and pressures and their physical properties including viscoelasticity, flammability, miscibility, and surface properties need to be considered for their acceptability with the IM process. In IM the material experiences high pressures and the pressure history in processing affects material properties such as shrinkage and residual stresses at the end of the process (Bayer et al., 1984). The injection and clamping pressure effects material densification or reduction in specific volume (Carrasco et al., 2010)

Challenges with the injection moulding process with respect to pharmaceutical drug product development are inevitable; therefore the selection criteria for materials or polymers for injection moulding need to be established. Although injection moulding was introduced by Speiser in 1964 as a pharmaceutical technology to produce sustained-release dosage forms and solid solutions, its use within the pharmaceutical industry has been limited to date to a few specific applications (Speiser, 1969) (Wacker et al., 1991). Recently, researchers have been exploring the application of an injection moulding technique to fabricate matrix-releasing tablets (Quinten et al., 2009) (Vervaet et

al., 2008), capsules of pharmaceutical polymers (Eith et al., 1986) and drug releasing polymer matrices (Cuff and Raouf, 1998), (Barshalom et al., 2003).

Nowadays, researchers are trying to develop and adapt new technologies for processing of pharmaceuticals. The IM process can be either explored as a down-stream or independent single unit operation to develop drug delivery systems. The development of the moulding processes to design drug-polymer systems with advanced properties could result in new geometries of dosage forms with distinct properties compared to conventional drug delivery systems. A schematic representation of the HME and IM processes for pharmaceutical product development is provided in Figure 1.1. The formation of solid dispersions of poorly soluble API with pharmaceutical grade polymers and use of IM process to provide the solid dispersion and final dosage form in single unit operation is illustrated in this figure.
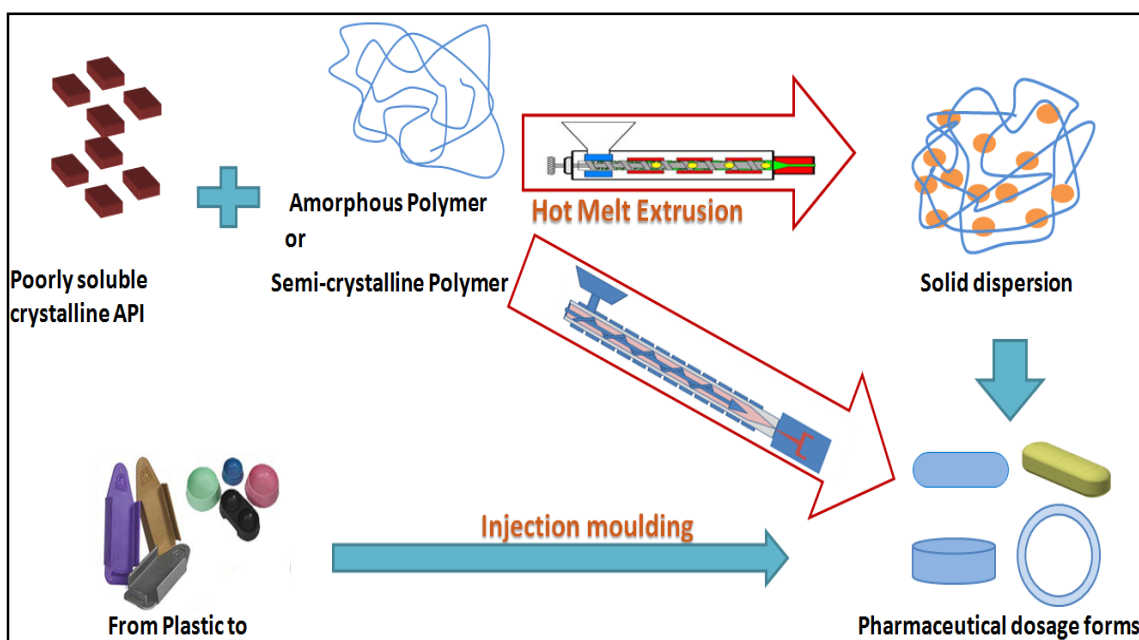
Figure 1.1 Schematic representation of application of HME and IM for NDDS

1.1 Theoretical considerations

The development of pharmaceutical drug-polymer systems using IM has several challenges associated with the process and product performance. Challenges associated with material properties can be addressed using theoretical calculations which provide pre-formulatory information about the selected materials. Prior to formulation development, the theoretical knowledge of drug-polymer miscibility and solubility in amorphous solid dispersions provides a better understanding of drug crystallisation and phase separation during shelf-life. The following parameters provide a better understanding about the miscibility and drug solubility in the polymeric carriers.

I.   Solubility parameters (δ)

II.   Interaction parameters (χ)

III.   Free energy of mixing(ΔG_{Mix})

IV.   Glass transition temperature of mixtures (Tg)

V.   Temperature-composition phase diagram

Details of the methods used to estimate these properties are provided in the pre-formulation chapter (chapter 4).

1.2 Challenges associated with IM of pharmaceutical drug-polymers systems

The challenges associated with injection moulding are mainly related to process and product performance.

1.2.1 Processing challenges

Most of the pharmaceutical polymer/carriers are not designed specifically for melt processing applications. Only a limited numbers of polymers such as Soluplus®, Affinosol® have been developed recently for HME application. However, IM of pharmaceutical grade polymer is challenging as it needs to have a suitable melt viscosity and melt rheology so that melt can flow inside the runner system and fill the mould cavity. Amorphous polymers soften on heating and exhibit poor lubricity hence often needs a plasticiser to aid the process by lowering processing temperatures and provide help to achieve optimum melt rheology. Most of the injection moulded part has a runner system for the filling of molten material in the mould cavity and when the part is cooled and ejected, the extra component gets separated from the main part and disposed. In the case of pharmaceutical drug delivery systems the wastage of moulded part is associated with high cost, health risks and regulatory concerns. The use of hot runner system could overcome the problem of wastage where the runner systems can be used as part of next injection moulding cycle.
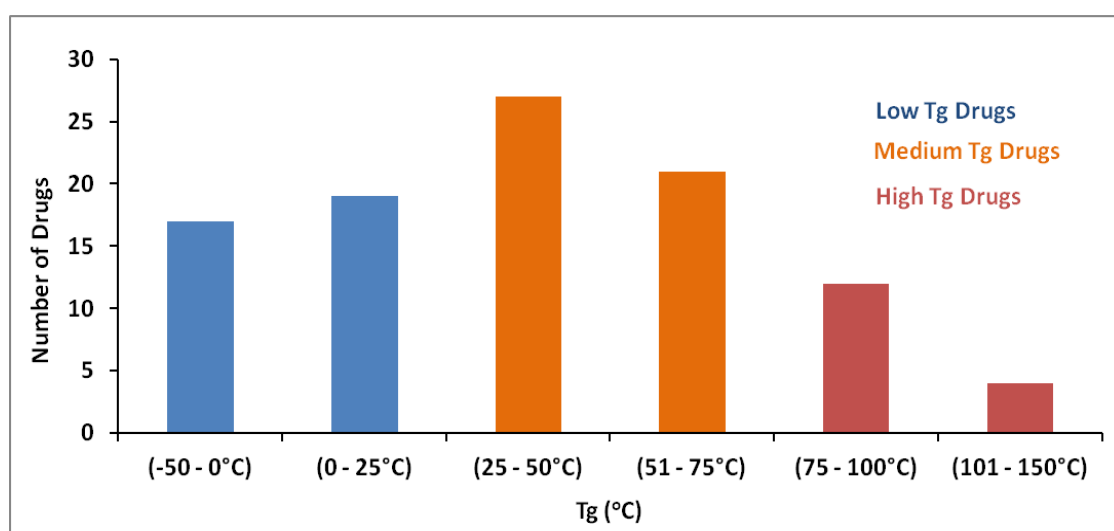
Figure 1.2: 100 APIs classified based on glass transition temperature (Tg) (Fukuoka et al., 1989)

Tg data of 100 APIs was compiled from the reported literature and classified in into three categories (Fukuoka et al., 1989). Figure 1.2 shows that approximately 1/3 of drugs ($\cong$ 36) fall in the range of - 50°C to 25 °C and which have a Tg less than the room temperature (RT) labelled as 'low Tg' drugs. Approximately 50% of the drugs fall in the range of 25°C to 75 °C labelled as 'medium Tg' drugs. 15% of drugs fall under 'high Tg' drugs and have Tg in the range of 75°C to 150 °C. Among which only 3% of show Tg higher than 100°C. The overall conclusion based on this figure can be drawn as most of the drugs fall in the low and medium Tg range and more than 60% of the drugs have Tg less than 50°C. Ibuprofen and felodipine (APIs) selected in this research have low and medium Tg, respectively. Rationale for the selection of APIs in this work was mainly based on their poor solubility and low Tg.

The selection of amorphous polymers for the solid dispersion usually depends on the intended application of the dosage form e.g immediate release, controlled release, fast release, delayed release etc. The Tg of amorphous polymers is an important consideration during selection, as high Tg polymers provide the higher Tg to the amorphous solid dispersion (formulation) and thus enhance its stability. However, high Tg polymer becomes a challenge for melt processing and often need plasticisers to aid the process. The majority of plastic grade polymers are semi-crystalline in nature and exhibit shear thinning behaviour and good melt rheology. The use of "low Tg" and/or "medium Tg" drugs as a plasticiser for pharmaceutical polymers will enhance the processability of polymers by HME and IM. In addition the need for other plasticisers which might destabilize the systems could be avoided.

1.2.2 Biopharmaceutical challenges:

Drug delivery products developed using injection moulding are highly dense, non-disintegrating and potentially challenging for oral drug delivery. Due to densification during injection moulding the dissolution of the dosage forms can be the rate limiting step hence the development of immediate release dosage form becomes challenging.

1.3 Research objectives

The main aim of this research is to investigate the injection moulding process to develop novel drug delivery systems (NDDS). The broad objective of the work is to understand the processing of pharmaceutical polymers by IM, explore injection mouding technology to produce pharmaceutical dosage forms, and to provide an understanding of the effect of the process variables on the properties of the moulded systems.

<u>Specific objectives of the research work include:</u>

1. To develop IM processes for pharmaceutical amorphous polymers and investigate its application for NDDS.

2. To understand the effect of IM processing history on the properties of injection moulded systems and to study the biopharmaceutical performance of amorphous solid dispersions or solid solutions achieved by HME and IM.

3. To understand the effect of additives such as modifiers and/or retardants on the performance of the moulded systems.

4. To investigate into the use of injection moulding to produce pharmaceutical dosage forms and to understand the relationship between materials,

processing conditions and performance, in particular drug release and stability.

In the present work, combinations of drug-polymers with different physicochemical properties were selected. Two poorly soluble model APIs belonging to biopharmaceutical classification system (BCS class II) and two pharmaceutical grade polymers were selected with the objective of obtaining NDDS with unique properties and drug release performance. A schematic representation of the drug-polymer combinations and systems developed in this work are presented in Figure 1.3. The Ibuprofen and felodipine exhibits low (-45 °C) and medium Tg (45 °C) respectively; whereas Soluplus® possess the low Tg (72 °C) compared to HPMCAS (120°C). The understanding of IM processing and stability of drug delivery systems obtained using these drug and polymer combinations was one of the main interest of this work.
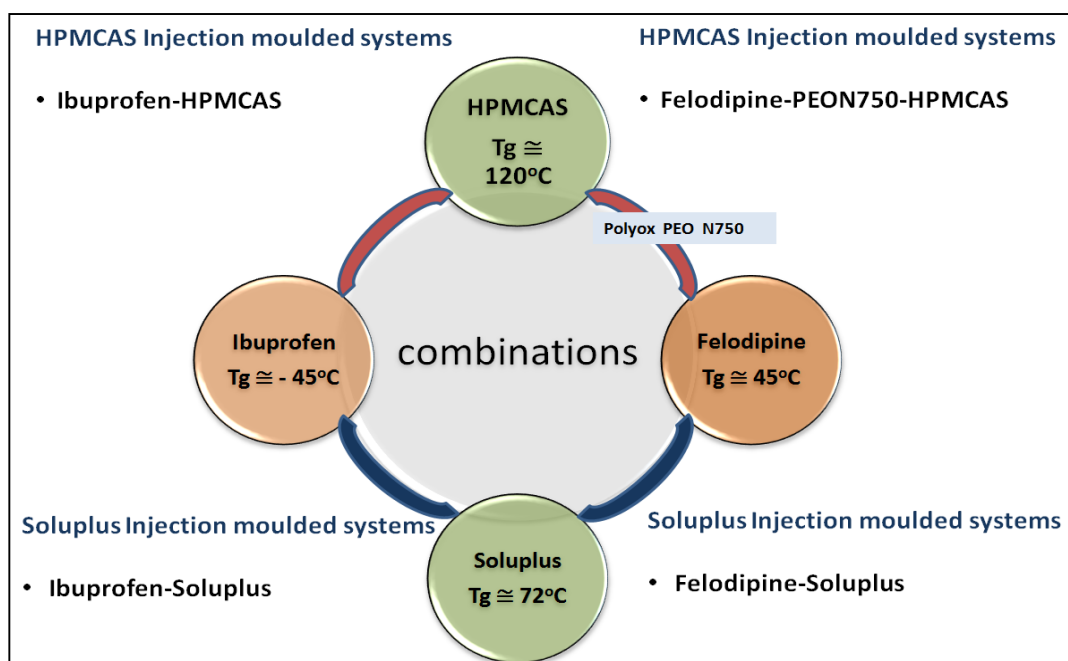
Figure 1.3: Drug polymer combinations used for processing using HME and IM

1.4 Thesis outline

Chapter 2 provides a general background and literature review and is divided into three sections. The first section provides information on poorly soluble drugs, biopharmaceutical classification systems and solubility enhancement approaches used for BCS II drugs. The middle section is focused on the concept of solid dispersions, drug carriers, polymers and methods of preparation. The final section provides an overview of HME and IM including their challenges and applications for drug delivery. The thesis structure is provided in Figure 1.4.

Chapter 3 describes the details of materials and methods used for this study and this chapter is sub-divided into two major sections; HPMCAS injection moulded systems and Soluplus® injection moulded systems. HPMCAS IM system provides information of both the HME and IM methods used to obtain Ibuprofen-HPMCAS systems and felodipine-PEON750-HPMCAS systems. Similarly; the Soluplus® IM system provides details of experimental conditions used to produce ibuprofen- Soluplus® systems and felodipine- Soluplus® systems. Details of all characterisation techniques used are provided within each section.

Chapter 4 provides the results and discussion of pre-formulation studies performed to understand the material properties.

Chapter 5 contains results and discussion of HPMAS IM systems; ibuprofen-HPMCAS systems and felodipine-PEON750-HPMCAS systems. The ibuprofen-HPMCAS moulded systems were investigated in detail to understand the processing and stability. Important outcomes of this research, such as understanding of surface crystallisation of ibuprofen, crystal habit,

biopharmaceutical performance, shrinkage and stability of IM systems are presented.
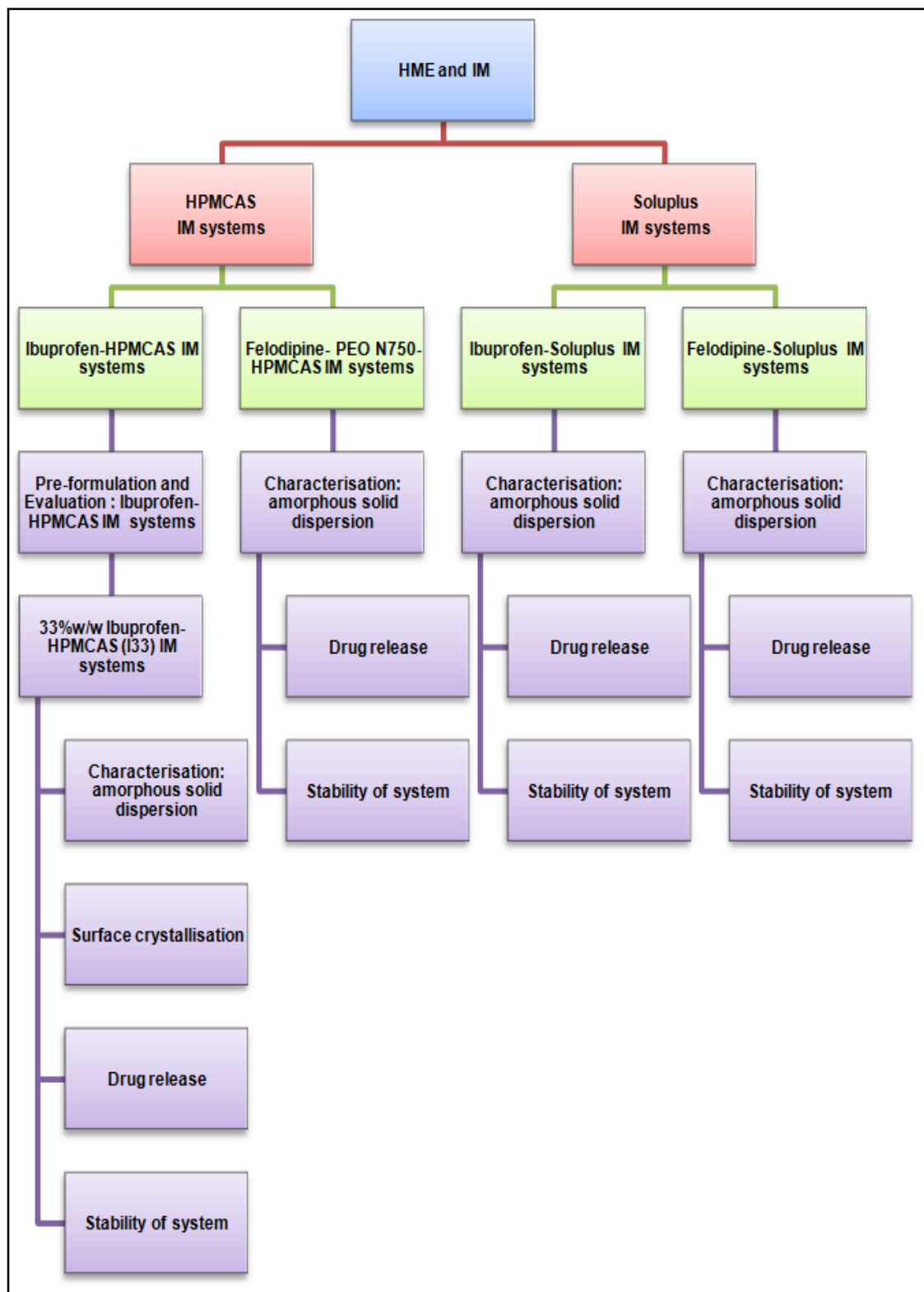
Figure 1.4: Schematic representation of the research structure

Chapter 6 contains the results and discussion of Soluplus® IM systems; ibuprofen-Soluplus® and felodipine-Soluplus®. The processing challenges associated with Soluplus® using HME and IM with the addition of ibuprofen and felodipine are discussed. Controlled release behaviour of the IM systems is also discussed.

Chapter 7 combines global discussion of results of pre-formulation, HPMCAS and Soluplus® injection moulded system

Chapter 8 contains an overall summary and conclusion of the work;

Chapter g suggestions for future work are presented in this chapter

Reference used within this thesis and appendix are provided in last section of thesis.

Chapter 2

Background

This chapter will provide relevant background information and a literature review of poorly soluble drugs, the biopharmaceutical classification system (BCS), and solid dispersion strategies used for solubility enhancement of active pharmaceutical ingredients (API). The objective of this chapter is also to review melt processing technologies used for development of solid dispersions and novel drug delivery systems. A schematic representation this chapter is shown in Figure 2.1.
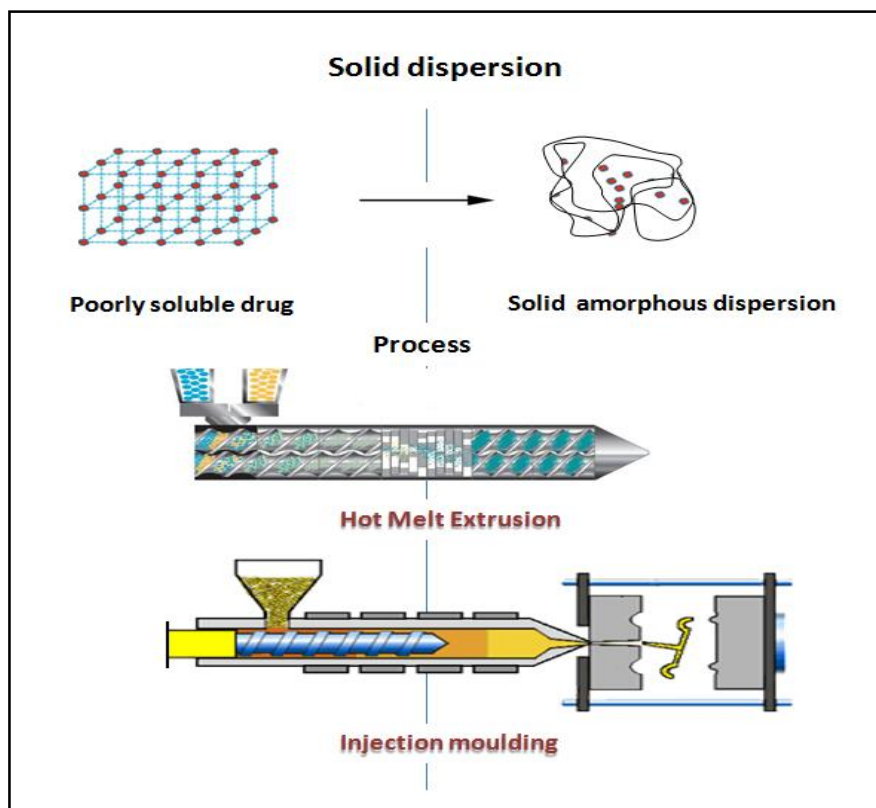
Figure 2.1: A schematic representation of background chapter

2.1 Poorly soluble drugs

Combinatorial chemistry and high throughput screening approaches are processes used in drug discovery to choose potential drug-like candidates after screening million's of compounds. The 'drug-like' compounds in early drug discovery are defined as compounds that have sufficient absorption, distribution, metabolism, excretion (ADME) properties and have sufficiently acceptable toxicity properties (Lipinski, 2000). The drug candidates chosen after this meticulous screening, however, can produce a drug with high or low aqueous solubility with high or low lipophilicity. The numbers of drug candidates with poor aqueous solubilities have increased in recent years and it is estimated that approximately 70% of new drug candidates have shown poor aqueous solubility (Ku and Dulin, 2012). Figure 2.2 shows currently marketed drugs and those under development (Babu and Nangia, 2011). Studies of the current globally marketed top 200 immediate release (IR) oral products showed that 40% of drugs are practically insoluble (<100 µg/ml) (Takagi et al., 2006).
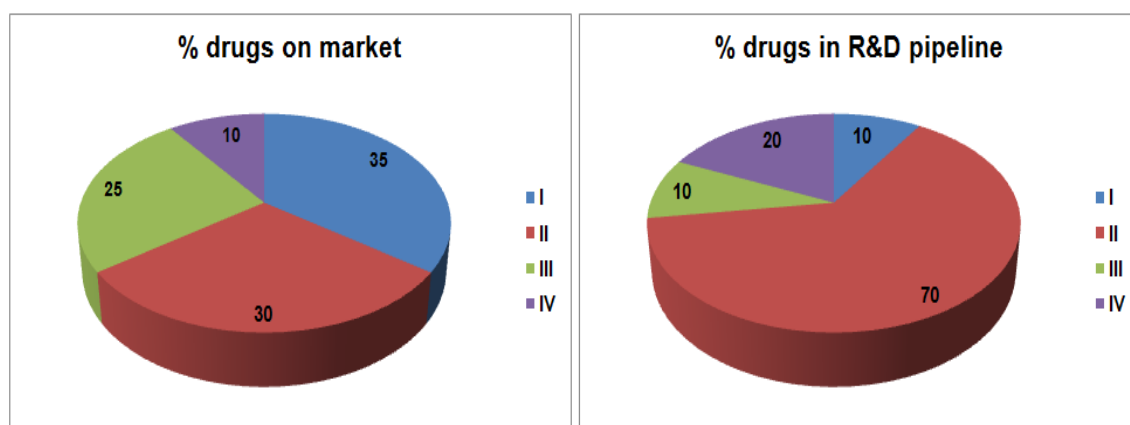
Figure 2.2: Low solubility drugs in the market and in the development pipeline according to the BCS (Babu and Nangia, 2011)

The poor aqueous solubility of drug candidates is critical in determination of its performance. In the case of orally administered drugs, a drug candidate

13

must undergo dissolution to get absorbed into the systemic (blood) circulation, and thus become bio-available. Complete absorption of the drug candidate after oral administration will be based on the events depicted in Figure 2.3. Moreover, the events are relatively important to each other and the rate at which they occur (Dressman and Reppas, 2000). Hence, in the case of poorly soluble drugs the dissolution becomes a rate-limiting step for absorption. When the solubility of the drug candidate is less than 0.1mg/mL (<100 µg/ml), it is considered to be practically insoluble (Table 2.1).

Table 2.1: Solubility definitions in the USP (Stegemann et al., 2007)

Description forms (solubility definition)	Parts of solvent required for one part of solute	Solubility range (mg/ml)	Solubility assigned (mg/ml)
Very soluble (VS)	<1	>1000	1000
Freely soluble (FS)	From 1 to 10	100-1000	100
Soluble	From 10 to 30	33-100	33
Sparingly soluble (SPS)	From 30 to 100	10-33	10
Slightly soluble (SS)	From 100 to 1000	1-10	1
Very slightly soluble (VSS)	From 1000 to 10,000	0.1-1	0.1
Practically insoluble (PI)[a]	>10,000	<0.1	0.01
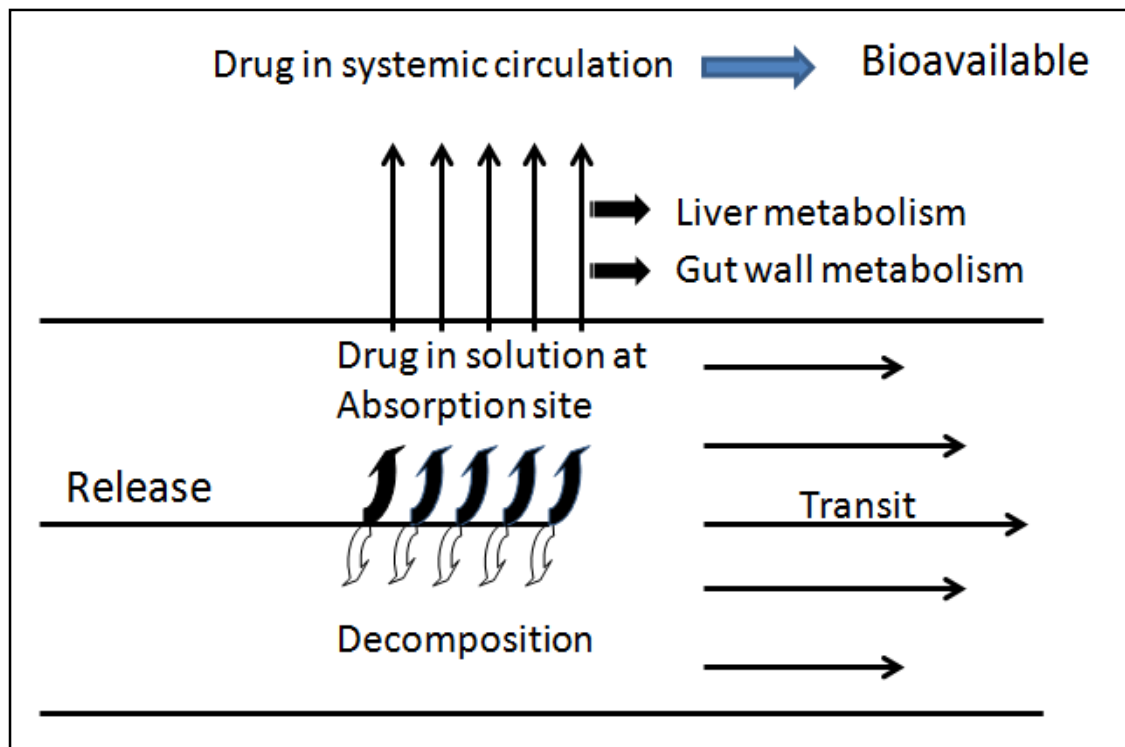
Figure 2.3: Events in the gastrointestinal tract following administration of an oral dosage form (adapted from Dressman and Reppas, 2000)

2.2   Biopharmaceutical classification system (BCS)

The BCS is a scientific framework used for the classification of drug substances based on their aqueous solubility and gastrointestinal permeability (FDA, 2000). It basically classifies a drug candidate into one of the four categories based on the solubilities and the permeability characteristics (Figure 2.4). Class I drug candidates are highly soluble and highly permeable. The drug candidates classified in class I should not be less than 90% absorbed. Class II and Class III candidates are the mirror images of each other. Class II drugs are poorly soluble therefore, exhibit poor performance during the dissolution; however, they are highly membrane permeable. Class III drugs are highly soluble but challenging because of poor lipophilicity. Class IV drugs have neither sufficient solubility nor permeability for complete absorption. From the biopharmaceutical point of view, the BCS scheme is a very useful and used as a decision-making tool in

formulation development. It is now a widely used tool for making strategies for formulation development of drug candidates.
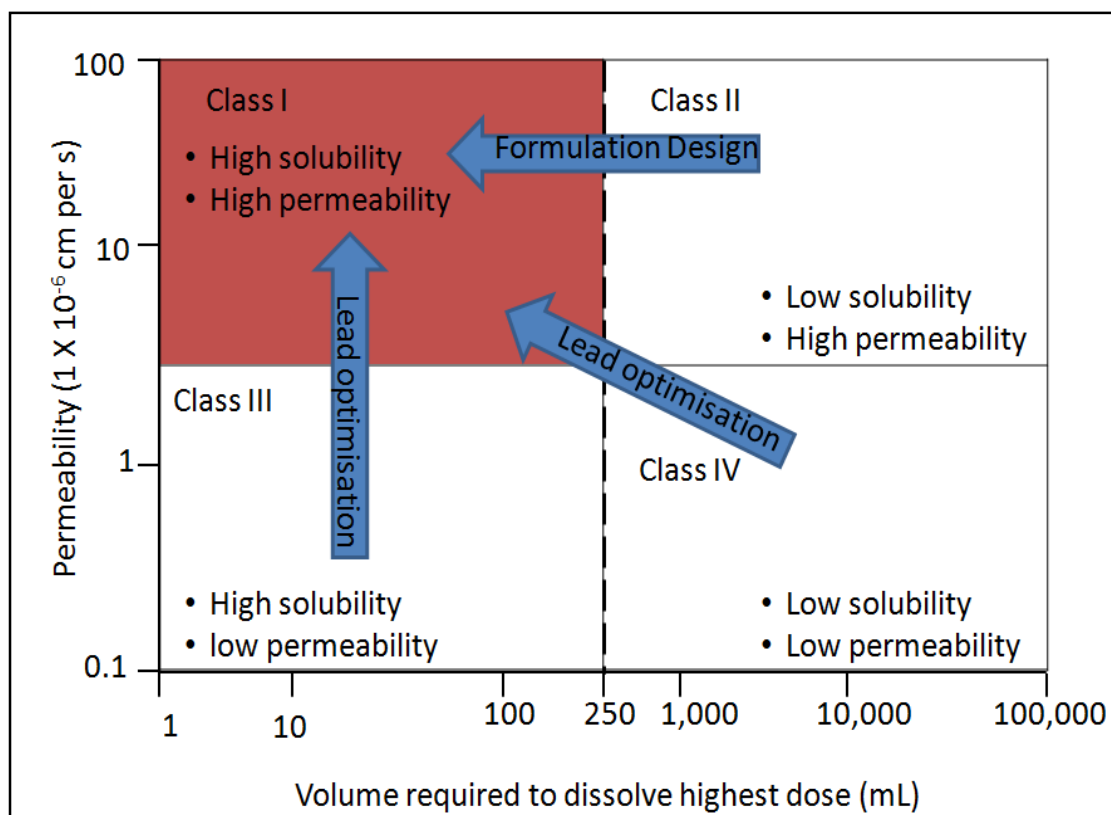
Figure 2.4: BCS classification of drugs (Rautio et al., 2008)

Recently, modified version of BCS called Biopharmaceutics Drug Disposition Classification System (BDDCS) was proposed to better predict drug disposition (Wu and Benet, 2005). BDDCS was developed based on the realisation that the high permeability characteristics of BCS class I and class II drug allow ready access to metabolising enzyme within hepatocytes and thus there is also good correlation between the drug metabolism and permeability defined under BCS. Instead of permeability the BDDCS categorises drug substances using major route of drug elimination or drug metabolism as follows (Chen and Yu, 2009; Larregieu and Benet, 2014):

Class I: High solubility, extensive metabolism

Class II: Low solubility, extensive metabolism

Class III: High solubility, poor metabolism

Class IV: Low solubility, poor metabolism

2.3 Formulation strategies based on BCS

As presented in Figure 2.4; the BCS classification is a great help in the understanding of physicochemical and biopharmaceutical properties of the drug candidates. A common approach for formulation development after its classification will be to try to shift all other classes of drugs to class I, which has both good solubility and lipophilicity. Low permeability of the drugs in class III and class IV would lead to strategies for optimisation of drug candidate properties; for example, lead optimisation which involves chemical structure modification, formation of prodrugs (Amidon et al., 1995) (Rautio et al., 2008). The absorption of class III is generally modified by formulation of dosage forms containing permeation enhancers such as fatty acids, bile salts, surfactants, polysaccharides etc. As the majority of drugs fall drugs into BCS II and most of the new drug discovered also show poor solubility despite their good lipophilicity. Therefore, formulation strategies are mainly focused on solubility enhancement of poorly soluble drugs.

2.4 Strategies for poorly soluble drugs (BCS II)

Solubility of a material is an intrinsic property that can be only influenced by the chemical modification of the molecule such as a salt formation or pro-drug formation. Dissolution of material, in contrast, is an extrinsic property which can be influenced by various factors such as chemical, physical or crystallographic modifications such as like particle size, complexation, surface property modification, co-crystallisation etc. (Stegemann et al., 2007). Formulation approaches for BCSII drugs are presented in Figure 2.5 .
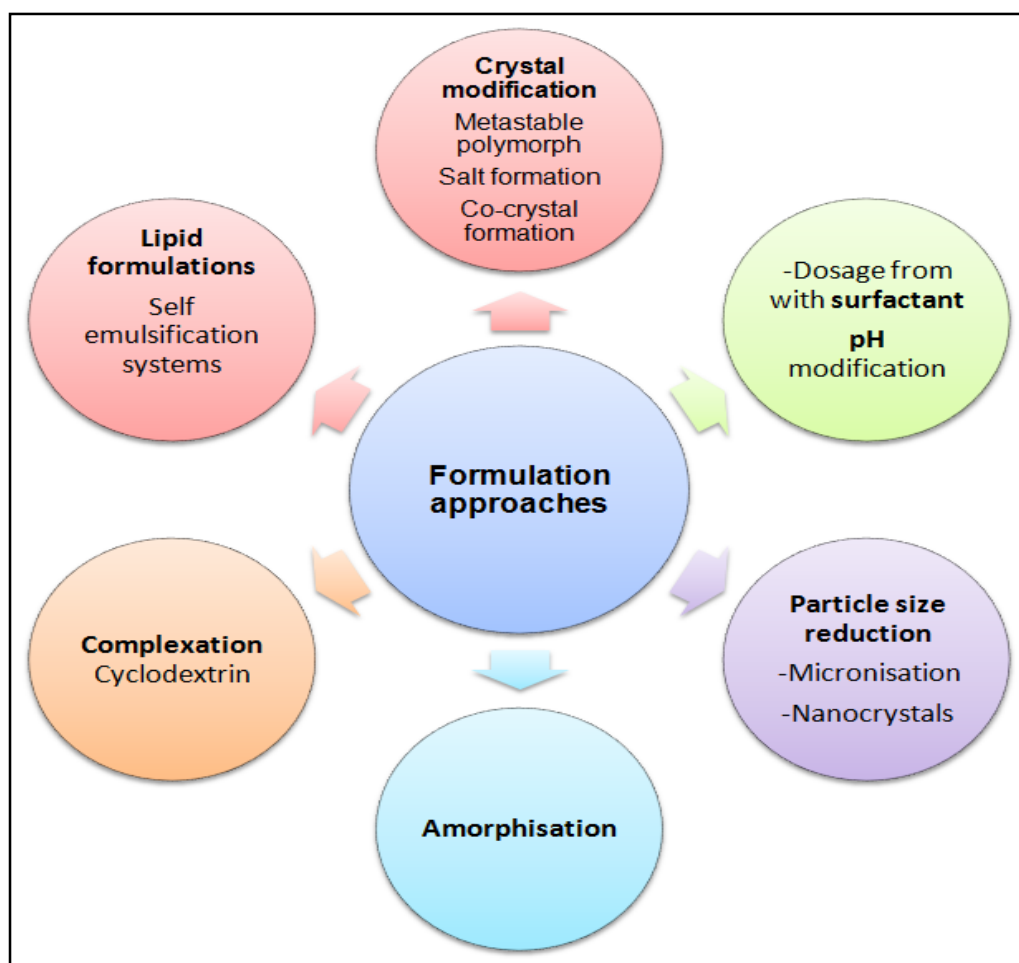
Figure 2.5: Formulation approaches used for solubility enhancement of poorly soluble drugs

2.4.1 Crystal modification

Polymorphism and salt formation are widely used approaches in the area of crystal modification of pharmaceutical drugs. Polymorphs are defined as a material with the same chemical composition, but differ in their lattice structure and/or molecular conformation (Rodriguez-Spong et al., 2004). Polymorphs exhibit different physicochemical properties such as melting point, solubility, density and stability. Generally a metastable polymorph shows higher kinetic solubility than a more thermodynamically more stable polymorph (Blagden et al., 2007). Salt formation is the common approach used for ionisable drugs in the pharmaceutical industry for the enhancement of solubility and the dissolution

rate. Salts are formed by transfer of a proton from an acid to a base. When the pka difference (ΔpKa) between an acid and a base is greater than 3, a strong ionic bond can be formed (Childs et al., 2007). The dissolution rate enhancement of the corresponding salt form compared to the free form is mainly because of the counter ion containing salt changes the pH at dissolving surface of the salt particle in the diffusion layer (Serajuddin, 2007). In recent years, the formation of co-crystals of poorly soluble drugs has been also widely investigated for crystal modification to improve the dissolution rate. Co-crystals are broadly defined as crystalline materials comprised of at least two different components (Schultheiss and Newman, 2009).

Pharmaceutical co-crystals are typically composed of active pharmaceutical ingredient (API) and co-formers in stoichiometric ratio. In many cases, it was seen that the API and co-formers require the formation of a hydrogen bond (H-bond) to form stable co-crystals. Generally ΔpKa is considered to be a reliable indicator for distinguishing salts and cocrystals, molecular complexes are thought to be co-crystals when the ΔpKa difference is less than 0 (Childs et al., 2007). There are many reports about the use of co-crystal approaches to modify the physiochemical properties of several APIs including carbamazepine, theophylline, itraconazole, norfloxacin, indomethacin (Vishweshwar et al., 2006) (Jones et al., 2006) (Childs et al., 2007) (Basavoju et al., 2006), to enhance the dissolution rate and oral bioavailability (Jung et al., 2010) (Jung et al., 2010) (McNamara et al., 2006) (McNamara et al., 2006) (Bak et al., 2008).

2.4.2 Particle size reduction

Reduction of the drug particle size to the micron or nano size is a widely used approach for solubility enhancement of poorly soluble drugs. According to the Noyes-Whitney equation the rate of dissolution (J) is directly proportional to the surface area (A) of the particles and inversely proportional to the boundary layer thickness (h).

$$J = \frac{D\,A}{h}\ (Cs - C)$$
Equation 2.1

Where J is the rate of dissolution, D is the diffusion co-efficient, h is boundary layer thickness, Cs is the saturation solubility, C amount of drug dissolved at time T.

Therefore, a reduction in particle size will increase the dissolution rate to a significant extent by increasing the surface area (Horter and Dressman, 2001) and decreasing boundary layer thickness (Mosharraf and Nystrom, 1995). Therefore, the micronisation of drug particles leads to a decrease in particle size by a factor of 5 which will enhance dissolution by 5 fold. A micronisation approach has successfully enhanced the bioavailability of some poorly soluble drugs such as griseofulvin, digoxin and felodipine (Atkinson et al., 1962) (Jounela et al., 1975; Scholz et al., 2002).
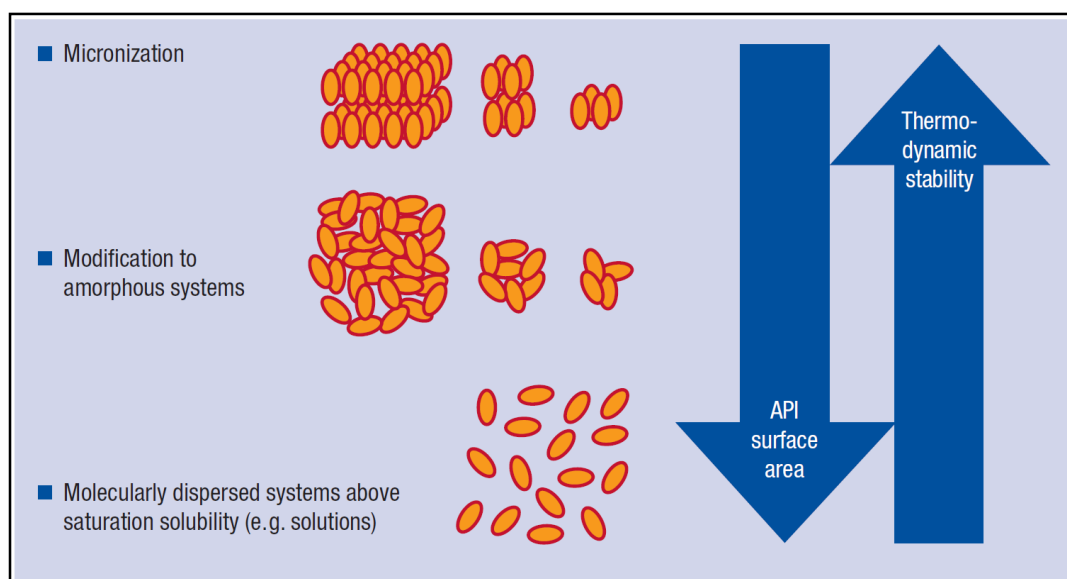
Figure 2.6: Surface area of the drug particles vs thermodynamic stability (Kolter et al., 2012)

Reduction of the drug particles to a nanometer size (< 1 µm) could be more advantageous as it will provide a greater surface area and decrease the boundary layer thickness (Figure 2.6). In addition to this factor, it will also increase the saturation solubility (Muller and Peters, 1998). Nanocrystals can be produced by wet milling, high-pressure homogenisation and controlled precipitation (Shegokar and Mueller, 2010). There are numerous reports on the solubility enhancement of poorly soluble drugs by nanosizing techniques. Drug candidates like Cilostazol, Curcumin, Danazol, Fenofibrate and Nitrendipine are the examples which have been formulated in nanocrystals and showed a significant enhancement in bioavailability.

2.4.3 Complexation: Cyclodextrin complexation

Cyclodextrins are useful functional excipients in the formulation of poorly soluble drugs and have wide popularity from a pharmaceutical perspective because of their ability to interact with drugs and form inclusion complexes (Rajewski and Stella, 1996). There are more than 10 marketed solid, liquid and semisolid dosage forms available with cyclodextrin complexes (Brewster and Loftsson, 2007). Cyclodextrins are oligosaccharides, contain a relatively hydrophobic or lipophilic central cavity and hydrophilic outer core and surface (Loftsson and Brewster, 1996). Cyclodextrins are used either as solublisers or to form solid dispersions with poorly soluble drugs to enhance their bioavailability (Figueiras et al., 2007) (Al Omari et al., 2006) (Cirri et al., 2005)

2.4.4 Amorphisation

In a crystalline solid, three-dimensional long range order normally exists, whereas in the case of the amorphous state, this order does not exist and the position of molecules relative to one another is more random as in the liquid state. The amorphous character may be induced in the solid by four common means (Figure 2.7). These include condensation from vapour state, supercooling of melt, mechanical activation of the crystalline mass and rapid precipitation from solution (Hancock and Zograf, 1997). Amorphous solid forms are markedly more soluble than their crystalline counterparts (Hancock and Parks, 2000). Formation to amorphous solids or formulation to amorphous solid dispersion (ASD) is used as a tool to enhance bioavailability by taking the solubility advantage offered by the amorphous solid.
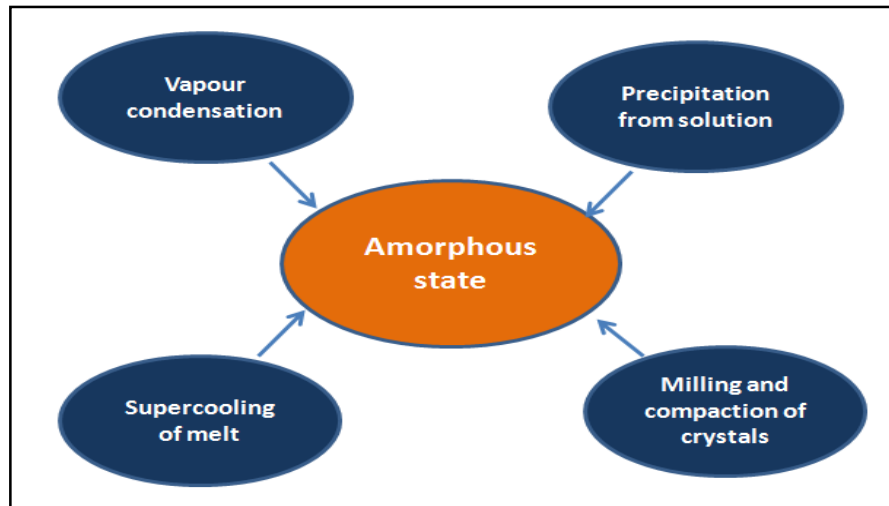
Figure 2.7: Schematic representation of most common ways by which the amorphous form is induced in pharmaceutical systems.

Figure 2.8 represents the enthalpy (H) or specific volume (V) of a material as a function of temperature. In crystalline materials, we may see at very low temperatures a small increase in enthalpy and specific volume with respect to the temperature indicative of a certain heat capacity (Cp) and thermal expansion coefficient (α). When a crystalline material reaches its melting temperature (Tm) discontinuity in both H and V represent a first-order transition to liquid state. Upon rapid cooling beyond its melting temperature values of H and V may follow equilibrium or first order in "supercooled region". On further cooling a change in slope is seen at a characteristic temperature called the "glass transition temperature" (Tg) (Figure 2.8). Tg is a significant property for the characterisation of pharmaceutical solids. At Tg the properties of the glassy material deviate from those of the equilibrium supercooled liquid to give a nonequilibrium state having even higher H and V than the supercooled liquid (Hancock and Zograf, 1997). The critical temperature T_K is known as the Kauzmann temperature and is thought to mark the lower limit of the experimental glass transition (Tg) and to be

the point at which the configurational entropy of the system reaches zero (Ediger et al., 1996) (Angell et al., 1986).
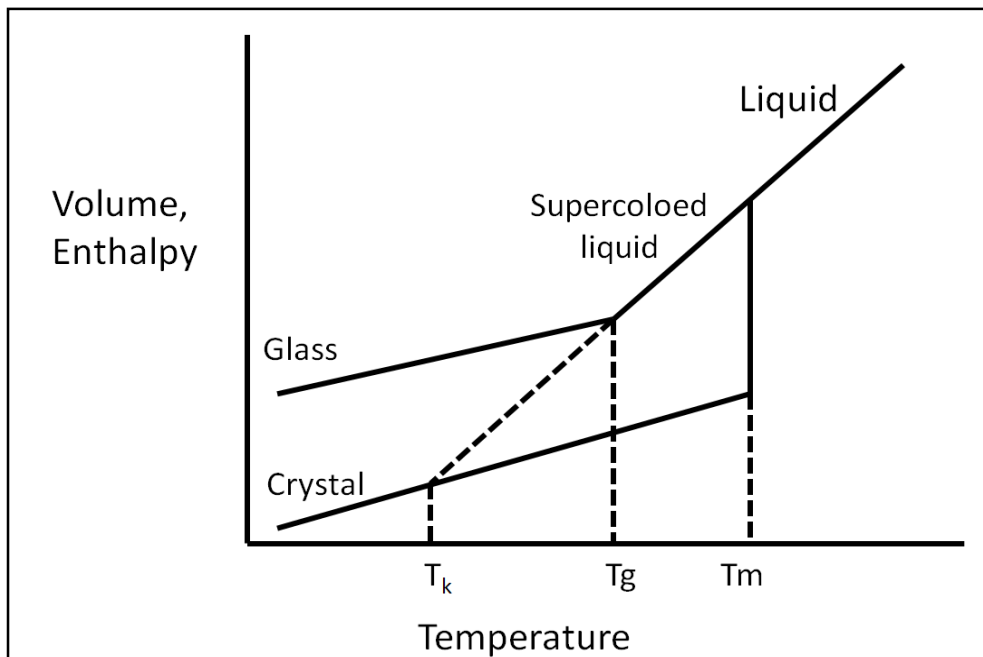
Figure 2.8: Schematic depiction of the variation of enthalpy (or volume) with temperature (adapted from Hancock and Zograf, 1997)

The amorphous state possesses higher internal energy than crystalline solids e.g Pikal et al. studied the series of β-lactam antibiotic (cephalosporins ≈25 kJ,mol^{-1}) using a solution calorimetry method (Pikal et al., 1978). This indicates that an amorphous state should have higher thermodynamic properties such as enthalpy, entropy, heat capacity than the crystalline state and greater molecular motions. The high internal energy and specific volume of an amorphous state can lead to an increased dissolution rate and enhanced bioavailability (Hancock and Zograf, 1997). However, these properties would also create the possibility that during processing or storage, the amorphous state may spontaneously convert back to the crystalline state (Yoshioka et al., 1994). The stabilisation of amorphous form or to obtain a stable

24

amorphous formulation, the solid dispersion (SD) approach has received wide acceptance in the area of pharmaceutical drug delivery.

2.5 Solid dispersion

During the last 30-40 years, the solid dispersions approach has become greatly accepted, adapted and recently commercialised for the formulation development of drug candidates which suffer from poor solubility. The definition of solid dispersion was first given in 1971 by Chiou and Riegelman in their excellent review "Dispersion of one or more active ingredient in an inert carrier or matrix at solid state prepared by the melting (fusion), solvent, or melting-solvent method". (Chiou and Riegelman, 1971)

2.5.1 Classification of solid dispersion

There are a number of ways by which the solid dispersions are classified. Classification based on molecular arrangements is given in Table 2.2.

Table 2.2: Classification of solid dispersion (Singh *et al.,* 2011)

Type		Matrix *	Drug * *	Remarks	No. of phases
1	**Eutectic**	C	C	The first type of prepared solid dispersion	2
2	**Amorphous precipitation in crystalline matrix**	C	A	Rarely encountered	2
3	**Solid solution**	C	M		
	Continuous solid solution	C	M	Miscible at all compositions, never prepared	1
	Discontinuous solid solution	C	M	Partially miscible, 2 phases even though drug is molecularly dispersed	2

	Substitutional solution	C	M	Molecular diameter of drug differs than 15% from the matrix diameter. In that case the drug and matrix are substitutional. Can be continuous or discontinuous. When discontinuous 2 phases even though drug is molecularly dispersed.	1 or 2
	Interstitial solid solutions	C	M	Drug molecular diameter less than 59% of matrix diameter. Usually limited miscibility, discontinuous	
4	**Glass suspension**	A	C	Particle size of dispersed phase dependent on cooling rate. Obtained after crystallisation of drug in amorphous matrix.	
5	**Glass suspension**	A	A	Particle size of dispersed phase dependent on cooling rate. Obtained after crystallisation of drug in amorphous matrix.	
6	**Glass solution**	A	M	Requires miscibility or solid solubility, complex formation or upon fast cooling, evaporation during preparation	

*A: matrix in amorphous state, C: matrix in crystalline state

** A: drug dispersed as an amorphous cluster in the matrix, C: drug dispersed as crystalline particles in the matrix, M: drug molecularly dispersed throughout the matrix

The Chiou and Riegelman proposed classification based on the major fast drug release mechanisms accordingly it was classified into six groups as explained below: (Chiou and Riegelman, 1971)

2.5.1.1 Simple eutectic mixtures

Eutectic mixtures can be prepared by rapid solidification of fused liquid of two components which shows a complete liquid miscibility and negligible solid-solid solubility (Figure 2.9). When a mixture of component A and component B with composition E is cooled both A and B will crystallise out simultaneously to form a eutectic mixtures. These mixtures are usually prepared by rapid cooling to comelt two components in order to obtain the fine crystals of two components. The carriers are usually crystalline in nature, e.g. urea, which dissolve rapidly in aqueous medium and release the fine drug crystals thus resulting in an enhanced dissolution rate and improved bioavailability.
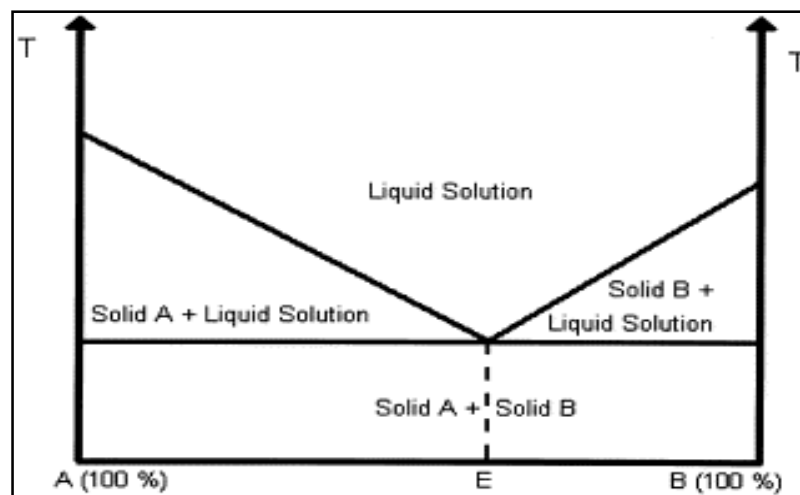
Figure 2.9: Phase diagram for a eutectic system (adapted from Leuner and Dressman, 2000)

e.g Eutectic mixtures of sulphathiazole-urea system (Sekiguchi and Obi, 1961) Urea-acetaminophen (Goldberg et al., 1966)

2.5.1.2 Solid solutions

Solid solutions are comparable to liquid solutions and consist of one phase irrespective of the number of components (Leuner and Dressman, 2000). Solid solutions consist of a solid solute dissolved in a solid solvent. In the case of solid

27

solutions, poorly soluble drug molecules are dispersed in an inert carrier with a relatively good aqueous solubility and dispersed drug particle size is reduced to molecular dimensions (Goldberg et al., 1965).

Continuous solid solutions

Continuous solid solutions are an ideal type of solid solution where two components are miscible in all preparations. Theoretically, this means that bonding strength between the two components is stronger than the bonding strength between molecules of the individual component. There are no reports of this type of solid solution in the pharmaceutical literature to date.

Discontinuous solid solutions

In the case of discontinuous solid solutions, there is a limited solubility of one component in the other. Goldberg suggested the that the term 'solid solution' should only be applied when the mutual solubility of the two components exceeds 5% (Goldberg et al., 1965). Chiou and Riegelman in 1969 reported the first amorphous solid solutions system for solubility enhancement of the griesofulvin (Chiou and Riegelman, 1969) .

Substitutional crystalline solid solutions, interstitial crystalline solid solutions and amorphous solid solutions

Classical solid solutions have a crystalline structure, in which a solute molecule either substitutes for a solvent molecule in the crystal lattice or fits into the interstices between the solvent molecules. In the case of substitutional crystalline solid solutions, substitution of a solute molecule for a solvent molecule

can only be possible when the size difference between the two molecules is less than 15% (Figure 2.10)
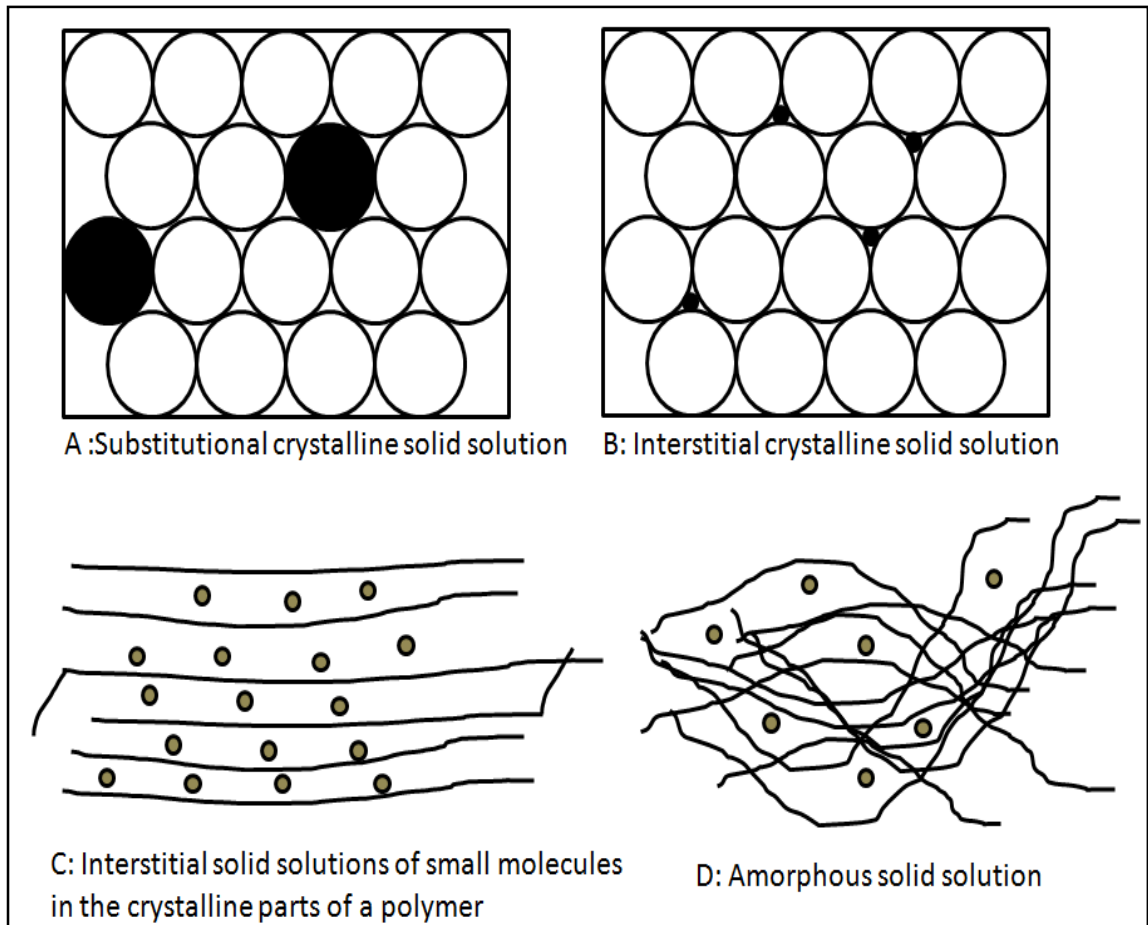
Figure 2.10: Solid solutions (referred from (Leuner and Dressman, 2000).

Whereas, in the case of interstitial crystalline solid solutions the dissolved molecule occupies the interstitial space between the solvent molecules in the crystal lattice (Figure 2.10B and Figure 2.10C). The two crucial criteria for the formation of interstitial crystalline solid solutions are first, the solute molecule diameter should not be longer the 0.59 of the solvent molecule's diameters (Reed-Hill, 1964). Second, the volume of the solute molecule should be less than 20 % of the solvent.

In amorphous solid solutions, the solute molecules are dispersed molecularly but irregularly within an amorphous solvent. (Figure 2.10D). The

dispersion of griseofulvin in citric acid was the first report of an amorphous soild

solution where the dissolution rate of the griseofulvin was increased significantly

due to the formation of a molecular level dispersion (Chiou and Riegelman 1969).

Other carriers reported in early studies were urea, sucrose, dextrose and

galactose. Recently the use of polymeric carriers to form amorphous solid

solutions has increased as the polymer itself is present in an amorphous polymer

chain network. Moreover, solute molecules may act like plasticisers, leading to a

reduction in Tg of a polymer. The details of polymeric carriers are presented in

tabular format in the next section (Table 2.3).

2.5.1.3 Glass solutions and glass suspensions

A glass solution is defined as a homogenous glassy system in which a

solute dissolves in a glassy solvent or carrier. Citric acid is capable of forming a

amorphous glass. Glassy solutions of griesofulvin, phenobarbital and

hexobarbital were reported with citric acid, which showed a marked increase in

dissolution rate (Chiou and Riegelman, 1969). The term glass suspension refers

to a mixture in which precipitated particles are suspended in a glassy solvent. e.g

crystallisation of benzophenone in hydrocarbon glass forms an invisible to

opaque appearance (Keller and Breen, 1965).

2.5.1.4 Amorphous precipitation of drug in crystalline carrier

This is a similar dispersion to a eutectic mixture, the only difference being

that the drug may precipitate as an amorphous form in a crystalline carrier. In

eutectic mixtures both the drug and carrier crystallise out simultaneously from

melting and solvent evaporation. Amorphous precipited novobiocin has a higher

solubility than its crystalline form (Mullins and Macek, 1960).

2.5.1.5 Compound or complex formation between drug and carrier

This group is not directly considered as class of solid dispersion; however the possibility of forming complexes cannot be overlooked. This group generally describes the possibility of formation of complexes between drug and inert carrier and that could ultimately change the dissolution rate. e.g the formation of insoluble complexes of anti-depressant (phenobarbital) with Polyethylene glycol 4000 or 6000 was shown to reduce its dissolution rate and permeation through the gut wall of rats (Singh et al., 1966).

2.5.1.6 Miscellaneous

It is possible that a solid dispersion may not entirely belong to one of the classes above mentioned, but may be formed from a combination of different groups. e.g Griseofulvin dispersed at high concentrations in polyethylene glycol may exist as individual molecule and as microcrystalline particles. The coprecipitates of reserpine with bile steroids (deoxycholic acid) were shown to increase blepharoptotoc activity of reserpine in mice. Exact physical properties of this system have not been elucidated, however the possibility of formation of a clathrate compound (inclusion compound) was considered in which a molecular dispersion of reserpine forms in hollow channels of bile clatharates (Ferguson, 1964).

2.5.2 Current trends and future prospective of solid dispersion

In general solid dispersion technology deals with a group of solids containing at least two components usually a hydrophobic drug and hydrophilic carrier. The carrier or matrix former could be crystalline or amorphous in nature. Figure 2.11 gives an overview on the compositions and properties of four generations of solid dispersions (Vo et al., 2013) .

The first generation of solid dispersion is where usually crystalline matrix formers such as urea, mannitol, citric acid were used to form eutectic mixtures. Due to the crystalline nature of the carriers, this type of solid dispersion exhibited low solubility and possessed low stability. During the development of second generation dispersions, the concept of the dispersion of an active into an amorphous polymer matrix became popularised e.g. polyethylene glycol, polyvinyl pyrrolidone. This generation of solid dispersions had improved dissolution rate and thereby improved bioavailability. In an amorphous solid dispersion, the API is dispersed at a molecular level amorphous particles or small crystals and exists in a supersaturated state in amorphous carriers because of forced solubilisation (Tanaka et al., 2006) (Urbanetz, 2006). Amorphous carriers can also increase dispersability and wettability of the API as well as may serve to inhibit the precipitation of drug during dissolution in aqueous media (Chauhan et al., 2013).
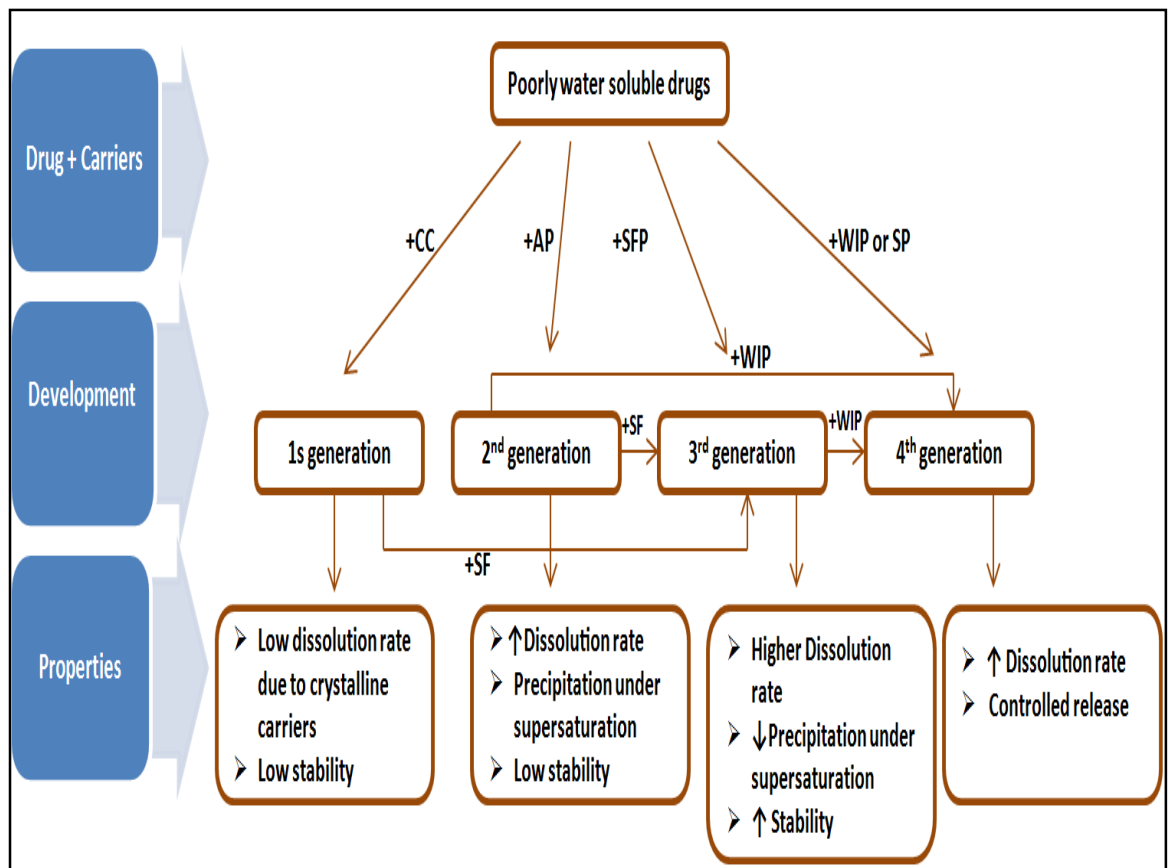
Figure 2.11:Composition and properties of four generations of solid dispersions. CC: crystalline carrier, AP: amorphous polymer, SFP: surfactant polymer, WIP: water insoluble polymer, SP: swellable polymer, SF: surfactant, (↑): increase, (↓): decrease (adapted from Vo et al., 2013)

The third generation of solid dispersion involves the use of surface active agents or self-emulsifiers. These agents were introduced as carriers or additives and showed a significant improvement in overcoming the above problems such as precipitation and recrystallisation. e.g Poloxamer, Compritol 888 ATO , gelucire 44/14 Soluplus® and emulsifiers such as sodium lauryl sulfate (SLS) Tween 80, d-alpha tocopheryl polyethylene glycol 1000 succinate (TPGS 1000).

Fourth generation solid dispersions are controlled release solid dispersions (CRSD) usually containing poorly water soluble drugs with a shorter

biological half-life. CRSD are designed to achieve two targets: firstly, solubility enhancement and secondly, extended release of the API in a controlled manner. There are many advantages of this type of solid dispersion: improved patient compliance due to reduced dosing frequency, decreased side effects, constant, prolonged therapeutic effect of poorly soluble drug release (Desai et al., 2006). The CRSDs have two main drug release mechanisms: diffusion and erosion. The use of water insoluble amorphous carriers and swellable polymers can dictate the mechanism of drug release. e.g Eudragit RSPO and ethyl cellulose are pH dependent solubule and water insoluble polymers respectively, and were used to obtain a sustained release of nitrendipine (Cui et al., 2003). Whereas the water soluble nature of polyethylene oxide (PEO) gave a controlled release of aceclofenac by diffusion through a swellable matrix of PEO (Tran et al., 2010). The details of carriers used in solid dispersions are compiled in Table 2.3.

Table 2.3: Carriers used for Solid dispersion and their properties (Paudel et al., 2013)

Carriers	M.Wt (Range) (kDa)	Tg (Tm) (°C)	Solubility parameters $(cal/cm^3)^{1/2}$	Hygroscopicity (moisture at 75%RH/RT)
Cellulosic derivatives: hydroxyl (ether)*				
HPMC 2910	10–1500	148.2–151.1	23.8	~10
HPMCAS-MF	80	117.3–120	31.2	6–7
HPMC-E5 (2906)	10–1500	152	–	–
Na-CMC	90–700		–	–
HPMC-P 55	10–1500	138	28	7–8
HPMC-AS HG	55–93	117.9–120	–	–
HPC (L-HPC)	50–1250	105 (220)		6–7
MCC	36	(260–270)		-
Vinyl polymers				
(OH of secondary alcohol)*-PVA				
PVP K 30	50	170–174	27.7	40%
PVP K 25	28–34			35–40%
PVP-VA64	45–70	106.0–110.0		<10% (50% RH)
PVP VA 37				
Kollicoat IR	45			
PVA 22000	20			
Soluplus®	90-140	72	31.22	~12

Carriers	M.Wt (Range) (kDa)	Tg (Tm) (°C)	Solubility parameters (cal/cm^3)$^{1/2}$	Hygroscopicity (moisture at 75%RH/RT)
Lipidic carriers				
Gelucire 44/14		-44		≈1% (<60% RH)
Gelucire 50/13		-50		
Compritol 888 ATO				
Sterotex K NF				
Poly(ethylene oxide) & derivatives				
Polyox N750		- 50		
PEG 4000	2.6–3.8	(50–58)		<2.5%
PEG6000	7.3–9.3	−22.71 (55–63)		<1%
PEG20000	15–25	−41 (60–63)		NH
Poloxamer 407	9.84–14.6			
Carbohydrates: hydroxyl (ether)*- dextrin				
Lactose	0.3423	232		
Arabia gum				
Stevia-G				
Glucosyl hesperidin				
PHPMA (poly[N-(2-hydroxypropyl)methacrylate])	20	-		
Eudragit E 100	47	48	19.3	
NaPMM	135			
Polyacrylic acid (PAA)	100	100–105 & 126		
Carbopol 940	104.4	100–105		

2.5.3 Polymers

A polymer is defined as a chemical compound or mixture of compounds consisting of repeating structural units, created through a process of polymerisation. This term describes a molecule whose structure is composed of multiple repeating units, from which originates a characteristic of high relative molecular mass and properties. The chemical structure, physico-chemical properties and applications of three pharmaceutical grade polymers selected in this research are presented in this section

2.5.3.1 Hydroxy propyl methyl cellulose acetate succinate (HPMCAS)

HPMCAS is cellulose ether, formed by alkylation of cellulose ether. Hypromellose acetate succinate is a mixture of acetic acid and monosuccinic acid esters of hydroxypropylmethyl cellulose. The nature of substituted i.e Alkyl, aryl, hydroxy-alkyl, other substituted alkyls, etc., degree of substitution, i.e. number of free and esterified hydroxyl groups dictates the polymer's physical properties (Figure 2.12).
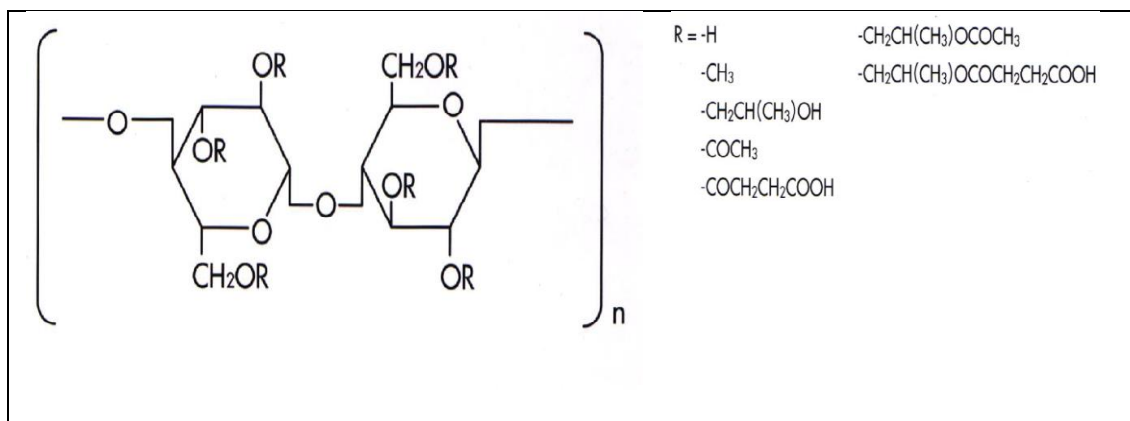
Figure 2.12: Structure of HPMCAS

HPMCAS is available in several grades which mainly vary with the extent of substitution of acetyl and succinoyl groups. An increase in substitution of

methoxy and acetyl groups increases the hydrophobicity of the polymer. Succinic acid remains un-ionised below pH 5 (Table 2.4). In pharmaceutical applications, it is mainly used for film and enteric coatings of oral dosage forms such as tablets and granules. It is insoluble in stomach fluid, but dissolves rapidly in the upper intestine. It is widely used for solid amorphous dispersion applications and is reported to have a higher drug dissolution rate (e.g nifedipine) and inhibit the recrystallisation of drugs from the polymer matrix (Tanno et al., 2004).

Table 2.4: Various grade and nature substitution of HPMCAS

Type	Content of substituent's (%)				Soluble at pH
	Succinoyl	Acetyl	Methoxyl	Hydroxypropoxyl	
HPMCAS-LF	14.8	7.3	7.1	22.7	5.5 and higher
HPMCAS-MF	11.0	9.3	7.4	23.0	6.0 and higher
HPMCAS-HF	7.8	11.1	7.4	23.5	6.5 and higher

Properties and application of HPMCAS

The unique properties of HPMCAS make it suitable for amorphous solid dispersions and spray-dried dispersions. Some of the properties of HPMCAS are summarised below (Friesen et al., 2008):

1. It has a high Tg in its un-ionized state. The high Tg of HPMCAS directly correlates to the drug having low molecular mobility, and is thus responsible for the physical stability of HPMCAS amorphous dispersions.

2. It is highly soluble in organic solvents, e.g. acetone, methanol; this allows applications for enteric coating and spray dried dispersions.

3. HPMCAS gets partially ionized and at pH above 5, the charge on the polymer minimises the formation of large polymer aggregates, allowing drug-polymer colloids (e.g amorphous nanostructures) to remain stable.

4. HPMCAS is amphiphilic in nature; hence it is a polymer of choice for solubility enhancement of poorly soluble drugs and stabiliser of re-crystallisation during dissolution from amorphous dispersion.

5. The amphiphillic nature of HPMCAS allows insoluble drug molecules to interact with a hydrophobic region, whereas hydrophilic regions allow these structures to be stable as colloids in aqueous solutions.

As reported in Table 2.4 HPMCAS is available with various degrees of substitution of acetate and succinate groups. The degree of substituents and the nature of substitution on the HPMCAS backbone decides its pH dependency and hydrophilic-lipophillic properties. The official monograph in national formulary (NF) reported that HPMCAS is a cellulosic polymer substituted on the hydroxyls : methoxy, with a mass content of 12-28 wt %; hydroxypropyl with a mass content of 4-23 wt %; acetate, with a mass content of 2-16 wt %; and succinate, with a mass content of 4-28 wt % The nature of these substitution gives unique properties to the polymer (Figure 2.13).
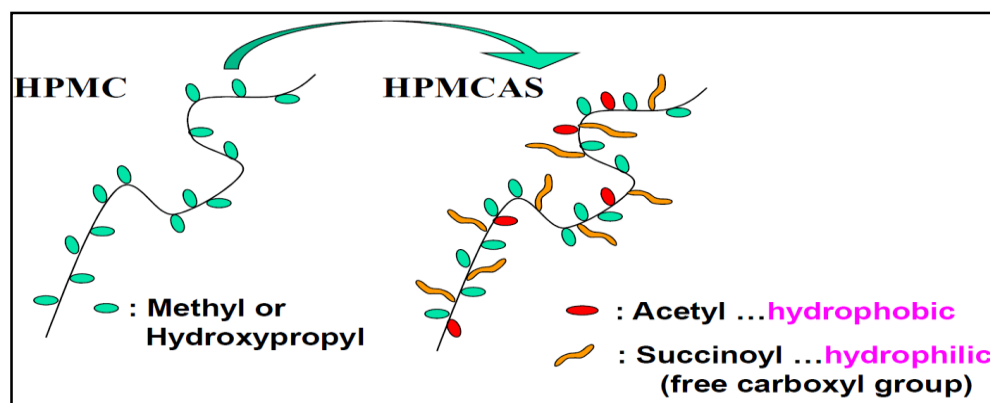
Figure 2.13: Schematic of nature of substituent and degree of substitution (adapted from ShinEstu AOQAT)

The succinate (hydrophilic) groups of HPMCAS have pKa of 5, Therefore, at pH below 4 less than 10% of polymer will be ionised and at least 50% of polymer will be ionised about pH value 5 or higher (Figure 2.14) The methoxy and acetate substituents are relatively hydrophobic and due to these HPMCAS is water-insoluble when un-ionised (about pH > 5) and remains predominantly colloidal at intestinal pH levels (6-7.5).
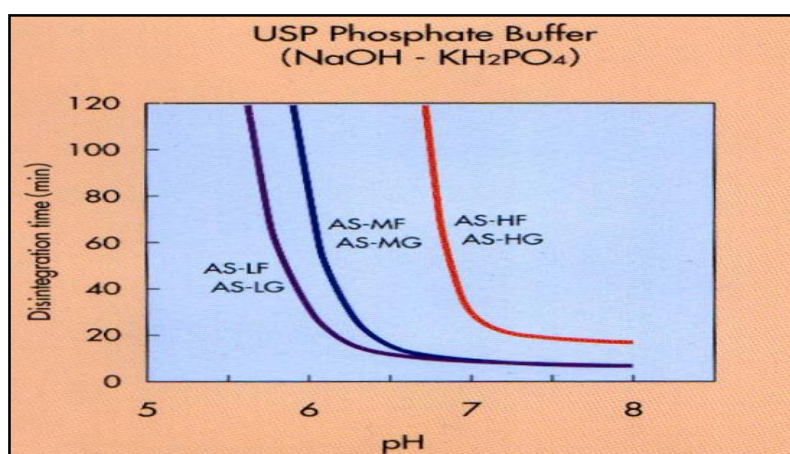
Figure 2.14: HPMCAS film solubility at various pH (adapted from ShinEstu AOQAT)

The substitutions also the affect Tg of the HPMCAS as reported by Friesen (Friesen et al., 2008). Under dry conditions Tg of HPMCAS is 120°C. The HPMCAS-LF grade shows a decrease in Tg due to the plasticisation effect of water compared to other grades owing to its higher substitution of succinic acid groups (hydrophilic groups) (Figure 2.15). However, relative water absorption was less even at 75% RH, only 6% water absorbed by the HPMCAS, HPMC absorbed 10% while PVP absorbed 23% of water. As a result the Tg of HPMCAS remained at 70°C even when equilibrated at high RH (75%). This observation indicates the excellent physical stability of HPMCAS based solid dispersions. HPMCAS has been used as a carrier or stabiliser for a number of Pfizer compounds of spray dried solid dispersions (Friesen et al., 2008). A floating and

sustained release dosage form composed of nicardipine hydrochloride and HPMCAS was prepared using a twin-screw extruder.
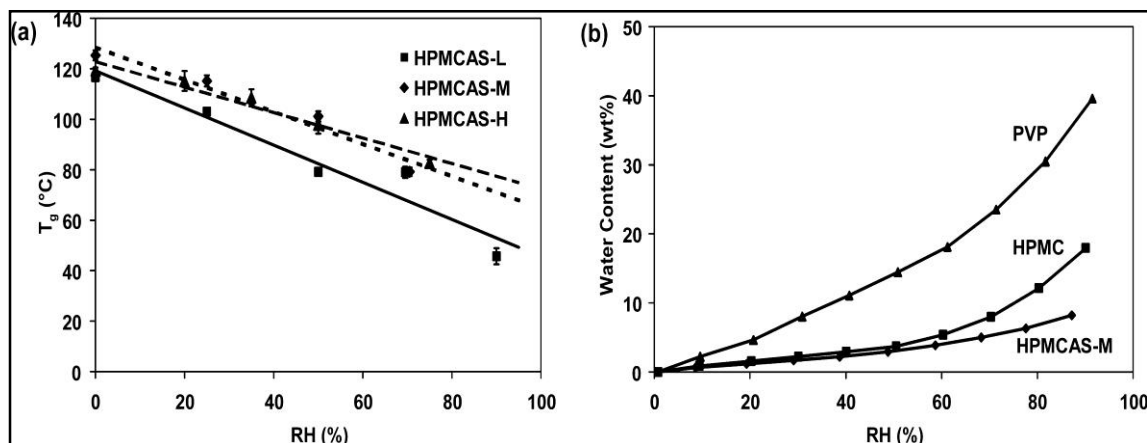
Figure 2.15: Effect of RH on polymer properties: (a) Tg versus the RH to which samples were equilibrated (at ambient temperature) for HPMCAS and (b) equilibrium water absorption versus RH for HPMCAS, PVP, and HPMC measured at 25 °C (adapted from Friesen et al; 2008)

2.5.3.2 Soluplus®

Soluplus® is a polyvinyl caprolactum-polyvinyl acetate-polyethylene glycol graft co-polymer. It has an amphiphilic chemical structure and is regarded as a polymeric stabiliser. It is an innovative excipient developed by BASF and was specifically designed to be used in HME to obtain solid solutions of poorly soluble drugs.
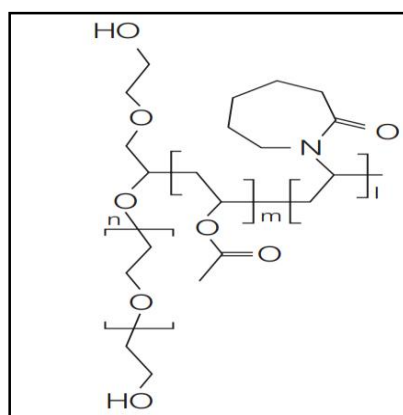
Figure 2.16: **Chemical structure of Soluplus®**

41

Table 2.5: Properties of Soluplus®

Chemical structure :	PEG6000/Vinylcaprolactam/vinylacetate (13/57/30)
Appearance:	White to yellowish free-flowing granules
Molecular weight :	118 000 g/mol
K value (1% ethanol) :	31- 41
Tg :	72 °C
CMC	7.6mg/L~7.6ppm
Solubility	acetone (up to 50%) methanol (up to 45%), ethanol (up to 25%) and Soluble in water.

Soluplus® at higher concentration forms colloidal polymer micelles in aqueous solution thus may result in a cloudy or turbid solution. This phenomenon is more pronounced at elevated temperatures above the lower critical solution temperature (LCST) hence heated above this temperatures Soluplus® forms large polymeric micelles and turns into a more turbid solution this process is reversible upon cooling the solution.

Soluplus® is a good solubiliser for poorly soluble drugs and the saturation solubility of various drugs has been studied in 10% polymer solution and phosphate buffer (Kolter et al., 2012)
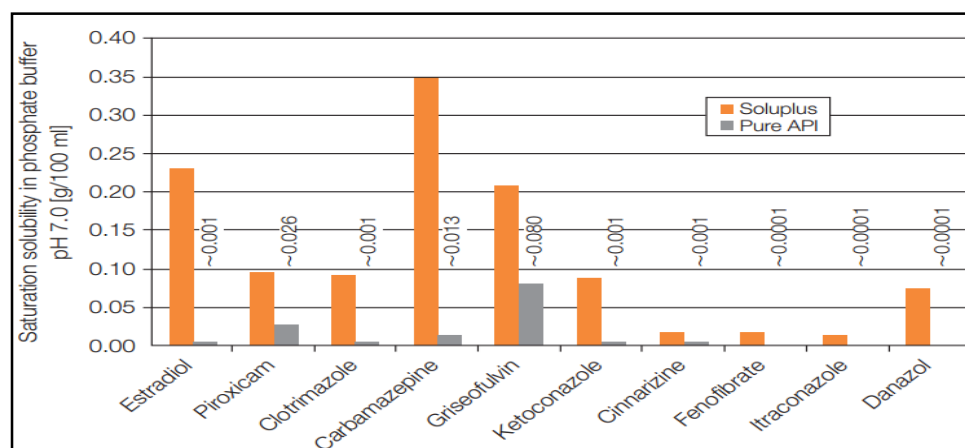
Figure 2.5: Saturated solubility of various drugs (Kolter et al., 2012)

The saturation solubility of drug in polymer solution is increased compared to the phosphate buffer which clearly shows solubilisation effects of Soluplus®. Soluplus® is used for solubility enhancement and for obtaining solid solutions with poorly soluble drugs. Soluplus® was used as a carrier for solubility enhancement of poorly soluble drugs (BCS II) such as fenofibrate, danazol, itraconzole. Both in-vivo and in-vitro testing showed higher solubility and high level of C_{max} and AUC with almost a 5 fold increase compared to the crystalline drug (Linn et al., 2012) .

2.5.3.3 Polyethylene oxide (PEO)

PEO is a white, water soluble, non-ionic polymer. The typical properties of PEO are mentioned in the Table 2.6.

Table 2.6: Typical properties of PEO

Appearance	Off-white powder
Crystalline melting point⁽ DSC), ⁰C	62-69
Odour	Slightly smells ammonic
Melt flow temperature, (⁰C)	>98
Volatiles content, as packaged, % by wt (at 105⁰C)	<1.0
Alkaline earth Metals, % by wt as CaO, max	1.0
Powder bulk density (kg/m³)	(304-593)
Polymer density, (kg/m³)	1.15-1.26
Moisture content, as Packaged, %	<1
Heat of Fusion, cal/gm	33
Solution pH	8-10

Properties and applications of PEO

1. PEO can be cross-linked to form hydrogels (Di Colo et al., 2001) and therefore exhibits water retention characteristics. It is a good film former and PEO films can be made by both melting and solvent casting methods.

2. Upon exposure to water or gastric juices, PEO hydrates and swells rapidly to form a hydrogel, hence it can be used to make a controlled release matrix system. Controlled release of drugs can be obtained by swelling and diffusion or swelling and erosion from PEO matrices (Kim, 1998)

3. PEO has mucosal bioadhesive properties and generally the higher molecular weight grades of PEO (4000000) have the highest levels of adhesion (Cappello et al., 2006).

4. PEO has good flow lubricity and compaction properties and hence is suitable for direct compaction (Dimitrov and Lambov, 1999). It is used as a carrier for solid dispersions of poorly soluble drugs using melt extrusion (Prodduturi et al., 2007).

2.5.4 Methods to achieve solid dispersions or solid solutions

In the early 1960s, when the concept of solid dispersions of poorly soluble drugs in the inert carrier was becoming popular, three principle methods were reported; melting/fusion, solvent and solvent-melting. The solvent method involved dissolving of physical mixtures of drugs and carriers in a common solvent followed by evaporation of the solvent to obtain a solid dispersion. In one example of the solvent-melting approach, the drug phase (spirnonolactone) could be dissolved in liquid solvent and then incorporating this solution into the polymer melt (Polyethylene glycol 6000). Some of the solid dispersion preparations are mentioned in Figure 2.17.
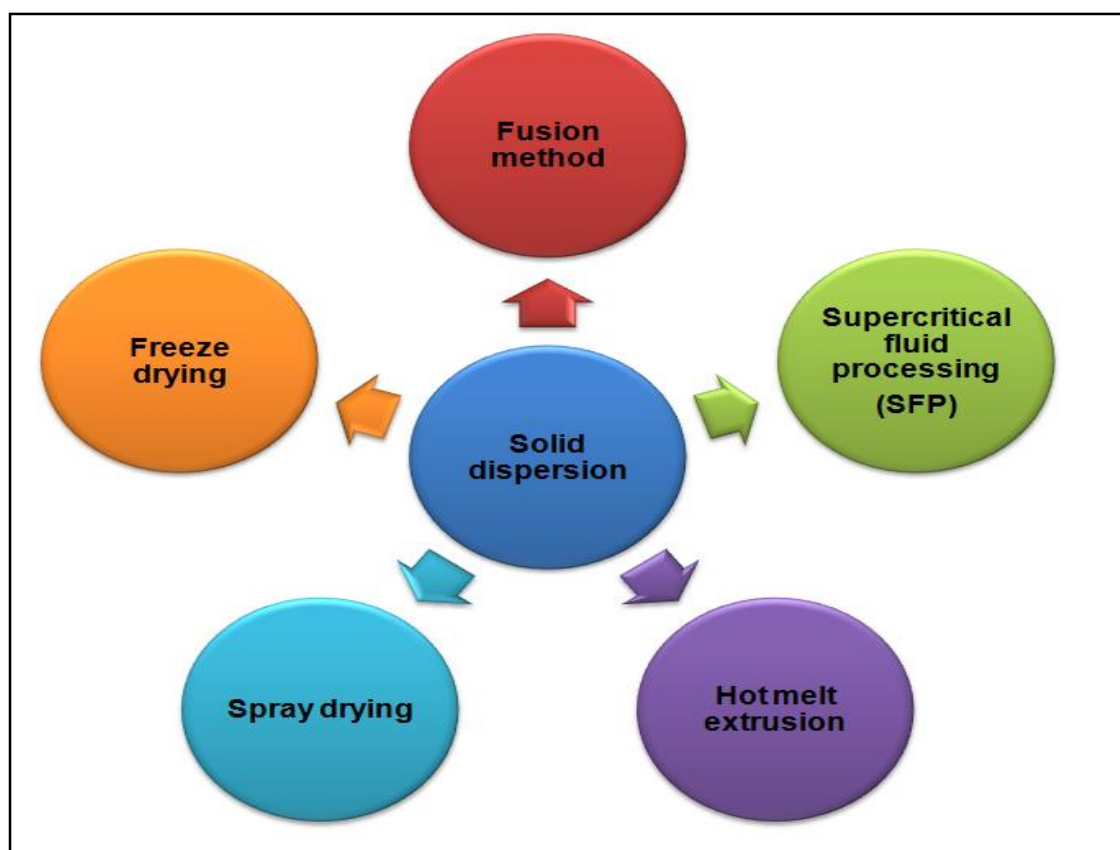
Figure 2.17: Methods to achieve solid dispersions

2.5.4.1 Solvent methods (solvent evaporation methods)

In the case of solvent evaporation methods the solid dispersion is prepared by evaporation of solvent from a solution containing a drug and carrier. This technique has solved problems associated with melting methods such as decomposition. However, the prerequisite of this method is that the carrier and drug should have sufficient solubility in the selected solvent or co-solvent. Usually carriers are hydrophilic in nature and drugs are hydrophobic in nature (Sahoo et al., 2011), hence the use of water as a solvent is limited. Organic solvents such as methanol, ethanol, ethyl acetate, acetone are used alone or used in a mixture with water. The complete removal of solvents upon evaporation is nearly impossible, hence the residual solvent in the products may cause instability, e.g.

water lowers the Tg and acts to plasticise the system leading to phase separation (Vo et al., 2013).

2.5.4.1.1 Spray drying

Spray drying is an efficient manufacturing technology for solid dispersions because it permits rapid removal of solvent and results in rapid transformation of the drug carrier solution to drug-carrier particles (Paudel et al., 2013). In this technique, the drug–carrier solution or suspension is pumped from the reservoir and atomised into fine droplets which give a higher surface area for evaporation and results in the formation of a solid dispersion within seconds. In a solid dispersion drug dispersed in an amorphous form leads in higher dissolution and solubility. Examples of available solid dispersion products prepared by spray drying are Incivek® and Intelence® (Weuts et al., 2011).

2.5.4.1.2 Freeze drying

This process consists of two main steps: freezing and lyophilisation. The drug–carrier solution is immersed in liquid nitrogen until it is fully frozen and the frozen solution is then lyophilized (van Drooge et al., 2004). The advantage of this method is the minimized risk of phase separation whereas a disadvantage is that most organic solvents posses the low freezing temperature and do not stay frozen during sublimation. Furthermore, the solvents should have a sufficiently high vapour pressure.

2.5.4.1.3 Supercritical fluid processing

In supercritical fluid processing, supercritical carbon dioxide (CO_2) is used as a solubilising agent for the drug and the carrier and sprayed through a nozzle into an expansion vessel with lower pressure. The rapid expansion leads to the

generation of small solid dispersion particles with desirable size distribution (Moneghini et al., 2001). The problem associated with supercritical fluids is scale-up and selectivity of the process.

2.5.4.2 Hot melt methods

Sekiguchi and Obi reported the hot melt approach for the first time using a drug carrier mixture. The example used was sulphathiazole (drug) and carrier (Urea). These were melted together at temperatures above the eutectic point and rapidly cooled in an ice bath. Cooling leads to supersaturation, but due to the solidification the drug becomes trapped in the carrier matrix. This process ensures a solid dispersion formation, whether it forms a molecular dispersion or not depends on the degree of supersaturation and rate of cooling. In other words, the process has an effect on the properties of the dispersion and product properties can be varied by changing processing history. Goldberg later discussed the advantages of solid solutions over eutectic mixtures in a series of the publications (Goldberg et al., 1965) (Goldberg et al., 1966)

The significant improvement in bioavailability was attributed to two factors, first the reduction in particle size to the molecular level and second, once the carrier is dissolved in the dissolution media and released the drug is molecularly dispersed in the dissolution media (Goldberg et al., 1966). Taylor and Zografi further provided an explanation for the improvement in dissolution rate that the drug has no crystal structure in the solid solution and therefore the energy required to break the crystalline structure of the drug before it can dissolve is not a limitation of the drug getting released from the solid solution (Taylor and Zografi, 1997). The high dissolution rate of solid solutions thus, maintains the supersatured solution for absorption however, supersaturated solutions have a

tendency to get crystallised or precipitate out as metastable polymorphs during dissolution. In some cases, carriers (polymers) used for solid solutions inhibit the precipitation of the drug from supersaturated solution (Simonelli et al., 1976) (Simonelli et al., 1976) (Hilton and Summers, 1986)

In the case of hot melt methods, the preparation method used for making the dispersion also has a significant effect on the nature of the dispersion. Several attempts were made to study the effect of melt processing parameters on the properties of dispersions. These include reports by Sekiguchi and Obi, Chiou and Riegelman where they accelerated the cooling rate by snap-cooling on a stainless-steel plate (Chiou and Riegelman, 1971). Kanig introduced different variations of spraying hot melt onto a cold surface (Kanig, 1964). Recent approaches include the use of HME and a number of groups have published enhancement of poor solubility of drugs by HME. A further approach was used to prepare solid solution drugs by injection moulding demonstrated by Wacker in 1991 (Wacker et al., 1991).

2.6 Hot melt extrusion

HME is the process of pushing a polymer/substance by the action of a rotating screw at elevated temperature through a die to form a product. The schematic of the extrusion process is shown in the Figure 2.18. In the extrusion process, the molten polymer phase can function as a thermal binder and act as a matrix former, solubiliser or drug release retardant upon cooling and solidification (Repka et al., 2007). Therefore, solvents and binders are not necessary which can reduce the number of unit operations, processing steps and time consuming post- processing drying steps.
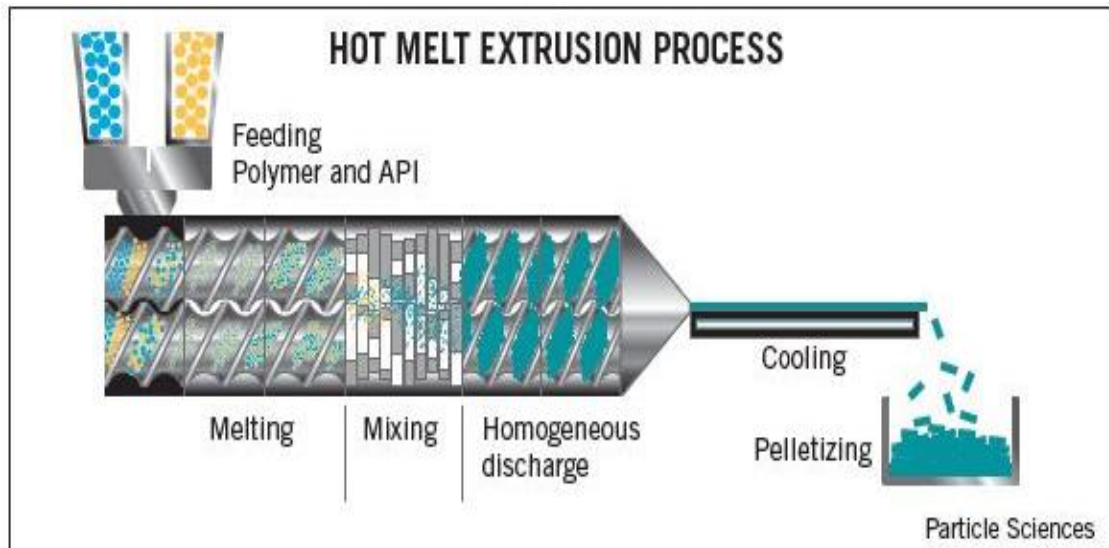
Figure 2.18: Schematic diagram of hot melt extrusion (Adapted from particle science Inc.)

A uniform particulate dispersion within the molten polymer can be achieved by intense mixing and agitation imposed by the action of the rotation of screws causing de-aggregation of suspended particles.

2.6.1 Type of extruders

Pharmaceutical extruders (Figure 2.19) are much evolved and adapted to mix actives with carriers as well as for wet granulation. The pharmaceutical class extruder has to meet regulatory requirements and differ from plastics extruder in term of contact parts. The contact part must not be reactive, adsorptive with pharmaceutical product and also they must meet their design as per regulatory guidelines for cleaning and validation. Pharmaceutical extrudes are typically made of surgical grade stainless steel.

Figure 2.19: Thermo Scientific Pharmalab HME 16

The extrusion process can be categorised either as ram extrusion or screw extrusion. Ram extrusion is based on the principle of positive displacement by high pressure to push softened or molten material through a die to produce uniform extrudate. Screw extruders are based on the conveying mechanism of rotating screws that carries material forward through a die and forms intended shape. Screw extruders consist of a minimum of three distinct parts; a conveying system for transport of the material and intense mixing, a die to form shapes, and auxiliary equipment such as cooler, pelletiser, calendaring rollers, for finished product. Twin screw extruders are most accepted for the processing of pharmaceutical products and have several advantages over single screw extruders such as easier material feeding, high kneading and dispersing capacities (Figure 2.20). Extruder and screw design have a significant effect on shear and residence time (Repka et al., 2007) (Crowley et al., 2007).
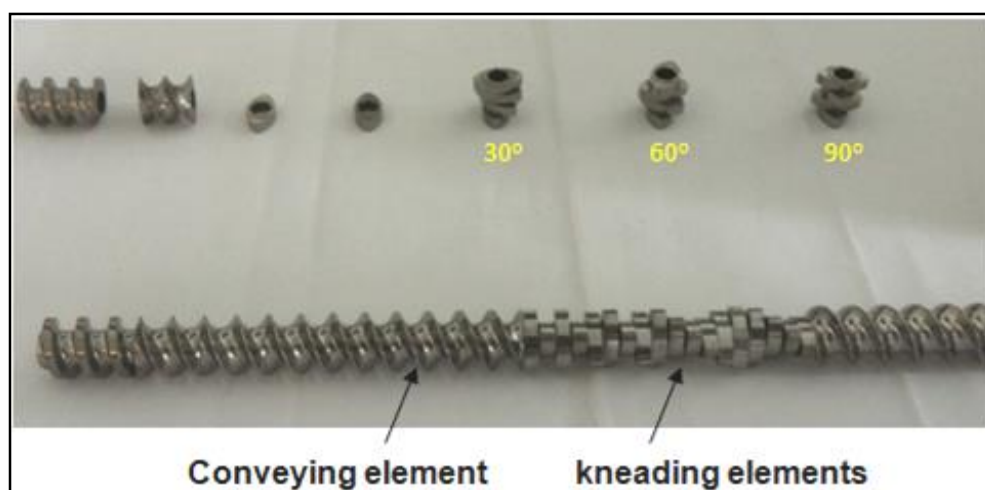
Figure 2.20: HME screws and kneading elements

2.6.2 Applications of HME for solid dispersions and drug delivery

As explained earlier, there is a significant effect of particle size on the rate of dissolution of the drug. HME is one of the main process used to disperse the drugs in polymer matrices aiming to obtain a molecular level dispersion (Breitenbach, 2002) (Forster et al., 2001a; Kinoshita et al., 2002)

In general, the more the particle size is reduced the lower will be the thermodynamic stability. Energy is required when a drug is to leave its crystalline state. Transforming the drug into an amorphous state means bringing it into a higher energy state; in order to achieve this crystal lattice energy must be overcome. The crystalline state of a substance is the only thermodynamically favoured energy state. When a drug is transformed into an amorphous state both the physical and chemical stability is often limited, therefore, amorphous drug molecules often tend to re-crystallise to achieve a thermodynamically stable configuration. To address this issue the formulation to an amorphous solid dispersion is a common approach to stabilise if the "freezing effect" is sufficient due to a high Tg of the system or better by interactions, such as hydrogen

51

bonding between the dispersed drug and the carrier (often polymeric or amorphous) (Breitenbach, 2002).
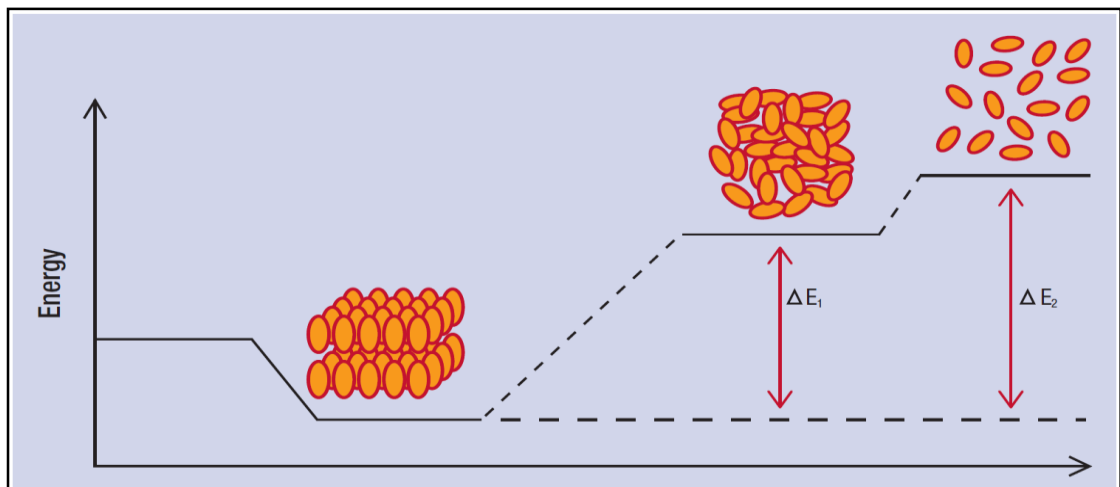
Figure 2.21 Stability of crystalline state (Kolter et al., 2012)

The question of how does the HME process help to generate an amorphous solid dispersion can be explained by referring to Figure 2.21. The crystal lattice energy of the drug has to be overcome to transform it into an amorphous state (Hancock and Parks, 2000). In addition to this, the drug and polymer need to be blended and co-dispersed subsequently. The extruder achieves both these functions by applying shear stress to both drug and polymer. Under temperature and energy provided by friction due to shear stress overcomes the crystal lattice energy and softens the polymer. The rotating screws and different kneading elements make conditions suitable for dispersion and with the right choice of process parameters and drug-polymer combination a solid solution can be obtained. Melt extrusion may be applied to disperse a drug in a polymer matrix down to the molecular level, therefore it is a technology that gives broad perspective to the amorphous glass or solid solution approach as a delivery system.
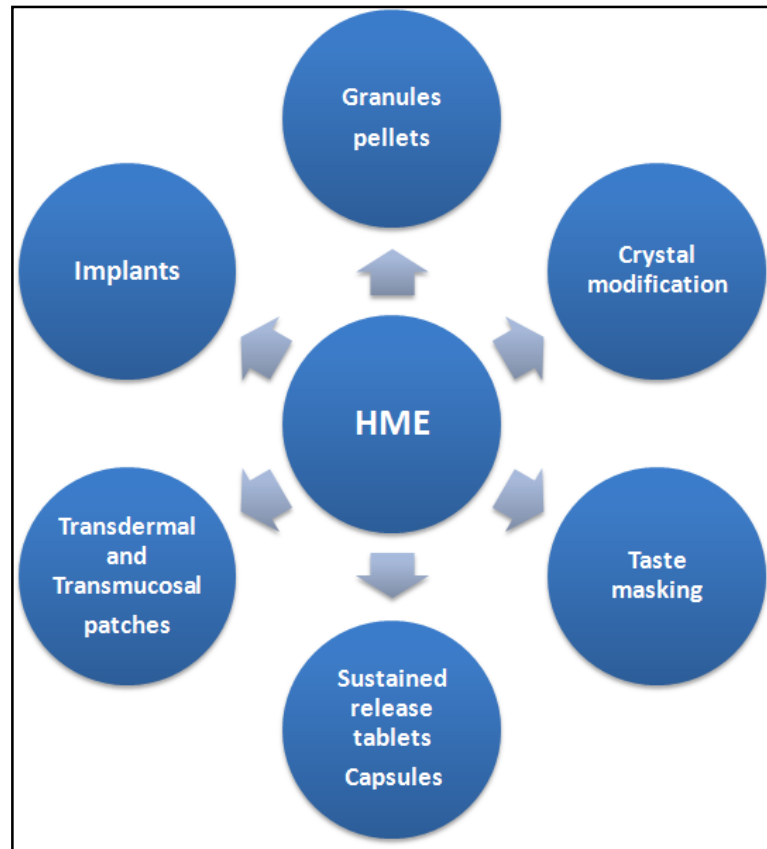
Figure 2.22: Pharmaceutical applications of HME

The range of pharmaceutical products made using HME are mentioned in Figure 2.22 and details of the application have been provided in an excellent review by Repka (Repka et al., 2007), A number of products made using HME are listed in Table 2.7.

Table 2.7: Currently marketed and developed drug products produced utilizing hot melt extrusion technology (adapted from (Shah et al., 2013)

Product name	Indication	HME purpose	Company
Lacrisert® (Opthalmic Insert)	Dry eye syndrome	Shaped system	Merck
Zoladex™ (Goserelin Acetate Injectable Implant)	Prostate cancer	Shaped system	AstraZeneca
Implanon® (Etonogestrel Implant)	Contraceptive	Shaped system	Organon
Gris-PEG (Griseofulvin)	Anti-fungal	Crystalline dispersion	Pedinol Pharmacal Inc.
NuvaRing® (Etonogestrel, Ethinyl Estradiol depot system)	Contraceptive	Shaped system	Merck
Norvir® (Ritonavir)	Anti-viral (HIV)	Amorphous dispersion	Abbott Laboratories
Kaletra® (Ritonavir/Lopinavir)	Anti-viral (HIV)	Amorphous dispersion	Abbott Laboratories
Eucreas® (Vildagliptin/Metformin HCl)	Diabetes	Melt granulation	Novartis
Zithromax® (Azythromycin enteric-coated multiparticulates)	Anti-biotic	Melt congeal	Pfizer
Orzurdex® (Dexamethasone Implantable Device)	Macular edema	Shaped system	Allergan
Fenoglide™ (Fenofibrate)	Dyslipidemia	MeltDose® (solid dispersion)	Life Cycle Pharma
Anacetrapib (Under Development)	Atherosclerosis	Amorphous dispersion	Merck
Posaconazole (Under Development)	Antifungal	Amorphous dispersion	Merck

2.6.3 Examples of NDDS by HME

2.6.3.1 Contraceptive Intravaginal rings

A contraceptive vaginal ring containing ethinyl estradiol and etonorgestrel has been prepared by melt extrusion (Figure 2.23). Coaxial fibres containing various concentrations of steroids in the polymer (polyethylene vinylacetate copolymers) were prepared and the drug release measurements were carried out (van Laarhoven et al., 2002). The process involves blending of steroid and a polymer mixture in twin screw extrusion and the steroid was completely dissolved in molten polymer. After cooling, cooled strands were obtained and converted into fine pellets (core). For the preparation of coaxial fibres a co-extrusion process was used where the membrane polymer and core polymer were passed through a spinneret to form coaxial fibres.

Figure 2.23 : Nuvaring: contracetive vaginal ring (adapted from Merck products)

2.6.3.2 Floating and sustained release dosage forms

A floating sustained release dosage form composed of nicardipine hydrochloride and hydroxypropylmethylcellulose acetate succinate (HPMCAS) was prepared using a twin-screw extruder (Nakamichi et al., 2001). By

adjustment of high pressure screw elements in the immediate vicinity of the die outlet and by controlling the barrel temperature, a porous or puffed dosage form was obtained. This was very successfully used as a floating dosage form containing enteric coating polymer used for longer retention in the stomach. A sustained release formulation of isosorbide nitrates in combination with polyvinyl acetate has processed using HME. In vitro release of isosorbide nitrates with polyvinylacetate showed that even at low polymer concentration the sustaining effect of the polymer was sufficient to delay the release.

2.6.4 Advantages and limitation of HME

There are a number of advantages and limitations of HME and some of those are mentioned in this section.

2.6.4.1 Advantages

Continuous and solvent free process: HME is a single unit operation, and continuous process so it avoids problems with batch processes associated with conventional pharmaceutical processing therefore avoiding batch to batch variability, wastage and time. Moreover, processing without organic solvents makes HME a green and solvent free process.

High yield and scalable: HME has a high yield capacity and is readily scalable from small scale to the manufacturing scale.

Versatile and PAT enabled: HME is capable for the development of a variety of dosage forms for wide applications. Extrusion also facilitates process analytical tools (PAT) for in-line monitoring of process for quality testing as emphasised by FDA (FDA guideline 2004). Extrusion barrel can be equipped with processing monitoring tools such as NIR (Kelly et al., 2012), Raman (De Beer et al., 2011) to characterise properties of the product during and after HME.

56

2.6.4.2 Limitations

High temperature and shear can be a major drawback of the HME process. To date, the relatively limited number of FDA approved polymers available for pharmaceutical applications and very few of those polymers are suitable for melt processing. High processing temperatures, suitable rheology, degradation are among the top material related challenges associated with HME. However, these issues can be addressed by engineering and formulation approaches. The use of plasticisers can lower processing temperatures and soften polymers by lowering the Tg. The process variables such as shear, screw speed, feed rate and residence time can reduce degradation by affecting the mixing intensity.

2.7 Injection moulding

Injection moulding is the most commonly used manufacturing process for the fabrication of intricate plastic parts with excellent dimensional accuracy. A large number of items associated with our daily life are produced by injection moulding. Typical product categories include housewares, toys, automotive parts, furniture, rigid packaging items, appliances and medical devices. The injection moulding process requires the use of an injection unit, raw plastic material and a mould. It is a process of forming an article by forcing molten polymer under pressure into a mould where it is cooled, solidified and subsequently released by opening the two halves of the mould.

Injection moulding is widely applied in the plastic processing industry but is a relatively new technique to the pharmaceutical industry. Therefore the introduction of the injection moulding process to FDA approved pharmaceutical polymers and biodegradable materials are of great interest. Recently, researchers have begun to explore the application of injection moulding to matrix-releasing tablets, capsules of pharmaceutical polymers and rods of biodegradable materials.

2.7.1 Key parameters of the injection moulding process

The injection moulding process is generally influenced by the following parameters:

- ➢ Polymer type (semi-crystalline or amorphous)
- ➢ Physical properties of the polymer in its molten and solid form
- ➢ Screw design
- ➢ Mould and runner design

➢ Set injection moulding conditions

The polymer type and their physical properties significantly influence processing by the injection moulding process. In injection moulding it is very important to achieve a suitable polymer melt viscosity to flow and mould. Generally, thermoplastic semi-crystalline polymers are melted above their melting temperature and the desired melt viscosity can be achieved by set temperature. However, amorphous polymers do not melt and soften on heating hence, those often requires processing with plasticiser and additives. Typically, injection moulding machines are designed with a single screw and the function of the screw is to guide material along the barrel, melt it and inject into mould cavity. Sometimes the single screw of injection moulding machine limits its application, particularly when materials are in powder form or mixing of components is required. Design of the mould and injection moulding conditions decide the properties of moulded part as well as the total time required for the injection moulding cycle.

2.7.2 Injection moulding process

Injection moulding of polymers is a high speed technique to produce quality parts with great accuracy in large numbers. During processing, the polymer is melted by the action of a rotating screw and injected in molten form under pressure into a mould. The result is that the mould cavity is exactly copied by the molten polymer, neglecting shrinkage. Sufficient pressure is applied to maintain packing during cooling and solidification. After cooling, the mould opens and the part is ejected. The injection moulding process is then repeated. Schematic of an injection moulding machine is provided in the Figure 2.24.
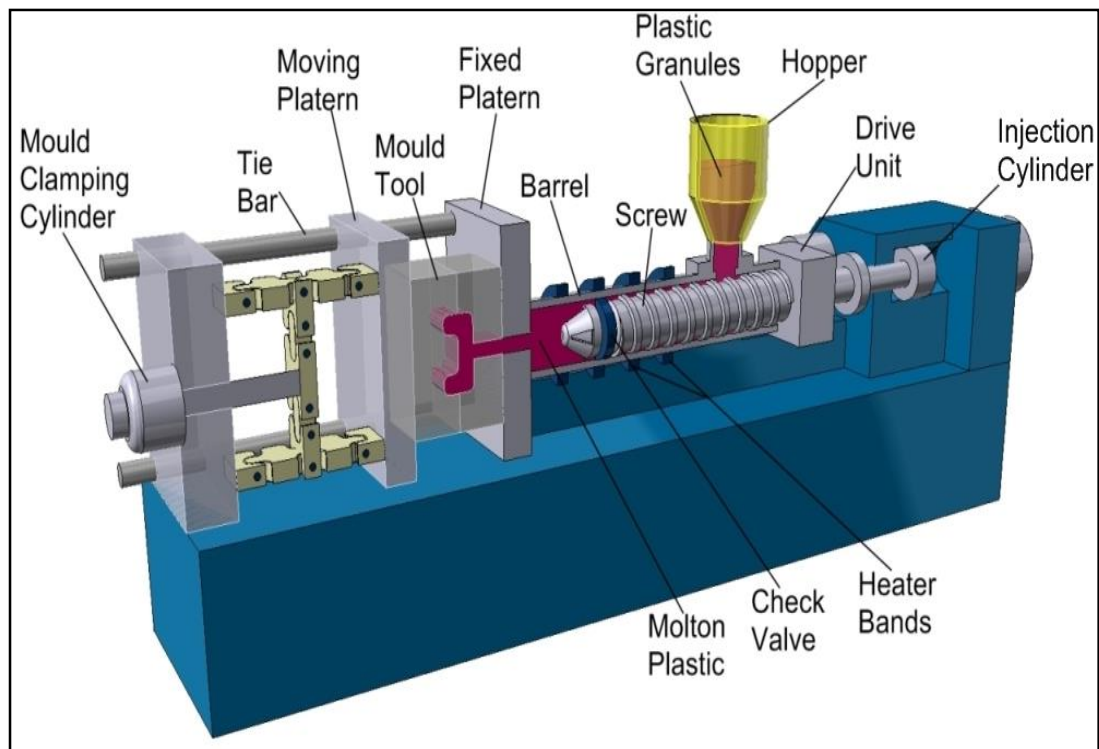
Figure 2.24: **Schematic of an injection moulding machine (adapted from Rutland plastics)**

2.7.3 Steps of the injection moulding process

The typical injection moulding process comprises six steps and can be tailored to specific material and product specifications. The moulding process consists of the following stages:

2.7.3.1 Clamping

Clamping unit is what holds the mould under pressure during the injection and cooling (Figure 2.25). Basically, it holds the two halves of the mould which are called fixed and moving platen. The closing of two halves of mould ensures the formation of mould cavity. Injection moulding machine can be categorised based on the amount of clamping force that the machine can exert and this force keeps the mould closed during injection process. The typical clamping force can vary from 5 tonnes to over 9000 tonnes.
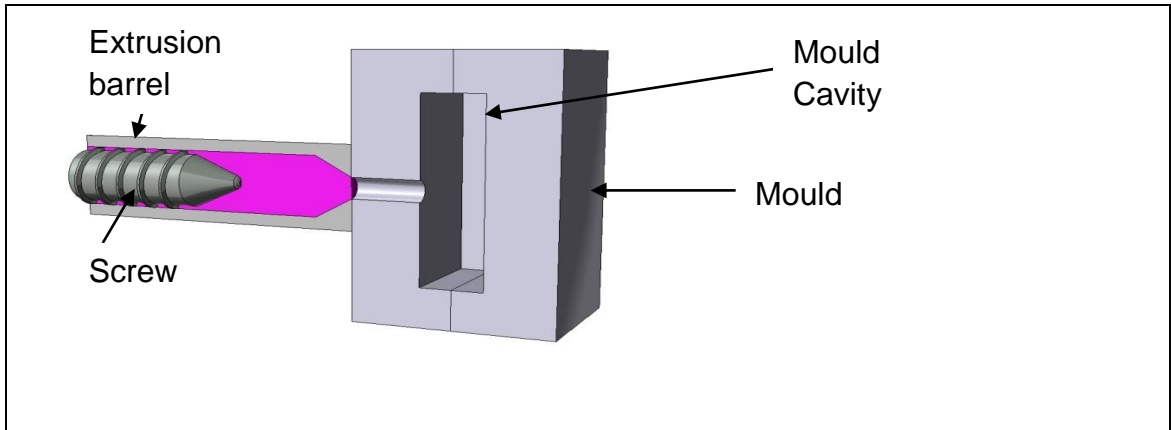
Figure 2.25: **Closing of mould; screw guided back with pressure and ready to inject molten polymer (adapted from Rutland plastics)**

2.7.3.2 Injection

During injection phase, the pellets feed into the barrel where they are heated until they reach molten form. The single screw within the extrusion barrel guide the material forward and force to the end of the barrel. Once the enough material has accumulated in front of the screw, the injection process begins. The screw pushes the molten polymer at a certain speed in to the mould cavity through a runner system. The injection pressure and speed are controlled by the action of the screw (Figure 2.26).
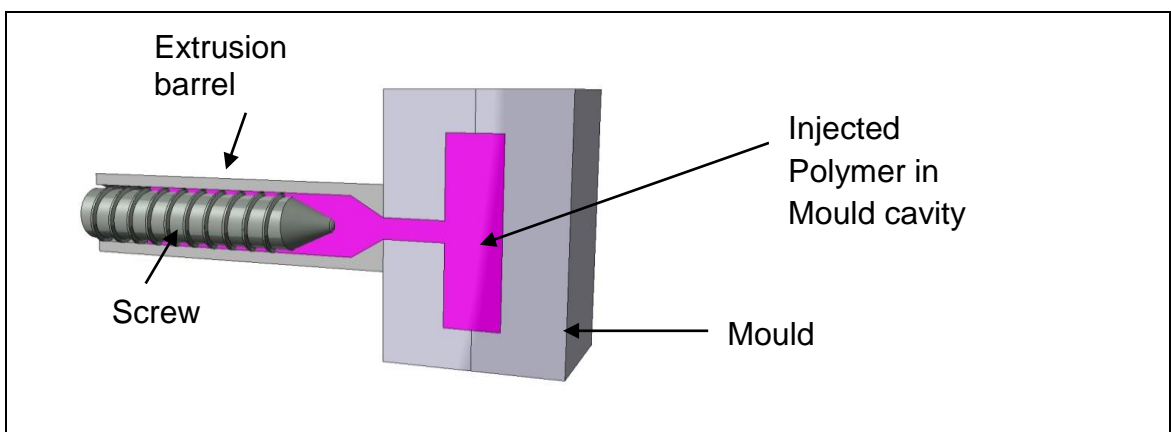
Figure 2.26: Injection of molten polymer (adapted from Rutland plastics)

2.7.3.3 Packing

After the molten polymer has been injected into the mould, pressure is applied to ensure all cavities are filled. The holding pressure applied at this stage can influence the properties of the moulded part such as densification and shrinkage.

2.7.3.4 Cooling and plasticisation

The parts are then allowed to solidify in the mould. Meanwhile, the screw is rotated and forced backwards as it prepares the next shot of molten polymer. Two processes happen simultaneously at this stage, i.e. part cooling and plasticisation. The mold temperature usually set at the required temperature, which influences the cooling rate of the part. The properties of the moulded product could be greatly influenced by the rate of cooling. The rapid cooling provides the "quenching effect" which likely to induce amorphous content in the moulded products. Plasticisation ensures the melting and preparation of shot volume for the next IM cycle.

2.7.3.5 Opening

The moving platen moves away from the fixed platen separating the mould tool.

2.7.3.6 Ejection

Sliding pins aid ejection of the completed moulding from the injection mould tool (Figure 2.27).
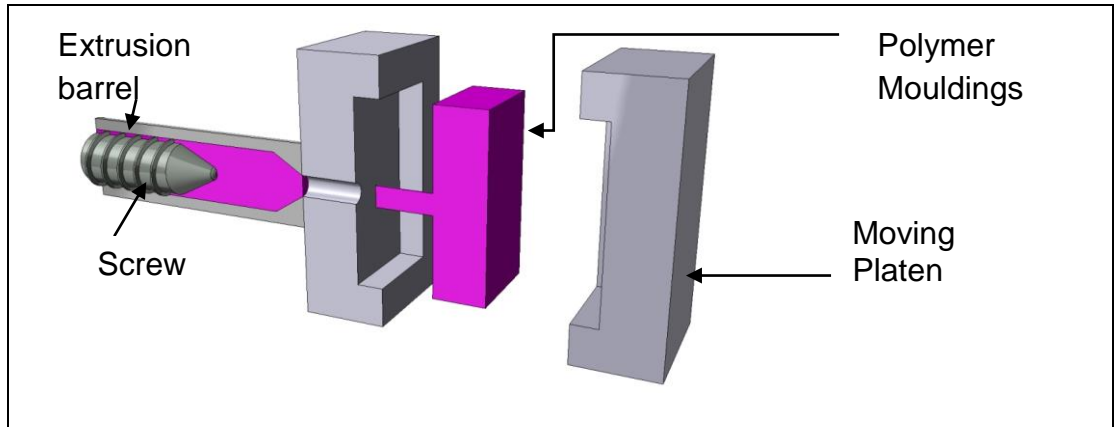
Figure 2.27: Final step: Opening and ejection of the moulded part (adapted from Rutland plastics)

The length of time from closing the mould to ejecting the finished plastic moulding is one injection moulding cycle, known as the cycle time (Figure 2.28 and Figure 2.29)
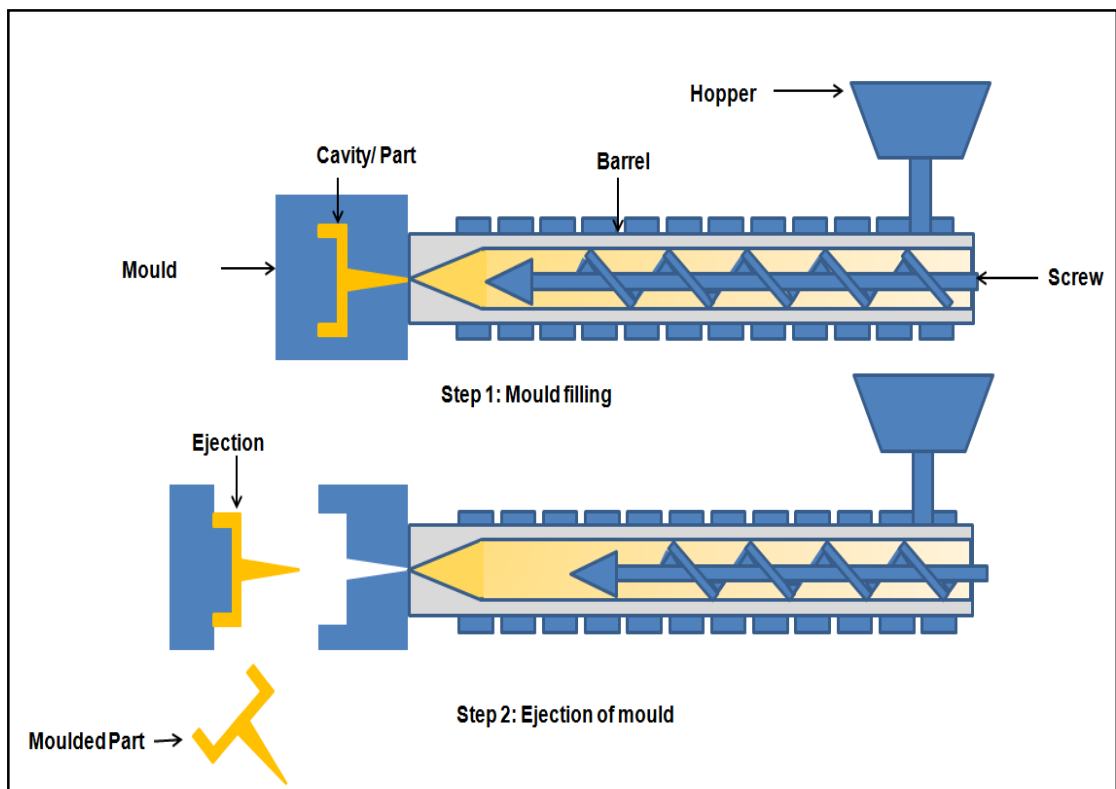
Figure 2.28: Schematic of the injection moulding process
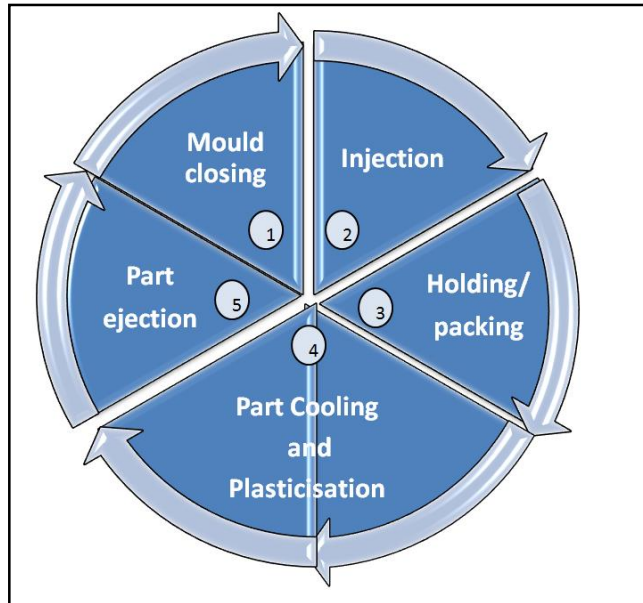
Figure 2.29: Injection moulding cycle

2.7.4 Injection moulding process variables

High quality injection moulding requires control and monitoring of four main parameters**:**

I   Shot volume: Determines the amount of polymer to be injected.

II   Pressures: Packing pressure, clamping pressure and extrusion back pressure during plasticisation.

III   Temperatures: Set temperature of the barrel, nozzle, runners and mould cavity.

IV   Speeds: Injection speed determines the rate at which the polymer is injected into the cavity.

2.7.4.1 Pressures

In injection moulding the material experiences high pressure and this pressure history during processing affects material properties such as shrinkage, residual stresses and density at the end of the process. ((Bayer et al., 1984). The

injection and clamping pressures effect material densification or specific volume (Carrasco et al., 2010). Inappropriate selection of shot size and/or injection speed can result in incomplete mould filling, sinking or flashing (i.e. excess material).

2.7.4.2 Temperatures

Polymer viscosity is dependent on temperature. In injection moulding, melt temperature is kept above the materials melt temperature for semi-crystalline polymers. Barrel temperature is profiled to optimise solids conveying and melting of the polymer. Excessive exposure to high operating temperatures may result in material degradation, surface imperfection, burned parts etc. The mould cavity is generally cooled to promote solidification, allowing the part to be ejected. Mechanical properties of the part are heavily dependent upon the cooling rate particularly for semi-crystalline polymers.

2.7.4.3 Speeds

Injection moulding is a high speed process and the amount of time a material experiences thermal, shear or deformation forces depends on the speed of the process. Injection speed affects the shear strain rates experienced by the molten polymer and also governs the time required to fill the mould cavity.

2.7.5 Advantages of injection moulding

There are number of advantages of injection mouding process and some the advantages are mentioned below

1. The ability to produce components with excellent dimensional accuracy. It is a single unit operation with minimal post production work required.

2. Full automation can be achieved with a high throughput; the process is well suited to the manufacture of pharmaceutical dosage forms such as tablets and capsules, in addition to more complex designs.

3. Modification of material properties is possible through control of injection moulding conditions such as pack pressure and mould temperature; these influence polymer densification and crystallisation and can potentially be used to alter pharmaceutical performance.

4. IM is an emerging technology for the development of pharmaceutical fast and controlled release dosage forms in a single step and there is a strong potential to develop intellectual property (IP).

2.7.6 Challenges related to injection moulding process with respect to pharma formulations

2.7.6.1 Material properties

Polymers exhibit different properties such as rheology and degree of crystallinity, hence they show different behaviour during injection moulding. Commonly used polymers for injection moulding are thermoplastic and almost 90% of injection moulded products are made up of these polymers. Both amorphous (e.g polyurethane, poly vinyl chloride) and semi-crystalline (e.g nylon, polyethylene, poly L-lactic acid) polymers differ from each other in terms of their behaviour in the injection moulding process and the finished product characteristics (Table 2.8).

Table 2.8: **Amorphous vs semi-crystalline thermoplastic polymers**.
(Adapted from **(Zema et al., 2012)**

	Amorphous	**Semi-crystalline**
Injection moulding behaviour	soften on heating	melt on heating
	poor lubricity	good lubricity
Injection moulding product characteristics	limited and isotropic shrinkage	marked and anisotropic shrinkage
	high impact strength	low impact strength
	transparent	opaque

The polymer and other process additives for the injection moulding can be chosen on the basis of it's equipment, time, and cost of the process as well as considering the desired properties required in the final product to suit the intended application. Whenever it's demand to improve product properties, it may involve the use of extra components, critical and expensive processes. Hence, to balance the product quality with consideration of formulation and processing aspect different polymer additives for injection moulding are employed by the plastic industries:

1) Fillers (e.g talc, mica starch) are used to decrease the thermoplastic percentage, thus reduces cost.

2) Reinforcements (e.g graphite, glass fibre, clays), these are added generally in 10-40% by weight in the formulation to give mechanical strength and stiffness to the final product.

3) Colourants e.g diazos, iron oxides, carbon black.

4) Plasticiser (e.g citrate ester for PLA, dioctyl phthalate for PVC) reduces the glass transition temperature of the polymers and hence improves the processibility and the flexibility of the moulded product.

5) A substance which limits shrinkage and warpage of moulded part e.g carbon fibres, or substances which gives electrical conductivity e.g nickels.

Application of the injection moulding technique for pharmaceutical dosage form development however is very challenging as drug products are limited by strict qualitative and quantitative criteria, regulatory guidelines which basically ensure the quality, safety, and efficacy of the drug products. Moreover, in the case of pharmaceutical actives; dose, physico-chemical properties and stability are the main limitations which cannot be modified. Therefore, degradation of actives at processing temperatures as well as overall product properties during stability or storage needs to be considered.

The selected polymer for the injection moulding process should posses the following properties:

- Suitable melt rheology
- Thermal stability
- Stable behaviour upon mould cooling
- Lubricity
- Provide the desired drug release pattern

The application of the moulding process for development of pharmaceutical dosage forms is still limited, and generally been restricted to simple formulations. With reference to the previous classification, various categories of aids have also been used for the development of the moulded pharmaceutical formulations.

1) Reinforcements (e.g microcrystalline cellulose, hydroxylapatite)

2) Plasticisers are used to lower glass transition temperatures of polymers and thus allow process to carry out at lower temperatures; this effect gives a

freedom to operate an injection moulding process within the stable thermal profile of drug and/or excipients thus ensuring stability. (e.g dibutyl sebacate, DBS; glycerol, polyethylene glycol, PEG400)

3) Modifiers i.e substances that may be added to trigger or retard drug release performance (e.g disintegrants, polymeric carriers)

2.7.6.2 Screw design

Injection moulding machines are designed with a single screw. Hence, the material in the powder form cannot be fed or conveyed into screw barrel. It also limits application where high shear mixing or complex mixture of APIs and/or excipients is required. Therefore, high shear mixing and pelletisation using a twin-screw extruder is generally required prior to IM.

2.7.6.3 Shrinkage, densification:

Some polymers tend to shrink upon exposure to high temperatures and high pressures during moulding. Densification or decrease in the specific volume sometime can make the polymer matrix very rigid and less soluble. However, this can be minimised by changing processing conditions or addition of modifiers.

Shrinkage is a phenomenon associated with injection moulded products. The change of dimension of injection moulded products with respect to those of the cavity. The difference in the dimensions of mould cavity and of the moulded specimens may vary according to mould design and operation of moulding process (ASTM D955). ASTM D 955 - 08 (2014). Guidelines on "Standard Test Method of Measuring Shrinkage from Mold Dimensions of Thermoplastics" are intended to measure shrinkage from the mould cavity to moulded dimension of thermoplastic when parts will be made by compression or injection processes

with specified process conditions. This change in dimension mainly depends on the material properties, processing variables, mould and part design. In general, three types of shrinkage phenomenon are reported; first, in-mould shrinkage (shrinkage during processing), as-mould (skrinkage just after mould opening commonly referred as 'mould shrinkage') and post-shrinkage (time effects during storage, recrystallisation etc.) (Jansen et al., 1998). All materials have a specific *shrinkage* and the values are assigned to them by the material manufacturer. The shrinkage is nothing but a value can be used to predict how much difference there will be between the plastic product when it is first moulded and the plastic product after it has cooled (Bryce, 1996).

When heated, every material expands and when cooled, it shrinks. Plastics are no exception (Bryce, 1996). However, each material has distinct value for how much it will shrink when its cooled after heating. This value typically referred as shrinkage rate is listed as an inch / inch or meter/meter. ASTM D-955 (ISO 294-4) provides test guidelines for characterisation of shrinkage in both parallel to and across the direction of flow.

2.7.6.4 Factors and process variables affecting shrinkage:

Extensive research has been done into the as-mould shrinkage of injection moulded parts and experimental studies have reported that shrinkage is affected by processing parameters as well as mould geometry (Jansen et al., 1998; Rosato et al., 2000) (Isayev and Hariharan, 1985; Tjong et al., 1996). The studies reported that holding pressure has the most influential effect on shrinkage; higher holding pressures decreased mould shrinkage in all directions. The second most influential parameter was the injection temperature, where shrinkage was thought

to be reduced due to better pressure transmission. However, if the temperature of melt increased further the gate took a long time to freeze off and if this time exceeds the holding time of mouldings then shrinkage increases.

The process variable and factors affecting actual shrinkage are:

1. Size and shape of the part

2. Design and size and length of runners, machine nozzle and gates

3. Part wall thickness

4. Cooling channels and moulding cooling parameter i.e temperature and time

5. Flow pattern within the mould

6. Holding or packing pressure and time

Minimum shrinkage will occur when the maximum amount of material will be forced into the mould cavity for the longest possible time as a result of adequately sized flow channels, and when adequately high hold pressure is maintained until the plastic is thoroughly hardened. When low hold pressures are applied for a relatively short time, inadequate amount plastic is forced into the mould leading to high shrinkage. The viscosity of the molten plastic is also an important property to consider when setting the melt temperature, however high viscosity of materials sometime cause difficulty in maintaining adequate mould pressures.

2.7.7 Applications of injection moulding in drug delivery

Although injection moulding was introduced by Speiser in 1964 as a pharmaceutical technology to produce sustained-release dosage forms, its use within the pharmaceutical industry has been limited to a few applications. The major focus was given to the development of existing products with this

71

technology and aimed to reduce cost and time of manufacture. Later studies published on injection moulding have discussed more innovative applications, and unique designs as well as composition and functional characteristics of product. Table 2.9 lists a compilation of the work reported on injection moulding for pharmaceutical applications.

Preliminary evaluation of injection moulded tablets was reported using polyethylene glycol (PEG) as a carrier and microcrystalline cellulose (MCC) as a reinforcement for immediate release application (Cuff and Raouf, 1998). The authors reported significant benefits such as dust containment (friability) and content uniformity even with low dose drug (<1%). Moreover, the authors reported that this technique could be used in the development of non-disintegrating and prolonged release dosage forms by obtaining solid amorphous or solid molecular dispersions of actives in polymer matrices. Different geometries of dosage forms have also been developed using injection moulding. For example subcutaneous implants (Rothen-Weinhold et al., 1999) and intra-vaginal inserts (Rathbone et al., 2002)

2.7.8 Novel Drug Delivery Systems (NDDS)

2.7.8.1 Eaglet® Technology

This is a novel, patented technology for production of controlled release dosage forms using an injection moulding technology. In this case, a hydrophilic/erodible matrix containing the active substance is coated with an impermeable polymeric layer. The delivery device structure is designed to have a lateral opening on both sides for the liberation of the drug and release can be driven by diffusion or erosion based mechanisms (Figure 2.30). Zero-order

release rates can be controlled by restricting the area in contact with biological fluids. In particular the Egalet® ADPREM (Abuse Deterrent Prolonged Release Erodible Matrix) has developed the technology for administration of opiods (morphine and hydrocodone) to patients undergoing pain management therapy hence, reducing the need for frequent dosing and risk of abuse. (Hemmingsen et al., 2011)
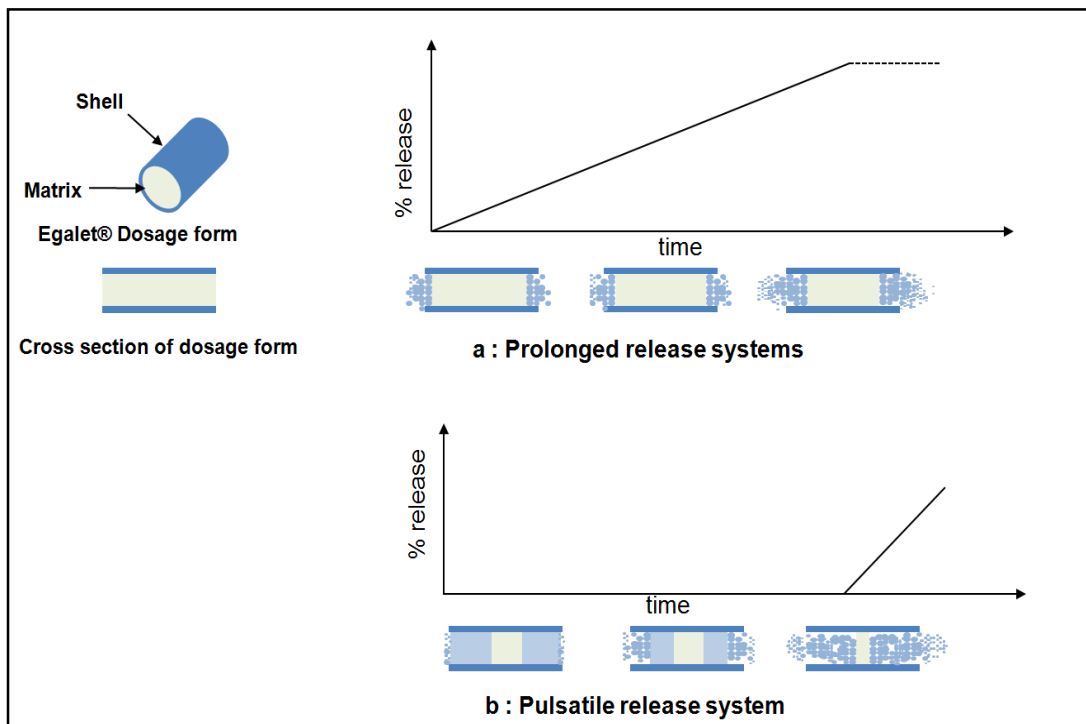
Figure 2.30: Outline and expected release profiles of Egalet® (Barshalom et al., 1991)

Egalet® Technology is based on a novel moulding process which involves the injection of two subsequent phases into same mould using a perpendicularly positioned nozzle. In the first step, a plunger is placed in the mould cavity which creates a tube shaped gap between the wall and the tube surface in which the coating material is injected as soon as it cools down, the plunger goes back, at the same time, the second phase is injected consisting injection of a drug containing layer. After cooling the moulding is ejected by a plunger.

2.7.8.2 Co-injection technique for bilayer devices

Vaz reported this innovative technology consisting of a bi-layer delivery system based on soy protein. This inovlves "sequential injection into a mould of skin (inner) and core (outer) from two different plasticating chambers through the same runner" (Vaz et al., 2003) (Figure 2.31). The processing aids used for processing of a soy protein were a platiciser (glycerol), a cross-linker (glycoxal) and re-inforcement with hydroxylapatite. The authors claimed that by changing the degree of cross-linking and by varying the skin layer thickness, drug release rate could be modified. Author presented the co-injection moulding technology for the delivery of encapsulated theophylline and the different release behaviour from the single layer and double layer device was obtained where later provided the controlled release.
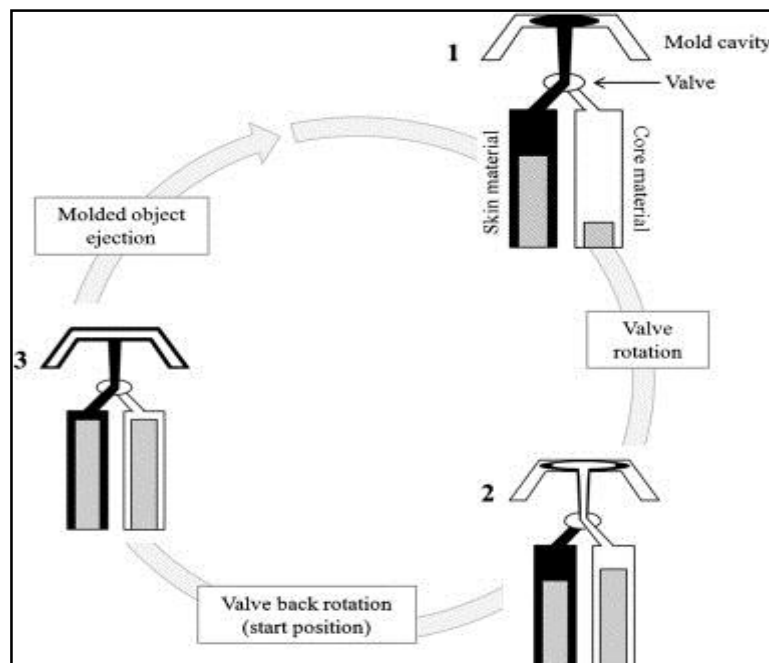
Figure 2.31 Outline of a co-injection process (Vaz et al., 2003)

2.7.8.3 Chronocap™:

Another reported device based on injection moulding is Chronocap™ which is based on Chronotropic™ oral drug delivery devices. It is a swallable/erodable device for pulsatile and/or chrotropic release of drug at the target site. e.g colonic release by hydrophilic cellulose derivative (Sangalli et al., 2004). In particular, Chronocap™ are shell devices and can be used as carrier to convey different formulations. These are made up of various hydroxypropyl cellulose (HPC) grades and shells of nominal thicknesses of 300, 600, 900 μm. These have exhibited satisfactory technological properties and performance for drug release applications.

Table 2.9: Injection moulding applications in drug delivery and relevant characteristics.(Zema et al., 2012)

Product	Polymer	Formulation	Equipment	Application
Oral capsules	Potato starch Gelatin	Starch/water or gelatin/water mixtures (around 15% water content)	Horizontal injection moulding machine (screw type)	Alternative system to gelatin dip-moulded capsules
IR(immediate release) tablets	PEG 6000 PEG 8000	*Drug*: different active ingredients (dispersed/dissolved in the molten carrier) *Reinforcement*: MCC	Horizontal injection moulding machine (screw type)	Alternative to immediate-release compressed tablets
Oral capsular device	HPC	*Plasticizer*: PEG 1500	Bench-top micro-moulding machine (plunger type)	Functional container for pulsatile/colonic release
Oral non-disintegrating matrices	Wheat starch EC	*Drug*: model active ingredient (sodium benzoate); metoprolol tartrate *Plasticizer*: glycerol, DBS *Release modifier*: HPMC, L-HPC, xanthan gum, PEO *Reinforcement*: MCC *Mould release agent*: silicon based spray	Horizontal injection moulding machine (screw type) Twin-screw mini-extruder + lab-scale vertical injection moulder	Alternative to compressed non-disintegrating oral matrices
Bi-layer device		*Drug*: theophylline *Cross-linker*: glyoxal *Plasticizer*: glycerol *Reinforcement*: hydroxylapatite	Twin-screw extruder + horizontal injection moulding machine (screw type)	Co-injected device for controlled release

Implantable matrices	PLA Polyanhydride copolymer PLC PLGA	*Drug*: valpreotide pamoato, gentamicine sulfate, fluconazole, praziquantel, 5-fluorouracil	Horizontal injection moulding machine (screw type)	Alternative to current implants
			Bench-top micro-moulding machine (plunger type)	
			Vertical injection moulding machine	
			Twin-screw mini-extruder + lab-scale vertical injection moulder	
Intravaginal inserts	PLC Ethylene vinyl acetate	*Drug:* progesterone, davipirine	Horizontal injection moulding machine	Alternative to current intravaginal inserts
			Twin-screw extruder + injection moulder (hydraulic or plunger-type)	
Oral multi-layer device	Impermeable shell: biodegradable polymers (*e.g.* EC)	*Drug*: carvedilole, opioids (*e.g.* hydrocodone, morphine)	Not specified	Double injected device for prolonged or pulsatile release
	Plug/matrix: soluble/erodible polymers (*e.g.* PEO)	*Plasticizers (shell)*: *e.g.* cetostearyl alcohol		

2.8 Summary

HME has become one the mainstream technologies for pharmaceutical research and development with more than 10 pharmaceutical products currently marketed. However, there are some challenges associated with HME in terms of material suitability such as thermolabile drugs, high processing temperatures required for polymer processing which may be associated with degradation. A number of engineering and formulation approaches have been proposed to address these issues. However, products obtained by HME are mostly in the form of an intermediate state which needs subsequent downstream processing to form into the dosage form. Therefore, injection moulding is thought to be an interesting technology as it offers a technological advantage to form a finished end product (dosage forms). Moreover, IM processing parameters have a major influence on the material properties. Therefore, IM was selected for the investigation during this research to further explore its applications in the pharmaceutical area.

Chapter 3

Materials and methods

In this chapter the materials, hot melt extrusion (HME) and injection moulding (IM) experimental procedure and the characterisation methods used throughout research are described in detail. The method section is sub-divided into three parts. The first part describes the methods used to obtain pre-formulation data on APIs and polymers to understand their miscibility, solubility and stability. The following parts describe the HME and IM processing parameters and chracterisation methods used for analysis of extruded pellets and injection moulded systems. The characterisation methodologies were focused on analysis of thermal, spectroscopic and drug release behaviour of the extruded and moulded products.

A general process schematic is provided in

Figure 3.1. The process consisted of extrusion of the drug and a polymer blend using a twin screw extruder. The products obtained were cooled and pelletised to 2 mm diameter pellets using a pelletiser. The pellets obtained were fed into the hopper of an injection moulding machine and moulded in to two shapes: tensile bars and tablets (caplets). Optimised HME and IM parameters are provided under each sub-chapter.
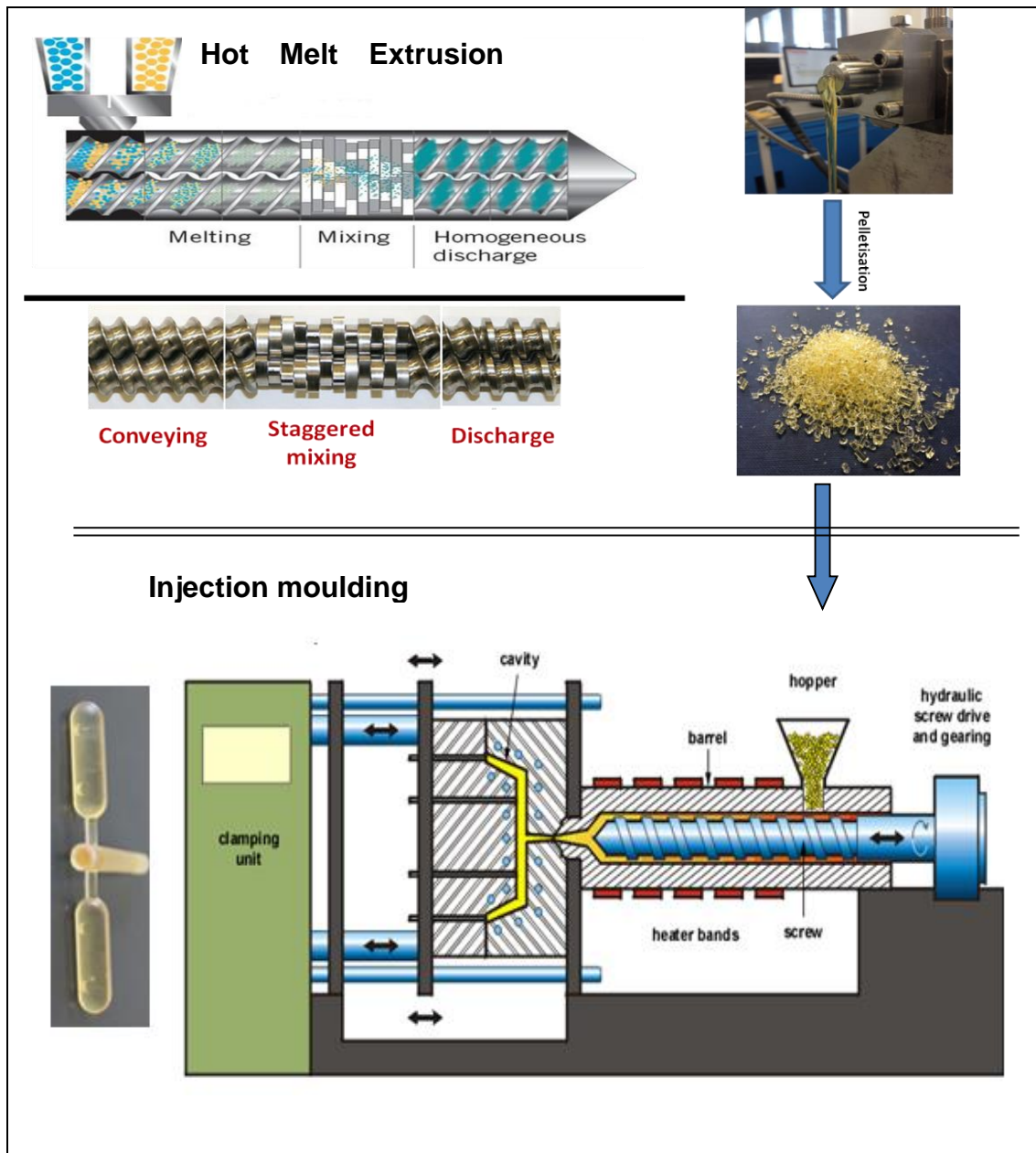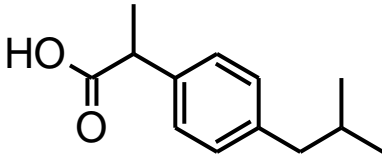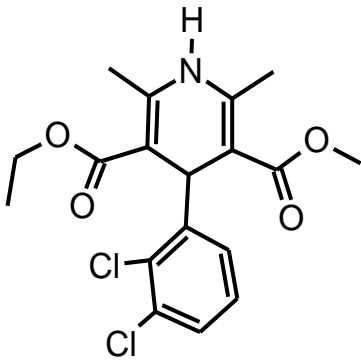
Figure 3.1: Schematic of HME and IM process for the product development

3.1 Materials

3.1.1 Active pharmaceutical ingredients (APIs)

The APIs used for this work and their details are mentioned in Table 3.1.

Table 3.1: List of APIs and physical properties

APIS	Source	Lot no
Ibuprofen	ALBEMARLE, USA	7050-1077
Felodipine	ShinEstu, Japan	1110003

Ibuprofen	Molecular Formula: $C_{13}H_{18}O_2$ Formula Weight: 206.28082 Composition: C(75.69%) H(8.80%) O(15.51%) Molar Refractivity: 60.77 ± 0.3 cm^3 Molar Volume: 200.3 ± 3.0 cm^3 Parachor: 497.6 ± 4.0 cm^3 Surface Tension: 38.0 ± 3.0 dyne/cm Density: 1.029 ± 0.06 g/cm^3 Polarizability: $24.09 \pm 0.5 \times 10^{-24}$cm^3 Average Mass: 206.2808 Da Melting point : 75-77°C Tg : -45°C
Felodipine	Molecular Formula: $C_{18}H_{19}Cl_2NO_4$ Formula Weight: 384.25376 Composition: C(56.26%) H(4.98%) Cl(18.45%) N(3.65%) O(16.66%) Molar Refractivity: 95.78 ± 0.3 cm^3 Molar Volume: 300.8 ± 3.0 cm^3 Parachor: 766.7 ± 6.0 cm^3 Surface Tension: 42.1 ± 3.0 dyne/cm Density: 1.277 ± 0.06 g/cm^3 Polarizability: $37.97 \pm 0.5 \times 10^{-24}$cm^3 Average Mass: 384.2538 Da Melting point : 145°C Tg: 45°C

3.1.2 Polymers

Three pharmaceutical grade polymers used for this study and details of suppliers, grade and lot numbers are mentioned in Table 3.2 and the chemical structure are provided in

Figure 3.2.

Table 3.2: List of polymers used in this research

Polymer	Source	Lot no.	Molecular weight	Tg (^{o}C)
HPMCAS-LF	ShinEstu, Japan	1023032	20133	120
Soluplus®	BASF, germany	HJ076	115000	72
Polyethylene oxide (Polyox N750)	Colorcon, UK	DT375497	300000	- 52

3.1.3 Chemicals and solvents

Specifications of the all solvents and chemicals used for this research are listed in Table 3.3

Table 3.3: Details of Chemical and solvent

Polymer	Source	Grade
Potassium dihydrogen phosphate	Sigma Aldrich, UK	AR
Sodium hydroxide	Sigma Aldrich UK	AR
Sodium phosphate Monobasic	Sigma Aldrich UK	AR
Sodium phosphate Dibasic	Sigma Aldrich UK	AR
Methanol	Sigma Aldrich UK	AR
Sodium lauryl Sulphate	Sigma Aldrich UK	AR

R = H, CH$_3$, CH$_2$CH(OH)CH$_3$,
COCH$_3$, COCH$_2$CH$_2$COOH,
CH$_2$CH(OCOCH$_3$)CH$_3$
CH$_2$CH(OCOCH$_2$CH$_2$COOH)CH$_3$

(A) HPMCAS

(B) Soluplus ®

(C) Poly (ethylene oxide
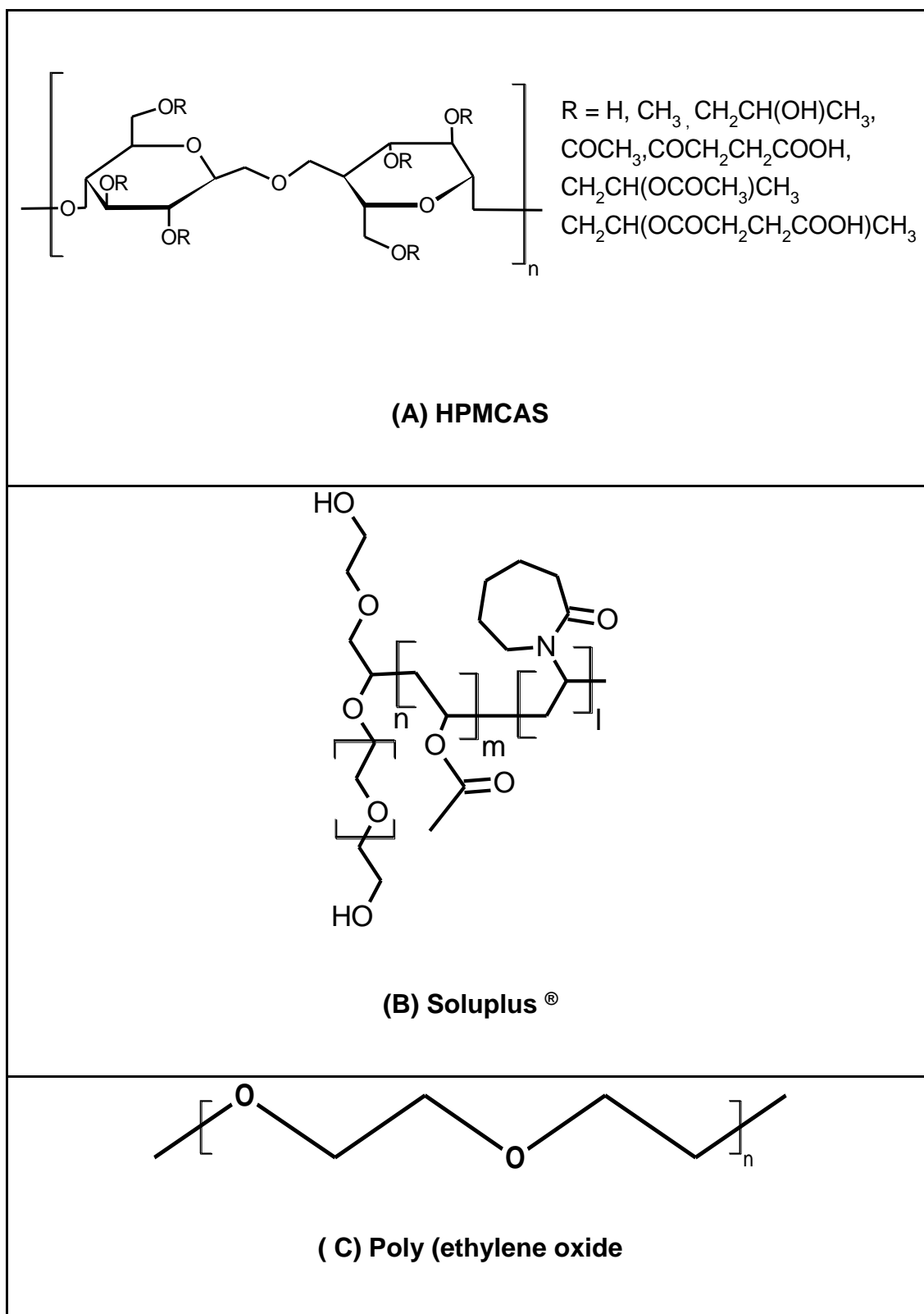
Figure 3.2: Chemical structures of polymers

3.1.4 Equipment

Specification of all the equipment used this research are provided in Table 3.4.

Table 3.4: Equipment specification

Equipment	Manufacturer	Specifications
Twin screw extruder	Thermo Scientific, UK	Pharmalab 16 mm co-rotating
Strand pelletiser	Thermo, UK	2-3 mm size pelletiser
Injection moulding	Fanuc Roboshot, Japan	5Tonne clamping force, 14 mm screw diameter
Scanning electron microscopy	FEI, UK	Quanta 400 SEM
DSC	TA Instruments UK	Q 2000
DMA	TA Instruments UK	Q800
NIR	Thermo Scientific, UK	Antaris II
Raman Spectroscopy	Renishaw, UK	Thermo Scientific
FTIR	Perkin Elmer, USA	ATR Frontier
PXRD	Bruker, USA	D8 powder diffractometer
TGA	TA Instruments, UK	Q 5000IR
Flow through cell (USP IV)	Sotax , Switzerland	CE7 smart open loop
Dissolution apparatus (USPII)	Copley Scientific UK	USP type II paddle test apparatus
Hot stage microscope	Linkam, UK	Zeiss Axioplan-2 microscope
UV	Jasco, UK	V-730 UV-visible
3D Laser microscope	Olympus, Japan	3D surface measurement

3.1.5 Software

Software used for data processing are listed in Table 3.5

Table 3.5: software used for processing of results

Software	Purpose
TA universal analysis	Thermal analysis
PowDLL converter	PXRD pattern analysis
TQ Analyst software	NIR spectra and Partial least square
GRAMS/AI™ Spectroscopy Software	Raman spectra analysis, FTIR spectra analysis
Jade 2010	PXRD pattern analysis
EVA	PXRD pattern software
Origin	Graph and analysis
ACD/Chem Sketch	Chemical drawing software

3.2 Methods

3.2.1 Pre-formulation studies: Characterisation of drugs and polymers

The drugs and the polymers were initially characterised to understand the solubility parameters (δ), glass transition temperature (Tg) and the drug-polymer solubility and miscibility. Temperature-composition phase diagrams were constructed for the four systems to predict stability of the amorphous solid dispersions.

3.2.1.1 Prediction of solubility parameters and glass transition temperature

Solubility parameters (δ) were calculated for the drugs (ibuprofen, felodipine) and the polymers (HPMCAS, Soluplus®) using the Van Krevelen and Hoftyzer's group contribution method (Adamska and Voelkel, 2005). The Tg of

85

each drug-polymer mixture was predicted theoretically using the Fox equation
(Fox and Flory, 1950)

$$\frac{1}{T_g} = \frac{W_{drug}}{T_g, drug} + \frac{1 - W_{drug}}{T_g, polymer}$$

(Equation 3.1)

Where, W_{drug} is the weight fraction of the drug, Tg drug is the glass transition temperature of the drug, Tg polymer is the glass transition temperature of the polymer.

3.2.1.2 Drug polymer solubility and miscibility:

The Flory-Huggins (F-H) interaction parameter (χ) and Gibbs free energy of mixing (ΔG_{mix}) were calculated to understand the drug polymer miscibility and solubility using the practical based approach of melting point depression. The temperature and composition dependent χ was calculated for drug-polymer amorphous solid dispersions made using the solvent evaporation method. The temperature composition phase diagram was established for all four systems using ΔG and χ.

The drug-polymer mixtures were physically mixed together in the different weight ratios (total weight 2 gm) and dissolved in 10 ml of acetone and stirred using a magnetic bead for 12 hrs to ensure complete dissolution. The solvent was removed by air-drying followed by vacuum drying at 30°C for 24hrs to ensure removal of any residual solvent. The resulting material was milled gently with a mortar and pestle and stored in desiccators before further testing. DSC studies were carried out using a DSC 2000 (TA instrument; UK). Indium standards were used to calibrate the DSC temperature and enthalpy scales. Approximately 5 mg of samples were hermetically sealed in the aluminium pan and an empty

86

aluminium pan was used as a reference. The pans were heated at 2°C/min in the temperature range of 0°C to 120°C for ibuprofen-HPMCAS and ibuprofen-Soluplus® samples. Similarly, felodipine-HPMCAS and felodipine-Soluplus® samples were analysed using the same DSC conditions except heated from 25°C to 160°C.

3.2.1.3 Melt rheology: Capillary rheometery

Capillary rheometry is pressure driven technique which mimics the flow through an extruder die or injection moulding nozzle. The shear viscosities of the HPMCAS, Soluplus®, ibuprofen-HPMCAS, Felodipine-PEO-HPMCAS ibuprofen-Soluplus®, (IBS) and felodipine-Soluplus (FDS) were studied using the twin bore (RH10) precision advanced capillary rheometer (Malvern Instruments, UK) using Flowmaster version 8.3.10 control software. The common crosshead was used to drive the piston at a range of speeds causing the melt to flow at a certain flow rate through capillary dies and the pressure drop at the entrance of the each capillary die was monitored. One barrel of the capillary rheometer was fitted with the capillary die of an L/D ratio of 16 and another was fitted with orifice die. The dimension of the capillary die used was (length X bore diameter X entrance angle): long length die (16X1X180), orifice die (0X1X180). Capillary dies were fitted into the bottom of the barrel and pressure transducers were positioned directly above the measure pressures with respective barrel. The apparent shear rate and shear stress at the wall of the capillary die, during the flow polymer through the die can be derived using Poiseulle relationship:

$$\text{Shear rate } (\gamma) = \frac{4Q}{\pi R^3} \text{ , Shear stress } (\tau_w) = \frac{R\Delta P}{2L} \text{ ,}$$

$$\text{Shear viscosity } (\eta) = \frac{\tau_w}{\gamma} \qquad \text{(Equation 3.2)}$$

Where, γ τ_w, denotes the wall shear rate (s^{-1}); wall shear stress (Pa) respectively, for the flow of fluids through a capillary radius R (m) and length L (m) at volumetric flow rate Q (m^3/s) across the pressure drop (ΔP). η denotes the shear viscosity which is a ratio of shear stress to shear rate.

3.2.2 Hot Melt extrusion (HME):

This section describes the general hot melt extrusion process and specific processing parameters used for the preparation for all four systems. Extrusion of drug- polymer blends was carried out using a co-rotating twin screw extruder (Pharmalab HME 16, Thermo Scientific, UK) with a screw diameter of 16mm and a screw length to diameter ratio of 40:1 (Figure 3.3). The extruder temperature profile was set to the required temperature with constant screw rotation speed. The blends were fed into the extruder at a constant feed rate using a gravimetric twin screw feeder (Barbender, Germany). Following extrusion the strands were cooled and pelletised in to 2mm size pellets.

Figure 3.3: Pharmalab HME 16 and screw configuration

Extruder screw configuration

The residence time and shear mixing of materials has a significant influence on the property of the extruded materials. The different screw elements were used to make the configuration. The screw configuration was used for the extrusion described in Table 3.6.

Table 3.6 Screw configurations ordered from feed to discharge

Length (D)a	Element type
28	Forwarding
2.25	30º
1.25	60 º
1	90 º
6	Forwarding
1.5	Discharge

a In terms of number of diameters, 1D = 16 mm]

3.2.2.1 Ibuprofen HPMCAS IM systems

Batches were prepared with the different percentage loading of ibuprofen in HPMCAS with ratios of ibuprofen: HPMCAS 1:2 (33%w/w), 1:2.5 (29%w/w) and 1:3 (25%w/w). Physical mixtures were prepared in 250 gm batch sizes for all batches and fed into a twin screw extruder (Pharmalab, Thermo Scientific, UK) at a processing temperature of 100°C at a screw speed of 200 rpm (Table 3.7). The feed rate was kept constant at 0.7 kg/hr. For batches containing mannitol the amount of ibuprofen was kept constant and the percentage loading of the mannitol was changed to keep HPMCAS: (ibuprofen:mannitol) mixture (60:40%) (Table 3.7).

3.2.2.2 Felodipine-PEO –HPMCAS systems

The blank system i.e PEON750-HPMCAS (20:80%w/w) was extruded to understand the processability of the HMPCAS with PEO N750. Felodipine containing pellets were prepared using HME contained felodipine-PEON750-HPMCAS (10:20:70%w/w/w) (Figure 3.4). The pellets were further used to obtain IM tablets and tensile bars. The optimised HME parameters for PEO-HPMCAS and FDH (Felodipine-PEON750-HPMCAS) are mentioned in the Table 3.8.

Table 3.7: Hot Melt Extrusion batches and parameters used for the ibuprofen-HPMCAS systems

Batch name	Composition and Ratio	HME Parameters											
		Screw speed (rpm)	Temperature Profile										
					Mixing			Conveying zone					
I33 Pellets	Ibuprofen: HPMCAS 1:2 (33% w/w)	200	**Die**	10	9	8	7	6	5	4	3	2	
			100	100	100	100	100	100	90	70	50	20	
I29 Pellets	Ibuprofen: HPMCAS 1:2.5 (29 % w/w)	200	**Die**	10	9	8	7	6	5	4	3	2	
			100	100	100	100	100	100	90	70	50	20	
I25 Pellets	Ibuprofen: HPMCAS 1:3 (25% w/w)	200	**Die**	10	9	8	7	6	5	4	3	2	
			100	100	100	100	100	100	90	70	50	20	
IM33 Pellets	Ibuprofen:man-nitol:HPMCAS 33:7:60%W/W/W	200	**Die**	10	9	8	7	6	5	4	3	2	
			110	110	110	110	110	110	90	70	50	20	
IM29 Pellets	Ibuprofen:man-nitol:HPMCAS 29:11:60%W/W/W	200	**Die**	10	9	8	7	6	5	4	3	2	
			110	110	110	110	110	110	90	70	50	20	
IM25 Pellets	Ibuprofen:man-nitol:HPMCAS 25:15:60%W/W/W	200	**Die**	10	9	8	7	6	5	4	3	2	
			110	110	110	110	110	110	90	70	50	20	

Table 3.8: HME parameters for PEO-HPMCAS and FDH batch

Batch name	Composition and Ratio	HME Parameters											
PEO-HPMCAS	PEON750-HPMCAS-LG (20:70%w/w)	**Screw speed (rpm)** 200	temperature										

Table 3.8: HME parameters for PEO-HPMCAS and FDH batch

Batch name	Composition and Ratio	HME Parameters
PEO-HPMCAS	PEON750-HPMCAS-LG (20:70%w/w)	**Screw speed (rpm)** 200 — Temperature Profile (Mixing / Conveying zone); Feed rate(kg/hr) 0.6
FDH	Felodipine-PEON750-HPMCAS-LG (10:20:70% w/w/w)	**Screw speed (rpm)** 200 — Temperature Profile; Feed rate(kg/hr) 0.6

Temperature Profile (PEO-HPMCAS) — Mixing | Conveying zone

Die	10	9	8	7	6	5	4	3	2
140	140	140	140	140	140	120	70	50	25

Feed rate(kg/hr) 0.6

Temperature Profile (FDH)

Die	10	9	8	7	6	5	4	3	2
140	140	140	140	140	140	120	70	50	25

Feed rate(kg/hr) 0.6
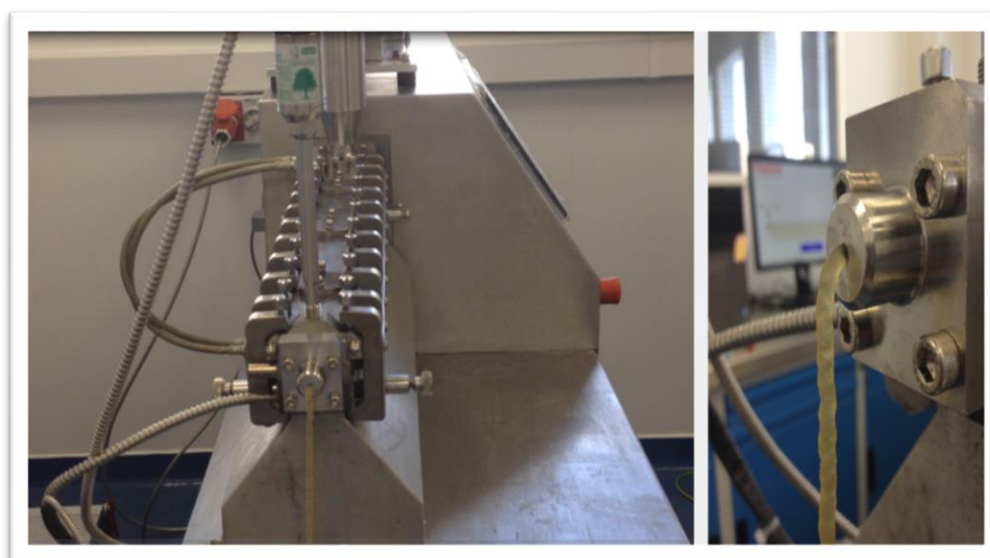
Figure 3.4: HME of Felodipine-PEO-HPMCAS (FDH) systems

3.2.2.3 Soluplus® IM systems

The processability of the Soluplus® using HME was studied with and without the addition of APIs. The Soluplus® was dried at 55°C for 12hrs before processing by HME. Batches were prepared with addition of 10%w/w of drug. The details about batches are as follows:

- Ibuprofen-Soluplus® (IBS) (10:90%w/w)

- Felodipine-Soluplus® (FDS) (10:90%w/w)

The physical mixture for 300gm batch size was prepared and extruded into pellets using a Pharmalab HME 16 (Thermo scientific, Germany). The details of HME parameters are presented Table 3.9 and Figure 3.5 shows the HME products of FDS and IBS batches, respectively

Table 3.9: HME of Soluplus®, IBS abd FDS batches

Batch name	Composition and Ratio	HME Parameters										
Soluplus®	100%w/w	Screw speed (rpm) 200	**Temperature Profile**									
					Mixing		Conveying zone					
			Die	10	9	8	7	6	5	4	3	2
			150	150	140	140	140	140	120	70	50	25
			Feed rate(kg/hr) 0.40									
IBS	Ibuprofen-Soluplus® (10:90%w/w)	Screw speed (rpm) 200	Die	10	9	8	7	6	5	4	3	2
			130	130	130	130	130	130	120	70	50	25
			Feed rate(kg/hr)0.40									
FDS	Felodipine Soluplus® (10:90%w/w)	Screw speed (rpm) 200	Die	10	9	8	7	6	5	4	3	2
			150	140	140	140	140	140	120	70	50	25
			Feed rate(kg/hr)0.40									
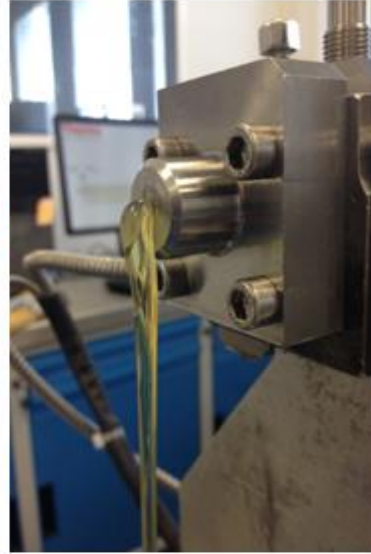
Ibuprofen-Soluplus® (IBS)Pellets   **Felodipine-Soluplus® (FDS) Pellets**

Figure 3.5: Hot melt extrusion of Soluplus® systems and extruded pellets of IBS and FDS

3.2.3 Injection moulding

Extruded Pellets of were fed into an IM machine (Fanuc Roboshot S-2000i5A) where they were melted and injected in the mould cavity. The dumbbell shaped moulds were prepared and used to explore the mechanical properties of the materials. Dimensions of tensile bar were: Length: 76mm. Neck dimensions: 33mm × 2mm × 5 mm. The injection moulded tablets (caplets) were prepared using a mould cavity with the dimension: Length (20mm) x width (6 mm) X thickness (4.30 mm). Figure 3.6 shows the IM machine and mould cavity used for the moulding.
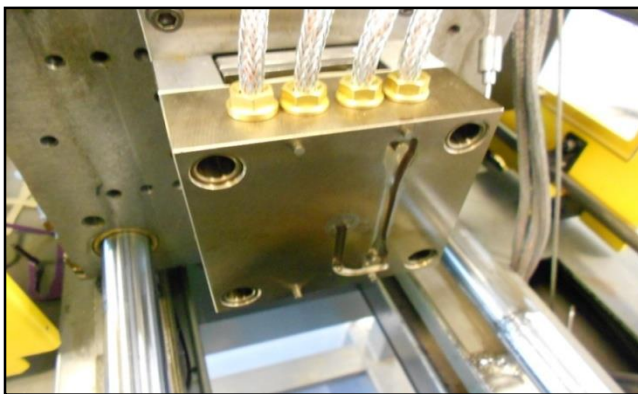
Figure 3.6: FANUC Roboshot i5A injection moulding machine, tensile bar and tablet mould design

A HAAKE MiniJet (Thermo Scientific, Germany) injection molding machine was used to produce the injection moulded tablets. The injection moulding machine has a heated cylinder for melting the polymer. For making the tablets, Ibuprofen-HPMCAS extruded pellets and Ibuprofen-mannitol-HPMCAS extruded pellets were melted at 120°C in the cylinder for 5min to achieve melting. Polymer melt was injected at a pressure of 600 bar for 1sec by a pneumatically driven piston into a tablet (caplet) shaped mould (Figure 3.6). The mould temperature was kept constant at 25°C for all batches. Tablets were packed at three different packing pressures i.e 400, 600, 800 bar at same pack time of 5 sec.

Table 3.10: Injection moulding batches and parameters

Batch Name	Composition and Ratio	IM Parameters			
		Cylinder Temperature (ºC)	Injection	Mould Packing	
		Cylinder*	Injection pressure (Bar)	Pack Pressure (Bar)	Pack time (Sec)
I33 Tablet	Ibuprofen:HPMCAS Pellets 1:2 (33% w/w)	120	600	400 / 600 / 800	5
I29 Tablet	Ibuprofen:HPMCAS Pellets 1:2.5(29% w/w)	120	600	400 / 600 / 800	5
I25 Tablet	Ibuprofen:HPMC AS Pellets 1:3(25% w/w)	120	600	400 / 600 / 800	5
IM33	Ibuprofen:Mannitol: HPMCAS Pellets 33:7:60% w/w/w	120	600	400 / 600 / 800	5
IM29 Tablet	Ibuprofen:Mannitol: HPMCAS Pellets 29:11:60%w/w/w	120	600	400 / 600 / 800	5
IM25 Tablet	Ibuprofen:Mannitol: HPMCAS Pellets 25:15:60%w/w/w	120	600	400 / 600 / 800	5

∗All batches were kept for 5min at stated temperature to ensure melting.

3.2.3.1 Effect of process parameters using DoE (33% ibuprofen-HPMCAS system)

To investigate the crystallisation kinetics and understand the surface crystallisation of ibuprofen the 33% ibuprofen-HPMCAS (I33) batch size was selected and extrusion was carried out using parameters mentioned in Table 3.7. Extruded I 33 pellets were then used to produce moulded tensile bars and tablets. All the products developed for the ibuprofen-HPMCAS system and their characterisation scheme presented in the Figure 3.7. A 3^2 factorial design was applied to understand the effect of injection moulding process variables on crystallisation kinetics and shrinkage rate.
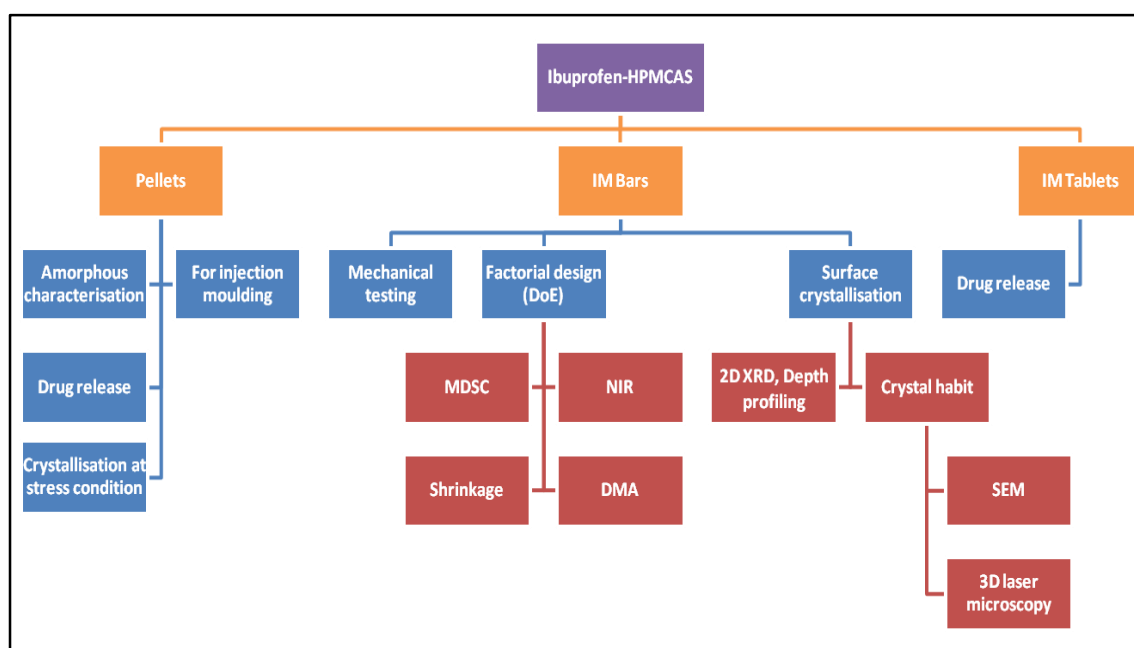
Figure 3.7 Ibuprofen-HPMCAS extruded and moulded products and characterization methods

3.2.3.1.1 3^2 factorial design for Injection moulding

I33 extruded pellets prepared using HME were used in design of experiment studies (for IM (Fanuc Roboshot Japan) to obtain tensile bar specimens. Factorial design was applied to understand the effect of process

variables on the properties of injection moulded system. The conditions used for injection the fixed process parameters such as shot size, injection speed, pack time, cooling time are mentioned in the Table 3.11 and process variable are mentioned in the Table 3.12. The pack pressure and mould temperature were used as the process variables as these parameters were considered to have a significant influence on the crystallisation and shrinkage.

Table 3.11: 3^2 injection moulding parameter

Temp (ºC)	Shot size parameter			Process parameters		
	Shot size (mm)	Screw Speed (rpm)	Back Pressure (bar)	Injection speed (mm/s)	Mould Packing Time (sec)	Mould Cooling Time(sec)
120	19	30	80	100	20	15

Table 3.12: injection moulded process variables

Batch no.	Process variable	
	Mould packing pressure (bar) (X1)	Mould cooling temperature (ºC) (X2)
B01	300	10
B02	500	10
B03	700	10
B04	300	20
B05	500	20
B06	700	20
B07	300	30
B08	500	30
B09	700	30

* B1 to B9 is experimental code assigned

3.2.3.1.2 Stability (stress) testing

To study material properties, the nature of the ibuprofen dispersion in the polymer matrix and the phenomenon of the surface crystallisation of ibuprofen from IM system, the IM bars (B01-B09) were exposed to different stress conditions listed in Table 3.13

Table 3.13: Environmental (stress) conditions

Accelerated		Middle		Control (RT)	
Temperature (^{o}C)	Humidity %	Temperature (^{o}C)	Humidity %	Temperature (^{o}C)	Humidity %
40	75	40	60	25	60

3.2.3.2 Felodipine-PEO –HPMCAS systems

The extruded pellets were used to produce IM tablets and tensile bars. The optimised IM processing parameters for PEO-HPMCAS and FDH moulded systems are mentioned in the Table 3.14.

Table 3.14 Injection moulding condition for tensile bars and tablets: PEO-HPMCAS and FDH systems

Batch	Injection moulding conditions
PEO-HPMCAS PEON750-HPMCAS (20:70%w/w) **Tensile bars**	• Temperature profile(^{o}C) | Nozzle	Zone 4	Zone 3	Zone 2	Zone 1
---	---	---	---	---
140	140	140	140	30	 • Shot size : 23 mm • Injection speed : 100 mm/s • Pack pressure : 300 bar • Pack time: 20 sec • Mould temperature: 20°C • Cooling time: 15 sec

PEO-HPMCAS PEON750-HPMCAS (20:70%w/w) **Tablets**	• Temperature profile (°C) <table><tr><td>Nozzle</td><td>Zone 4</td><td>Zone 3</td><td>Zone 2</td><td>Zone 1</td></tr><tr><td>140</td><td>140</td><td>140</td><td>120</td><td>30</td></tr></table> • Shot size : 14 mm • Injection speed : 120 mm/s • Pack pressure : 300 bar, 15 sec, 100 bar 10sec • Pack time: 25 sec • Mould Temperature : 20°C • Cooling time : 20 sec
FDH Felodipine-PEON750-HPMCAS (10:20:70% w/w/w) **Tensile bars**	• Temperature profile (°C) <table><tr><td>Nozzle</td><td>Zone 4</td><td>Zone 3</td><td>Zone 2</td><td>Zone 1</td></tr><tr><td>140</td><td>140</td><td>140</td><td>120</td><td>30</td></tr></table> • Shot size : 23 mm • Injection speed : 100 mm/s • Pack pressure : 300 bar • Pack time: 20 sec • Mould temperature: 20°C • Cooling time : 20 sec
FDH Felodipine-PEON750-HPMCAS (10:20:70% w/w/w) **Tensile bars**	• Temperature profile (°C) <table><tr><td>Nozzle</td><td>Zone 4</td><td>Zone 3</td><td>Zone 2</td><td>Zone 1</td></tr><tr><td>140</td><td>140</td><td>140</td><td>120</td><td>30</td></tr></table> • Shot size : 14 mm • Injection speed : 100 mm/s • Pack pressure : 900 bar • Pack time: 20 sec • Mould temperature: 20°C • Cooling time : 20 sec

3.2.3.3 Soluplus® IM systems

In this section details of IM processing parameters used for ibuprofen-Soluplus® and felodipine-Soluplus® moulded systems are mentioned in Table 3.15.

Table 3.15 Injection moulding conditions for Soluplus® IM batches

Batch name	Injection moulding conditions
Soluplus® **Tensile bars**	• Temperature profile (ºC) <table><tr><td>Nozzle</td><td>Zone 4</td><td>Zone 3</td><td>Zone 2</td><td>Zone 1</td></tr><tr><td>150</td><td>150</td><td>150</td><td>150</td><td>30</td></tr></table>• Shot size : 23mm • Injection speed : 120 mm/s • Pack pressure 500 Bar, 15 sec; 100Bar, 10sec Pack time: 20sec • Mould temperature: 70ºC • Cooling time: 5 Sec
Soluplus® **Tablets**	• Temperature profile (ºC) <table><tr><td>Nozzle</td><td>Zone 4</td><td>Zone 3</td><td>Zone 2</td><td>Zone 1</td></tr><tr><td>150</td><td>150</td><td>150</td><td>150</td><td>30</td></tr></table>• Shot size: 16 mm • Injection speed: 120 mm/s • Pack pressure: 500 bar, 15 sec; 100 bar, 10sec • Pack time: 30 sec • Mould Temperature : 60ºC • Cooling time : 30 sec
IBS Ibuprofen- Soluplus (10:90%w/w) **Tensile bars**	• Temperature profile (ºC) <table><tr><td>Nozzle</td><td>Zone 4</td><td>Zone 3</td><td>Zone 2</td><td>Zone 1</td></tr><tr><td>135</td><td>135</td><td>135</td><td>120</td><td>30</td></tr></table>• Shot size : 23 mm • Injection speed : 120 mm/s • Pack pressure : 500 bar • Pack time: 10 sec • Mould temperature: 55ºC • Cooling time : 10 sec

IBS Ibuprofen- Soluplus (10:90%w/w) **Tablets**	• Temperature profile (^{o}C) | Nozzle	Zone 4	Zone 3	Zone 2	Zone 1
135	135	135	135	30 | • Shot size : 16 mm • Injection speed : 120 mm/s • Pack pressure : 500 bar • Pack time: 20 sec • Mould temperature: 50°C • Cooling time : 20 sec
FDS Felodipine - Soluplus (10:90%w/w) **Tensile bars**	• Temperature profile (^{o}C) | Nozzle	Zone 4	Zone 3	Zone 2	Zone 1
150	150	150	130	30 | • Shot size : 23 mm • Injection speed : 120 mm/s • Pack pressure : 500 bar • Pack time: 20 sec • Mould temperature: 55°C • Cooling time : 10 sec
FDS Felodipine - Soluplus (10:90%w/w) **Tablets**	• Temperature profile (^{o}C) | Nozzle	Zone 4	Zone 3	Zone 2	Zone 1
150	150	150	130	30 | • Shot size : 17 mm • Injection speed : 120 mm/s • Pack pressure : 500 bar • Pack time: 20 sec • Mould temperature: 55°C • Cooling time : 20 sec

3.2.4 Characterisation of Extruded and Injection moulded systems

Extruded pellets, injection moulded tablets and tensile bars were characterised using thermal, mechanical, and spectroscopic techniques. In vitro drug release was also performed to understand the dissolution rate of drug from dosage forms.

3.2.4.1 Differential scanning calorimetry

Thermal profiles of pure ibuprofen, mannitol, HPMCAS, physical mixtures, extruded pellets and injection moulded tablets were characterised using DSC Q2000 (TA instruments) at temperature range from 0 to 150°C at a heating rate of 10°C/min. For an analysis of the moulded tablets, a section from the middle of the tablet was obtained. I33 moulded tablets are soft in nature and thr sample from middle was obtained by slicing surface with sharp scalpels. The Tg of HPMCAS was characterized using MDSC condition, where the sample was heated at an underlying heating rate of 5°C/min with modulation period of 60 sec and amplitude of ±1°C/min. The felodipine-HPMCAS (FDH), ibuprofen-Soluplus® (IBS), felodipine-Soluplus® (IBS) extruded pellets and moulded samples were also analysed using MDSC condition mentioned earlier. The results were analysed using TA Instruments universal analysis 2000 software.

The stability samples of I33 and FDH moulded systems were analysed at each stress condition by taking surface samples of the moulded bar using MDSC heat only condition. These MDSC conditions were chosen to calculate the degree of crystallinity (% crystallisation) and rate of surface crystallisation of ibuprofen from moulded bars. The surface of the moulded systems was taken over specific time after the exposure to the stress conditions. The samples were heated at an

underlying heating rate of 5°C/min and period of 60 sec. Rate of crystallisation I33 systems was monitored for 4 weeks by taking samples after 1, 2, 3, 7, 14, 21, and 28 days.

3.2.4.2 Mechanical characterisation

The mechanical testing of moulded systems was performed to understand the plasticisation effect of drugs on the polymer. Dumbbell shaped mould was used to explore the mechanical properties of the material. The dimensions of tensile bar were: Length: 76mm. Neck dimensions: 33mm × 2mm (thickness) × 5 mm (Width). An Instron tensometer (Figure 3.8) was equipped with a temperature controlled chamber to maintain temperature. A load cell of 1 KN was used and samples were tested at three extension rates 10 mm/min, 100 mm/min, and 500 mm/min.
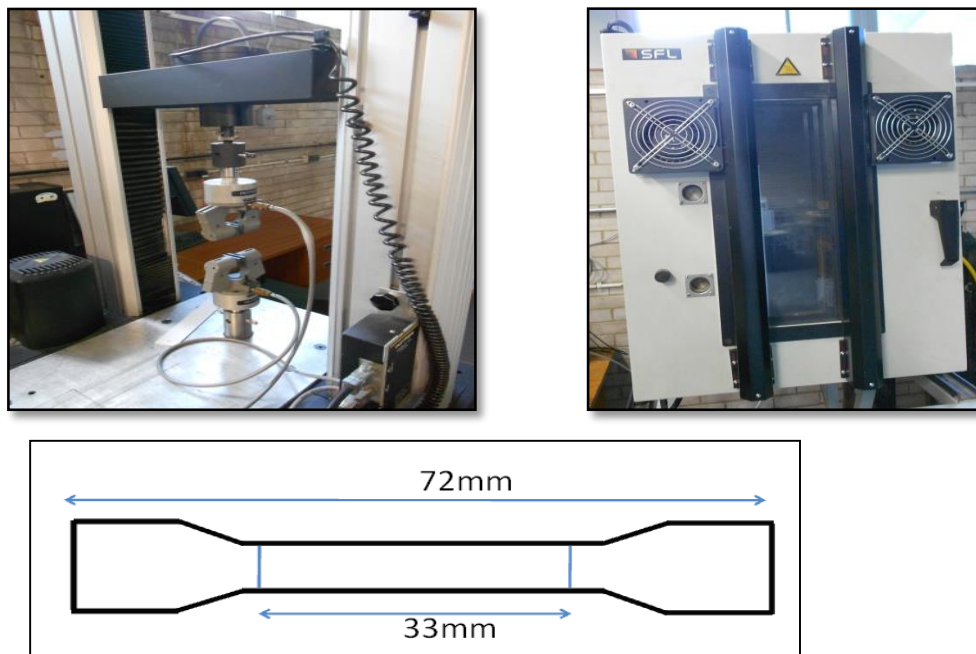
Figure 3.8: Instron tensometer and temperature controlled chamber and schematic of injection moulded bar

3.2.4.3 Raman spectroscopy

A laser radiation of wavelength 785nm was focused on the sample by the 100x objective lens. Raman backscattered radiation was collected by a high numerical aperture lens and passed through a con-focal aperture to a detection system. Weak signals are first separated from the laser Rayleigh background by a notch filter and afterwards analysed spectrally by a Charged Coupled Detector (CCD). A ReniShaw Raman Microscope was used. Samples were analysed at 50% laser power with an exposure of 10 times/sec and a spectral accumulation of a 1s with removal of a cosmic ray. Raman spectra of pure Ibuprofen, felodipine, mannitol, HPMCAS, Soluplus®, PEO N750, physical mixtures, extruded pellets and moulded tablets were analysed using Raman microscopy.

For 33% Ibuprofen-HPMCAS I33 moulded tablets, studies were planned to observe the surface crystallisation from the moulded tablets and hence spectras were acquired from both the middle and the surface of the tablets. Furthermore, to study the moisture induced surface crystallisation the I33 tablets were exposed at 43% and 75% relative humidity in a closed environment using saturated salt solutions of potassium carbonate and sodium chloride respectively. A Raman spectrum of the surface samples was monitored over 1 week, 2 weeks and 3 months.

3.2.4.4 Hot stage microscopy:

The possibility of crystallisation of I33 tablets (ibuprofen) at non-sink condition was studied using hot stage microscopy. I33 tablets were studied using hot stage microscopy (Carl Zeiss; Axioplan 2 imging). The experimental conditions were used to observe the dissolution of tablets at different pH levels.

Tablets were immersed in a petri dish containing 10ml of Phosphate buffer pH 7.2 and in another case 0.1N HCL. The solution temperature was maintained at 37°C using a hot stage. For this work, plane polarized light was focused using a 20 x objectives on the edge of the tablet and images were taken every 30 mins for 6 hrs. For imaging and data processing, Axiovision release 4.6.6 SP1 software was used.

3.2.4.5 Scanning electron microscopy

Scanning electron microscopy was used to visualise the morphology of the I33 tablet surfaces. Each tablet surface was gold coated with a layer thickness of 30nm. SEM images were taken using an FEI Quanta 400 scanning electron microscope under high vacuum with a voltage of 20KV and a working distance of 10mm at various magnification levels. SEM studies were designed to analyse the tablet surface after in-vitro dissolution of 33% Ibuprofen-HPMCAS tablets (I 33 tab) and 33% ibuprofen-mannitol HPMCAS tablets (IM33 tab) at time points of 3 hrs and 6 hrs.

3.2.4.6 3D laser microscopy: surface crystal orientation and roughness

For a detailed understanding of the orientation of the surface crystals the scans were performed at various regions of each I33 molded bar exposed to different stress conditions. The 3D measuring laser microscope (Lext OLS 4000 Olympus) with 20x objective lens (Mplan ApoN lens) was used for the surface scanning. The scanning area selected was 646 x 646 µm. The surface roughness evaluation made using the measured height parameters.

3.2.4.7 Dynamic Mechanical Analysis (DMA)

Thermo-mechanical evaluation was carried out using a DMA Q800 by subjecting moulded bars with dimensions of 16 mm gauge length, 5 mm width, 2 mm thickness to dynamic tensile deformation.

Test conditions:

Mode: DMA- multi-strain frequency

Method: Temperature ramp and frequency sweep

Frequency: Amplitude test: 5Hz with 16 μm deformation

Temperature: 20- 85°C with heating rate of 2°C/min

3.2.4.8 Near Infrared Spectroscopy (NIR):

NIR spectroscopy was performed on the pure crystalline ibuprofen and amorphous HPMCAS samples using an Antaris II NIR spectrometer (Thermo Scientific, UK). Physical mixtures were prepared by mixing the drug and the polymer in different proportions to obtain 10% w/w, 20% w/w, 30% w/w, 40% w/w, 50 % w/w, 60%w/w ibuprofen-HPMCAS mixtures. The samples were added to 10 ml glass vials and placed on the top of the light source for measurement of absorbance (Figure 3.9).

Figure 3.9: NIR of extruded pellets

Each sample analysis was performed in triplicate and reading consisted of 32 individual spectra at a resolution of 8 cm^{-1}, scanned over the region of 4000–10,000 cm^{-1} wave-numbers (2500–1000 nm wavelength) using Thermo Scientific RESULT software. Measured spectra were then stored for the subsequent analysis. A calibration curve was plotted using the calibration standards and used for quantification to determine the degree of crystallinity (% crystallisation) at each stability point.

3.2.4.9 2 dimensional (2D) X ray diffraction

The crystal habit, surface crystal orientation of I33 moulded systems was studied using 2D XRDIntact moulded samples were exposed, at room temperature, to CoKα radiation (1.7906 Å; 45 kV X 40mA) in a two dimensional X-ray diffractometer (D8 Discover 2D, Bruker with a 140 mm diameter window VÅNTEC-500 detector) (Figure 3.10). XRD patterns were collected, using a 0.8 mm collimator set at 6° angle of incidence and an area detector (angular range 36°) set at an angle of diffraction at 12° 2θ. The irradiated area can be described by an ellipse with a major axis of 5120 μm and minor axis of 1120 μm. Data analyses were performed using commercially available software (JADE 2010). Figure 3.11 shows the depth profiling samples used for the testing.

For depth profiling the following experimental conditions were used:

- Instrument details: Bruker microdiffractometer with copper radiation (45kV/40mA), incident beam graphite monochromater, 0.05 mm collimator, and a two-dimensional multi-wire detector (Figure 3.10).

- One measurement frame centered at 18°/9° (2θ/ω) with a 120 s/frame dwell

- 2D detector images converted to 1D intensity vs. 2θ patterns

- JADE 2010 used for data analysis
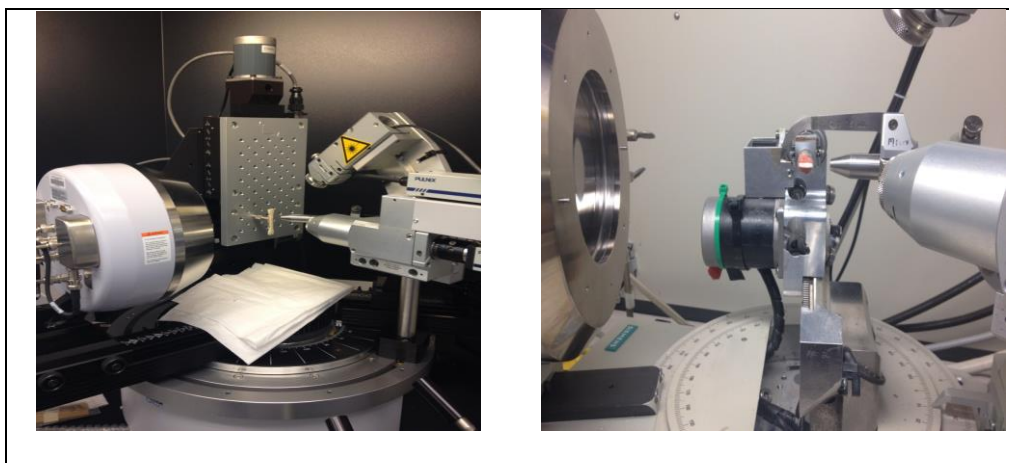
Figure 3.10: Depth profiling with 2D diffractometer
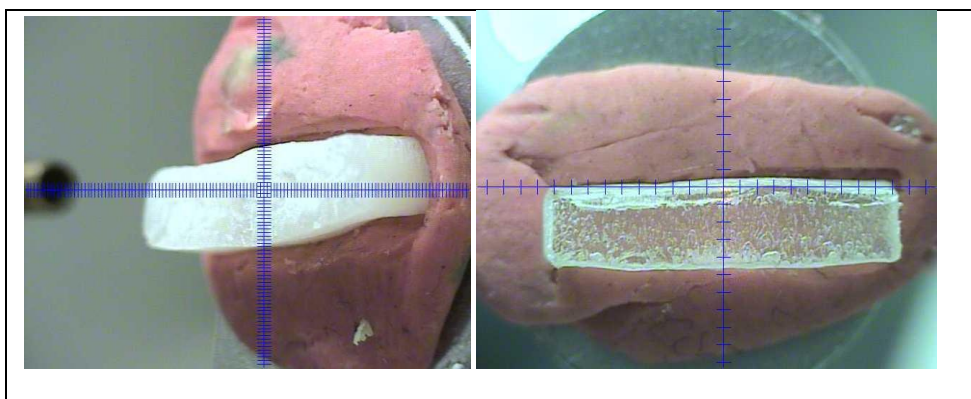
Figure 3.11: I33 moulded bar 40°C 75%RH exposed bar (left), 25°C 60% exposed bar (right)

3.2.4.10 Fourier transforms Infra-red spectroscopy (FTIR)

FTIR spectroscopic analysis of the samples was performed using a Spectrum 100 with a universal single bounces Diamond ATR attachment (Perkin Elmer, USA). This incorporated an optical system that allowed data collection in the range of 660 to 3500 cm^{-1} with resolution of 0.5 cm^{-1}. The spectra obtained were analysed using GRAMS/AI™ spectroscopy software (Thermo scientific, UK). The spectra were taken to understand the functional group vibrations and involvement of drug and polymer functional groups for the formation of hydrogen bonds.

3.2.4.11 Shrinkage

Ibuprofen-HPMCAS systems were tend to shrink after moulding hence to understand the shrinkage phenomenon the samples were exposed to different stress conditions. The 4cm injection moulded bars of both the HPMCAS and Soluplus® IM systems were kept at different stress condition as described in Table 3.13. The shrinkage rate at these three conditions was monitored for a period of 6 months. Changes in the length, width and thickness were monitored and used for the calculation of surface area and % length shrinkage ratio.

3.2.4.12 In-vitro drug release

USP II apparatus: Paddle

A calibration curve was established for the ibuprofen in a phosphate buffer pH 7.2 from 2-10 µg/ml. The drug content of extruded pellets was analysed by dissolving 450 mg of pellets and tablets of each individual batch in 20 ml of methanol and further dilution with phosphate buffer pH 7.2. Dissolution testing was performed using USP apparatus II (Paddle). Tablets were weighed and placed in a dissolution vessel consisting of 900ml of dissolution media i.e Phosphate buffer pH 7.2. The buffer was maintained at 37°C and paddle rotation speed of 50rpm. 5 ml samples were withdrawn at each time point (5, 15, 30, 60, 90, 120, 150, 180, 240, 300, 360, 420 mins) and the same volume was replaced with buffer. Ibuprofen content in dissolution samples was analysed using UV (Jasco, UK) and the data was processed using PCP disso software V3.

USP IV apparatus: flow through-cell

A USP apparatus 4 (CE 7 Smart with piston Pump, Sotax AG, Switzerland) with 22.6mm flow cell was used for this study. The procedure for preparation of

the cell consisted of placing a 5mm ruby ball onto the apex of cell and approximately 8 gm of 1mm glass beads were added to the cone area to form a glass bead bed. The testing products (i.e pellets and tablets) were positioned on the top of glass bead bed. The details of experimental parameters used for testing of all four moulded tablets are as follows.

- Dissolution media:

  - For ibuprofen-HPMCAS and ibuprofen Soluplus® tablets: Phosphate buffer pH 7.2,

  - For Felodipine-PEO-HPMCAS and Felodipine-Soluplus® tablets: Phosphate buffer pH 6.5 with 1% SLS

- Flow rate: 4 ml/min,

- Temperature: 37.0±0.5°C, Loop configuration: Open loop

Chapter 4

Pre-formulation

In this chapter result of preformulation studies performed on the materials are discussed. The prediction of solubility parameters, glass transition temperature, estimation of drug-polymer miscibility and solubility were the main objectives of this study. The temperature-composition phase diagram was constructed to estimate the stability and performance.

4.1 Pre-formulation studies

The active pharmaceutical ingredients (APIs) i.e ibuprofen and the felodipine and the polymers i.e HPMCAS and Soluplus® were characterised using theoretical and practical methodologies to understand the material properties. Understanding of the physicochemical properties of the drug- polymer mixtures was the main objective of these pre-formulation studies.

4.1.1 Prediction of solubility parameters and glass transition temperature

The solubility parameter (δ) can be used to predict the miscibility of the two substances by measuring their cohesive energy density (CED) (Greenhalgh et al., 1999) (Verheyen et al., 2001). All inter-atomic and/or molecular interactions such as van der Waal's interaction, electrostatic interaction, induced or permanent dipole interactions, covalent bonds, ionic bonds and hydrogen bonds contribute to the cohesive energy of a substance (Hancock et al., 1997). Among the several reported methods to calculate solubility parameters the preferred methods used were the Van Krevelen and Hoftyzer's group contribution method (δ (MPa1/2) (Adamska and Voelkel, 2005).The solubility parameter in this approach is expressed in $(J/cm^3)^{1/2}$ or $MPa^{1/2}$ by the equation below (Van Krevelen and Te Nijenhuis, 2009)

$$\delta^2 = \delta_d^2 + \delta_p^2 + \delta_h^2$$ (Equation 4.1)

Where

$$\delta_d = \frac{\sum F_{di}}{V} \qquad \delta_p = \frac{\sqrt{\sum F_{pi}^2}}{V} \qquad \delta_h = \sqrt{\frac{\sum E_{hi}}{V}}$$ (Equation 4.2)

In these equations, δ is the total solubility parameter, δ_d is the contribution from dispersion forces, δ_p is the contribution from polar forces, δ_h is the contribution from hydrogen bonding, F_{di} is the molar attraction constant due to

the dispersion component, F_{pi} is the molar attraction constant due to the polar component, E_{hi} is the hydrogen bonding energy, and V is the molar volume (Van Krevelen, 1990). Generally, the selected drug–excipient blends with a difference in their solubility parameters ($\Delta\delta$) of < 7.0 MPa$^{1/2}$ are predicted to be miscible whereas those with $\Delta\delta$ of >10.0 MPa$^{1/2}$ are predicted to be immiscible with each other (Forster et al., 2001b) (Ghebremeskel et al., 2007; Greenhalgh et al., 1999). The solubility parameter (δ) and other physical properties of the selected drugs (ibuprofen and felodipine) and polymers (HPMCAS and Soluplus®) are presented in Table 4.1.

Table 4.1: Physical properties of ibuprofen, felodipine, HPMCAS, and Soluplus®

Compounds	Molecular Voume(V) (cm^3/mol)	Density (g/cm^3)	Molecular weight (g/mol)	Solubility parameter (δ) (MPa$^{1/2}$)
Ibuprofen	200.28	1.03	206.29	18.81 [a]
HPMCAS	15852.76	1.27	20133[a]	26.89 [a]
Felodipine	300.19	1.28	384.25	24.39 [b]
Soluplus®	116161.66	0.99	115000	31.22 [b]

[a]Calculated using the Van Krevelen and Hoftyzer's group contribution method

[b]Adapted from the reference (Tian et al., 2013)

The solubility parameter difference ($\Delta\delta$) of the four systems was calculated by subtracting solubility parameter of the drug from the polymer ($\Delta\delta$ = δ of polymer − δ of drug) and the $\Delta\delta$ values of the four systems is listed in Table 4.2.

Table 4.2: The solubility parameter difference (Δ*δ*) of drug polymer composition

Drug- polymer systems	Solubility parameters difference ($\Delta\delta$) (MPa$^{1/2}$)
Ibuprofen- HPMCAS	8.08
Felodipine- HPMCAS	2.50
Ibuprofen- Soluplus®	12.41
Felodipine - Soluplus®	6.83

In general, the solubility parameter difference ($\Delta\delta$) of the ibuprofen containing systems was higher compared to the felodipine containing systems. Ibuprofen-HPMCAS and ibuprofen-Soluplus® showed a solubility parameter difference ($\Delta\delta$) of 8.08 and 12.41, respectively, indicating that the ibuprofen-HPMCAS system could be partially miscible with each whereas the ibuprofen-Soluplus® system could be immiscible. The lowest difference in solubility parameters was observed for felodipine- HPMCAS systems with $\Delta\delta$ of 2.5 and slightly higher for the felodipine-Soluplus® system ($\Delta\delta$=6.83).

The prediction of solubility parameters provides valuable information on the miscibility of the selected systems. Although this method can be used as a tool to predict miscibility of the drug and polymers it has some limitations. For instance, it is difficult to estimate highly directional (e.g, hydrogen bonding) or long range (e.g., electrostatic) interactions of complex molecules using the group contribution method (Gupta et al., 2011). Hence, it is often necessary to confirm miscibility using experimental methods such as differential scanning calorimetry (DSC).

The glass transition temperature (Tg) of systems was calculated using Fox equation (Fox and Flory, 1950). The predicted Tg for different weight fractions of drug and polymer vs temperature is displayed in Figure 4.1. The Figure 4.1a shows a fall in the glass transition temperature of HPMCAS due to the addition of a different weight fraction of the ibuprofen and felodipine. Similarly, Figure 4.1b show that Tg falls for the Soluplus®, due to the addition of the ibuprofen and felodipine respectively (Figure 4.1).

Actual points in the graphs are representative of a Tg of the total mixture. In the case of HPMCAS the addition of ibuprofen has a major effect on the Tg of the polymer. HPMCAS has a Tg of 120°C and it is a predicted that the 10%w/w addition of ibuprofen will decrease Tg of the mixture to 93°C and 10%w/w addition of felodipine will shift Tg to 110°C. This suggests that the addition of a low Tg drug such as ibuprofen (- 45°C) to a high Tg polymer like HPMCAS leads to a reduction of the Tg of the mixture to a higher extent compared to the addition of a medium Tg drug like felodipine (45°C). This can be attributed to the higher plasticisation effect of ibuprofen than felodipine. Similarly for Soluplus® (Tg ≅ 72°C) the addition of ibuprofen significantly reduced the Tg of the mixture and the addition of 50%w/w of ibuprofen in Soluplus® will decrease Tg as low as 0°C while 50% w/w addition of felodipine will reduce Tg to 57 °C (Figure 4.1b).
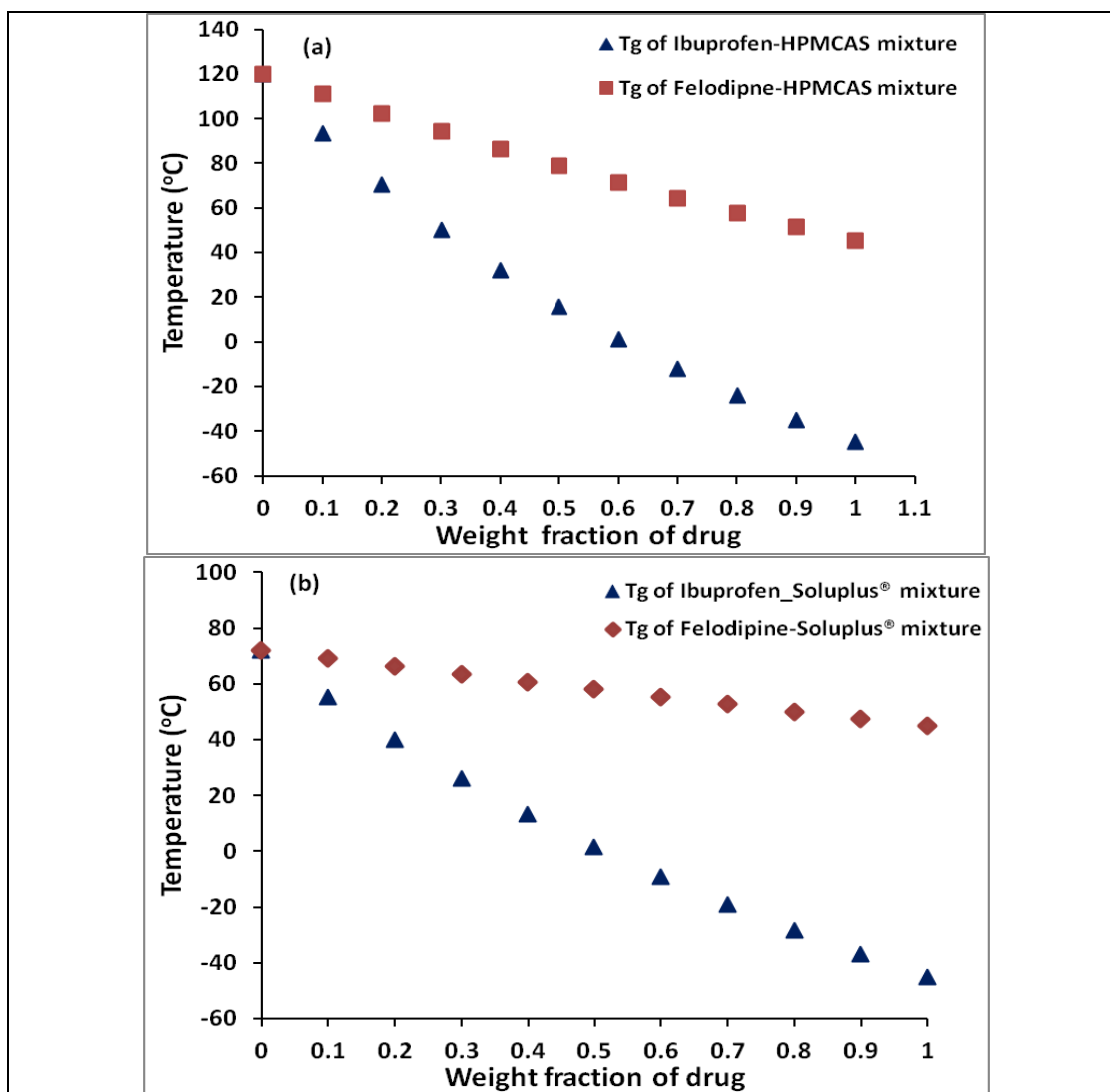
Figure 4.1: Glass transition temperature of the systems predicted based on the Fox equation – (a) Ibuprofen-HPMCAS, felodipine-HPMCAS (b) Ibuprofen-Soluplus®, felodipine-Soluplus®

4.1.2 Drug-polymer miscibility and solubility

The solubility of small molecule drugs in a polymer matrix system has a significant impact on the development of pharmaceutical dosage forms. The long-term stability of the formulated product is determined by whether the drug loading inside the polymer matrix is oversaturated or undersaturated (Zhao et al., 2011). The practical approach of melting point depression can used to calculate the Flory-Huggins (F-H) interaction parameters and free energy of mixing (Nishi and

Wang, 1975). The Flory-Huggins theory provides a practical indication of the miscibility of binary systems.

4.1.2.1 Theoretical considerations: Flory-Huggins interaction parameters (χ) and free energy of mixing (ΔG)

According to the Flory-Huggins (F-H) theory, the Gibbs free energy change that accompanies mixing of a drug-polymer binary system may be expressed as:

$$\Delta G_{mix} = \Delta H_{mix} - T\Delta S_{mix}$$

(Equation 4.3)

Where ΔH_{mix} is the enthalpic parameter and ΔS_{mix} is the entropic parameters. For a binary system of a polymer with a small molecule drug, the Gibbs mixing function written according to the F-H model is the sum of combinatorial terms plus interaction terms. Subsequently, the Gibbs free energy may be expressed as F-H interaction χ

$$\Delta G_{mix} = RT \left(\frac{\phi_{drug}}{N_A} \ln \phi_{drug} + \frac{\phi_{poly}}{N_B} \ln \phi_{poly} + \chi_{drug-poly} \phi_{drug} \phi_{poly} \right)$$

(Equation 4.4)

Where Φ is the volume fraction, N is the molar volume of drug or polymer χ is the F-H interaction parameter, R is the molar gas constant, and T is the temperature.

In the case of a drug-polymer mixture N_A may be defined as molecular size of the drug and $N_B = mN_A$, where m is the ratio of volume of polymer chain to drug molar volume chain

119

$$m = \dfrac{\dfrac{M_{W\ (poly)}}{\rho_{poly}}}{\dfrac{M_{W\ (drug)}}{\rho_{drug}}} \hspace{3cm} \text{(Equation 4.5)}$$

Where Mw (poly) is the molecular weight of the polymer and Mw (drug) the molecular weight of the drug, and ρ_{poly} and ρ_{drug} are the density of polymer and drug, respectively. Hence equation 4.5 for the free energy of mixing for binary (drug-polymer) systems may be written as:

$$\Delta G_{Mix} = RT \left(\phi_{drug} \ln \phi_{drug} + \frac{\phi_{poly}}{m} \ln \phi_{poly} + \chi_{drug-poly}\, \phi_{drug}\, \phi_{poly} \right)$$

(Equation 4.6)

Hence, the corresponding interaction parameter (χ) at a specific temperature may therefore be used for calculation of free energy of mixing (ΔG_{mix}). The drug-polymer interaction parameters can be predicted using melting point depression data collected from DSC studies (Caron et al., 2011; Marsac et al., 2006; Marsac et al., 2009; Sun et al., 2010; Tao et al., 2009).

$$\frac{1}{T_m} - \frac{1}{T_{m0}} = -\frac{R}{\Delta H}\left[\ln \phi_{drug} + \left(1 - \frac{1}{m}\right)\phi_{poly} + \chi_{drug-poly}\, \phi_{poly^2}\right]$$

(Equation 4.7)

Where T_m and T_{mo} are the melting points of the drug crystal in the mixture of drug/polymer ϕ volume fraction of drug, respectively, m is the molar volume; R is the real gas constant, and ΔH is the heat of fusion of the crystalline drug.

In practice, the interaction parameter (χ), displays complex dependence on the polymer composition, chain length and temperature. The correlation between interaction parameters and this variable cannot be simply determined (Zhao et al., 2011). Often temperature dependence of the interaction parameter is empirically written as the sum of two components to simplify studies. The

temperature dependence of interaction parameters can be calculated using the following equation

$$\chi_{drug-poly} = A + \frac{B}{T}$$ (Equation 4.8)

Where, A is the value of temperature-independent term (entropic contribution), B/T is the value of temperature-dependent term (enthalpic contribution). The dependence interaction parameter on volume fraction (composition) is negligible relative to the temperature and the first order relationship between χ and temperature is an additional assumption of the F-H polymer solution theory. The first order relationship between χ and 1/T can be used to extrapolate the value of χ for drug polymer systems outside the experimental temperature (Lin and Huang, 2010) (Dexi et al; 2010)(Zhao et al., 2011). Equation 4.9 can be further used to relate χ to temperature and used for obtaining F-H constants A and B. F-H constants A and B are important for the calculation of interaction parameters at a range of temperature, especially for the estimation at a lower temperature than glass transition (Tg) and room temperature. This estimation has an importance for calculating free energy of mixing (ΔG) of binary systems.

In this research, the four compositions (Ibuprofen-HPMCAS, ibuprofen-Soluplus®, felodipine-HPMCAS and felodpine-Soluplus®) were used for the injection moulding and drug polymer dispersions were preliminary studied to predict their miscibility and the solubility with each other using melting point depression approach.

4.1.2.2 Melting point depression and relationship between χ and T

The depression of melting point was developed by Nishi and Wang in 1975 to describe the interaction between pure amorphous and pure crystalline polymer (Nishi and Wang, 1975). The melting point of a drug occurs at a temperature when the chemical potential of the pure drug is equal to the chemical potential of the molten drug (Flory, 1953). If the drug is miscible with polymer, the chemical potential of drug in a mixture must be less than the chemical potential of pure amorphous drug. (Marsac et al., 2009). Strong exothermic mixing should cause a large depression in melting point while weaker exothermic, athermal, endothermic mixing should progressively cause less melting point depression. In contrast, if the drug and the polymer are immiscible with each other no melting point depression is expected since the chemical potential of the molten drug is unaltered by the presence of the polymer (Marsac et al., 2006; Marsac et al., 2009; Zhao et al., 2011) .

In the present study the melting point depression of the drug-polymer physical mixture was observed using DSC heating of the sample. A representative melting point depression of the ibuprofen - HPMCAS system is shown in Figure 4.2. The depression of melting point of the crystalline drug (ibuprofen) was observed in the presence of different concentrations of amorphous polymer (HPMCAS) due to the interaction between them near to the melting temperature of the drug (76°C). Figure 4.2 and Table 4.3 clearly shows depression of the melting point and when the concentration of ibuprofen was less than 40% w/w the absence of an endotherm confirmed the complete solubility of ibuprofen in HPMCAS below 40%w/w.
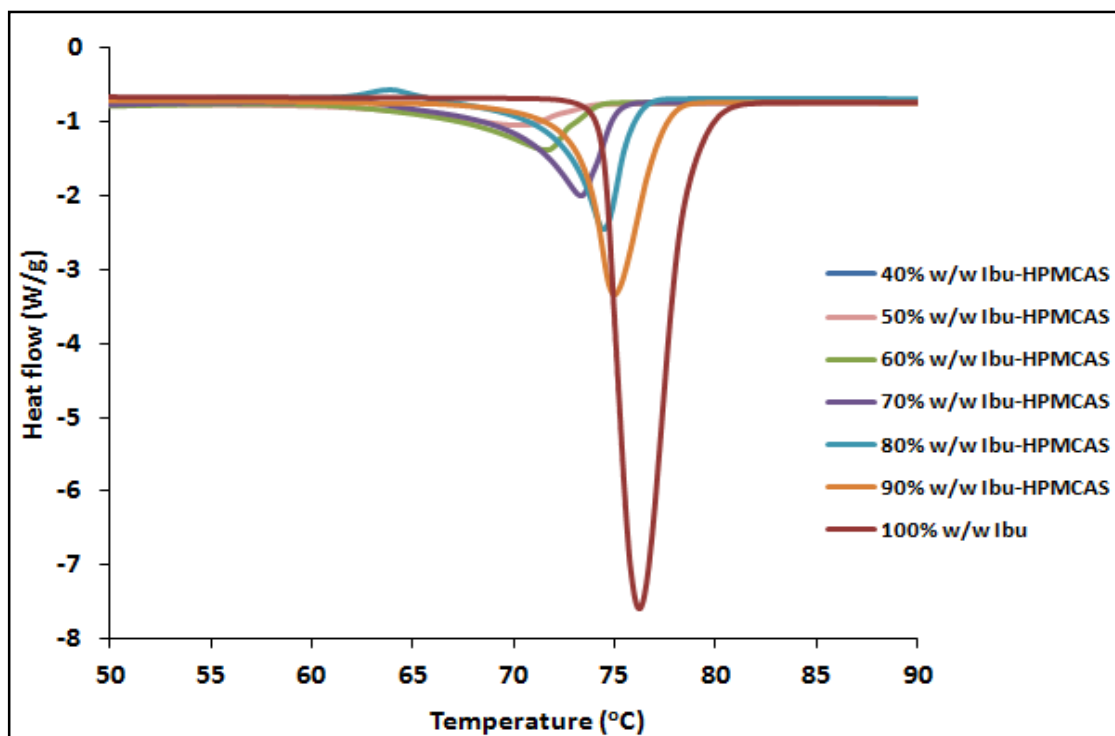
Figure 4.2: DSC thermogram of ibuprofen-HPMCAS mixtures measured at 2°C/min

Table 4.3 : Melting point depression of ibuprofen-HPMCAS

Weight fraction of drug	Temperature	1/T * 1000
0.4	69.6±0.21	2.929
0.5	70.4±0.23	2.907
0.6	72. 6±0.21	2.892
0.7	73.9±0.20	2.881
0.8	74.6±0.19	2.875
0.9	75.1±0.17	2.871
1	76.4±0.15	2.860

4.1.2.3 Interaction parameter (χ)

Melting point depression data collected from DSC studies was fitted with equation 4.8 to obtain the interaction parameter as a function of temperature. Ibuprofen-HPMCAS concentrations of less than 40% did not show a melting endotherm and for felodipine-HPMCAS no melting endotherm was observed for compositions less than 50%. In the case of Soluplus®, the ibuprofen-Soluplus® system did not show a melting endotherm below 50% composition and 60% in the case of felodipine-Soluplus® compositions. It suggests drug polymer binary systems exhibit an upper critical solution temperature (UCST) where the drug is completely miscible with the polymer (Tian et al., 2013). The temperature dependence of interaction parameters may be described as first order as shown by equation 4.9. A plot interaction parameter versus 1/T is shown in Figure 4.3.
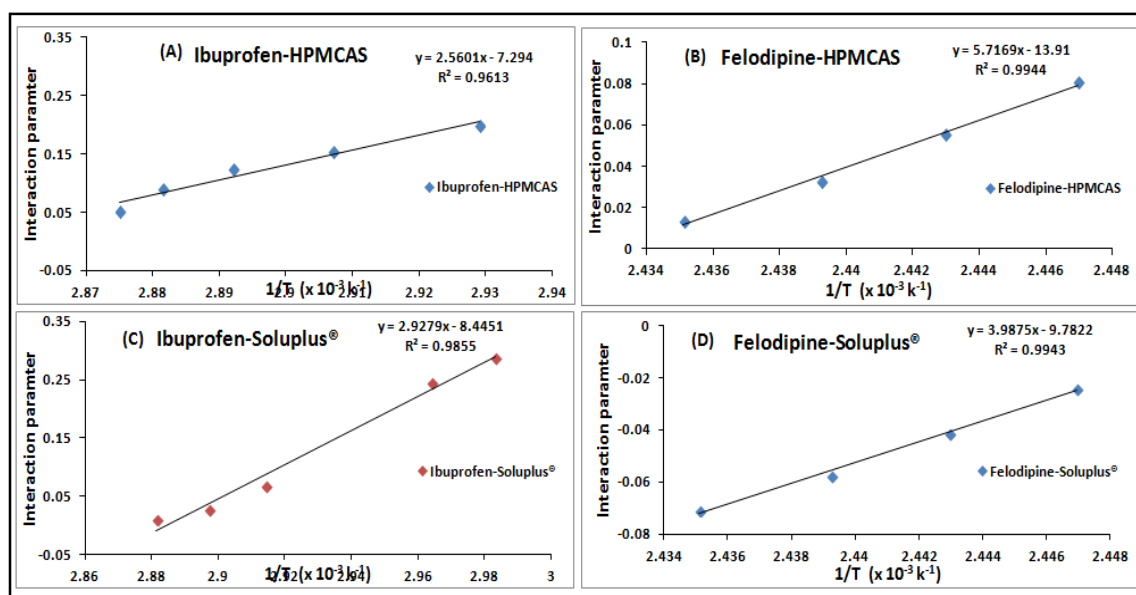
Figure 4.3: Variation of the interaction parameter X as a function of temperature (The solid line represents the line of best fit of equation 4.8 to experimental data)

A linear relationship between interaction parameter and 1/T was observed at a low drug concentration, whereas non-linearity at high drug concentrations

was observed. Similar observations were reported for indomethacin/PVA-VA system (Zhao et al., 2011). The linear relationship between temperature and interaction parameter allowed estimation of the F-H constants A and B as described in equation 4.9. Using the equation 4.9 the interaction parameter χ at RT (25°C) for the four systems was calculated and as reported in Table 4.4. The drug-polymer interaction parameter χ, obtained at 25°C is positive in all systems which suggest immiscibility at RT which is expected to decrease at elevated temperatures. For example, the HPMCAS composition has χ of 1.29 at 25°C and -0.43 at 100°C suggesting the good miscibility at elevated processing temperatures.

Table 4.4: F-H interaction constants A and B determined using linear regression analysis of experimental DSC data and interaction parameter, χ, calculated at 25°c using melting depression

Drug polymer systems	F-H constants		Interaction parameters
	A	B	χ
Ibuprofen-HPMCAS	-7.29	2560	1.29
Ibuprofen-Soluplus®	-8.44	2927	1.38
Felodipine-HPMCAS	-13.91	5716	5.26
Felodipine-Soluplus®	-9.78	3987	3.59

The calculated interaction parameters at RT suggest the interaction parameters higher than zero suggests immiscibility of the all drug polymer systems at 25C. However, the better interaction between the two components can be expected at higher temperature. The interaction parameters have a direct

influence on the free energy of mixing and hence the relationship between the temperature and ΔG is the reliable indicator of the miscibility.

4.1.2.4 Free energy of mixing (ΔG_{mix})

The free energy of mixing (ΔG_{mix}) of binary (drug-polymer) system gives information about the mixing of two components at a certain temperature. When $\Delta G_{mix} < 0$ for two compositions at respective temperature, suggesting the good miscibility with each other while immiscible when the $\Delta G_{mix} > 0$. Interestingly, free energy of mixing is dependent on both the temperature and composition (weight fraction) hence sometimes it's possible that the ΔG_{mix} can be negative at a lower weight fraction of drug and positive at a higher drug concentration at constant temperature.

The substitution of interaction parameters calculated at different temperatures into equation 4.7 can help to understand the variation in the Gibb's free energy of mixing as a function of drug composition and temperature. Figure 4.4 provides information about that Gibbs free energy of mixing for the four systems. Figure 4.4A and Figure 4.4B provides the free energy plot for the ibuprofen with HPMCAS and Soluplus® respectively. These plots are almost identical, although ibuprofen-HPMCAS has a slightly lower ΔG_{mix} compared to ibuprofen-Soluplus®. This suggests that mixing will be more favoured in the case of ibuprofen-HPMCAS.

In the case of felodipine containing systems the felodipine-HPMCAS system showed higher ΔGmix than felodipine-Soluplus® Figure 4.4C and Figure 4.4D show free energy plots for both systems. It is apparent that near the melting point of the drug (140°C) ΔGmix is negative and convex. At this temperature, the homogenous drug-polymer mixtures are generated and that are

126

thermodynamically stable at all drug-polymer weight fractions. For the felodipine-HPMCAS and felodipine-Soluplus® system temperatures ≥ 120°C favoured mixing at lower drug concentration of 40% and 70% respectively and positive values of system at higher drug concentration may indicate the systems tendency for phase separation at higher drug concentrations (Tian et al., 2013).
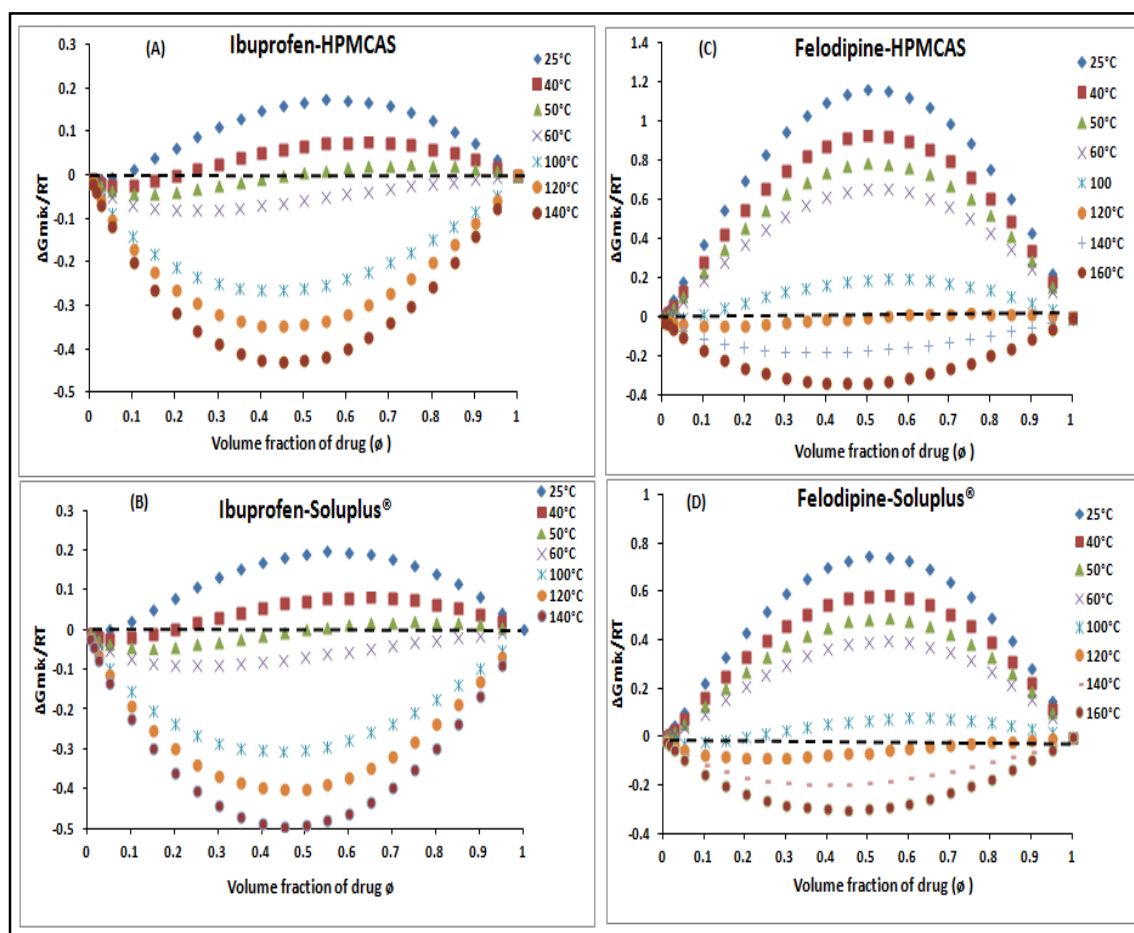
Figure 4.4: Plot of ΔGmix/RT as function of drug volume fraction and polymer (A) ibuprofen-HPMCAS (B) ibuprofen-Soluplus®; (C) Felodipine-HPMCAS(D) Felodipine-Soluplus® at various temperatures.

4.1.3 Temperature-composition phase diagram

Complete phase diagrams for ibuprofen-HPMCAS, ibuprofen-Soluplus®, felodipine-HPMCAS and felodipine-Soluplus® were obtained after understanding how ΔGmix varied with the temperature (T). The solubility and miscibility curve obtained from ΔGmix were combined with Tg of the mixtures to obtain the phase diagrams.

A typical phase diagram for a binary system is shown in the Figure 4.5. This is mainly composed of amorphous drug-polymer miscibility curve, crystalline drug-polymer solubility curve and the Tg of the solid dispersion. The concept of miscibility is well understood in polymer physics in which each polymer blend is stable in the amorphous state (Rubinstein and Colby, 2003). However, in the case of drug polymer solid dispersions complexity may arise as the amorphous drug dispersed in the solid dispersion is usually in a meta-stable state relative to the crystalline state and inclines to crystallise. Therefore, the drug-polymer dispersion would eventually reach equilibrium with regards to the crystalline drug and equilibrium composition of drug-polymer mixture would be the solubility of crystalline drug in the polymer (Qian et al., 2010).

The importance of drug polymer solubility and miscibility for the development of the stable amorphous dispersion is widely recognised. The temperature composition phase diagram can be used as a tool to assess the physical stability of the solid dispersion during formulation, process development and product shelf-life. The phase diagram consists of solubility, miscibility and Tg curves which intersect to form six different zones which provides valuable information on the thermodynamic stability of the drug- polymer system. It is assumed that the system is partially miscible above Tg (i.e Tc > Tg).
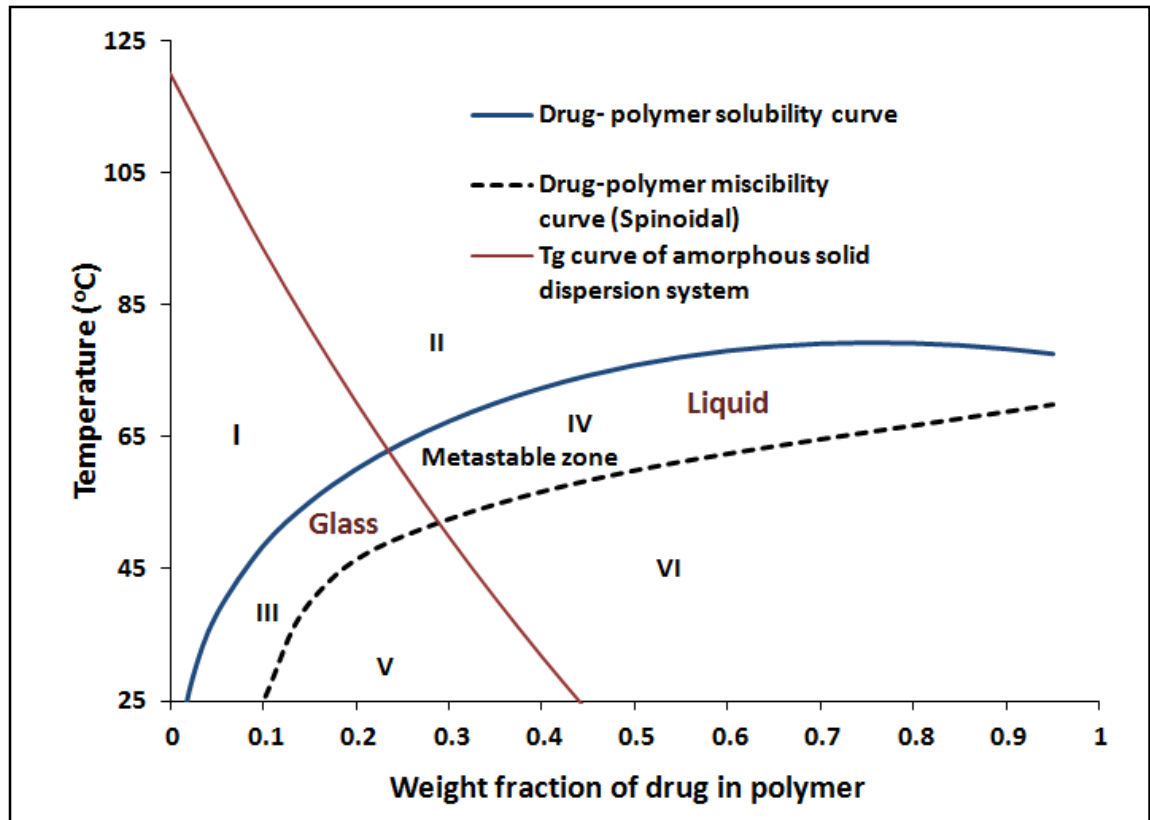
Figure 4.5: Representative drug-polymer phase diagrams

In theory, for drug concentrations above the miscibility curve, phase separation will be thermodynamically favoured and at equilibrium both a drug rich-phase and a polymer-rich phase coexist with two distinguished Tg values. However, solid dispersions made by practical processes such as spray drying or HME are well mixed kinetically and initially show a single Tg regardless of the drug loading. For simplicity, the Tg values shown in Figure 4.5 are correspond to a single Tg of the system.

As shown in the Figure 4.5 the miscibility, solubility and Tg curves separate the phase diagram into six different zones (zones I - VI) (Table 4.5). Since the amorphous form of the drug has a higher chemical potential than its crystalline counterpart, drug polymer miscibility (amorphous form solubility) is always higher than crystalline drug polymer solubility (Qian et al., 2010)

Table 4.5: Thermodynamic nature and destabilisation driving force for solid dispersions in zones I–VI of Figure 4.5

Zone	Thermodynamic Nature	Destabilization Driving Force
I	Thermodynamically stable glass	None
II	Thermodynamically stable liquid	None
III	Supersaturated glass	Crystallization of supersaturated drug
IV	Supersaturated liquid	Crystallization of supersaturated drug
V	Supersaturated and immiscible glass	Amorphous phase separation, crystallisation of supersaturated drug
VI	Supersaturated and immiscible liquid	Amorphous phase separation, crystallisation of supersaturated drug

The Tg curve defines the boundary between the equilibrium liquid (Zone II, IV, VI) and glass (I, III, V). The Tg curve is generally recognised as a kinetic boundary of molecular mobility and which usually represents two regions. Right of the Tg curve is the *equilibrium liquid* and in this region the structural relaxation occurs rapidly and solubility and miscibility can be measured at equilibrium. On the other hand, the left side of Tg curves is the non-equilibrium, glassy region where molecular mobility is considered to be very low and structural relaxation occurs slowly thus equilibrium solubility and miscibility cannot be strictly defined or measured experimentally. Interestingly, below Tg the stability of amorphous solid dispersions depends heavily on the kinetics of phase separation and/or crystallisation instead of thermodynamics.

The solubility curve is the boundary between the thermodynamically stable (Zone I and II) and meta-stable (zone III and IV). Regions I and II represent the maximum drug loading that can be achieved without the thermodynamic destabilisation of the system. Zones III and IV are defined respectively as 'supersaturated glass' and 'supersaturated liquid' and together this region is called the "metastable region". Crystallisation of supersaturated drug could arise from these metastable states upon destabilization. Especially in zone III a solid dispersion could be stabilised both thermodynamically (miscibility) and kinetically (restricted mobility). Zone V and VI are well below the miscibility and indicate complete phase immiscibility. Moreover, VI should be avoided as there are no thermodynamic or kinetic barriers for stability.

Phase diagrams of the four the systems are presented in Figure 4.6. The miscibility, solubility and Tg curves are plotted in order to obtain the complete temperature composition phase diagram. The dashed line referes to the spinoidal curve and to the right side of the curve the drug is present in an unstable state while on the left side of the curve the drug present in the metastable state. In case of ibuprofen (Figure 4.6a and Figure 4.6b), HPMCAS shows good miscibility and solubility with ibuprofen as compared to Soluplus®. Moreover, Tg of the system in the case of ibuprofen-HPMCAS composition was higher so zone III (supersatureted glass) was broader thus a kinetic barrier would stabilise the system due to restricted molecular mobility than in the case of ibuprofen-Soluplus® system.

(a) Ibuprofen- HPMCAS

- Solubility of Ibuprofen in HPMCAS
- Miscibility of Ibuprofen in HPMCAS
- Tg of mixture

Temperature (°C) vs. Weight fraction of drug

(b) Ibuprofen - Soluplus®

- Solubility of Ibuprofen in Soluplus®
- Miscibility of Ibuprofen in Soluplus®
- Tg of mixture

Temperature (°C) vs. Weight fraction of drug
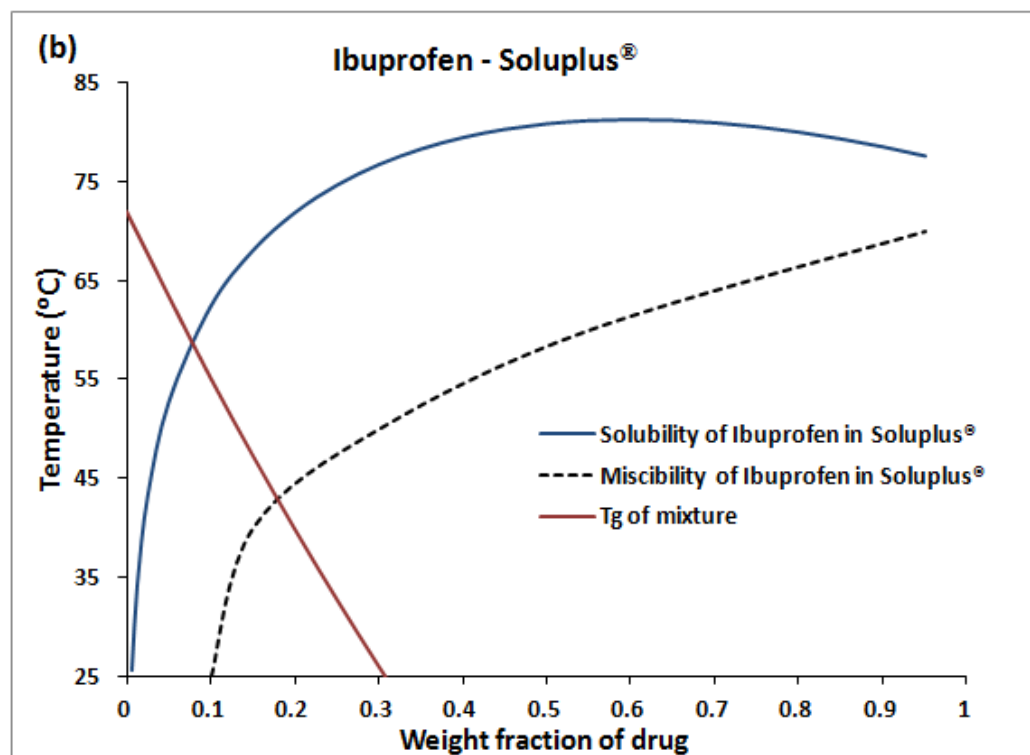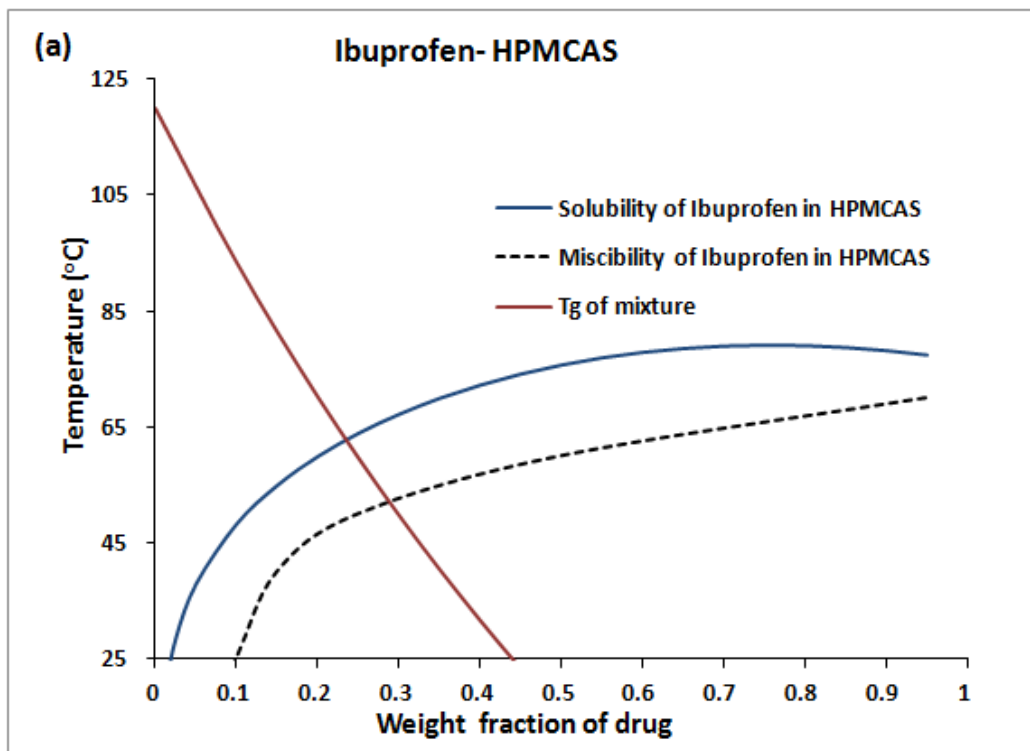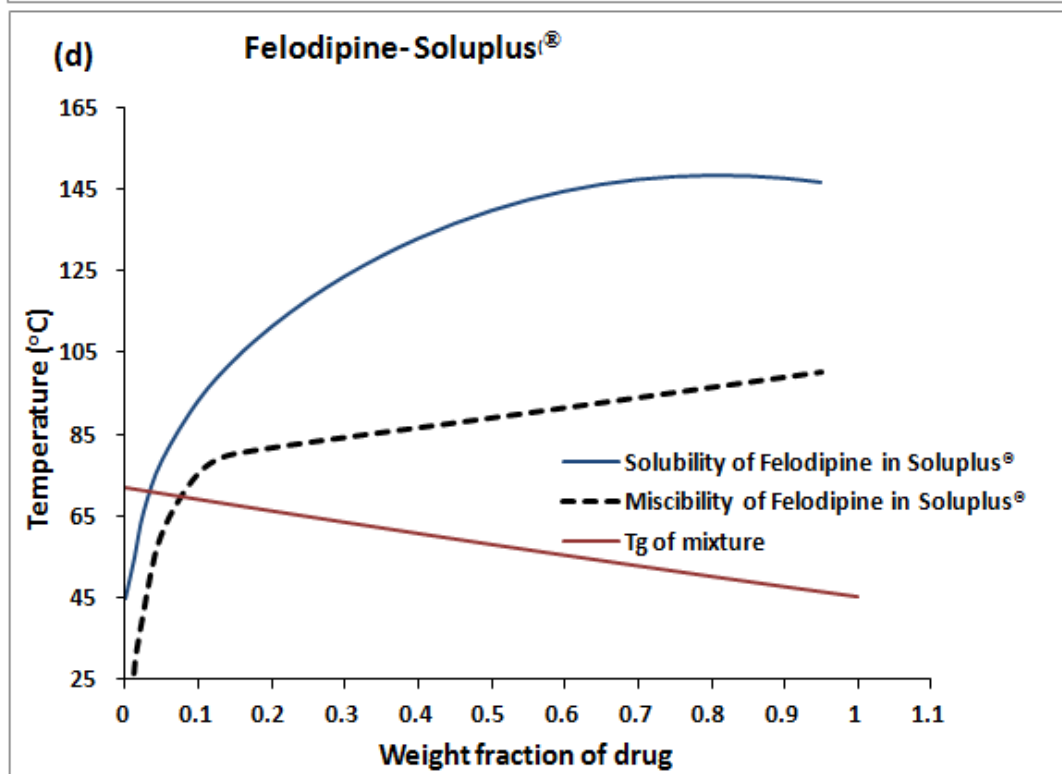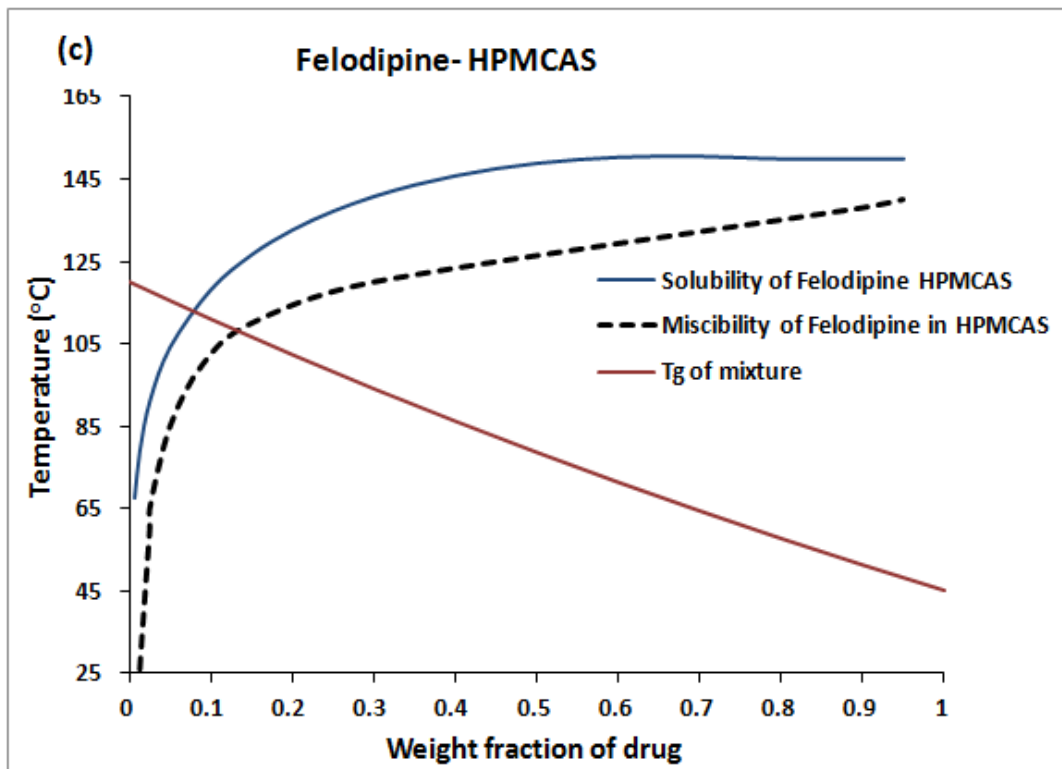
Figure 4.6: Binary phase diagram of (a) ibuprofen-HPMCAS; (b) ibuprofen-Soluplus® (C) Felodipine-HPMCAS (d) Felodipine-Soluplus®

In the case of felodipine systems, the felodipine-Soluplus® miscibility and solubility curves (Figure 4.6 d) shifted towards low temperatures indicating the good miscibility of felodipine with Soluplus® than HPMCAS at lower temperatures. However, due to High Tg of felodipine-HPMCAS system the Zone I , III, V are broader and indicating good stability compared with felodipine-Soluplus®. The phase diagram identified the region in which large energetic barriers (kinetic hinderance) for recrystallisation are apparent i.e kinetically and thermodyanamically favoured.

It was seen that ibuprofen has a good miscibility and solubility in HPMCAS compared Soluplus® on the other hand, the felodipine has good miscibility and solubility in Soluplus® compared to HPMCAS. For example, 10% w/w of felodipine will be miscible in Soluplus® at 70°C and it will get solubilise at 90°C. For the same concentration the miscibility and solubility of the felodipine in HPMCAS were predicted at higher temperature 105°C and 120°C respectively. The drug-miscibility results obtained from phase diagram are in good accordance with previously calculated solubility parameters.

This information on the drug polymer miscibility and solubility was very helpful to set the HME and IM processing parameters of the drug polymer systems.

Chapter 5

Results and discussion: HPMCAS IM systems

In this chapter results and discussion of HMCAS IM systems are provided. The chapter is subdivided into two main chapters Ibuprofen-HPMCAS and Felodipine-PEO-HPMCAS injection moulded systems. The processing aspects of both the systems and product properties of pellets and moulded system is discussed in this chapter.

5.1   Ibuprofen-HPMCAS injection moulded systems

The ibuprofen-HPMCAS (IBH) systems were processed using HME and IM with and without the addition of a release modifier (mannitol). The effect of drug-polymer composition on the process, product properties and drug release performance was studied at pre-formulation stage. The effect of IM process parameters such packing pressure and mould temperature on the surface crystallisation was studied in detail using 33% w/w Ibuprofen-HPMCAS (I33) systems.

5.1.1   Processability during extrusion and injection moulding

Pure Ibuprofen exhibits a low glass transition temperature of -45.1°C (Dudognon et al., 2008) and a melting endotherrm at 76.8±0.23°C. Mannitol exhibits a melting endotherm at 168.9±0.24°C (Figure 5.1). The Tg of HPMCAS was characterised using conventional and modulated DSC. The MDSC condition used provided good separation of Tg of HPMCAS at 120°C using the reversing heat flow signal (Figure 5.1 d). HPMCAS is cellulose ether, explored mainly as a carrier for solid dispersions. Solvent evaporation (Tanno et al., 2004) and spray dried dispersions (Friesen et al., 2008) were the solid dispersion methods used for dispersion, however, fewer applications have been explored for thermal processing of HPMCAS. Hence, the processibility of the polymer alone at 100°C using twin screw extrusion was evaluated, but excessive torque was observed and the extruder screws became blocked. The processing temperature was then increased in step of 10°C and at 160°C it was possible to extrude pure HPMCAS pellets. The mixture of ibuprofen and HPMCAS (1:2) processed using twin- screw extrusion at 100°C, smooth processing with torque of 30%, a flexible strand of 2 mm diameter was obtained and pelletised into 2 mm pellets. This confirms the

plasticisation effect of ibuprofen on HPMCAS. Similarly, other plasticisers are also used for HPMCAS; in order to lower the Tg and to improve processibility with extrusion. Plasticisers such as triacetin, diethyl citrate, and dioctyl phthalate have been used. 25%w/w triacetin in HPMCAS lowers Tg to as low as 49.0°C (Mehuys et al., 2005).
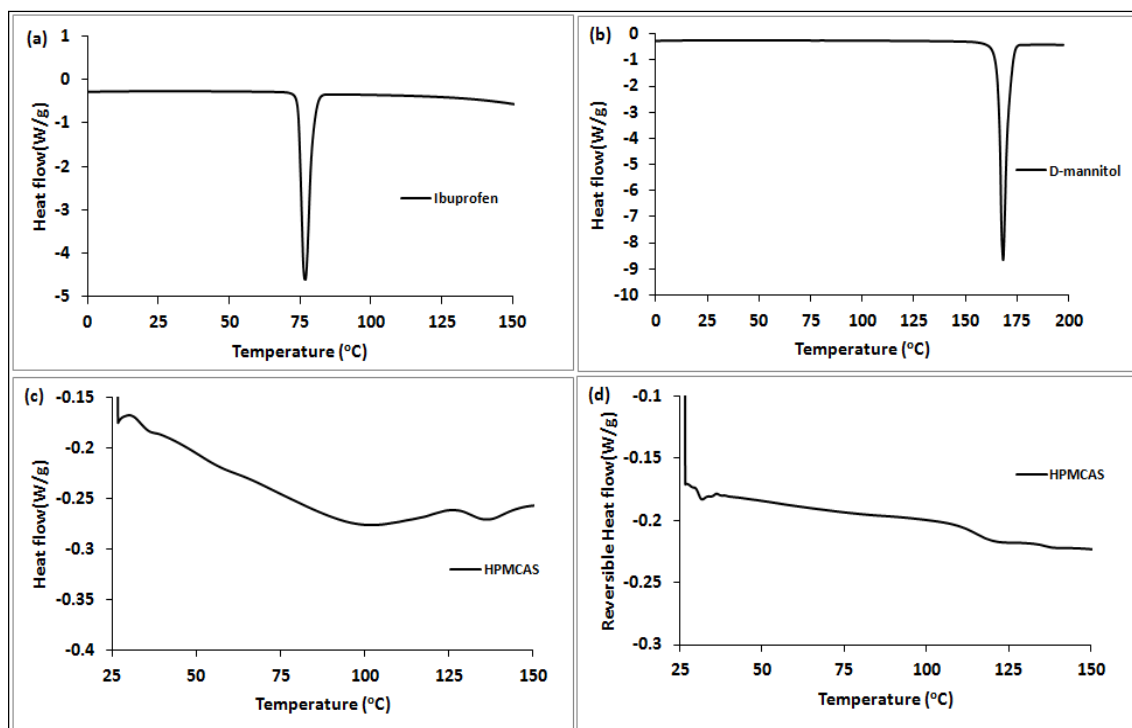
Figure 5.1: DSC thermo gram: (a) Pure Ibuprofen; (b) Mannitol; (c) HPMCAS heat flow (linear heating @5°C/min) (d) HPMCAS reversing heat flow (modulated heating @5°C/min)

The extrusion of Ibuprofen batches (I33, I29, and I25) and Ibuprofen mannitol (IM33, IM29, IM25) batches with different loadings of drug in HPMCAS was operated at the experimental conditions mentioned in Table 3.6. The torque associated with all batches is summarised in the Table 5.1. No significant change in torque with different loadings of drug and/or mannitol was observed which indicates a good processability under the stated experimental conditions

.

Table 5.1 Torque associated with the extrusion process

Ibuprofen-HPMCAS Batches(I)			Ibuprofen-D-mannitol-HPMCAS batches (IM)			
Percent Loading	Torque (%)	Motor power (kW)	Percent Loading		Torque (%)	Motor power (kW)
			Ibuprofen	Mannitol		
33	35-38	0.87-0.95	33	7	36-38	0.90-0.95
29	40-43	1.0 - 1.07	29	11	42-44	1.05-1.1
25	45-48	1.12-1.20	25	15	42-45	1.05-1.12

The powder state has poor flowability and powder cannot be fed into the throat of the injection moulding machine easily; also the single screw of the moulding machine does not provide intimate mixing. Hence, to ensure homogenous mixing and good feeding, the materials were pre-compounded into pellets using a twin screw extruder. In the case of injection moulding using the HAAKE MiniJet, processing parameters were kept constant except the packing pressure in order to understand the effect of densification on the properties of the moulded system. Here, the most important property considered was drug release from the tablet. Moulded tablets obtained using the HAAKE MiniJet are shown in the Table 5.2.

Table 5.2: Injection moulded tablets at packed at 600bar.

Ibuprofen tablets	33% Ibuprofen Tablet	29% Ibuprofen Tablet	25% Ibuprofen Tablet
Ibuprofen-mannitol Tablets	33% Ibuprofen, 7% Mannitol Tablet	29% Ibuprofen, 11% Mannitol Tablet	25% Ibuprofen, 15% Mannitol Tablet

5.1.2 Characterisation of extruded pellets and injection moulded tablets

Melt extruded pellets and injection moulded tablets were evaluated using thermal and spectroscopic techniques to understand the nature of amorphous drug dispersion and drug release from the polymer matrices.

5.1.2.1 Modulated Differential Scanning Calorimetry

Physical mixtures of Ibuprofen-HPMCAS and Ibuprofen-mannitol-HPMCAS batches characterised by DSC exhibited a sharp melting endotherm of ibuprofen at 76.8±0.23°C; indicating the crystalline nature of ibuprofen. The physical mixture containing mannitol also showed a sharp melting enotherm at 166.6±0.25°C indicating melting of the crystalline mannitol. Moreover, these results confirm that mannitol was did not solubilise in the molten ibuprofen-HPMCAS mixture and remained dispersed in the crystalline form. Similar behaviour was observed for extruded pellets where mannitol exhibited a melting endotherm at 166°C (Table 5.3d). Extruded pellets showed an absence of a sharp melting endotherm of ibuprofen indicating an amorphous dispersion of ibuprofen in HPMCAS (Figure 5.2c).
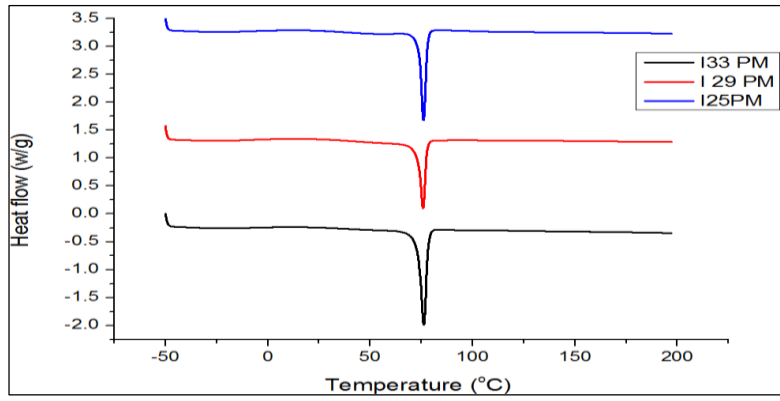
(a)
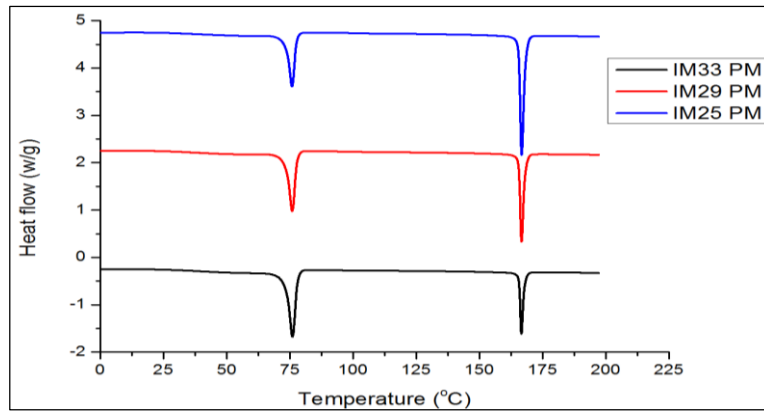
(b)
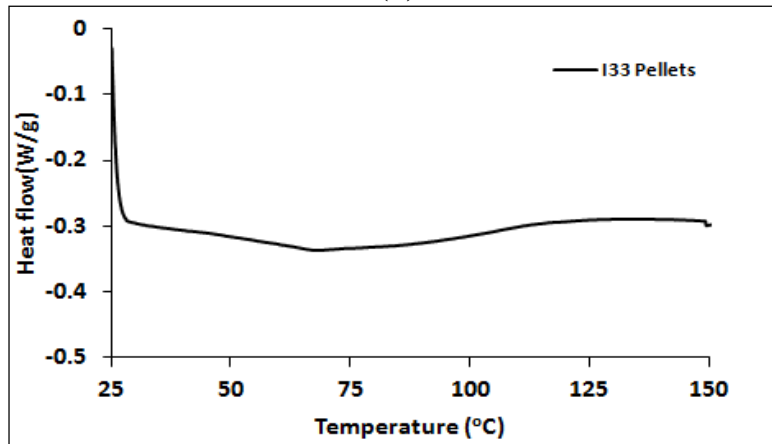
(c)
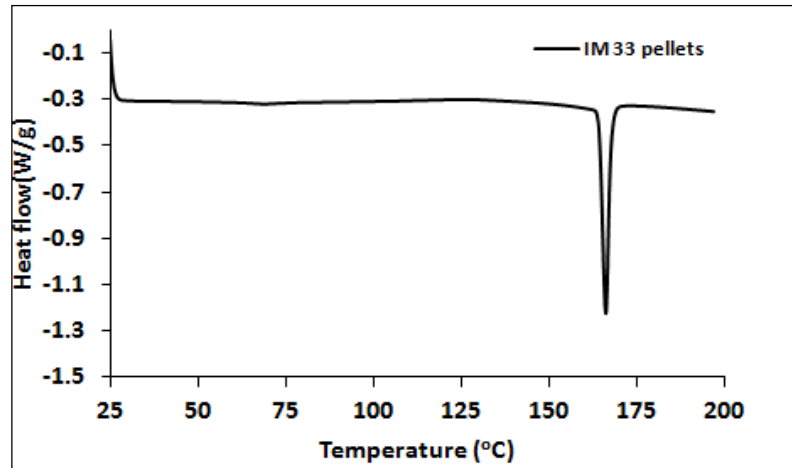
(d)

Figure 5.2: DSC thermogram: (a) Physical mixture of ibuprofen in HPMCAS (I33, I29, I25) (b)Physical mixture of Ibuprofen-mannitol-HPMCAS (IM33, IM29, IM25) (c) Ibuprofen-HPMCAS(I33) extruded pellets; (d) Ibuprofen-mannitol HPMCAS (IM33) extruded pellets (modulated heating rate 5°C/min)

Figure 5.3 shows the thermal profiles of moulded tablets packed at different packing pressures. The tablets prepared at different packing pressures of 400, 600, and 800 bar did not show any significant differences in thermal profiles. However, the absence of an ibuprofen melting endotherm in all samples confirms the formation of amorphous solid dispersion or amorphous molecular dispersion of ibuprofen with HPMCAS.

141
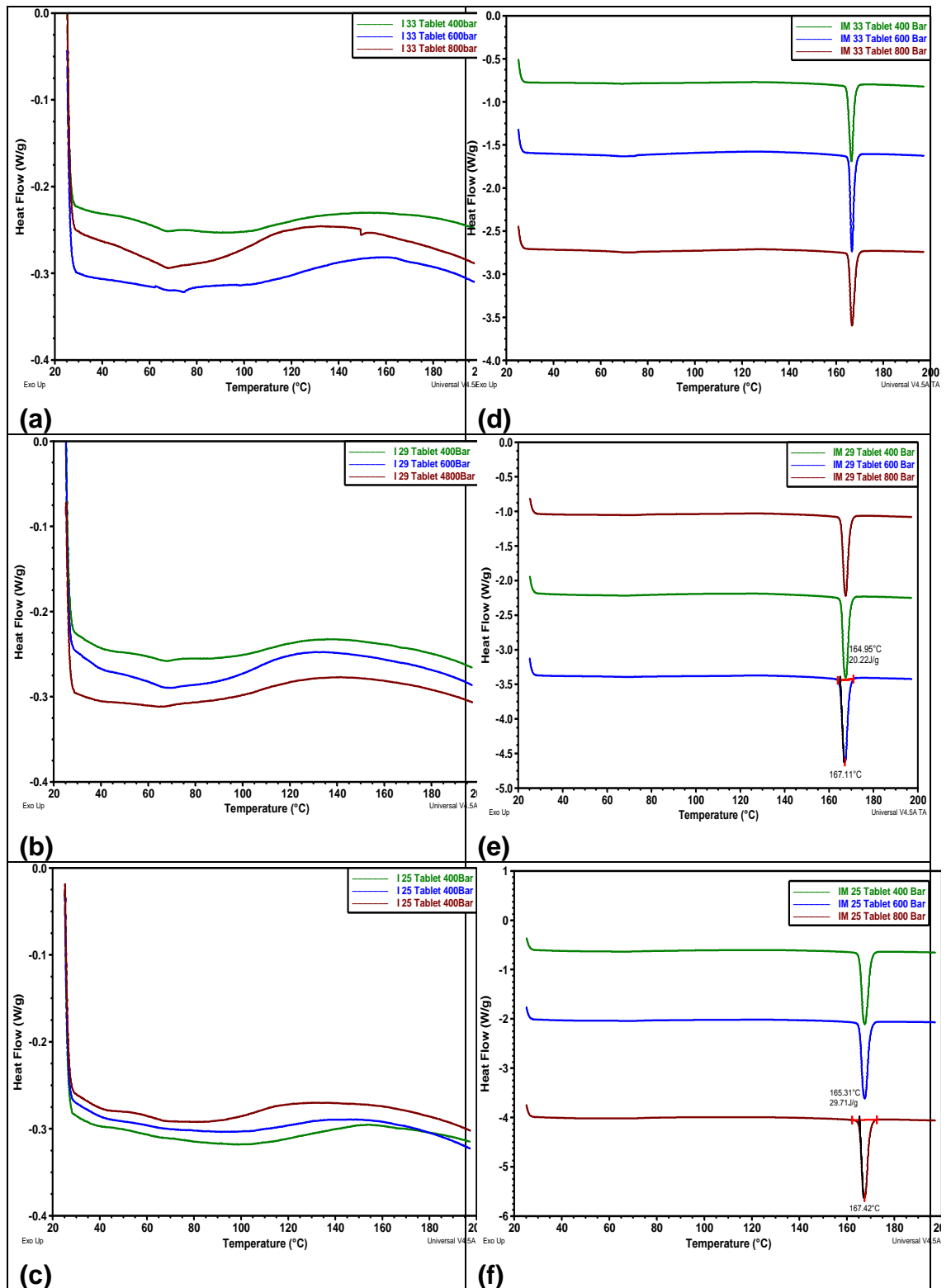
Figure 5.3: DSC Thermograms of injection moulded tablets packed at different packing pressures: (a) I33 Tablet; (b) I29 Tablet; (c) I25 Tablet (d) IM 33 Tablet e) IM29 Tablet (f) IM 25 Tablet (modulated heating rate 5°C/min)

5.1.2.2 Mechanical properties of moulded systems

Mechanical properties of the tensile bars prepared using pellets containing different amounts of ibuprofen and mannitol were determined using Instron tensile tester. The typical stress-strain profile was obtained by subjecting moulded bars at different extensions rates. The mechanical properties were such Young's modulus; ultimate tensile strength and extension at break were calculated based on the strain-strain profiles (Figure 5.4).
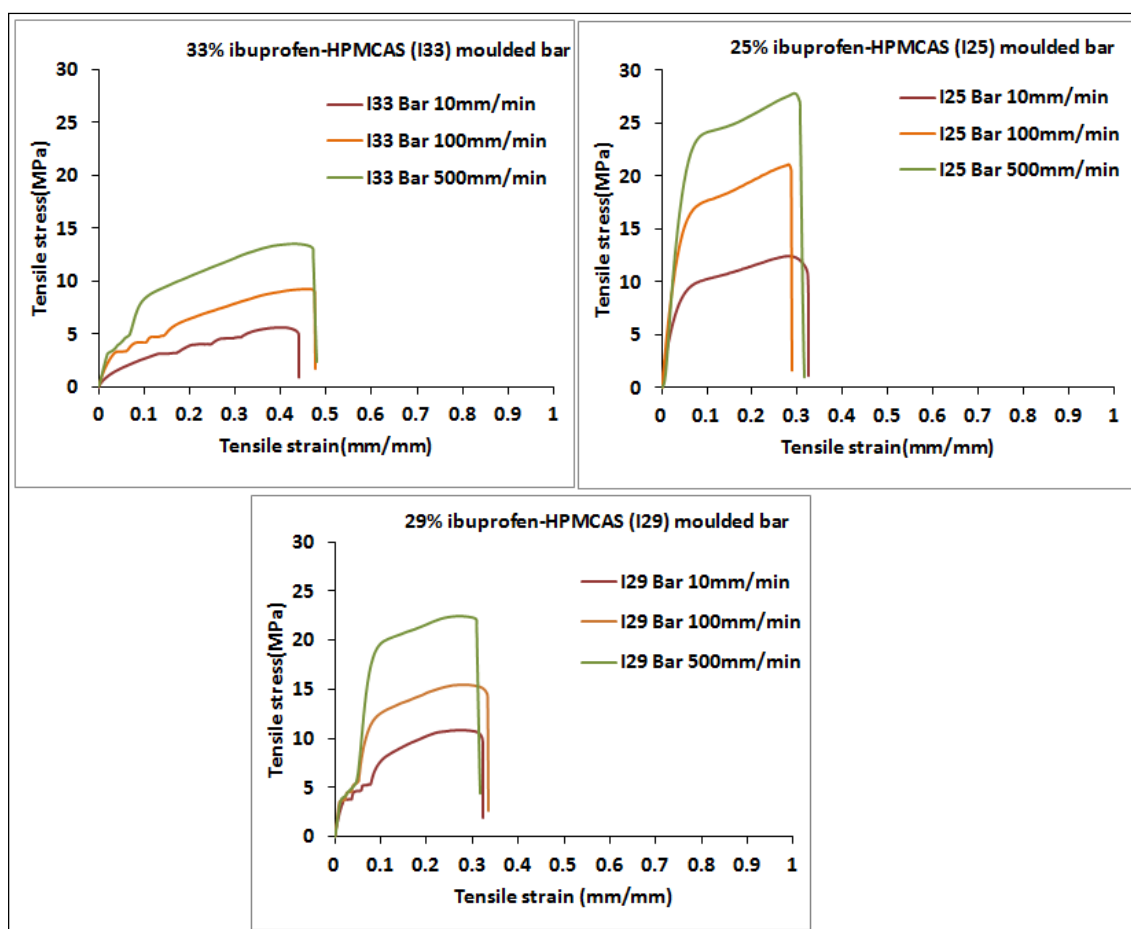
Figure 5.4: Stress-strain curve of injection moulded Ibuprofen-HPMCAS bar at ambient (RT) conditions

When comparing the I33 and the I25 mouldings at all experimental condition, the I25 moulded bars exhibited higher tensile strength and modulus than the I33 mouldings (Figure 5.4)

Table 5.3: Mechanical properties of injection moulded Bars

Batch	Extension Rate(mm/min)	Tensile Strength (MPa)	Young Modulus (MPa)	Extension at Break (mm)
I33 mould	10	5.68	35.57	14.53
	100	9.29	44.82	15.65
	500	14.84	74.43	15.41
I 29 mould	10	11.86	75.75	10.33
	100	14.07	98.59	10.50
	500	23.24	386.99	9.21
I 25 mould	10	13.31	135	10.04
	100	21.11	320	10.02
	500	27.84	447	10.03
IM33 mould	10	2.71	13.20	27
	100	5.90	22.84	24.03
	500	8.25	38.80	21.78

Low strength and stiffness in the case of the I33 mouldings can be explained by the plasticisation effect of the ibuprofen on HPMCAS. Plasticisation significantly changed the mechanical properties of the moulded bar as shown in the stress-strain curve Figure 5.4. The higher level of plasticiser decreased the strength and modulus, but increased extension at break indicating the flexible nature of the I33 mouldings compared to the I25 mouldings. The rate of deformation also has a significant effect on the mechanical behaviour of both I33 and I25 mouldings. For example, when I25 mouldings were extended at a low (10mm/min) rate it exhibited low strength (13.31MPa) and modulus (135MPa) however, when extended at moderate (100mm/min) to high (500mm/min) rate showed an increase in strength (27.84 MPa) modulus (447MPa) as shown in Table 5.3. The I29 moulded bar exhibited the tensile strength and modulus in

between the I33 and I25 mouldings. These results confirmed that the mechanical properties of Ibuprofen-HPMCAS injection moulded systems are dependent on the percentage of ibuprofen, which is responsible for the plasticisation of HPMCAS.
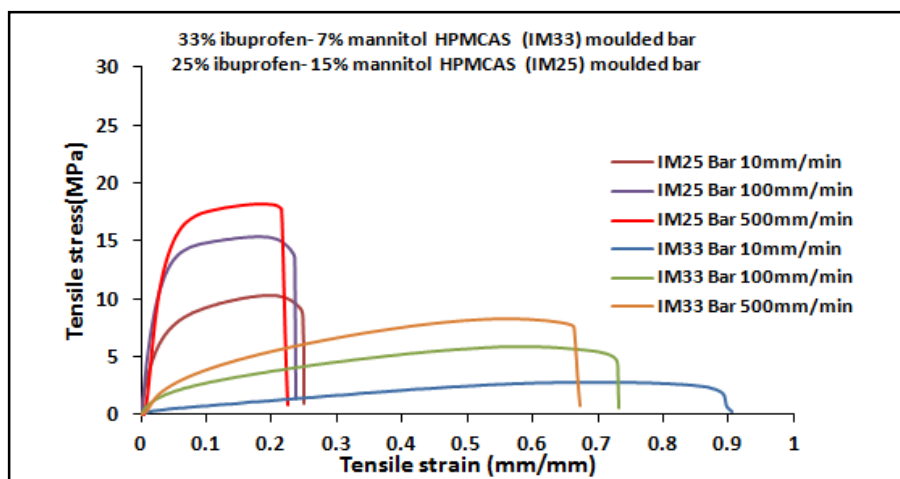
Figure 5.5: Stress-strain curve of injection moulded Ibuprofen-mannitol-HPMCAS bars at ambient (RT) conditions

Furthermore, different concentration of mannitol in the systems further decreased Young's modulus and ultimate tensile strength of the bar with increase in an extension at break. This confirms the of effect addition of a low Tg (7.4°C) substance manntiol on the mechanical properties of the bar (Yoshinari et al., 2003). When I33 bar compared with IM33 bar contains the same concentration of ibuprofen in the system except latter consists of 7% mannitol. The addition of mannitol had a significant effect on the mechanical strength of the bar where tensile strength and modulus of IM33 bar was reduced to approximately half than the I33 bar (Table 5.3). This indicates mannitol gets slightly dissolved in the molten mass of ibuprofen-HPMCAS at processing temperature (100°C). The stress-strain curve of IM33 and IM25 at all extension rates is presented in the

Figure 5.5. This clearly shows higher modulus and strength of IM 25 than IM33 where, higher ibuprofen decreased mechanical properties of the bar.

5.1.2.3 Raman Spectroscopy

A Raman spectrum in the 50–150 cm^{-1} regions contains information about vibrations and translations of the entire molecule in the lattice providing an indication of the level of crystallinity. These vibrations are characteristic of the crystal structure and sensitive to local order or disorder (Saerens et al., 2011). The spectra obtained from the fingerprint region (600-1800 cm^{-1}) composed of intra-molecular vibrations distinctive of atomic bonds, molecular conformations and the close molecular neighbouring (Hedoux et al., 2011). Ibuprofen shows a Raman band at 1608 cm^{-1} corresponding to a characteristic crystalline band (Figure 5.6). However, when ibuprofen is dissolved in solvent or processed as a hot melt extrudate with PVP it shows a peak at 1613 cm^{-1}. This shift to 1613 cm^{-1} is indicative of a molecular dispersion of ibuprofen in the polymer system (Breitenbach et al., 1999). The hot melt extruded pellets and injection moulded tablets displayed, this characteristic shift where the ibuprofen peak shifts to a higher wavelength of 1613 cm^{-1} (Figure 5.7 and Figure 5.8). This confirms that the ibuprofen has formed a molecular level dispersion with HPMCAS when processed into melt extruded pellets and injection moulded tablets.

HPMCAS shows -C=O bond stretching vibrations at 1745cm^{-1} and ibuprofen shows -C=O bond stretching at 1655 cm^{-1}. Ibuprofen shows the aryl -C=C stretching at two positions; 1575 cm^{-1} and 1608 cm^{-1} (Figure 5.9 and Figure 5.10) whereas mannitol does not show any Raman band in this region as it neither contains a carbonyl functional group nor an aromatic ring.
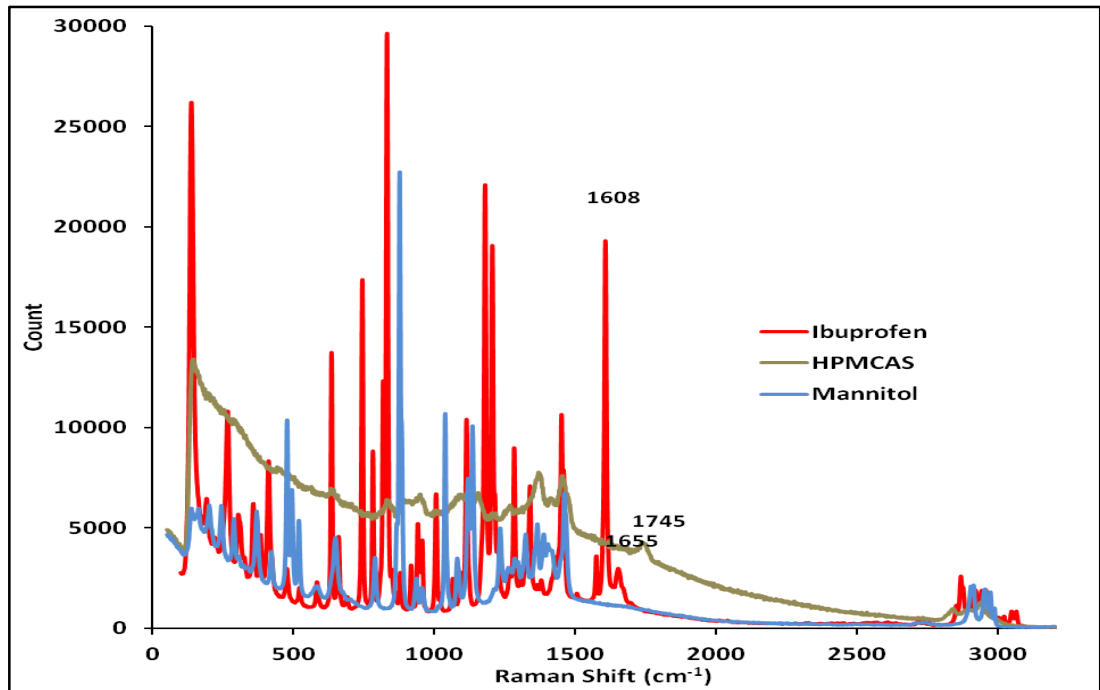
Figure 5.6: Raman spectra of pure ibuprofen, HPMCAS-LF and mannitol
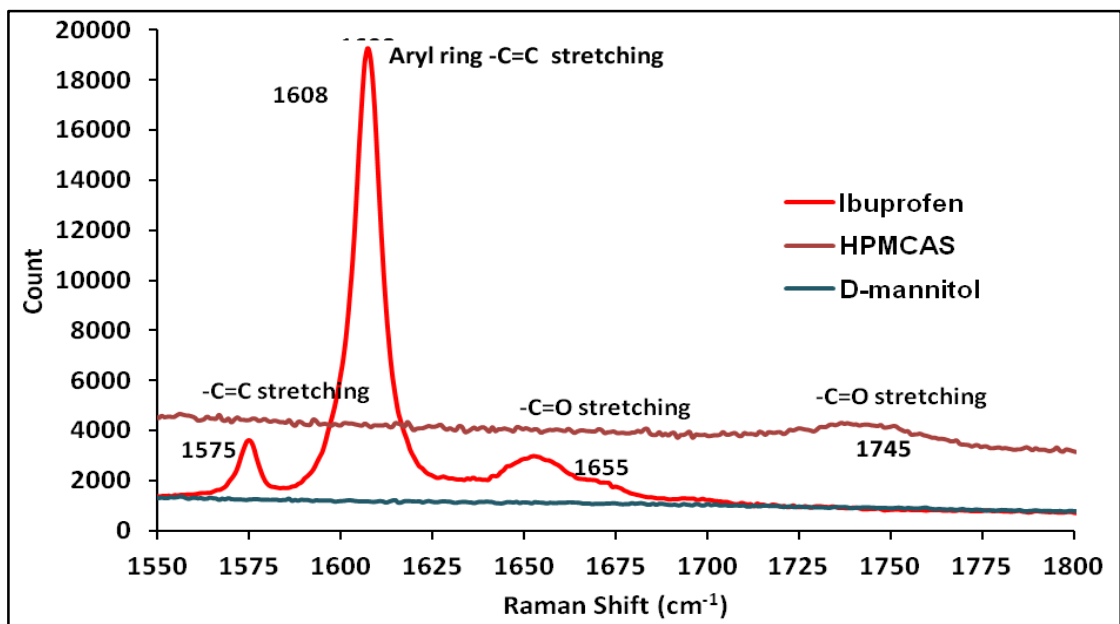
Figure 5.7: Raman spectra of pure ibuprofen, HPMCAS and mannitol (1550-1800cm^{-1})

Raman spectra of physical mixtures of ibuprofen 33%w/w ibuprofen-HPMCAS (I33 physcial mix) showed the Raman band of functional groups present in both the ibuprofen and the HPMCAS molecules (Figure 5.9). The analysis of extruded pellets and injection moulded tablet showed distinct shifts in the Raman spectrum in the 1550 to 1800 cm^{-1} region which corresponds to the fingerprint region of a drug molecule. The pure crystalline ibuprofen and the ibuprofen present in a physical mixture shows two distinct Raman band first, 1608 cm^{-1} corresponds to aryl –C=C stretching and second, 1650cm^{-1} bond corresponds to – C=O stretching vibrations . The hot melt extruded pellets (Figure 5.8) and injection molded tablets (Figure 5.9) showed a distinct peak shift at both positions. The ibuprofen crystal phase I (form I) exhibits Raman band at 1608cm^{-1} while Heduox et al. have reported Raman spectra of the low melting metastable phase II (form II) and glassy state, both exhibit the Raman band at 1613 cm^{-1}, this attributed to the similar local order in glassy (amorphous) and metastable states (Hedoux et al., 2011).
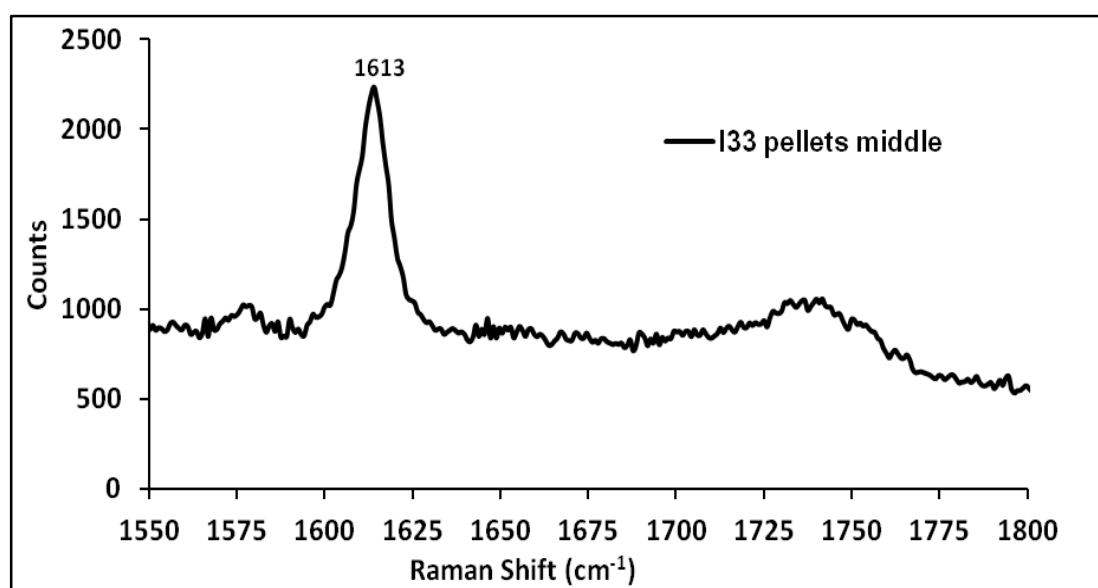
Figure 5.8: 33% ibuprofen HPMCAS melt extruded pellets (I 33 pellets)
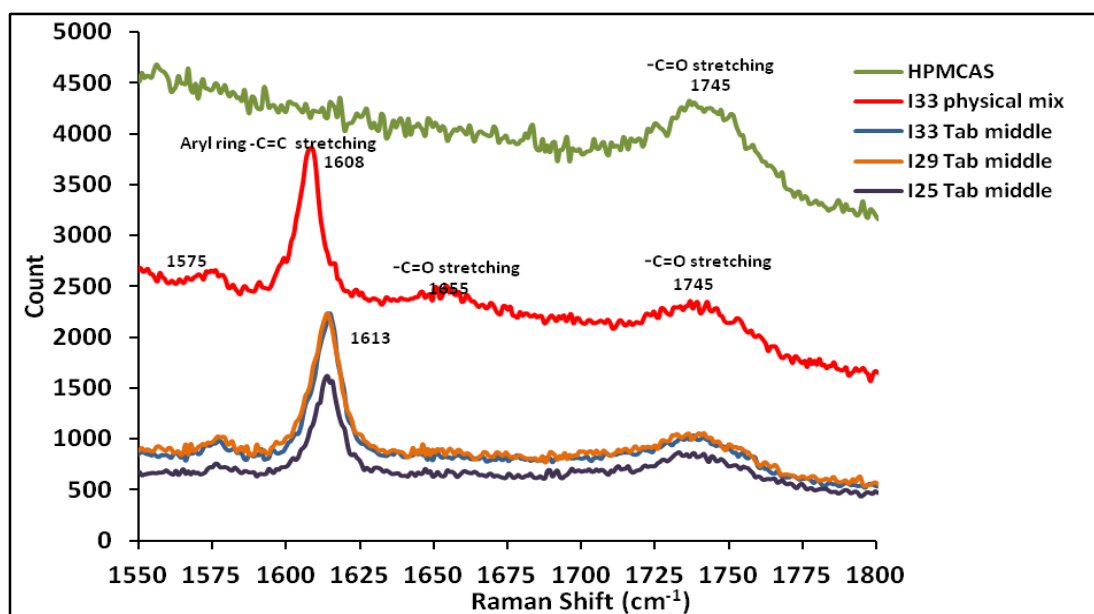
Figure 5.9: Raman shift for Ibuprofen-HPMCAS injection moulded tablets (spectra's taken after 24 hr storage at RT)
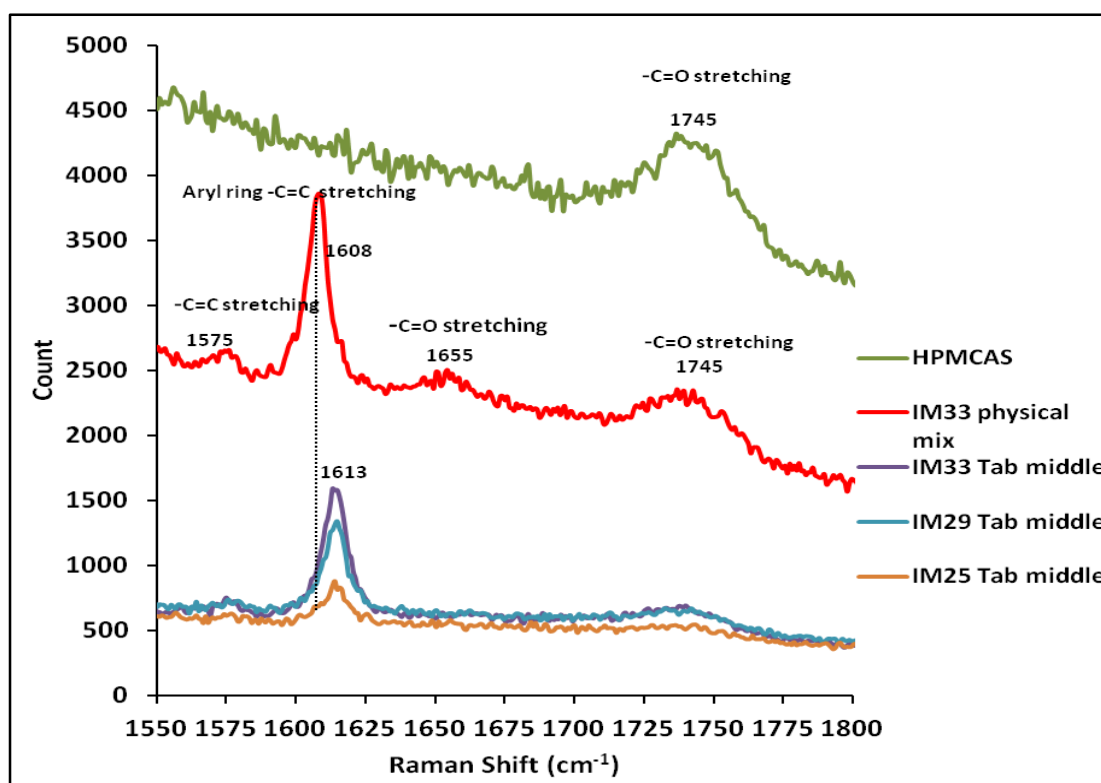
Figure 5.10: Raman shift for Ibuprofen-mannitol HPMCAS injection moulded tablets (spectra's taken after 24 hr storage at RT)

Rossi et al. have also studied vibrational properties of Ibuprofen-β cyclodextrin (CD) inclusion complexes using Raman scattering and explained the

numerical calculations. The region between 1550 to 1750 cm^{-1} was selected to understand the complexation induced changes in the ibuprofen spectrum. The complexation of ibuprofen with β-CD also showed the shift to 1613 cm^{-1} from 1608 cm^{-1} this effect was explained due to the involvement of atom belonging to the aryl ring -C=C group of ibuprofen was affected by the complexation process (Rossi et al., 2009). Similar shifts in the melt extruded pellets and the injection moulded system suggest the formation of the disordered (amorphous) state. The mannitol containing injection moulded system (IM) showed similar behaviour (Figure 5.10).

Carbonyl stretching of ibuprofen was seen at 1655 cm^{-1} due to the presence of ibuprofen dimer (two caboxylic acid functional groups of ibuprofen form a H-bond). The frequency downshift of this band was reported as a result of complexation. The extruded pellets and injection moulded system does not show the band at 1655 cm^{-1}. It confirms the absence of a dimer between carboxylic acid functional groups of two ibuprofen molecules, rather, showed the large higher frequency shift to 1745 cm^{-1} in the same region as HPMCAS indicates the formation of a H-bond between the ibuprofen and HPMCAS (Figure 5.9)

A comparison between spectra obtained from the surface and middle part of the tablets revealed an important phenomenon of surface crystallisation of ibuprofen from injection moulded tablets. A sample from the middle section of the tablet exhibited a Raman band at 1613.04 cm^{-1} however, surface samples exhibited at 1608.52 cm^{-1} with an increase in the relative intensity of the Raman band. Moreover, the localization -C=O stretching was seen at 1655 cm^{-1} (Figure 5.10 and Figure 5.11 Figure 5.12). The back shifts of Raman bands and increased

relative intensity of peaks confirms the surface crystallisation of amorphous ibuprofen. Langkilde et al. have also explained the differences between Raman spectra from different crystal forms of a compound, or between crystalline and amorphous forms (Langkilde et al., 1997) .
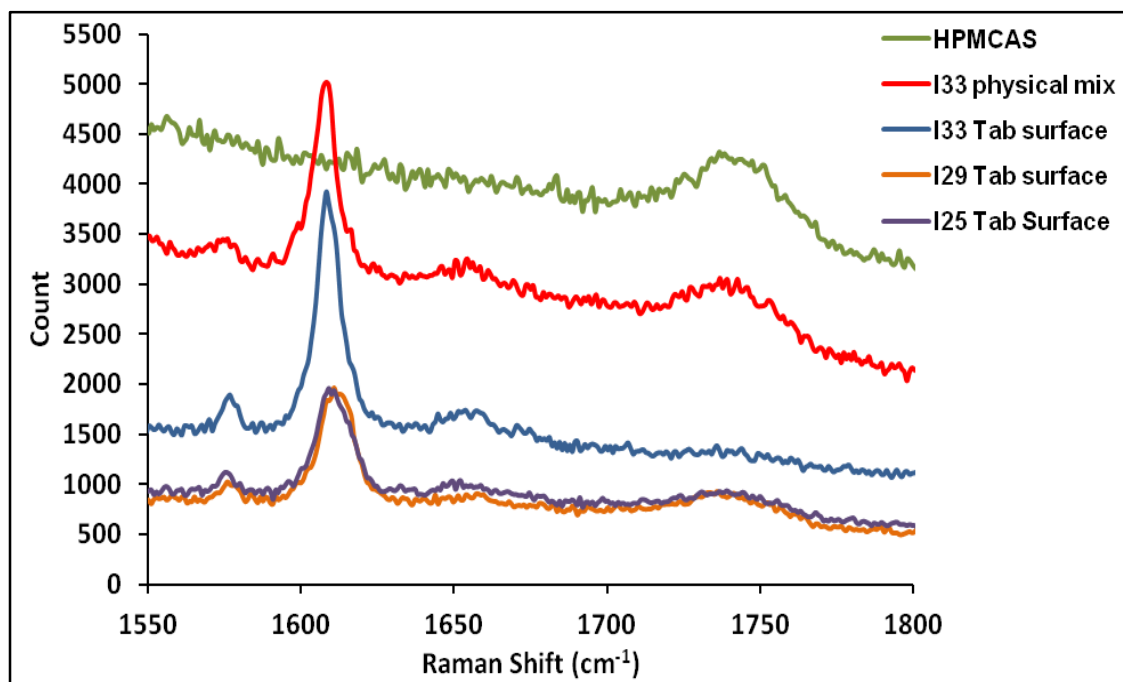
Figure 5.11: Surface spectra of Ibuprofen-HPMCAS injection moulded tablets (spectra's taken after 24 hr storage at RT)

The Figure 5.13 shows the clear difference in the Raman spectra of the surface crystallised tablets and the middle amorphous core. The difference in the spectrum indicates that ibuprofen dispersed inside the polymer matrix is in amorphous state, whereas phase separation leads to crystallisation on the surface.
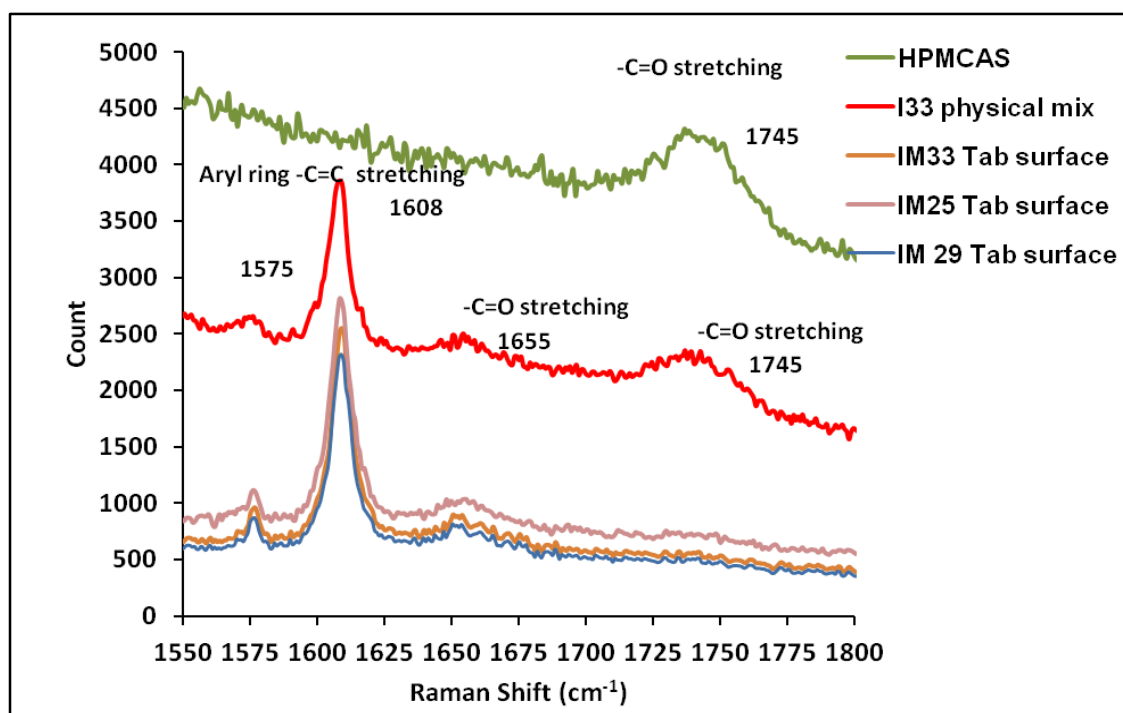
Figure 5.12: Surface spectra of Ibuprofen-mannitol-HPMCAS injection moulded tablets (spectra's taken after 24 hr storage at RT)
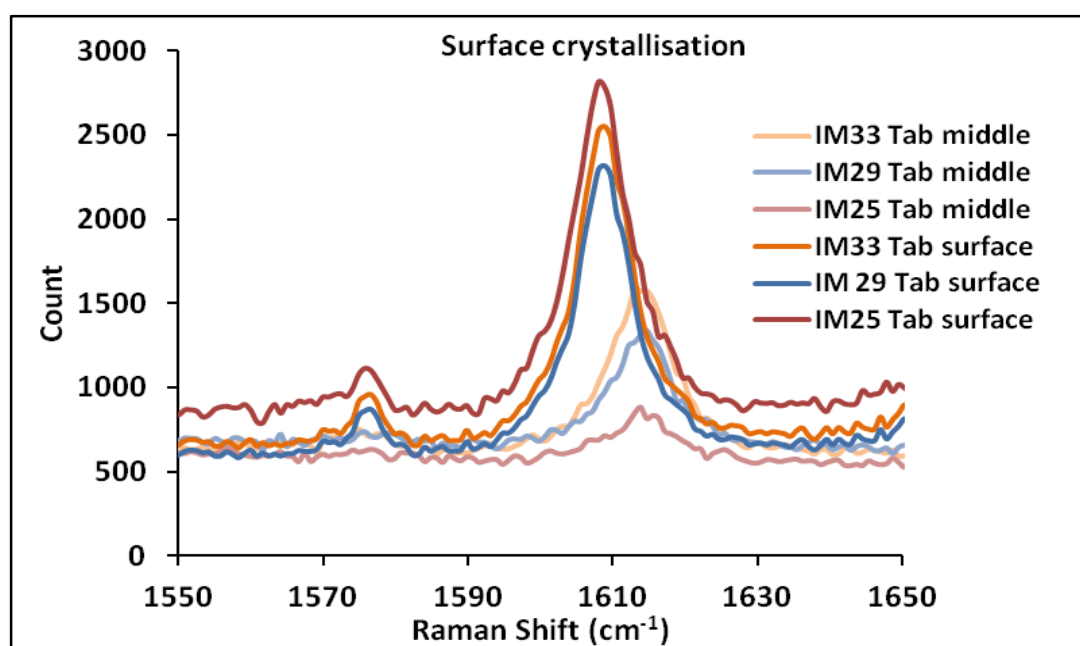
Figure 5.13: Surface crystallisation from injection moulded tablets (spectra's taken after 24 hr storage at RT)

152

5.1.2.4 Raman spectroscopy: Moisture induced surface crystallisation

Although the amorphous molecular dispersion of ibuprofen was achieved in HPMCAS through HME and IM processes, surface crystallisation was observed. It was important to understand the surface crystallisation under different humidity conditions at a constant temperature as moisture favours the crystallisation. Ibuprofen shows a crystalline band at 1608 cm^{-1} and the shift in this peak to 1613 cm^{-1} is indicative of a molecular level dispersion of the ibuprofen (Breitenbach et al., 1999). When moulded tablets were exposed to the different RH the shift back to 1608 cm^{-1} was observed with increased peak intensity over the period which confirms the tendency of amorphous drug to surface crystallise with moisture. Tablets exposed to 75%RH showed a higher relative peak intensity of 1608cm^{-1} peak than 43%RH (Figure 5.14). This suggests a higher crystallisation rate at 75% as well as the sensitivity of Raman signal to the degree of crystallinity. According to Langkilde, the differences in the Raman spectra can be seen for the different crystal and/or amorphous forms. These studies showed that amorphous, nanocrystalline and microcrystalline forms of ketoprofen showed an increase in the relative intensity of peaks as particle size increases (Langkilde et al., 1997).
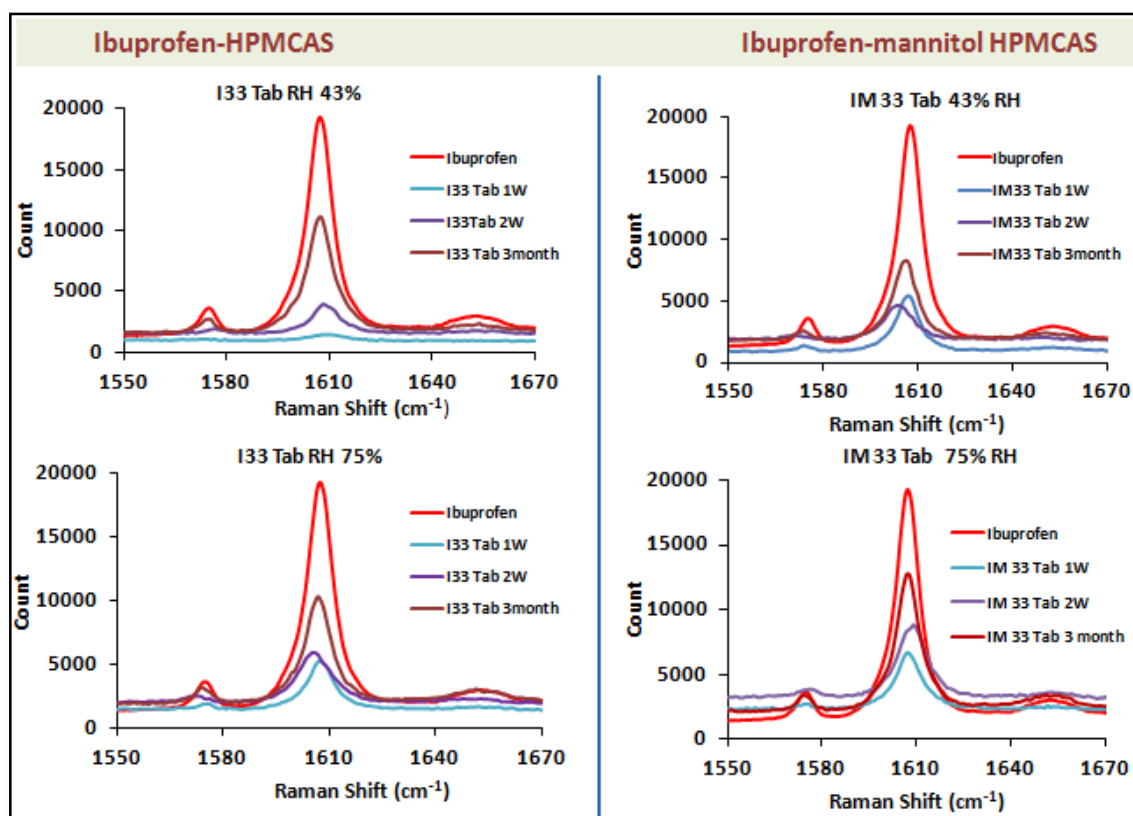
Figure 5.14: Raman spectra- moisture induced surface crystallisation

5.1.2.5 FTIR

Infrared (IR) spectroscopy deals with the Infrared region of the electromagnetic spectrum. Mid-IR, ranging approximately ranging from 4000–400 cm^{-1} (2.5–25 μm), is used to characterise the fundamental vibrations and associated vibration-rotations of a molecule. IR spectroscopy is a well established technique for characterising inter-molecular interactions such as hydrogen bonding (H-bond) (Jeffrey, 1997) (Murthy and Rao, 1968) and has been extensively used to understand the drug-polymer interactions in amorphous dispersions (Taylor and Zografi, 1997; Taylor and Zografi, 1998) ((Miyazaki et al., 2004; Weuts et al., 2005). In general, the H-bond between a drug and polymer can be formed when there is one proton donor and a proton acceptor. If these hetero interactions between drug and polymer differ in strength or extent relative to the self association of these systems, then that change will be reflected by a

154

change in peak position and shape of the IR spectrum for the functional groups in the specific interactions (Kestur et al., 2011)

Bras et al. studied the molecular motions in the amorphous ibuprofen using broadband dielectric spectroscopy (BDS), in order to probe inter-molecular H-bonding between the ibuprofen molecules. The IR spectroscopy was used to analyse both supercooled liquid (amorphous) and crystalline ibuprofen. The free C=0 group of carboxylic acid has a characteristic frequency of 1760 cm^{-1} appears as a sharp peak and in the presence of hydrogen bonds, these stretching is perturbed and shifts to lower wave numbers (1700-1725 cm^{-1}) (Bras et al., 2008) (Silverstein et al., 1981). When FTIR studies on supercooled (amorphous) and crystalline ibuprofen were done by Bras et al. it was observed that both amorphous and crystalline ibuprofen showed a downward shift at C=O stretching. The authors concluded that ibuprofen molecules in both phases exist almost in the form of hydrogen bonded aggregates (Bras et al., 2008). However the major difference seen was lowering the peak intensity and broadening of bands in the spectrum for the amorphous phase due to disorder or a less organised structure. The frequency shift at other positions in IR also gives valuable information on the amorphous phase formation and H-bond involvement.
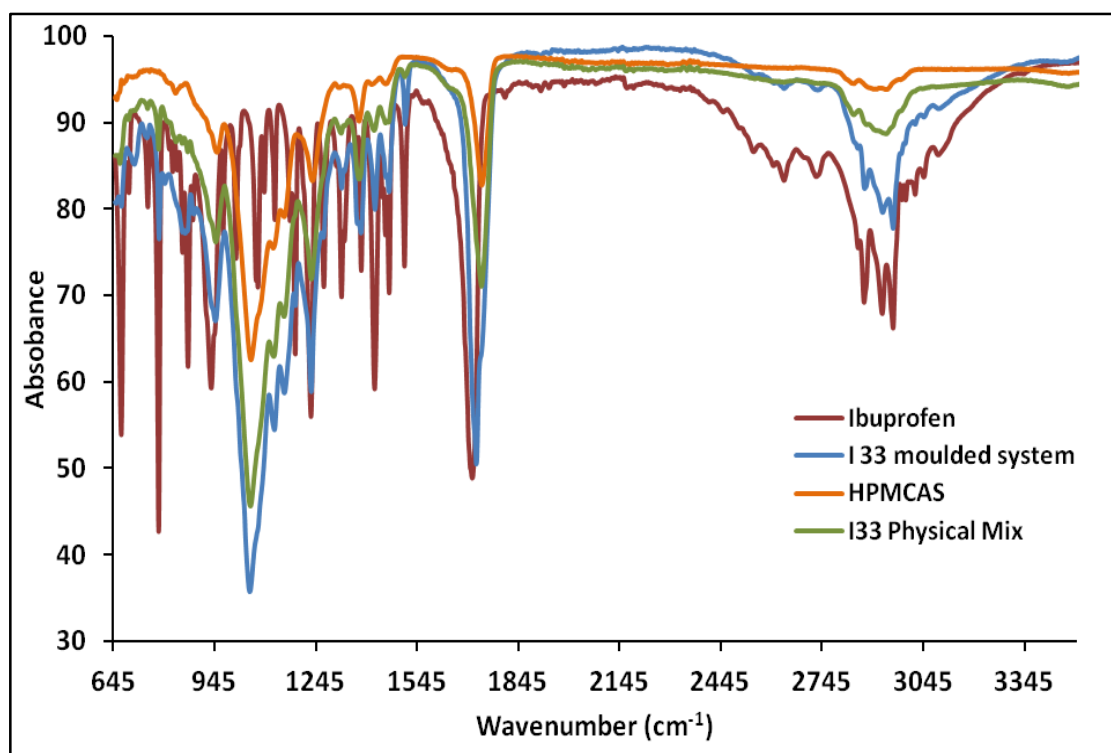
Figure 5.15: FTIR spectra of pure ibuprofen, HPMCAS, 33% Ibuprofen HPMCAS physical Mix (I33), 33% ibuprofen-HPMCAS moulded system

In the case of ibuprofen-HPMCAS systems, the pure crystalline ibuprofen showed a peak at -C=O stretching at 1708cm-1 and pure HPMCAS showed carbonyl stretching at 1735cm-1 this clearly indicates ibuprofen formed a inter-molecular H-bond within ibuprofen molecules (dimer) and the presence of a free -C=O group in the case of HPMCAS (Figure 5.15, Figure 5.16b). Vueba et al. assessed the conformational stability of ibuprofen using vibrational spectroscopy by both Raman and FTIR and marked the positions of functional group (Vueba et al., 2008). IR peaks of pure ibuprofen, physical mixture and moulded systems are summarised in Table 5.4, where changes at peak positions are also mentioned. Ibuprofen-HPMCAS moulded (I33) system showed -C=O stretching at 1720 cm^{-1} and broadening in the region suggests the formation of H-bonds between Ibuprofen and HPMCAS Figure 5.16b. It might be because of the

formation of a dimer between and drug and polymer instead of two molecules of ibuprofen.
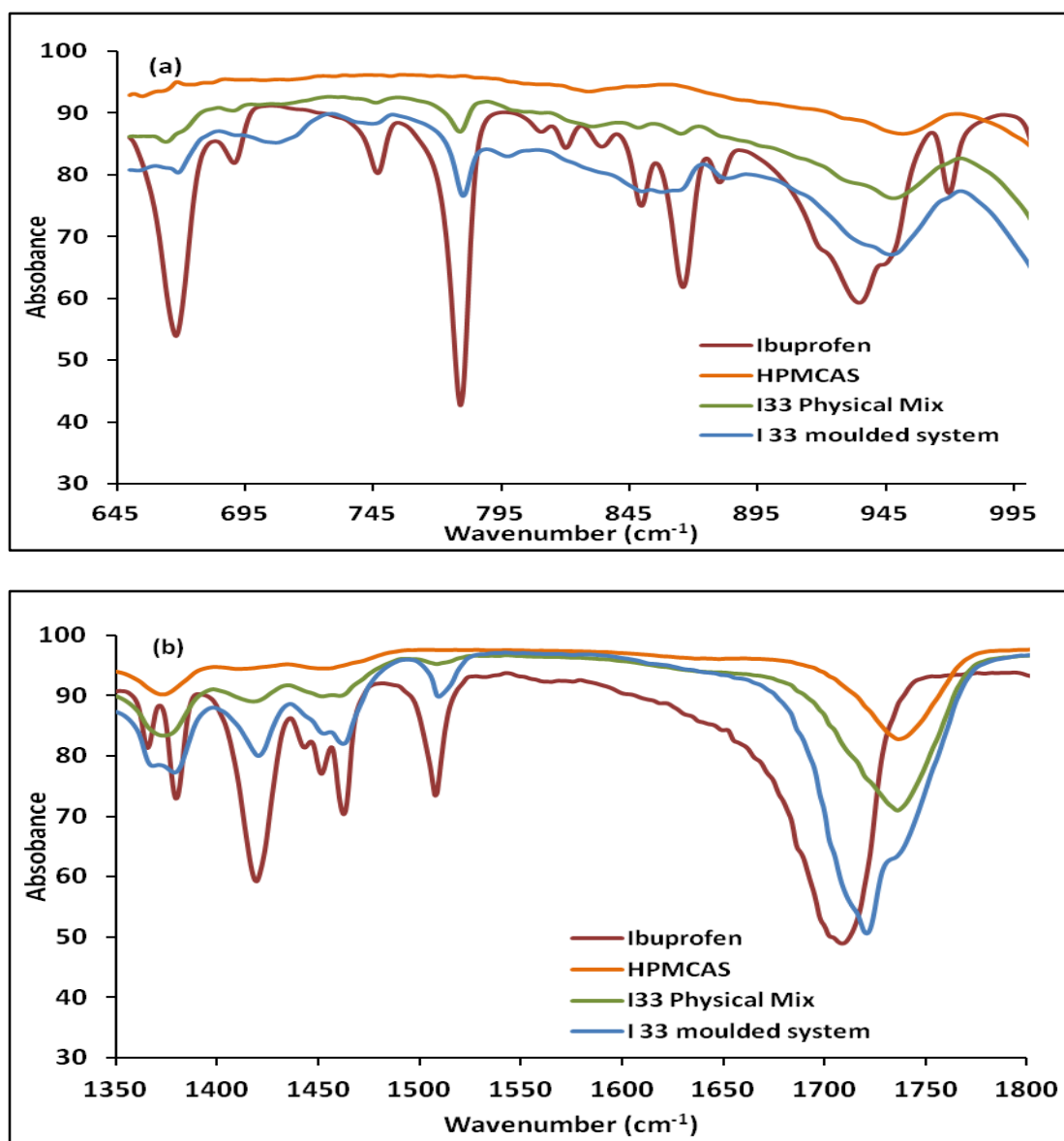
Figure 5.16: FTIR of Ibuprofen, HPMCAS, Ibuprofen-HPMCAS PM and I33 moulded system (a) 645 to 980 cm^{-1} region (b) 1350 to 1800 cm^{-1} region

Table 5.4: FTIR functional group of ibuprofen-HPMCAS

Functional group	Ibuprofen	Ibuprofen-HPMCAS Physical mix	Injection moulded tablets
CH$_3$ rock; C=O out-of-plane wagg	778	778	780
CH$_3$ rocking, CO-H bending(H-bonded)	921	944	950
CO-H bending(H-bonded)	1419	1419	1420
C-OH bending	1124	1124	1124
C-OH CO-H bending (H-bonded)	1231	1231	1231
C-OH bending modes	1365	1365	1365
CO-H bending (H-bonded)	1420	1420	1418
CH$_3$ Assymetic deformation	1462	1462	1462
C - C (aromatic) stretching	1507	1507	1509
C = O stretching	1708	1735	1720
C-OH bending modes	1365	1361	1361

The carbonyl stretching of surface samples of the I33 moulded systems after 7 day was observed at 1708 cm^{-1} whereas middle sample has shown at 1720 cm^{-1}. These results indicate surface crystallised ibuprofen caused the back shift due to dimer formation between two ibuprofen molecules (Figure 5.17 and Figure 5.18)
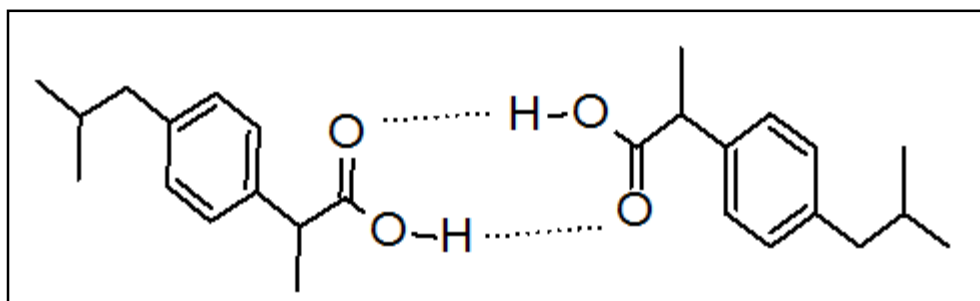
Figure 5.17: Ibuprofen dimer (H-bond)

Surface crystallised ibuprofen showed identical FTIR spectra to that of pure ibuprofen. When ibuprofen- polyethylene glycol(PEG) solid dispersions

were analyzed using FTIR, it was seen that ibuprofen formed a molecular level dispersion with PEG and showed the carbonyl band at higher wave number (1732 cm^{-1}). When the drug was dispersed at more than 50% wt ratio in a polymer, this showed a shift back to a lower wavenumber (1705 cm^{-1}). This has been interpreted as the saturation of the drug in a polymer and dimerisation of the ibuprofen becoming the precursor for crystallisation for the drug (Chan and Kazarian, 2006).
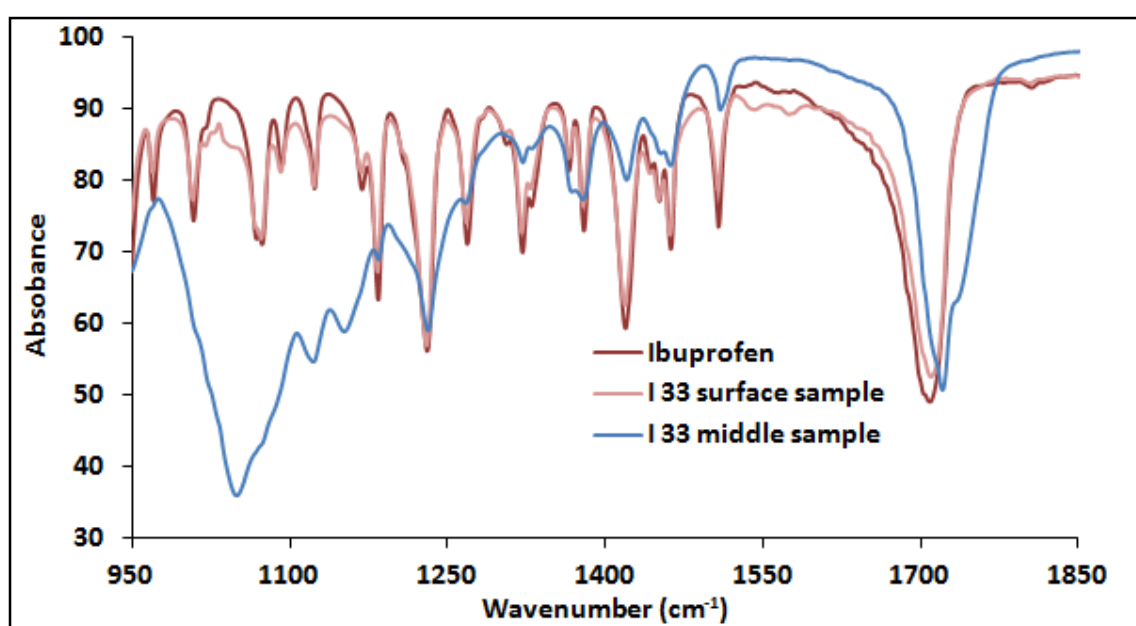
Figure 5.18: FTIR of I33 surface crystallised sample after 7 day at RT (945 to 1800 cm^{-1})

5.1.2.6 Hot stage microscopy

Microscopic studies on the I33 Tab (33% ibuprofen- HPMCAS Tab) in 0.1NHCL and in phosphate buffer pH 7.2 have provided an insight into the crystallisation behaviour of a dispersed amorphous drug during dissolution in the GI tract under non-sink conditions. Crystallisation of the ibuprofen was seen after 3hrs in the case of tablets immersed in phosphate buffer pH 7.2 (Figure 5.19). Poor wettability of the tablet surface was observed in the first hour which could be attributed to the hydrophobicity of the HPMCAS and the surface properties of moulded systems. A slight improvement in wettablility was observed in the case of tablets with dispersed mannitol however, a significant effect was only observed in the drug release rate, which will be described later. Tablets immersed in 0.1NHCL solution (pH 1.2) did not show any sign of the surface erosion and the absence of the surface crystals confirms the limited solubility of HPMCAS in an acidic environment (Figure 5.20). The HPMCAS has a pH dependent solubility and does not ionise below pH 5.5 therefore retards drug release at gastric pH and release the drug in the small intestine. The possibility of the ibuprofen crystallisation during dissolution under non-sink conditions was investigated using the microscopic studies.

33% Ibuprofen-HPMCAS (I33)tablets		
5min	30mins	30mins
120min	240 min	300 min
350 min	380 min	420 min
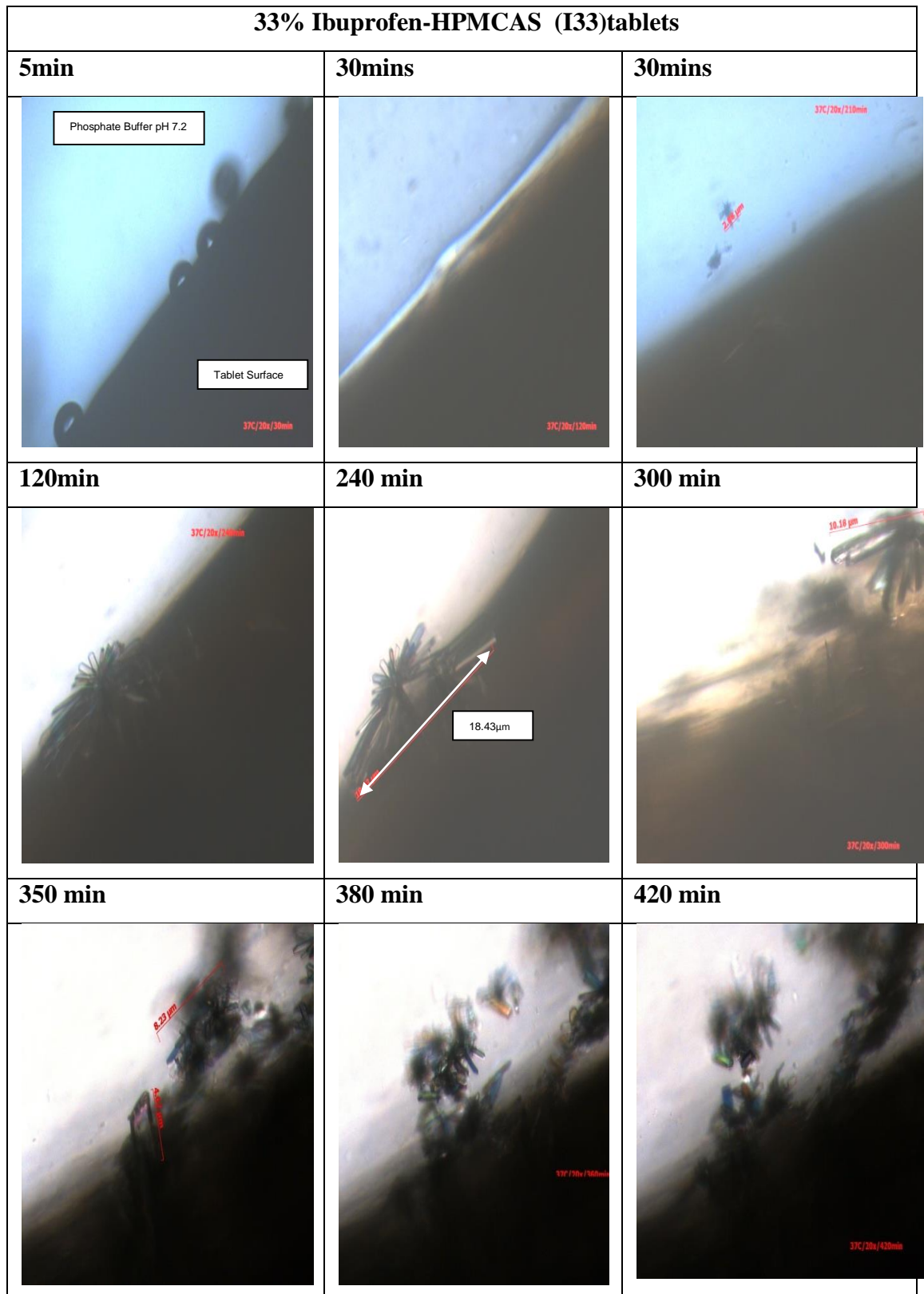
Figure 5.19: Hot stage microscopy: surface images of I 33 Tab (33% Ibuprofen- HPMCAS tablet) immersed in Phosphate buffer pH 7.2 at 37°C.

161

33% Ibuprofen-HPMCAS (I33)tablets		
5min	30mins	30mins
120min	240 min	300 min
350 min	380 min	420 min
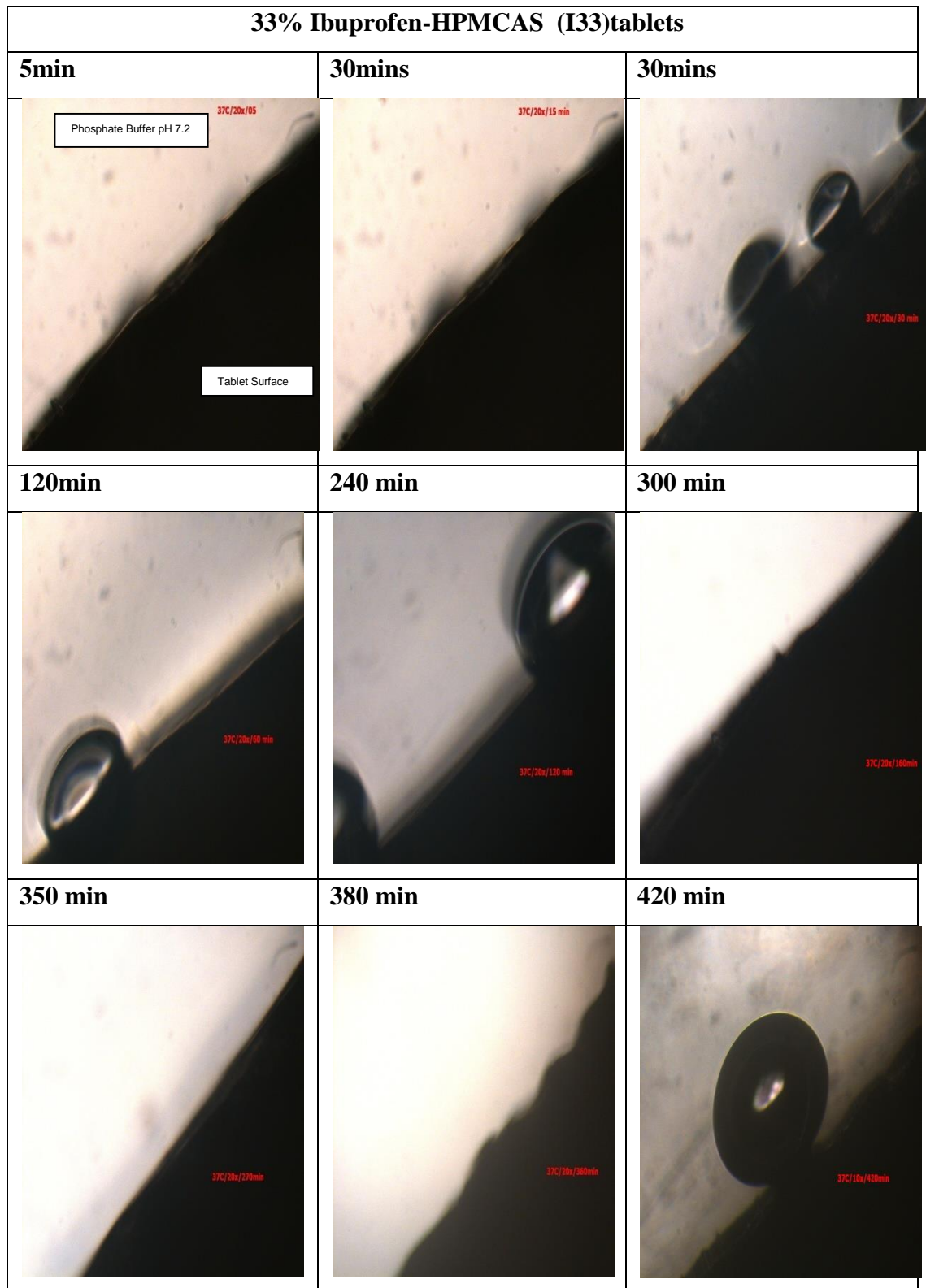
Figure 5.20: Hot stage microscopy: surface images of I 33 Tab (33% Ibuprofen- HPMCAS tablet) immersed 0.1N HCL at 37°C.

5.1.2.7   In-vitro release studies

Ibuprofen-HPMCAS and ibuprofen-mannitol-HPMCAS injection moulded tablets were subjected to the dissolution testing using USP II apparatus. The drug release from extruded pellets was also studied. Drug release from extruded pellets of ibuprofen (I33, I29, I25) and ibuprofen-mannitol-HPMCAS (IM33, IM29, IM25) batches in phosphate buffer showed the rapid release with almost 100% release in 2hrs in all the cases (Figure 5.21).
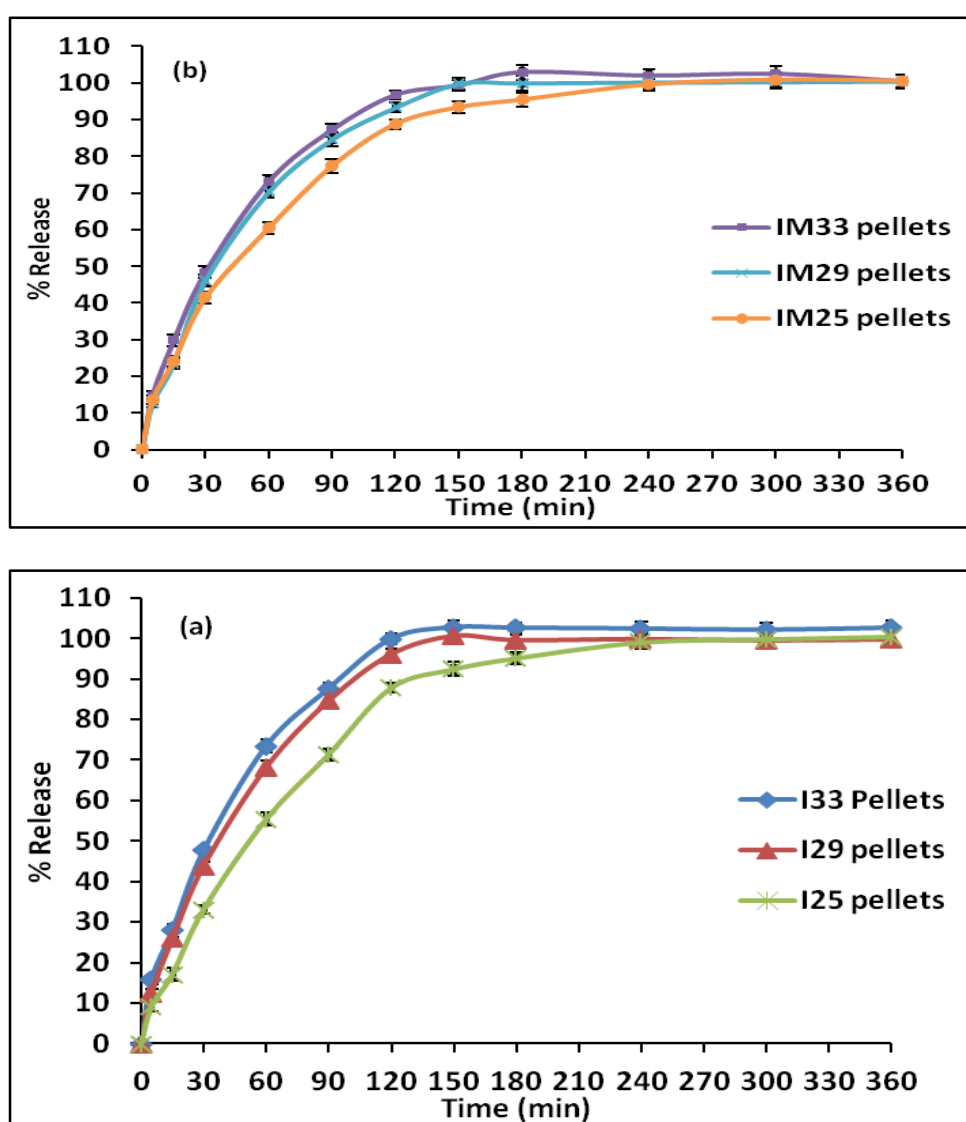
Figure 5.21: In-vitro release from extruded pellets of (a) Ibuprofen-HPMCAS and (b) Ibuprofen-mannitol HPMCAS in phosphate buffer pH 7.2 (n=3)

163

Tablet dissolution and drug-release in phosphate buffer pH 7.2 using USP II method showed erosion of the tablet surface rather than swelling and diffusion (Figure 5.23). Surface imaging of ibuprofen and ibuprofen mannitol tablets showed a smooth tablet surface (Figure 5.22). In vitro-dissolution after 3 and 6 hrs showed no signs of the pore formation in the case of ibuprofen tablets. However, tablets containing mannitol showed surface roughness and pore formation after 6hrs (Figure 5.24).

I33 Tab : 33% Ibu- HPMCAS

IM 33 Tab: 33% Ibu 7% mannitol - HPMCAS
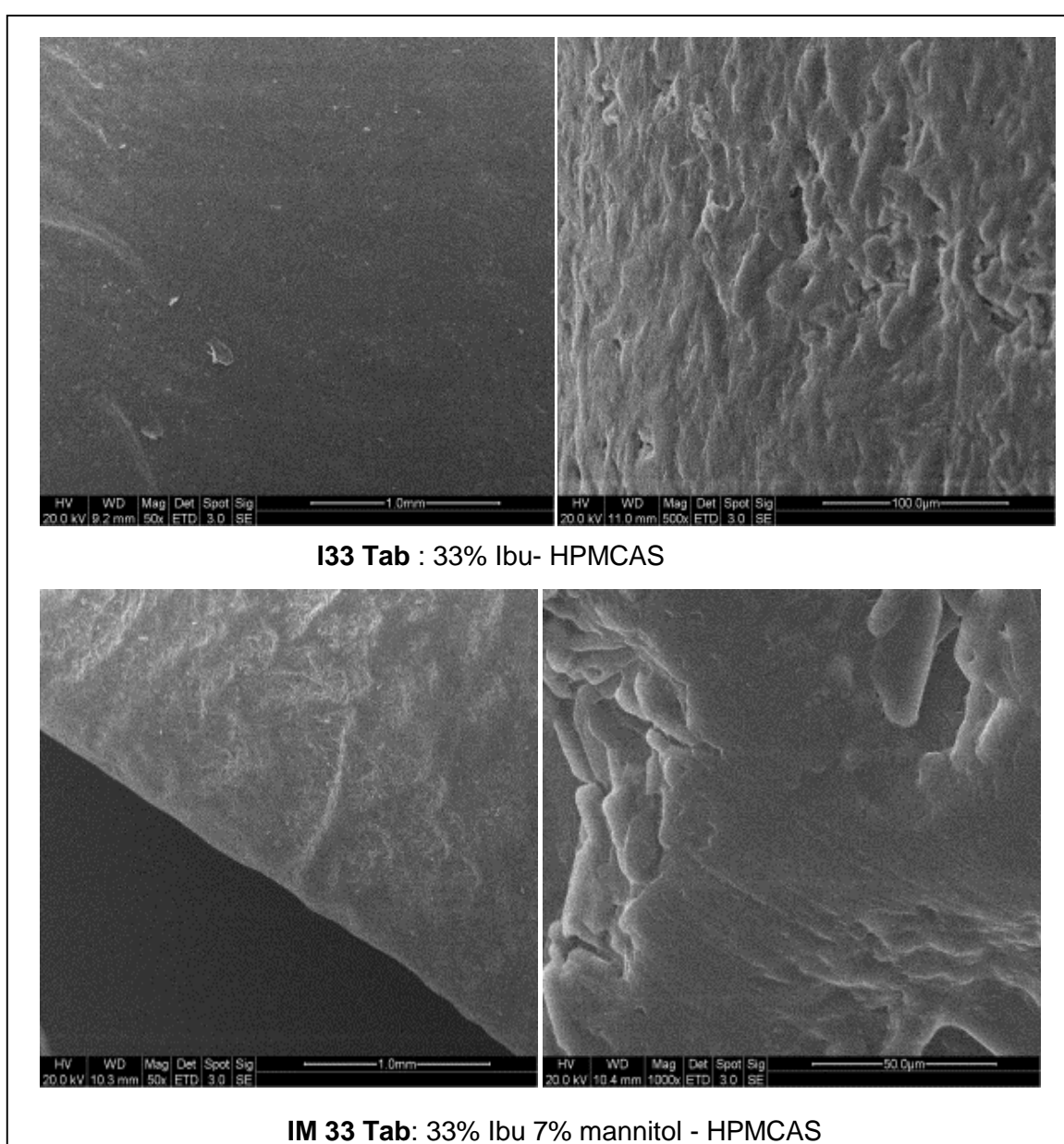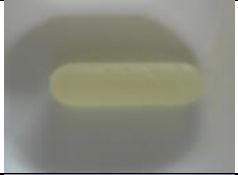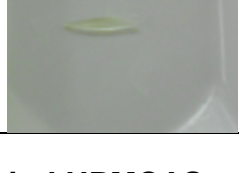
Figure 5.22: SEM surface images of I33 and IM33 tablet before dissolution

Time of tablet dissolution (min)	I33 Tab	I 29 Tab	I 25 Tab
0			
30			
60			
120			
180			
240			
300			
360			

(a) Ibuprofen-HPMCAS tablets

Time of tablet dissolution	IM33	IM29	IM25
0			
30			
60			
120			
180			
240			
300			
360			

(a) Ibuprofen-Mannitol HPMCAS tablets

Figure 5.23: (a) Ibuprofen Tablet: Tablet erosion and surface at specific time after dissolution (I33) (I29); (I25) Tab; (b) Ibuprofen mannitol Tablet: Tablet erosion and surface at specific time after dissolution (IM33); (IM29); (IM25)

Hydrophilic mannitol causes some pore formation during dissolution and thus accelerates the drug release from the moulded tablet. Moulded tablets showed slower release of ibuprofen as compared to pellets; where almost 50% drug release was observed in 150 mins and 80% release in 240 mins (Figure 5.25). 100% drug release was observed after 6 hrs for every injection moulded tablet. Ibuprofen tablets packed under the different packing pressures did not show any significant difference in the drug release (Figure 5.26).
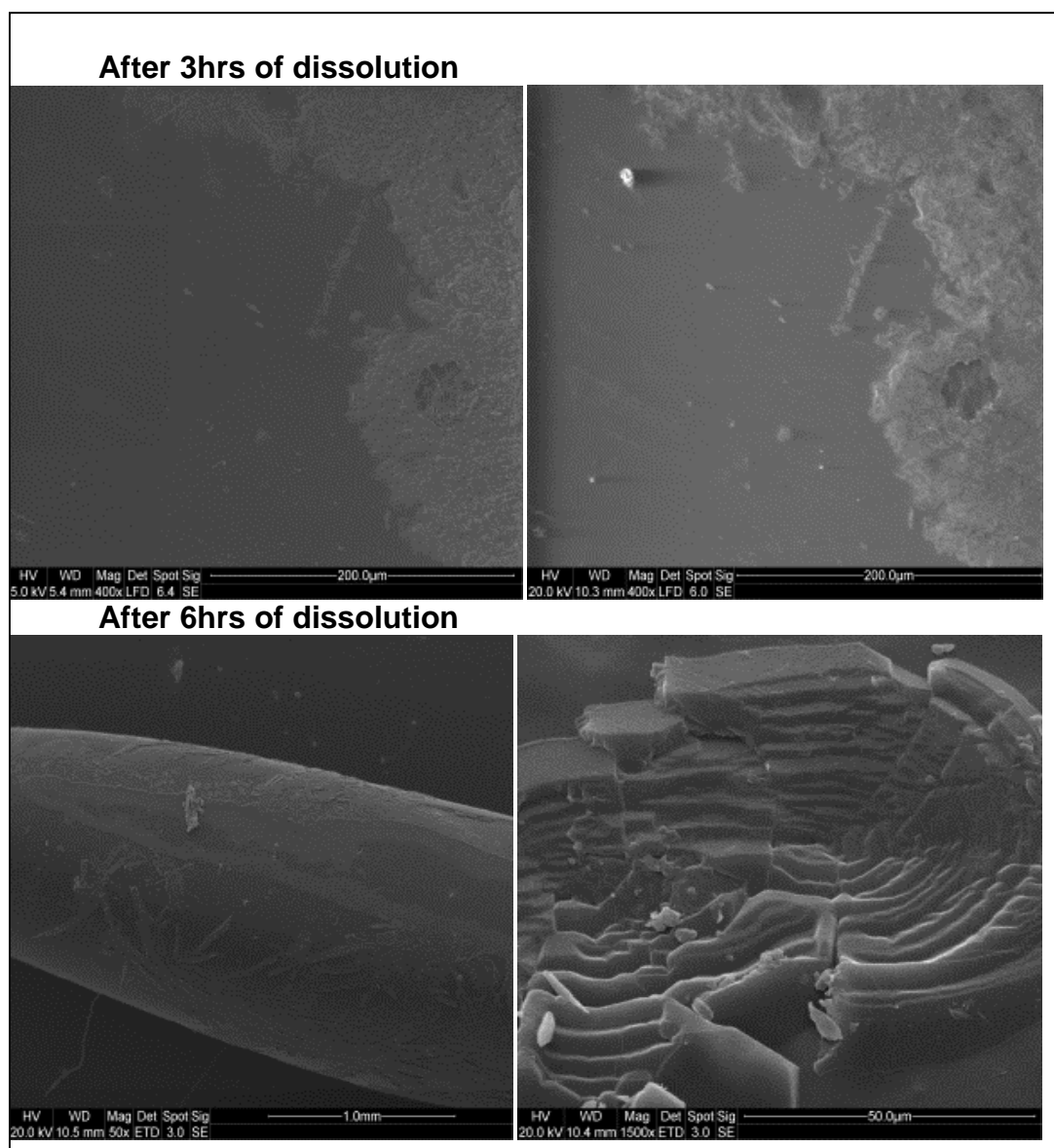
(a) I33 Tab: 33% Ibuprofen- HPMCAS Tab

After 3hrs of dissolution
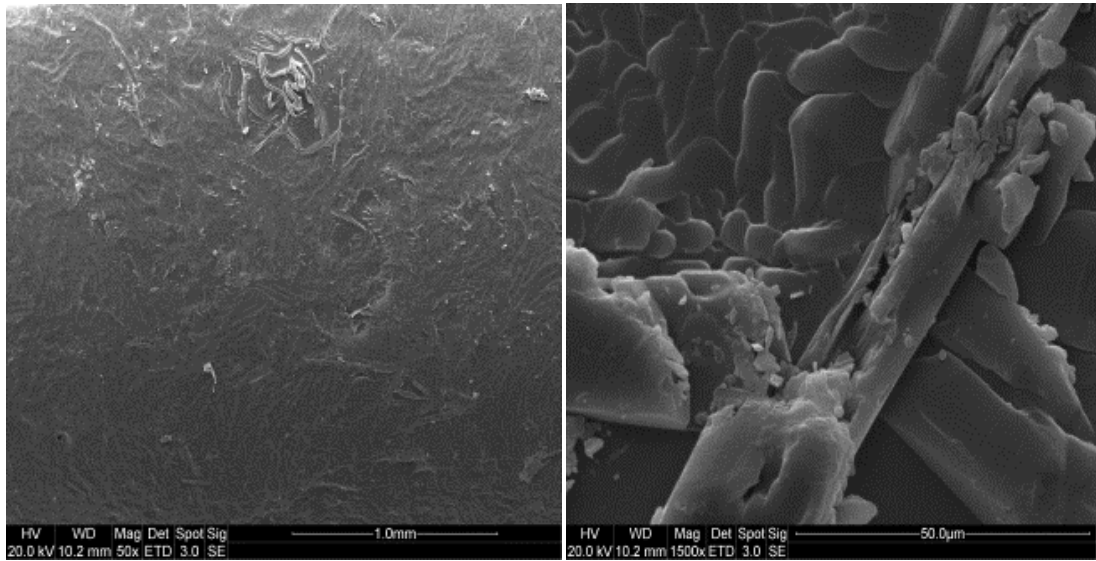
After 6hrs of dissolution
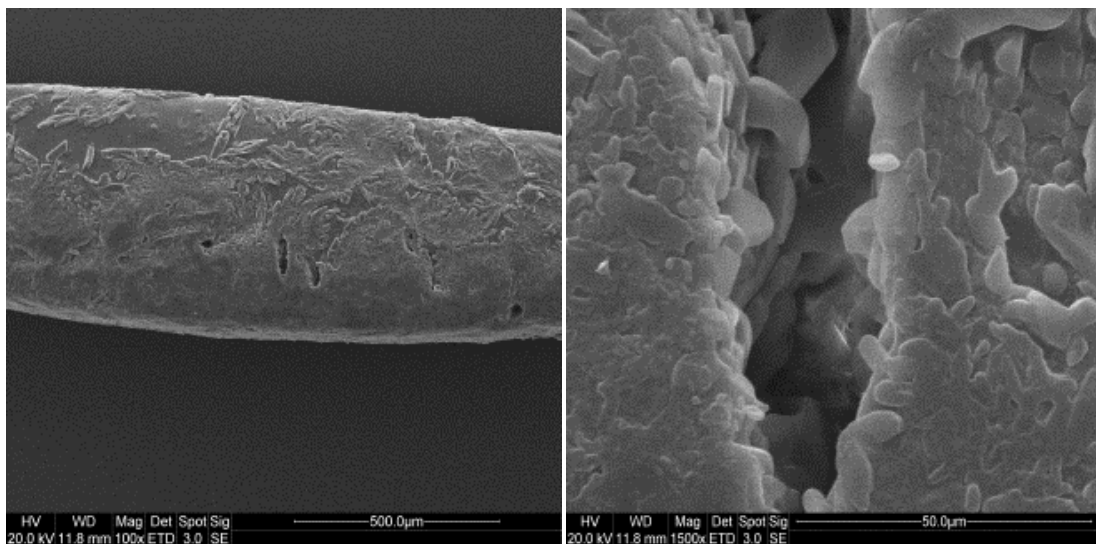
(b) IM 33 Tab: 33% Ibu, 7% mannitol - HPMCAS

Figure 5.24: SEM images of (a) I33 and (b) IM33 Tablet after in-vitro dissolution
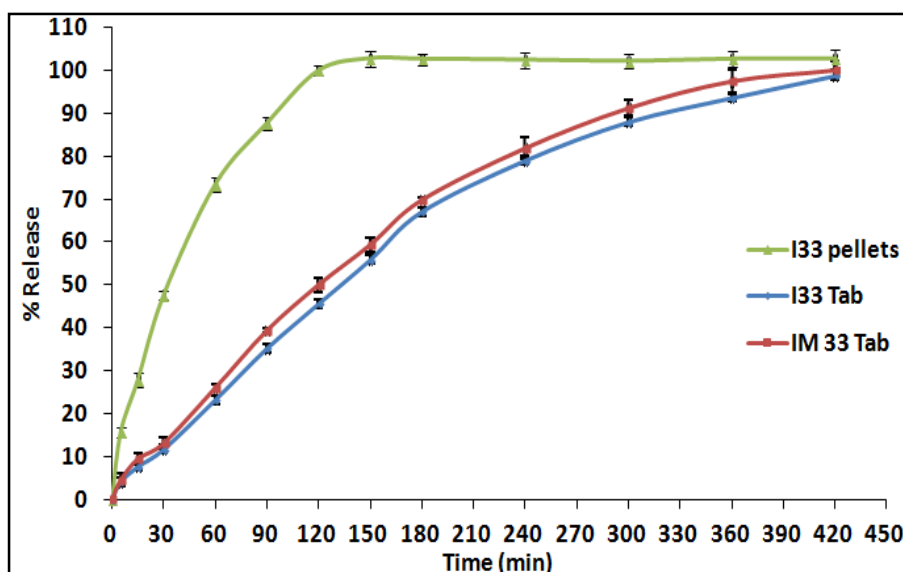
Figure 5.25: Drug release from 33% ibuprofen-HPMCAS systems: I33 pellets, I33 tablets and IM33 tablets in phosphate buffer pH 7.2 (n=6)

The controlled release behaviour of moulded systems can be explained by two reasons, firstly, hydrophobicity of HPMCAS and secondly, by densification during the injection moulding process. The nature of substituent's i.e methoxy and acetyl makes HPMCAS hydrophobic and hence the polymer surface shows poor wettability. The particle size had an influential effect on the drug release where smaller extruded pellets provided higher surface area during dissolution than injection moulded tablets.
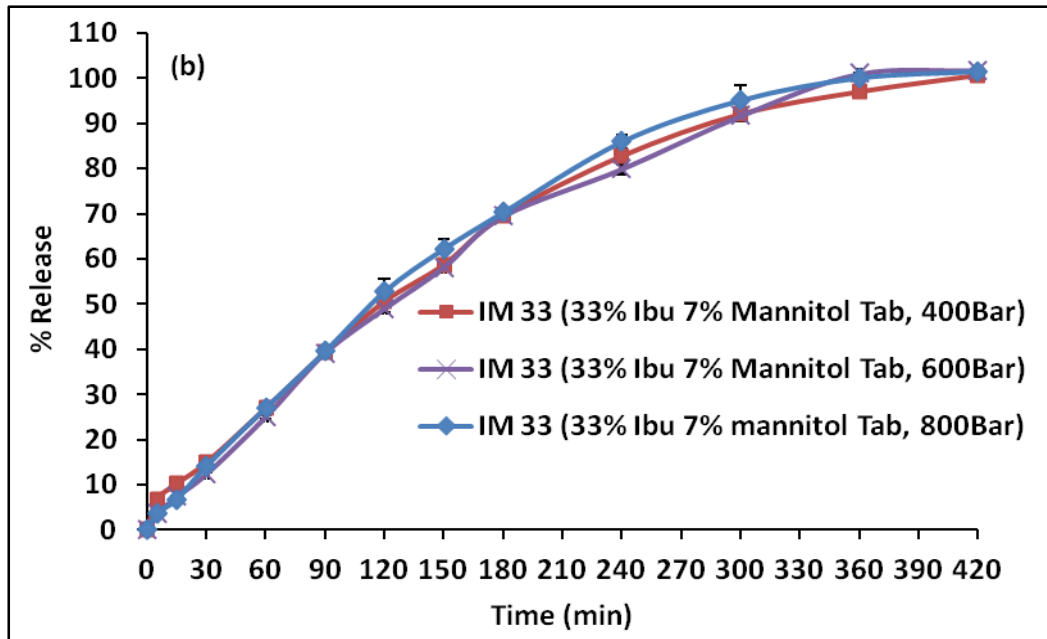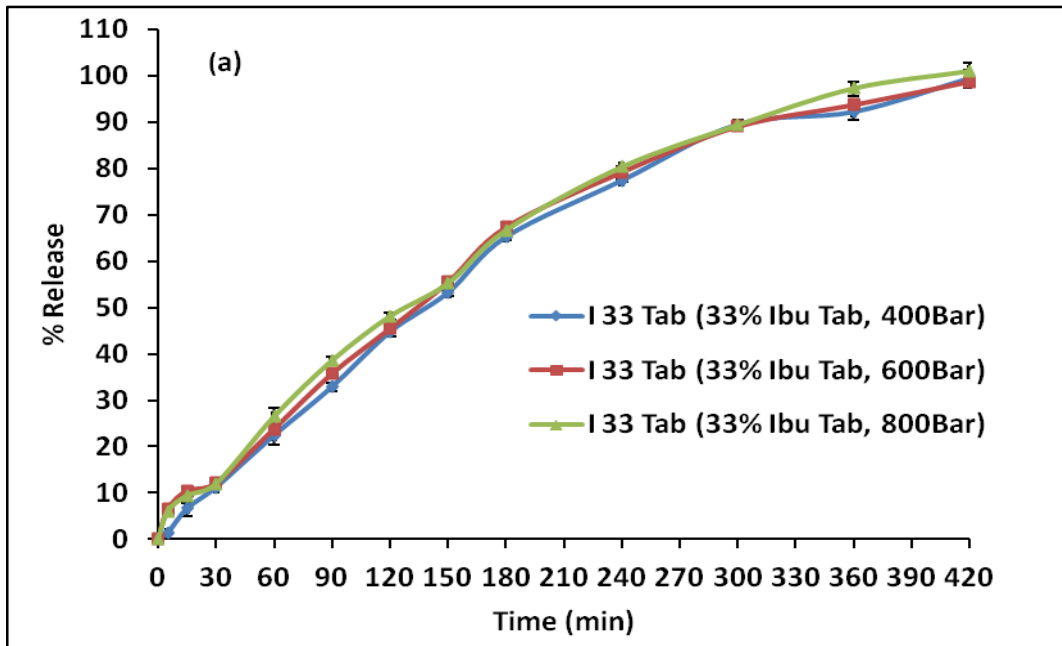
Figure 5.26: In-vitro release from injection moulded tablets of same strength and packed at different pressure; (a) Ibuprofen-HPMCAS and (b) Ibuprofen-D-mannitol HPMCAS in phosphate buffer pH7.2. (n=3)

5.1.3 Effect of processing parameters using DoE

The crystallisation of ibuprofen on the surface of the tablets and tensile bar was observed, which was confirmed during Raman spectroscopy analysis. The 33% ibuprofen-HPMCAS (I33) system (moulded bars) was studied in detail to understand the effect of injection moulding process variables i.e the packing pressure and mould temperature, on the properties of the moulded systems. The surface crystallisation kinetic was studied using MDSC and NIR. The change in molded bar (4cm) surface area due to the shrinkage and change of mechanical properties was studied using DMA. The data obtained using MDSC, NIR, shrinkage (surface area) and DMA was used to plot surface response curves to understand the effect of the injection moulding process variables on the crystallisation and shrinkage of I33 moulded bar.

5.1.3.1 Modulated DSC (MDSC)

The samples characterised immediately after moulding showed a single Tg at $38.1 \pm 0.23^{o}C$ whereas the absence of a sharp melting endotherm confirmed the formation of an amorphous molecular dispersion of the drug within the polymer (Figure 5.27). The middle section of bar showed a similar behaviour when analysed after 24hrs. However, the surface samples showed a small melting endotherm at $69.0 \pm 0.21^{o}C$ indicating the melting of the surface crystallised ibuprofen. Modulated DSC allowed a separation of thermal events on a reversing, non-reversing and reversing heat capacity curves (Rev Cp) (Coleman and Craig, 1996; Moffat et al., 2014; Qi and Craig, 2012; Royall et al., 1998) .
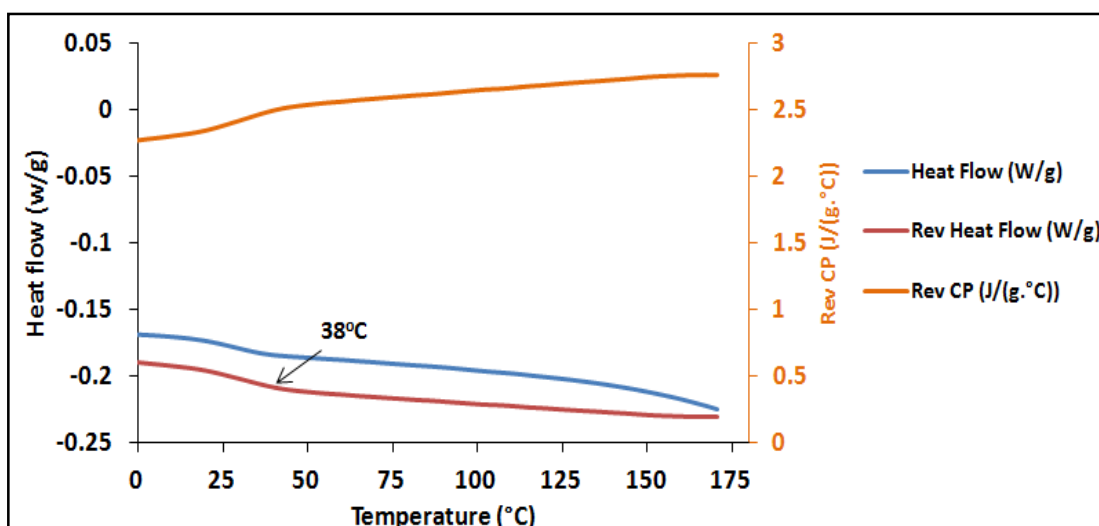
Figure 5.27: MDSC of ibuprofen-HPMCAS (I33) moulded tensile bar after the moulding (modulated heating rate 5°C/min)
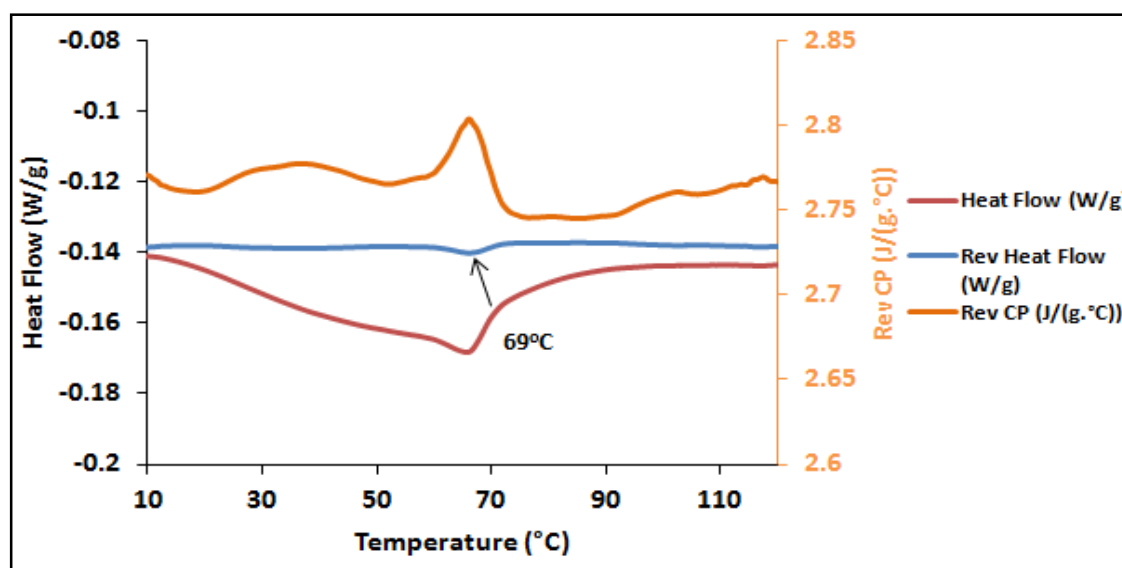
Figure 5.28: Phase separation of ibuprofen-HPMCAS (I33) moulded system: MDSC of surface sample of ibuprofen-HPMCAS (modulated heating rate 5°C/min)

The Reversing heat flow signals (Rev Cp) were monitored for the characterisation of Tg of the amorphous phase and the melting endotherm of the crystalline phase within the moulded samples. The increase in Rev Cp at 38°C represents the Tg and 69°C corresponds to crystalline ibuprofen (Figure 5.28). The specific heat capacity of the material is expected to increase at two steps during DSC heating; first, at Tg due to the higher molecular mobility and second,

at a fusion temperature of a compound. Complimentary results were obtained using DMA where, two tan δ peaks were observed in the same temperature region (explained in the section 5.1.3.3). Modulated DSC and DMA provided a good understanding of the thermal behaviour and phase separation of the moulded systems.

5.1.3.1.1 Crystallisation under stress conditions: prediction by MDSC

The crystallisation kinetics predicted for the nine batches which were kept at different stress conditions (temperature and humidity) as described in Table 3.13. Thermal analysis of surface samples taken for a period of one month at different intervals showed a melting endotherm of ibuprofen at 69-70°C with an increase in the melting enthalpy (Figure 5.29). The melting enthalpy (ΔH) was calculated by integration of area under melting endotherm and the formula used to calculate degree of crystallinity or % crystallisation is mentioned in the equation 5.1.

$$\% \text{ crystallsation } = \frac{\Delta Hs}{\Delta Hc} \times 100 \hspace{2cm} \text{(Equation 5.1)}$$

Where ΔHs is the melting enthalpy of surface crystallised sample at the stability time point; ΔHc is the melting enthalpy of the 33%w/w ibuprofen HPMCAS physical mixture.

A similar equation was used for prediction of the crystallisation kinetics from amorphous solid dispersion containing Cinnarizine-Soluplus®, efavirenz–polyvinylpyrrolidone (Tian et al., 2014a; Yang et al., 2010), fenofibrate and ketoconazole– Kollidon® VA 64 (Kanaujia et al., 2011).
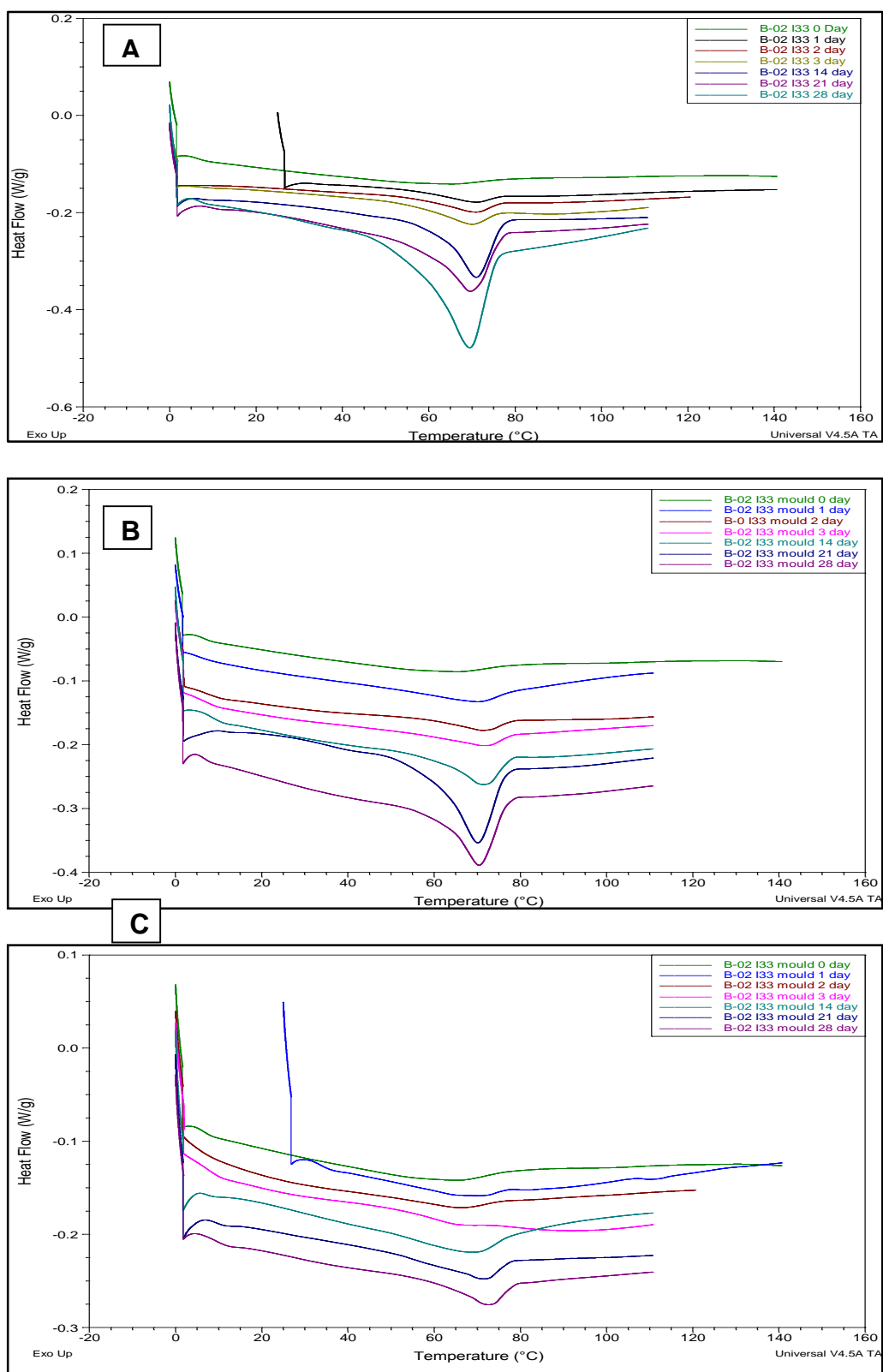
Figure 5.29: DSC thermograms of surface of ibuprofen-HPMCAS (I33) samples(B-02) exposed to stress condition: (A) 40°C 75%RH (B) 40°C 60%RH (C) 25°C 60%RH (modulated heating rate 5°C/min)

The Tg of of I33 system predicted by Fox equation indicated that the addition of ibuprofen would lower down the Tg of HPMCAS and the overall Tg of the system after addition of 33% ibuprofen could possibly lower the temperature around 45°C (Figure 5.28, Figure 4.1). Practically observed of Tg of the system using MDSC was at around 38°C. Therefore, it was interesting to evaluate the systems crystallisation above and below the Tg of the system.

Two storage temperatures were above the Tg of the system (40°C 75%RH and 40°C 60%RH) and one condition was below the Tg (25°C 60%RH). From DSC thermal profiles (Figure 5.29) the effect of stress condition on the melting enthalpy (ΔH) of the moulded system can be clearly seen. Calculated degrees of crystallinity (% crystallinity) of the moulded system at various stress conditions are displayed in the Figure 5.30. The predicted crystallization kinetics for all the batches have distinctively shown a higher degree of crystallization at 40°C compared to 25°C. Moreover, humidity also played an important role in the crystallisation i.e the higher %RH (75%) favoured the crystallisation kinetics than low RH (60%) when stored at similar storage temperature (40°C). In general, the different stress conditions had a significant effect on crystallisation ate.
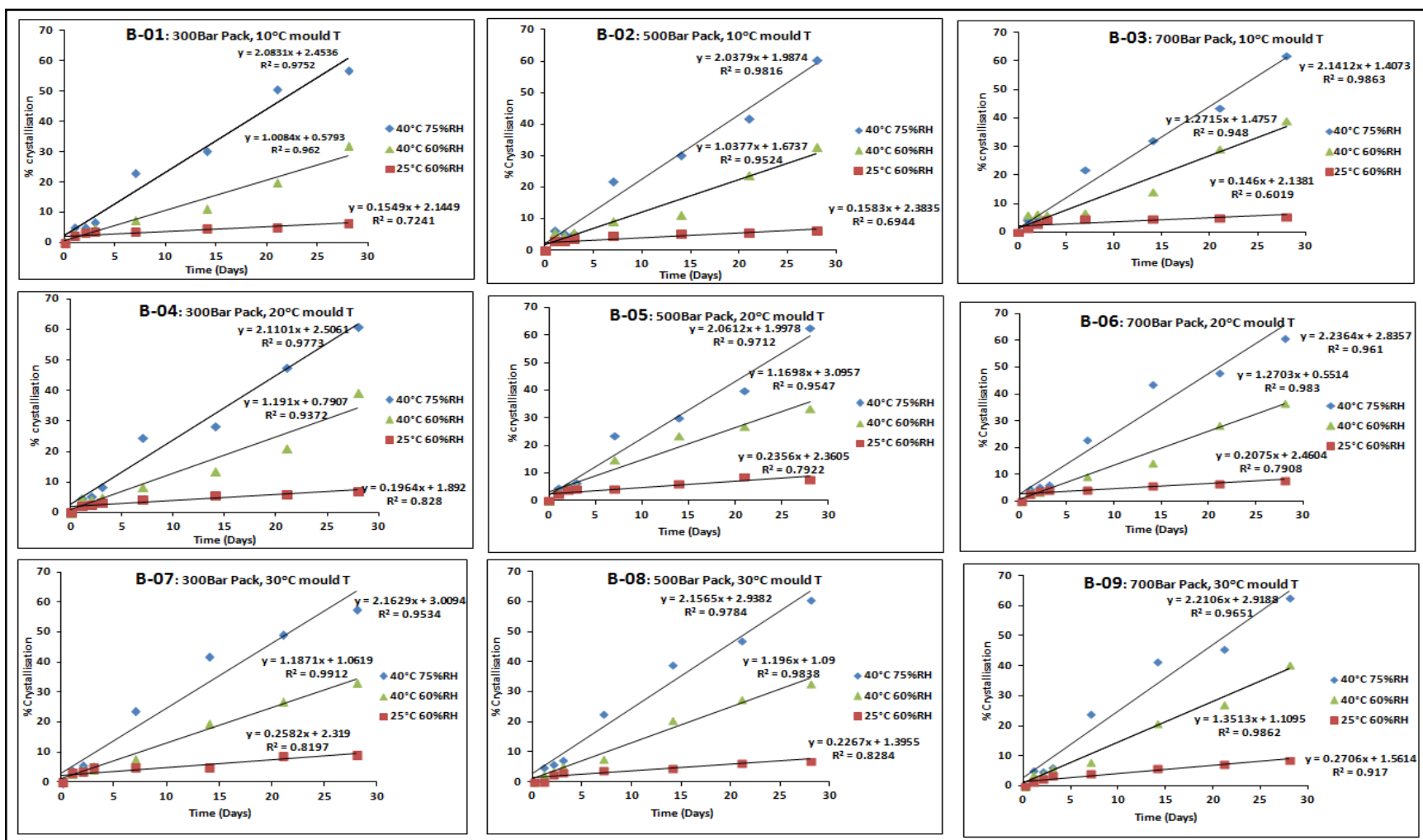
Figure 5.30: Crystallisation kinetics of I33 moulded systems stored at stress condition predicted by MDSC

176

After 7th day of storage, sigificant crystallinity was developed irrespective of the processing condition. It was seen that % crystallinity in the range of 22-23%, 7-9%, 3-4% at 40ºC 75%RH, 40ºC 60%RH, 25ºC 60%RH respectivey. The rate of crystallisation at stress conditions from all molded systems was calculated using the linear regression analysis the using equation mentioned as below

$$Y = mX + C \qquad\qquad\qquad \text{(Equation 5.2)}$$

Where Y is the % crystallised at a time t, X = time measured in days, m is the slope of the line, C is the intercept, Therefore, the slope of the line can be used to calculate the rate of % crystallisation/day. Batches (B-07, B-08, B-09) prepared at a high mould temperature (30ºC) showed a marginally higher rate of crystallization than the batches prepared at 10ºC and 20ºC this could be attributed to the melt quenching effect or rate of cooling of the melt (Table 5.5). Cooling rate has a significant influence on the properties of amorphous materials and rate of cooling has an effect on the nucleation from an amorphous state (Kelton, 1998). Slow cooling allows the maintenance of a steady-state nucleation rate, whereas rapid cooling prevents a full development of viable nuclei. Hence, rapid cooling not only facilitates glass formation, but also enhances the glass stability against the crystallisation (Yu, 2001). HPMCAS is relatively hydrophobic in nature due to its substitutients, however, when exposed to high RH (75%) conditions, it absorbs moisture and because of the platicisation effect of water, the Tg of the polymer decreases (Friesen et al., 2008).

When 40ºC 75%RH and 40ºC 60%RH systems were compared, the rate of crystallisation at 75%RH was observed to be the twice that of 60%RH (Table 5.5). This suggests that moisture-favoured crystallisation where the Tg of the

system was further decreased, leading to an increase in the molecular mobility. There are several reports on moisture-favoured crystallisation of APIs (Marsac et al., 2008; Marsac et al., 2010; Tian et al., 2014a). The systems stored at 25 °C 60%RH were least affected by the stress conditions as the storage temperature was below Tg of the system and the moisture level was similar to or less than the other conditions. Amorphous drugs shows higher molecular mobility above the Tg which favours crystallisation (Zhou et al., 2008).

Table 5.5: Rate of crystallisation (%)/day of I33 systems at stress condition

Batch number	Pack pressure	Mould Temp.	Rate of crystallisation (%)/day		
			40°C 75%RH	40°C 60%RH	25°C 60%RH
B-01	300	10	2.08	1.00	0.15
B-02	500	10	2.03	1.03	0.15
B-03	700	10	2.14	1.27	0.14
B-04	300	20	2.11	1.19	0.19
B-05	500	20	2.06	1.16	0.19
B-06	700	20	2.23	1.27	0.17
B-07	300	30	2.13	1.18	0.25
B-08	500	30	2.15	1.19	0.22
B-09	700	30	2.21	1.36	0.27

5.1.3.2 Near infrared spectroscopy

In NIR spectroscopy samples are irradiated with NIR light and some of the light is absorbed by the molecules, bringing them to a higher vibrational state. Only vibrations resulting in *changes in dipole movement* of a molecule can absorb IR radiation. The molecules need a permanent dipole to be IR active while some atomic molecule shows dipole induced by vibration. In general, R-H group shows strongest overtone as a diople movement is high, therefore O-H, N-H, C-H S-H groups are strong NIR absorbers (De Beer et al., 2011). In contrast H_2 does not absorb NIR radiation as it does not show a change in dipole movement during its vibration. Stretching and bending are the forms of vibrations which molecules may exhibit upon absorption of NIR energy. Stretching is a continuous change in bond length or interatomic distance along the axis while bending is due to a change in bond angle. For example, C-H group shows stretching at 2960 cm^{-1} and bending of C-H is at 1460 cm^{-1} (De Beer et al., 2011).

Second derivative NIR spectra in the 4000 cm^{-1}–10,000 cm^{-1} region for pure ibuprofen, HPMCAS and 33% ibuprofen-HPMCAS physical mixtures shown in the Figure 5.31. Pure crystalline ibuprofen shows intense NIR peaks while dilution with polymer (33% physical mixture) decreases the relative intensity of the peaks. A selected region between 4000 cm^{-1}– 4800 cm^{-1} is shown in Figure 5.32 . The reduction of peak intensity with concentration suggests good sensitivity of NIR for identification of different drug concentrations. This forms the basis for setting up a calibration curve with a physical mixture containing the different ibuprofen concentrations ranging from 10% to 60% by weight.
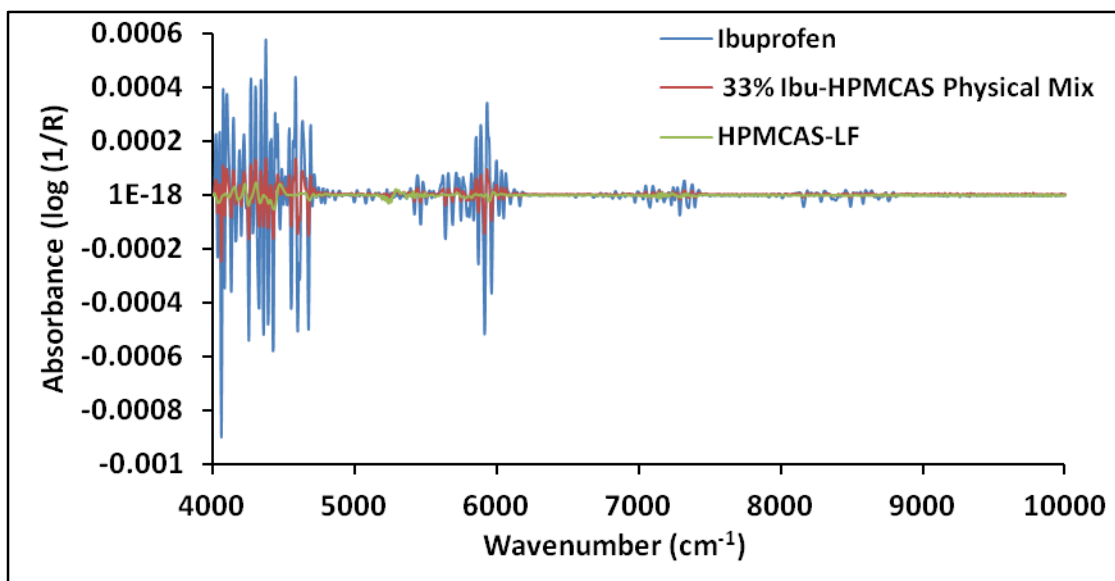
Figure 5.31: Second derivative of NIR spectra of ibuprofen, HPMCAS, 33% physical mixture
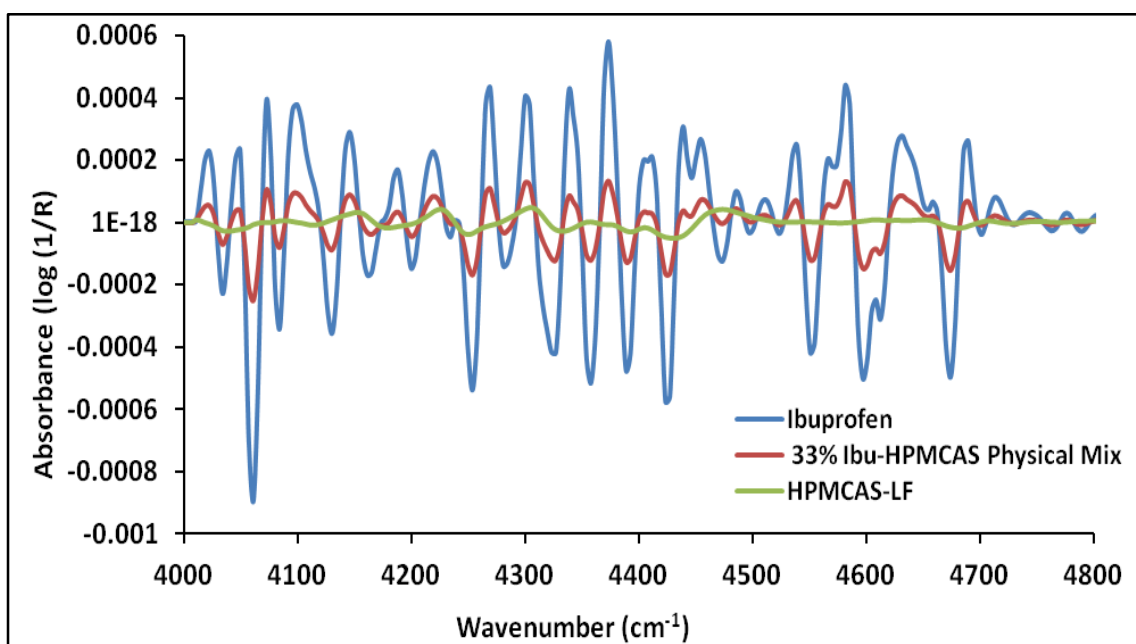
Figure 5.32: Second derivative of NIR spectra of ibuprofen, HPMCAS, 33% physical mixture in the 4000 cm^{-1}– 4800cm^{-1} range

Second derivative of NIR spectra of physical mixtures shown in Figure 5.33 and the Figure 5.34 shows the calibration curve and results of partial least squares regression analysis of NIR spectra using whole range (wavenumber 4000-10000 cm^{-1}). A good correlation was observed between the actual and

calculated concentrations of the ibuprofen (correlation coefficient 0.999). Validation standards containing known concentration of the ibuprofen (30%, 33% and 50% w/w) were accurately quantified using set calibration curve.
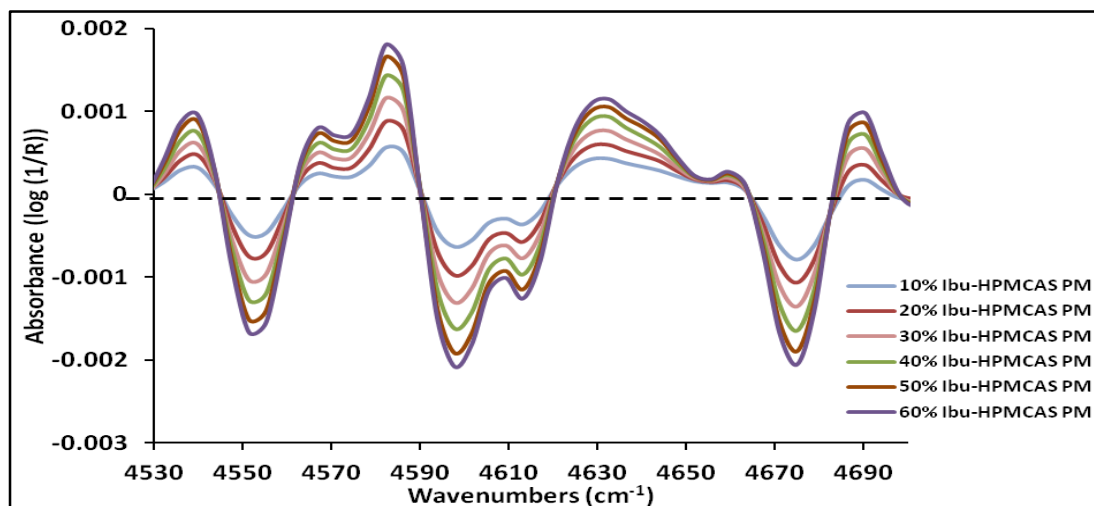
Figure 5.33: Second derivative of NIR of calibration standards : Ibu-HPMCAS physical mix
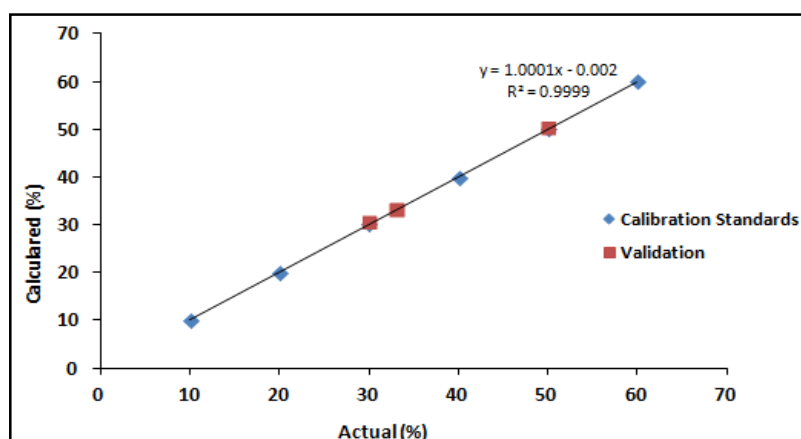
Figure 5.34: NIR calibration curve of ibuprofen-HPMCAS physical mixtures

NIR has been used as a process analytical tool (PAT) for analysis of wet granulation (Wikstrom et al., 2005) crystalline phases, polymorphic transformation (Aaltonen et al., 2003; Li et al., 2005) and co-crystal formation (Kelly et al., 2012). A transmission NIR method has been used to estimate the ibuprofen content of tablets (Meza et al., 2006). Injection moulded systems (B01-B09) analysed immediately after the moulding showed significant reduction in the

relative intensity of NIR peaks, indicating the formation of amorphous dispersion of ibuprofen in the HPMCAS matrix. The peak intensity of physical mixture containing similar drug-polymer weight ratio, i.e. 33% ibuprofen in HPMCAS (Figure 5.35,brown Line) showed sharp peaks due to the crystalline nature of ibuprofen, however moulded samples showed reduction in peak intensity due to the effect of the process on the material. Similar observations of the peak height reduction have been reported for the amorphous dispersion of tarcolimus in HPMCAS and HPC (Zidan et al., 2012).
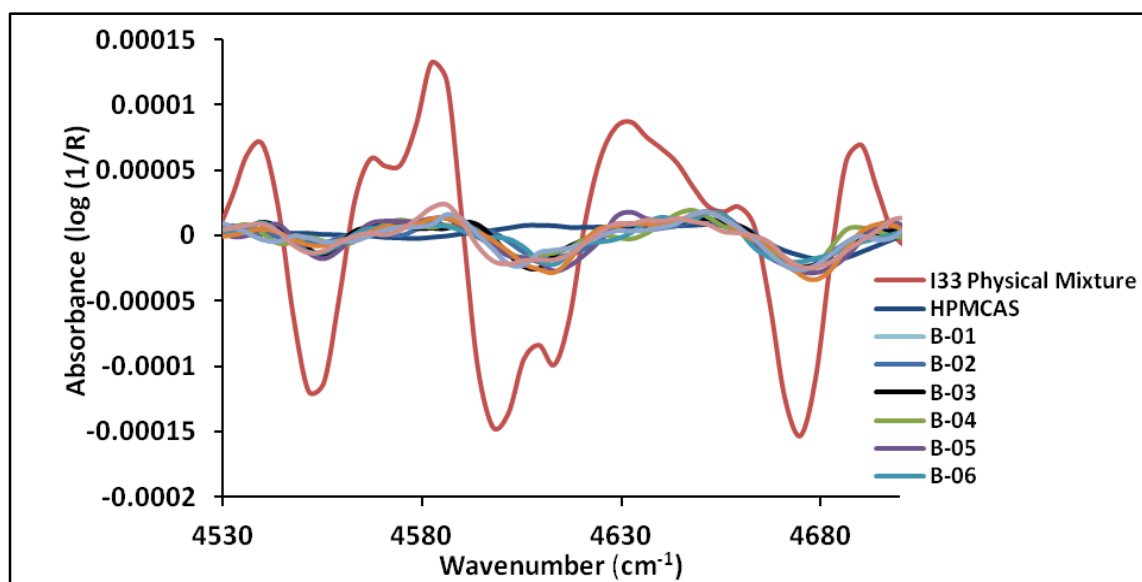
Figure 5.35: Second derivative of NIR spectra of I33 physical mixture and injection moulded samples
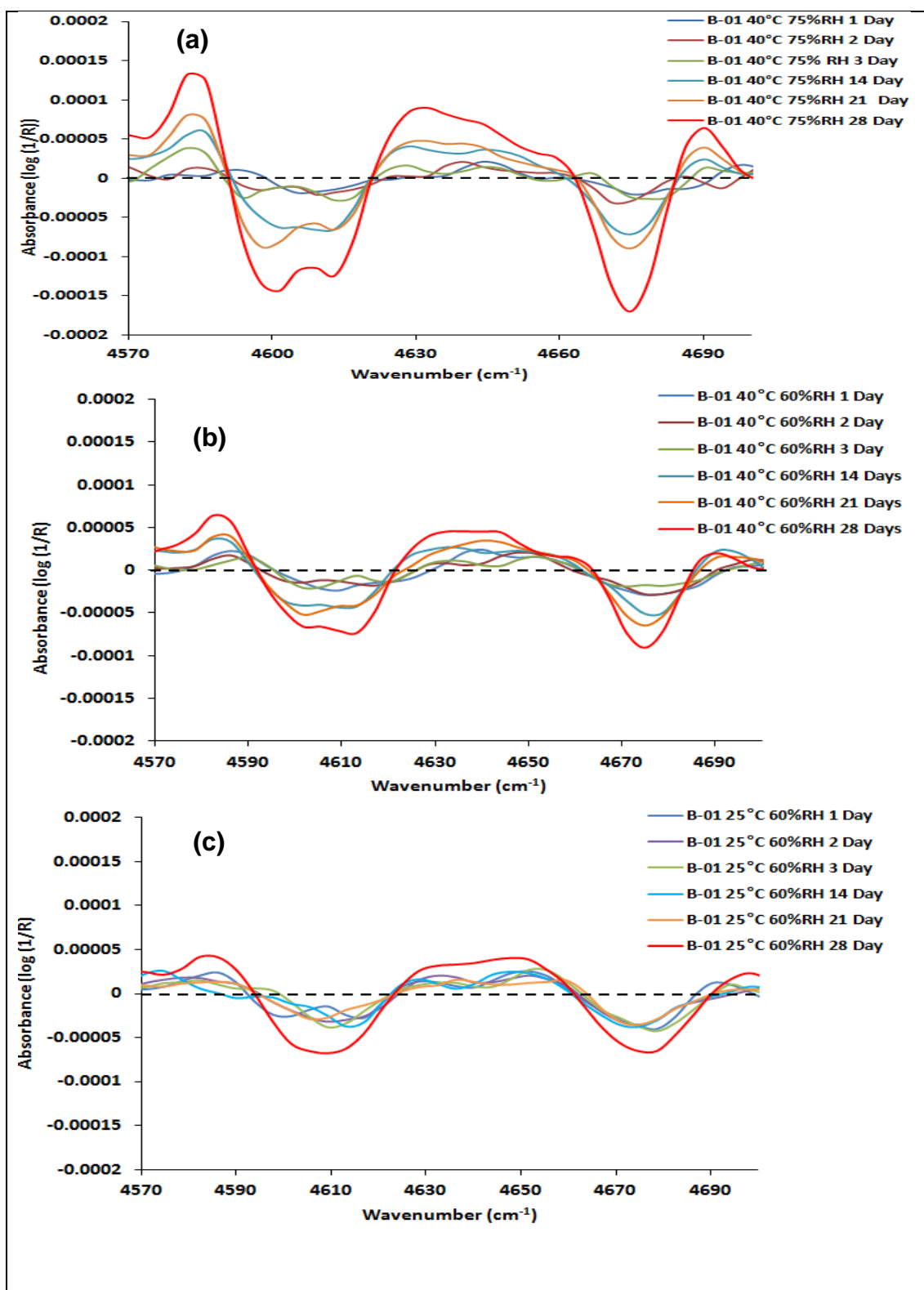
Figure 5.36: Second derivative of NIR spectra of surface crystallised bar (B-01) stored at (a) 40°C 75%RH (b) 40°C 60%RH (c) 25°C 60%RH

The second derivative NIR spectra of batch B-01 stored at three stress conditions are shown in the Figure 5.36. An increase in the relative peak intensity

with time was seen at all conditions. At 40°C 75% RH the relative increase in the peak intensity was high compared to 25 °C 60%RH due to the higher % crystallinity of the samples. The surface crystallisation measured by NIR was in good accordance with the MDSC results. The extreme condition (40°C 75% RH) favoured more rapid surface crystallisation compared to 40°C 60%RH which suggests an effect of moisture on the rate of the ibuprofen crystallisation.

The percent crystallinity and the crystallisation rate was quantified using the NIR calibration curve. The % crystallisation was plotted against time to obtain the rate of crystallisation (Figure 5.37). The crystallisation rate at 25°C 60%RH was approximately 0.2 %/day whereas at 40°C 75% RH it was about 2%/day. These finding suggests that the crystallisation rate at 25°C 60%RH was approximately one tenth of that at 40°C 75%. This difference was evidenced by both the effect of both Tg of moulded system and stress conditions (temperatures and moistures) on the crystallization rate as shown in Table 5.6 Batches (B-07, B-08, B-09) were prepared at a high mould temperature (30°C) showed a marginally higher rate of crystallization than the other conditions (10°C and 20°C). Similar trends were predicted earlier using MDSC suggesting that good sensitivity of the thermal and the spectroscopic techniques for the analysis of moulded systems.

Table 5.6: Rate of surface crystallisation (%)/day of I33 systems at stress condition measured by NIR

Batch number	Rate of crystallisation (%)/day		
	40ºC 75%RH	40ºC 60%RH	25ºC 60%RH
B-01: 300Bar Pack, 10ºC mould T	1.70	0.56	0.11
B-02: 500Bar Pack, 10ºC mould T	1.82	0.56	0.12
B-03: 700Bar Pack, 10ºC mould T	1.93	0.51	0.14
B-04: 300Bar Pack, 20ºC mold T	1.75	0.54	0.12
B-05: 500Bar Pack, 20ºC mould T	1.86	0.57	0.12
B-06: 700Bar Pack, 20ºC mould T	1.86	0.65	0.14
B-07: 300Bar Pack, 30ºC mould T	1.96	0.69	0.20
B-08: 500Bar Pack, 30ºC mould T	2.03	0.72	0.20
B-09: 700Bar Pack, 30ºC mould T	2.00	0.75	0.20
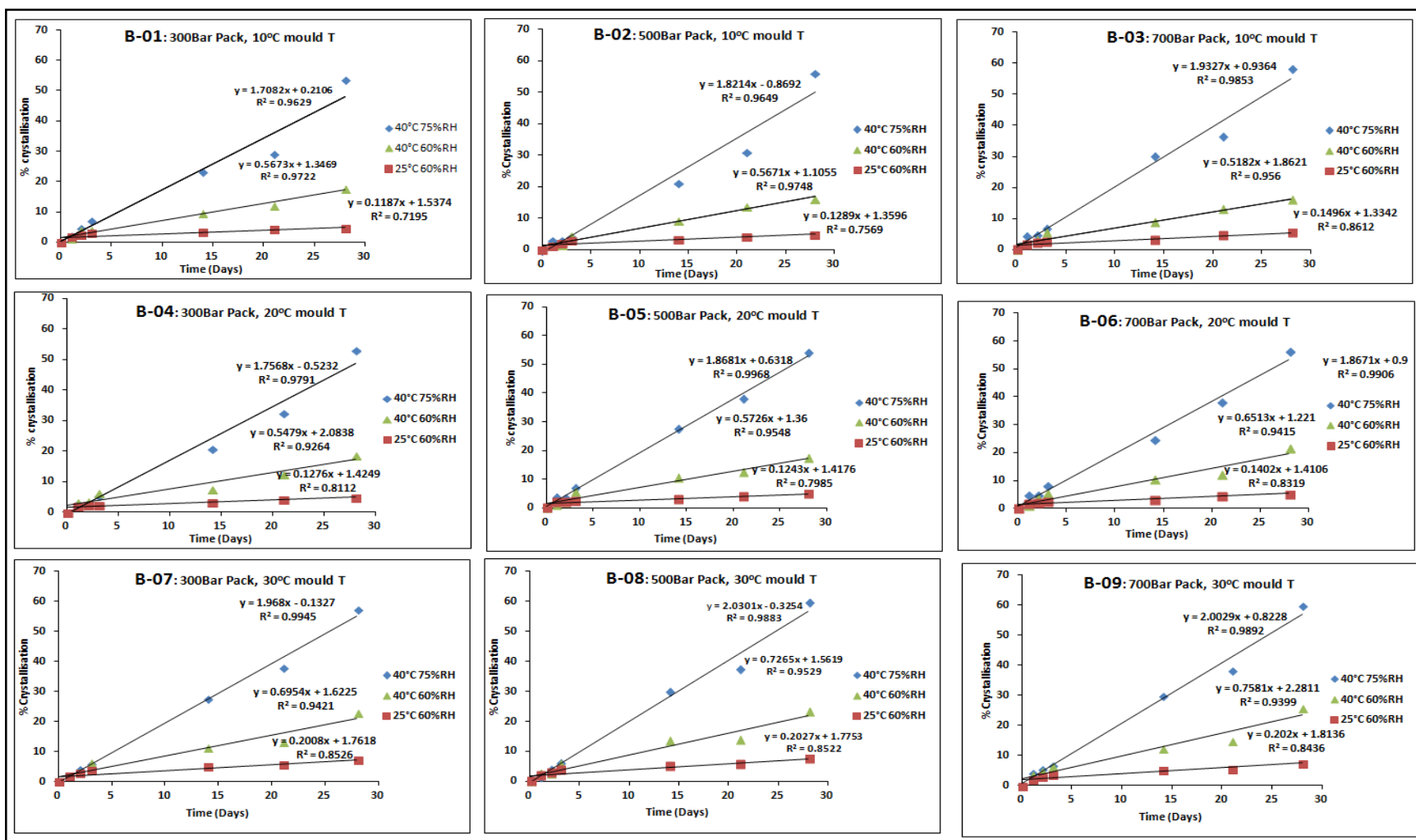
Figure 5.37: Crystallisation kinetics of I33 moulded systems predicted by NIR

5.1.3.3 Dynamic Mechanical Analysis

Dynamic mechanical analysis (DMA) can be used for the measurement of mechanical properties of a material as a function of temperature. Specifically, in DMA a variable sinusoidal stress is applied and the resultant sinusoidal strain is measured. In general, if the material being evaluated is purely elastic, the phase difference between the stress and strain sine wave is $0°$ i.e they are in phase, on the other hand, if the material is purely viscous the difference is $90°$ (Aitken et al., 1991) (Menard, 2008) (Figure 5.38). However, most real world materials, including polymers are viscoelastic in nature and exhibit a phase difference between those extremes. This resultant phase difference, together with the amplitude of stress and strain waves can be used to obtain a variety of fundamental material properties including the storage and loss modulus, tan δ, complex and dynamic viscosity.
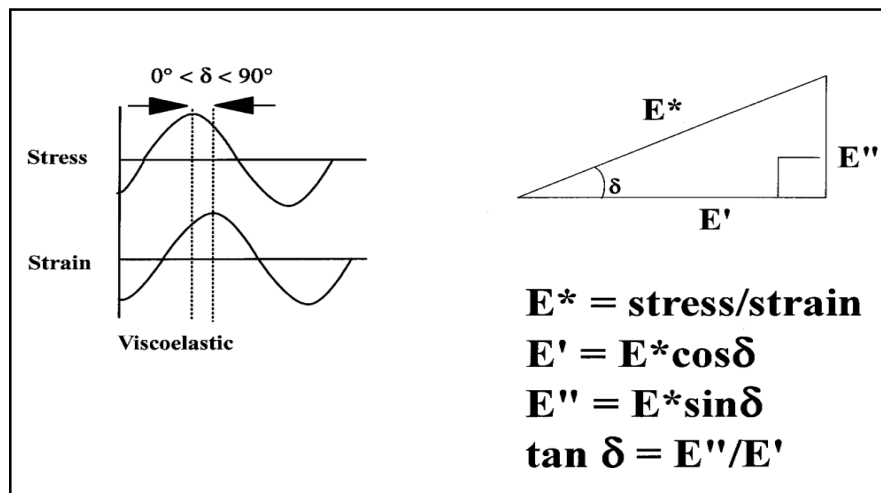
Figure 5.38. Vicoelasticity and complex modulus

In the case of the I33 moulded system DMA samples were analysed immediately after the moulding and also after the systems were kept at stress conditions. These showed significant changes in storage modulus and tan δ. Moulded bars analysed immediately after the moulding showed a single tan δ

around 58°C and a storage modulus of 11345 MPa. The storage modulus of the system has significantly fallen in the temperature region of 35 - 45°C. Fall in the storage modulus in the particular temperature range is indicative of glass transition. Tan δ is also sensitive to the molecular motion and correlated with the Tg of the systems (Menard, 2008). Both the fall in storage modulus (E′) and increased height of tan δ were considered as the Tg of polymers or polymer composites, e.g. polypropylene (Li et al., 2002), polycarbonates polyethylene terephthalate, polyethersulphone (Price, 2002). I33 moulded systems showed a single tan δ when analysed immediately after moulding Figure 5.39.
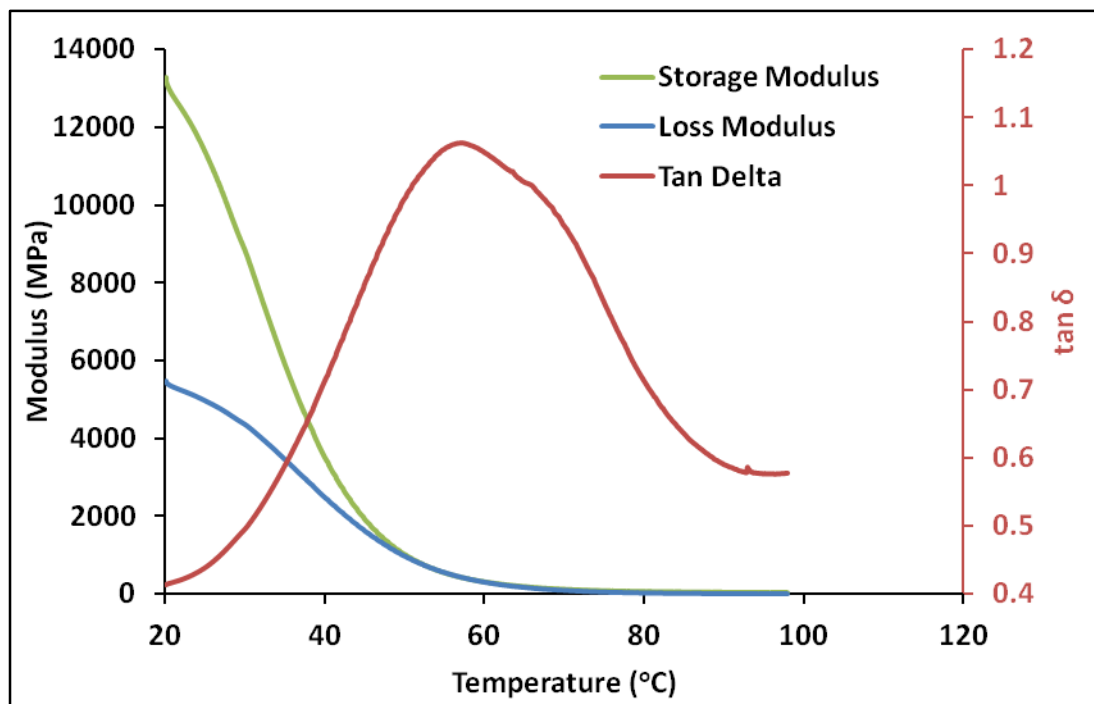
Figure 5.39: DMA of I33 injection moulded sample immediately after moulding
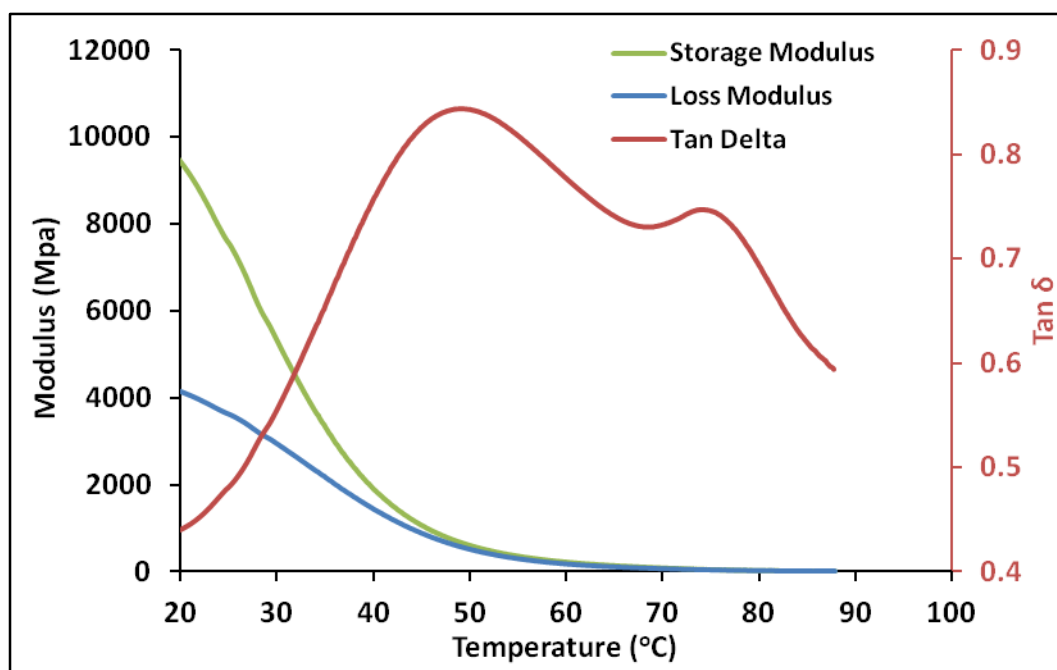
Figure 5.40: DMA of injection moulded sample after for 24hrs at RT

However, DMA of the I33 sample stored for 24 hours at ambient conditions (RT) showed the presence of two tan δ peaks which suggests the phase immiscibility and the phase separation of the system (Figure 5.40)

Moulded bars stored at stress conditions (40°C 75%RH and 25°C 60%RH), showed the changes and shifts in tan δ associated with amorphous and crystalline phases. The first tan δ was attributed to the amorphous phase, whereas the second tan δ peak was attributed to melting of crystalllised ibuprofen at temperature around 76-78°C. Interestingly, the monitored tan δ peak for 40°C 75%RH and for 25°C 60%RH samples showed a significant difference in height and position of tan δ peaks which could be clearly attributed to the rate of crystallization of the sample. Where, the 40°C 75% sample had approximately ten times higher crystallisation rate as compared to 25°C 60% (from MDSC and NIR results). The changes in tan δ at both the conditions are shown in Figure 5.41. The prominent phase changes was observed at 40°C 75% condition where

the first tan δ peak was gradually decreased from 45°C to 37°C whereas, slow crystallisation and the presence of major amorphous phase at 25°C 60% showed prominent first tan δ peak.
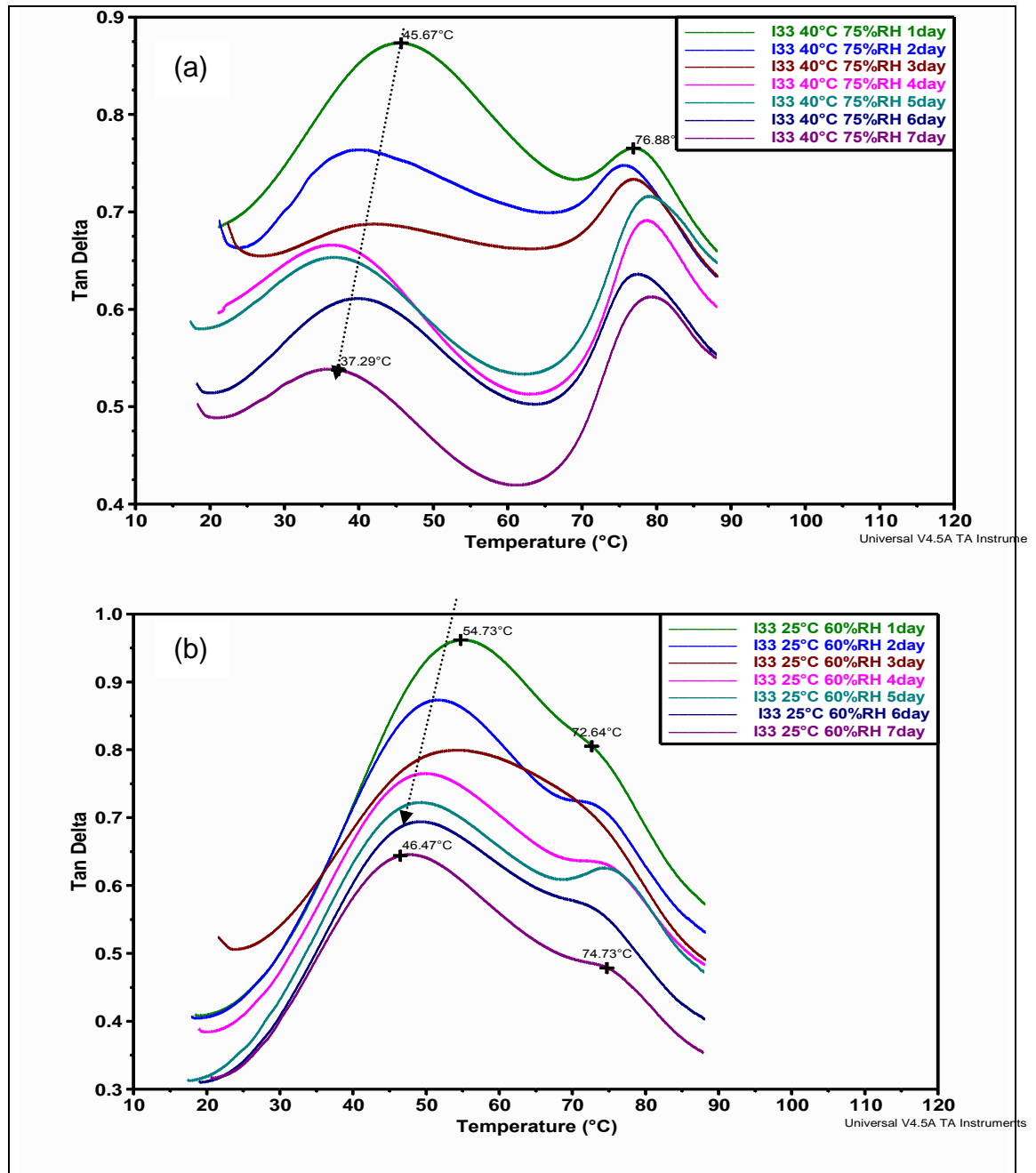
Figure 5.41: DMA: Tan Delta of I33 from 1day to 7days at (a) 40°C 75%RH (b) RH 25°C 60%RH

In order to understand the effect of crytsallisation on the mechanical properties of moulded systems (B01-B09) the samples were analysed after 7 days of exposure to the stress condition. The changes in storage modulus and

tan δ peaks were monitored to observe the effect of the physical aging process on the modulus and the molecular mobility of the moulded systems. The prominent effect of stress conditions was seen on tan δ. As observed using MDSC, on an average all batches were 20%, 8% and 2% crystallised at 40°C 75%RH, 40°C 60% RH, 25°C 60% RH respectively, after 7 days of storage. Tan δ peak changes for the moulded samples are presented in the Figure 5.43. Table 5.7 compares the storage modulus of the sample; immediately after moulding the sample was completely amorphous and there was no phase separation and the storage modulus was 11345 MPa. At 40°C 75% when the sample was 20% crystallised, storage modulus was decreased to 2000 MPa. These results suggest the adverse effect of the phase separation and crystallinity on the mechanical properties of the moulded systems.

Table 5.7: Storage and Loss modulus of sample after 7 days of stability (B01)

Stress condition (physical aging)	Storage modulus (MPa)	Tan Delta (tan δ)	
Before stability (0 day)			
RT	11345	**55**	
	After storage (7 day)	**Peak 1**	**Peak 2**
40°C 75%	2000		78
40°C 60%	3500	45.70	76.31
25°C 75%	5000	47.41	74.21
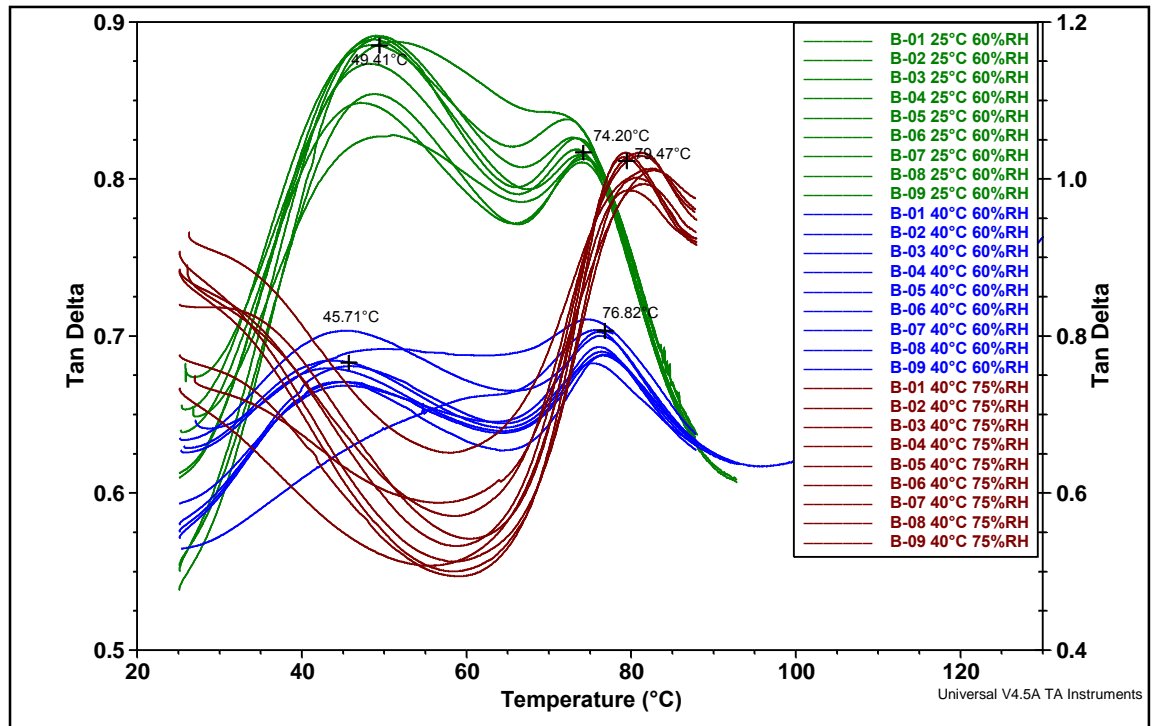
Figure 5.42: Tan δ of of I33 moulded batches at 7 day of storage

5.1.3.4 Shrinkage

In general, three types of shrinkage have been described in the injection moulding. Firstly, in-mould shrinkage occurs during processing; secondly, as-mould shrinkage often referred to as "mould shrinkage" which occurs just after mould opening and thirdly, post-shrinkage. Post shrinkage phenomenon is time dependent shrinkage which is largely influenced by physical aging, recrystallisation etc (Jansen et al., 1998). Tensile shaped, moulded bar obtained using the 3^2 factorial designs are shown in the Figure 5.43.
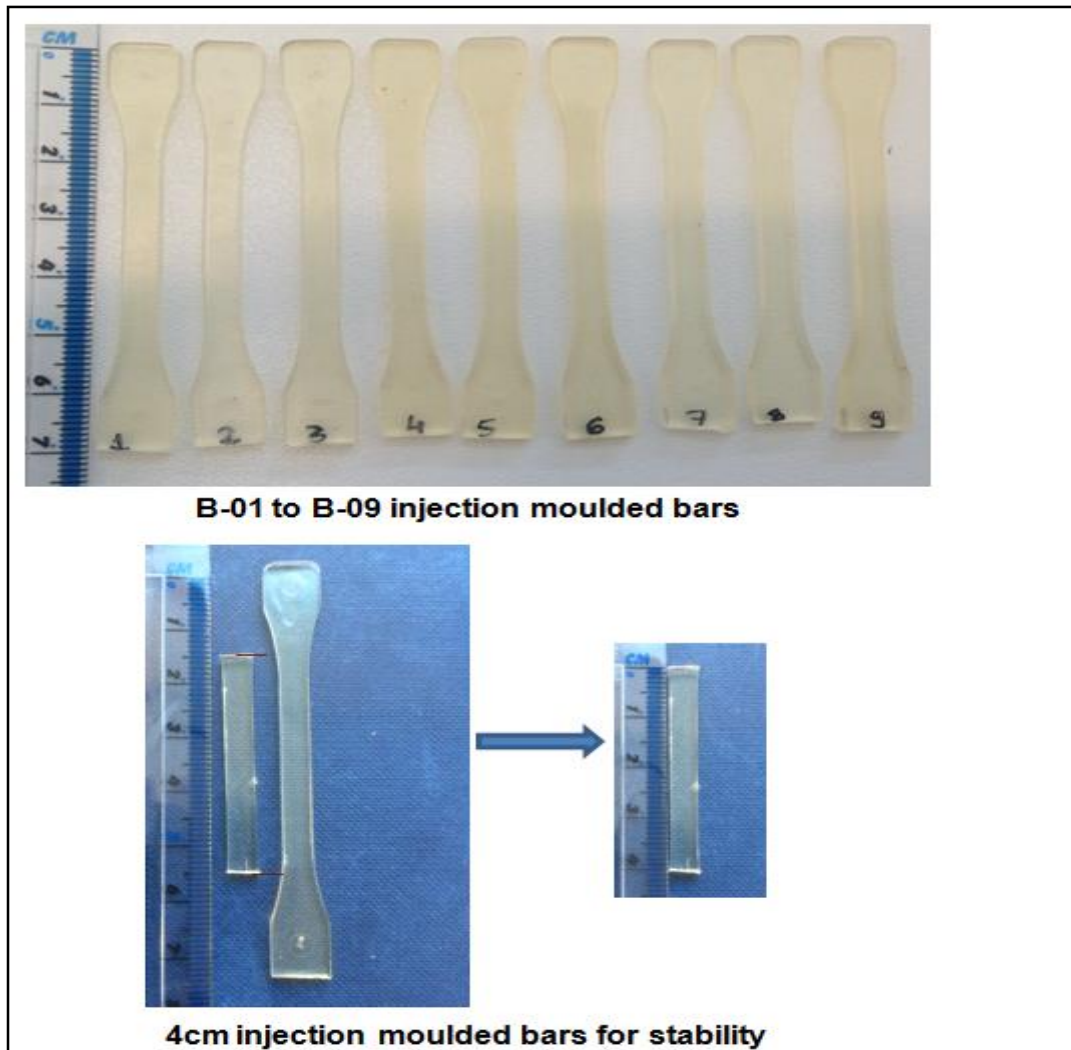
Figure 5.43: Injection moulded I33 batches for stability and shrinkage

I33 extruded and moulded bar (B-01-B-09) when kept at stress conditions showed a significant difference in shrinkage rate within 24hrs. Table 5.8 shows the comparative shrinkage from all I33 moulded batches and extruded bars. Extruded bar did not show any shrinkage even at extreme conditions. On the other hand, IM bars showed significant shrinkage at extreme conditions ($40^{o}C$ 75%) where all bars showed approximately 1 cm shrinkage and relatively less shrinkage was observed at $25^{o}C$ 60% (0.25 cm) and RT conditions (0.15 cm).

Table 5.8: Shrinkage from extruded and injection moulded systems

Batches	Original length (cm)	Length (cm) After 24hrs/1Day			
		40°C 75%	40°C 60%	25°C 60%	RT (Ambient)
Extruded bar	4.06	4.01	4.02	4.01	4.05
B-01	4.00	2.86	2.98	3.75	3.81
B-02	4.00	2.96	2.99	3.77	3.82
B-03	4.00	3.10	3.03	3.82	3.85
B-04	4.00	2.99	3.00	3.79	3.82
B-05	4.00	3.01	2.91	3.79	3.88
B-06	4.00	3.08	3.11	3.80	3.85
B-07	4.00	2.87	3.01	3.80	3.65
B-08	4.00	3.03	3.03	3.75	3.81
B-09	4.00	3.03	3.08	3.81	3.88

Batches B-03, B-06, B-09 packed at high packing pressures (700 bar) showed relatively less shrinkage compared to the other batches which were packed at low packing pressures this confirms the effect of packing pressure on the retardation of shrinkage rate. The effect of packing pressure on the shrinkage was previously reported for seven thermoplastic polymers and the key parameter for controlling the shrinkage was observed to be packing pressure (Jansen et al., 1998). Extruded systems containing the same concentration of ibuprofen did not does not show any shrinkage although the rate of crystallisation was similar. This confirms that plasticisation and/or recrystallisation of ibuprofen does not have a significant effect on shrinkage. However, the processing method used for the manufacturing of the systems does have major effect on the shrinkage. Figure

5.44 illustrate the difference in the shrinkage between the extruded and the IM system.
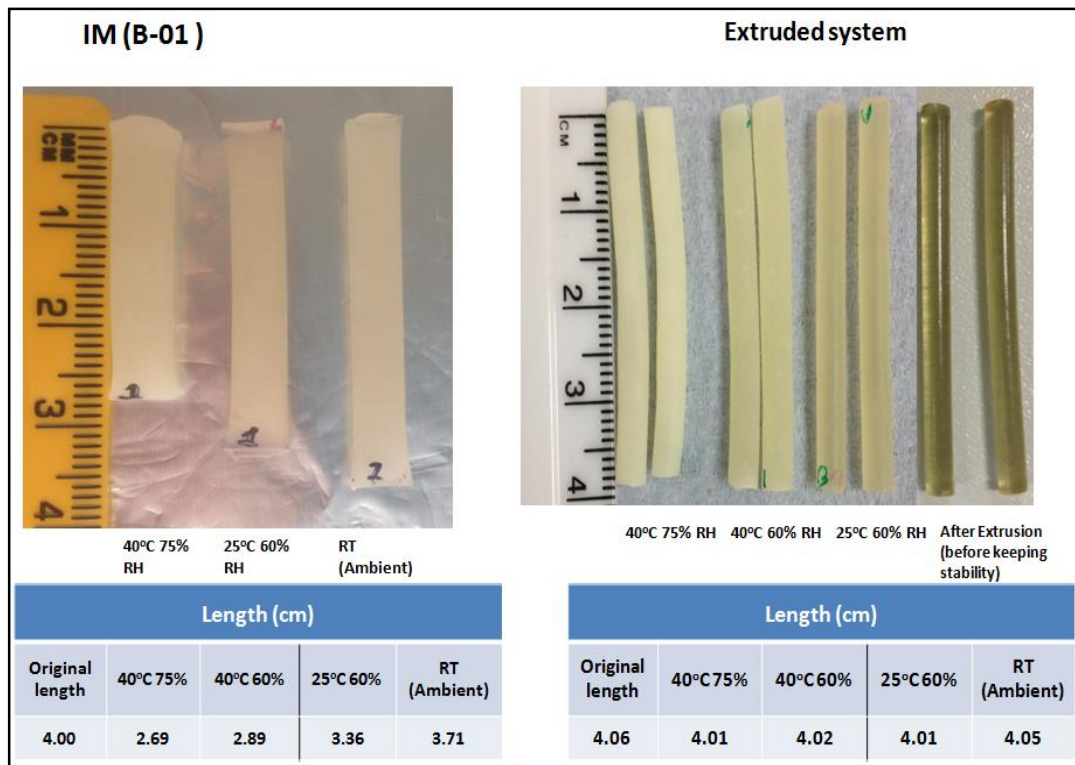
Figure 5.44: Comparative shrinkage of extruded and moulded system after 14days of storage

5.1.3.4.1 Surface area

Surface area of the moulded batches was calculated after the 1st day of moulding and exposure to the the stress conditions. As mentioned earlier, the batches kept at extreme stress temperatures (40ºC) showed high shrinkage rates, and changes were mostly associated with the length of a bar. The prominent change in surface area was seen after 24 hours of storage and higher surface area was seen in the bar kept at 25ºC 60%RH compared to 40ºC 75% and 40ºC 60%RH due to a lower shrinkage of the system. Shrinkage rate was directly proportional to the storage temperature, which also has a major influence on the surface area of the mould (Figure 5.45)
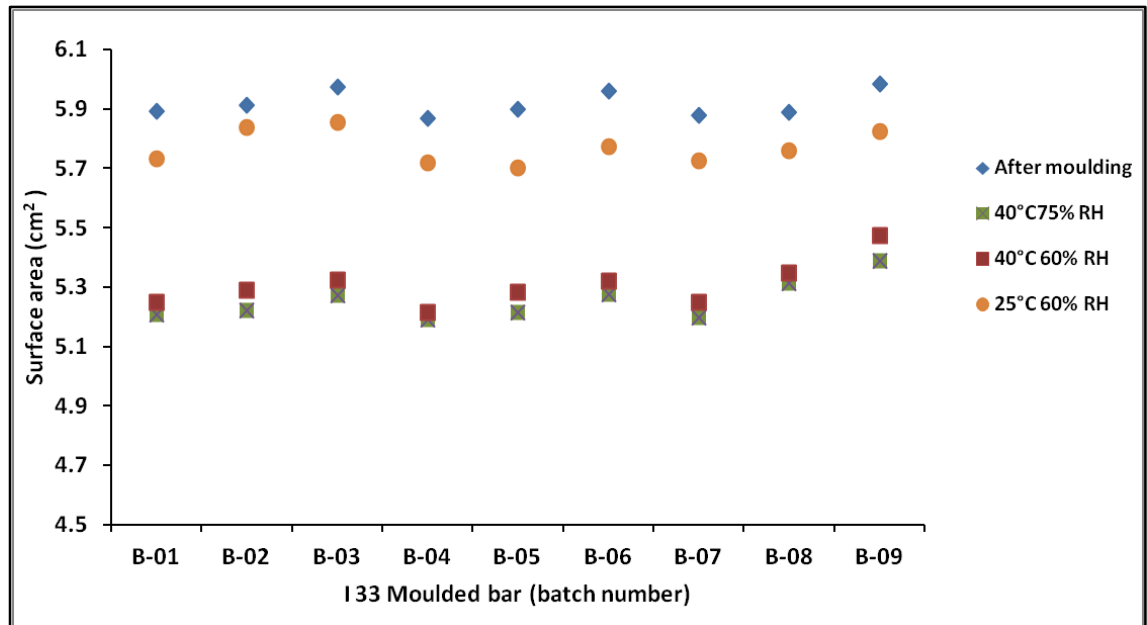
Figure 5.45: Surface area of moulded systems analysed after 1 day of storage

The % length shrinkage ratio of moulded bars was calculated using the following formula (Fei et al., 2013)

$$RS(\%) = \frac{So - Sp}{So} \; X \; 100 \qquad \text{(Equation 5.3)}$$

Where, S_o is length of I33 moulded parts before exposure to stress conditions. S_p is length of I33 moulded parts at stress condition after specific time.

Figure 5.46 shows the % length shrinkage ratio plotted against time for the period of 6 months. After 24hrs, approximately 28%, 25% and 3.5% shrinkage at 40ºC 75%, 40ºC 60%RH and 25ºC 60%RH respectively, was observed and thereafter only 8-10% change in the shrinkage was seen at all stress conditions (Figure 5.46b).
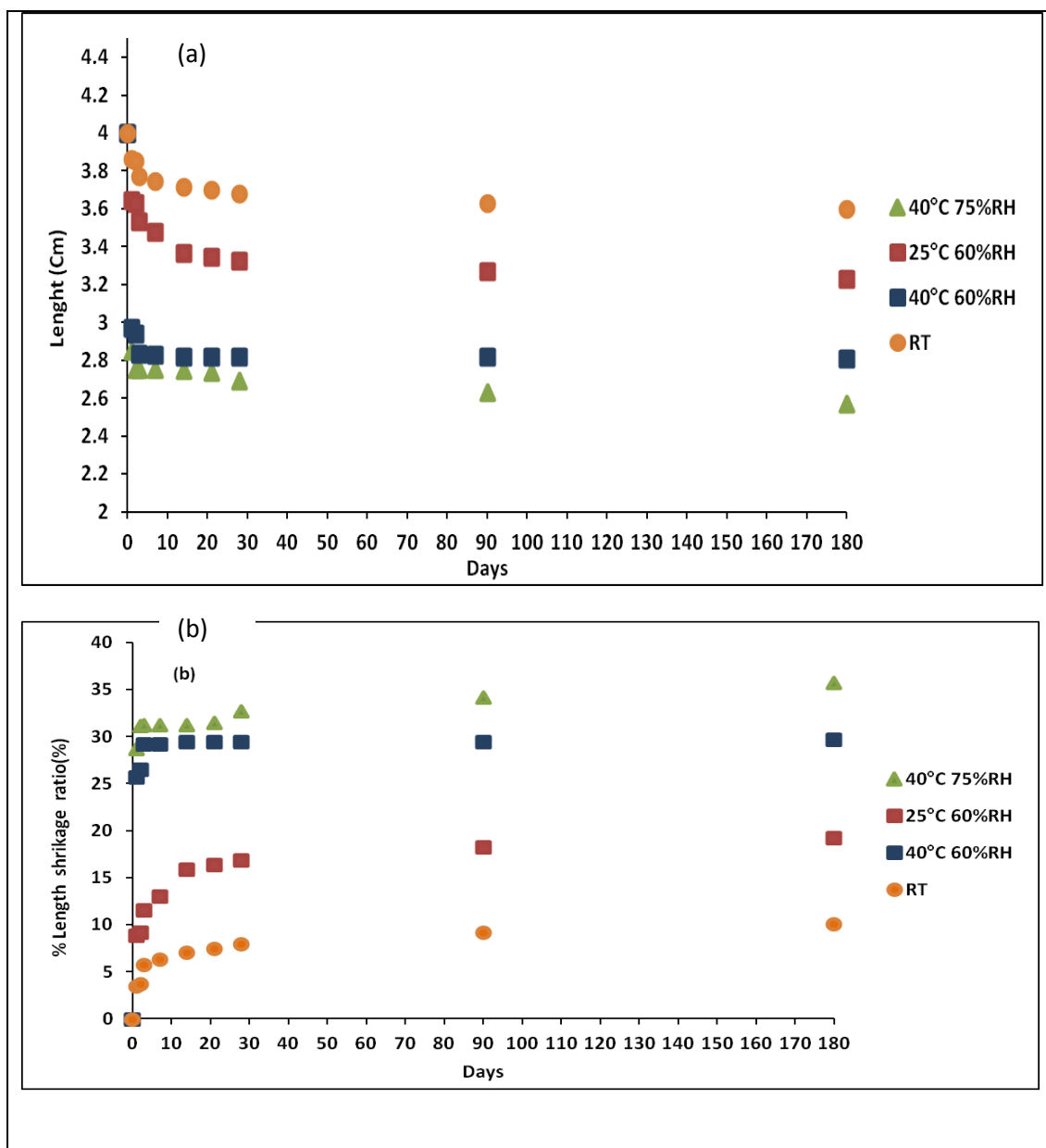
Figure 5.46: **Ibuprofen-HPMCAS (I33) shrinkage at different stability conditions: (a) length (b) % length shrinkage ratio**

The difference in shrinkage rate could be linked to glass transition temperature where higher temperature and humidity conditions favoured the decrease in Tg of the system and hence allowed polymer chain relaxation at a different rate leading to higher shrinkage at extreme conditions (40°C 75%RH). The shrinkage after 6 months for full length and 4 cm bar is shown in the Figure 5.47
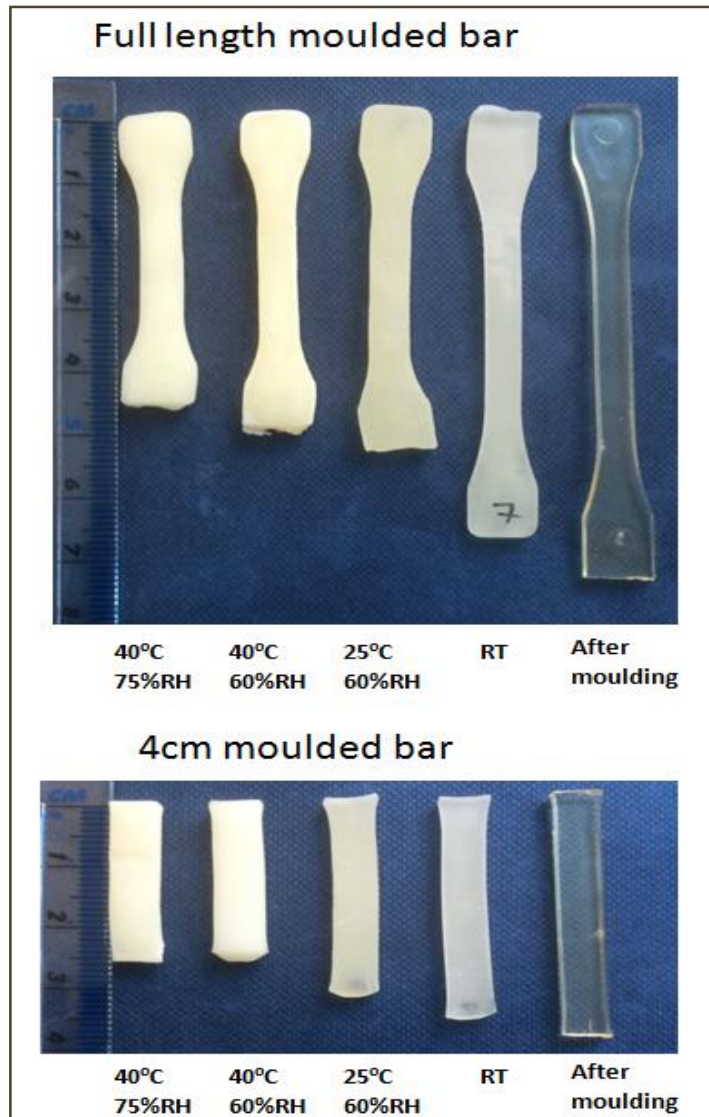
Figure 5.47: I33 mould shrinkage after 180 days of stability

The physical appearance of the moulded bars was seen different due to different % surface crystallisatinity. Moulded bar immediately after moulding were transparent in nature, however, due to phase separation and crystallisation the opacity of the bar increased at extreme stress conditions.

When thermoplastics are processed by IM, the dimensions of moulded parts, change as the material cools, these changes are often called as shrinkage or warpage and can be used to predict the appropriate mould geometry (Fischer, 2003). Although shrinkage is based on thermal contractions, there are other mechanisms which might be responsible for the dimensional changes after

demoulding (e.g. Inherent stresses, crysallisation, mechanical constrainst) (Zema et al., 2012). When HPMCAS was processed by IM using PEG1500 as a plasticiser to form the capsular shells the disk showed a similar tendency of shrinkage. The moulded disks thickness changed due to shrinkage and no significant effect of the amount of the plasticiser was observed. This indicates a shrinkage tendency of HPMCAS after IM.

5.1.3.5 Surface response methodology

The data obtained from the studies described in the earlier sections were compiled in Table 5.9 and was processed to obtain the surface response curves. The crystallisation and surface area data were analysed using multiple regression analysis and ANOVA.

5.1.3.5.1 Multiple regression analysis

The application of the statistical model analysis of variance (ANOVA) for processing of data provided information about the statistical significance of the results. ANOVA was applied for all the timepoints and regression coefficients were calculated and used when the P-value was significant (< 0.05). Non-significant variables were eliminated using the backward elimination method. The multiple regression equation used is mentioned below (Equation 5.4)

$$y = \beta_0 \; + \beta_1 \, X_1 \; + \beta_2 \, X_2 \; + \beta_{11} \, X_1^2 + \beta_{22} \, X_2^2 + \beta_{12} \, X_1 \, X_2 \qquad \text{(Equation 5.4)}$$

The process variables used for injection moulding have shown the significant effect on crystallisation and shrinkage under stress conditions. Crystallisation and shrinkage data is provided in Table 5.9.

Table 5.9: Crystallisation and surface area data at 40ºC 75% and 40ºC 60% 25 ºC 60%RH stress conditions

Batch name	Process Variables		% Crystallisation (MDSC)			% Crystallisation (NIR)				Surface Area (cm^2)				DMA
			40ºC 75%	40ºC 60%		40ºC 75%	40ºC 60%		25ºC 60%	40ºC 75%	40ºC 60%		25ºC 60%	25ºC 60%
	*X1	*X2	*C_{14}	*C_{14}	*C_{21}	*C_{14}	*C_{14}	*C_{21}	*C_{21}	*SA_{14}	*SA_{14}	*SA_{21}	*SA_{21}	*$\tan\delta_7$
B-01	300	10	23.56	11.06	19.90	22.12	9.67	12.18	4.20	5.170	5.21	5.20	5.45	72.29
B-02	500	10	21.79	11.15	23.71	21.5	9.21	12.83	4.20	5.184	5.24	5.21	5.49	73.37
B-03	700	10	20.85	11.09	29.27	23.91	9.92	12.01	4.20	5.226	5.26	5.25	5.53	74.18
B-04	300	20	25.83	13.57	21.30	24.74	9.89	12.68	4.21	5.165	5.20	5.21	5.49	72.5
B-05	500	20	22.44	15.06	27.00	27.48	10.56	13.44	4.01	5.203	5.25	5.20	5.54	72.72
B-06	700	20	23.24	14.43	28.45	26.54	10.27	13.12	4.67	5.224	5.28	5.20	5.58	73.7
B-07	300	30	23.89	19.41	26.89	27.59	12.26	13.38	4.98	5.280	5.30	5.20	5.57	73.53
B-08	500	30	22.83	20.57	27.50	29.92	13.57	13.87	5,01	5.320	5.32	5.25	5.57	74.4
B-09	700	30	24.90	21.09	27.37	29.86	12.4	14.88	5.06	5.327	5.34	5.31	5.64	74.24

*X1, X2 represents packing pressure and mould temperature; C_{14}, C_{21}, represents the crystallisation at 14 and 21 days SA_{14}, SA_{21}, represents the surface area at 14 and 21 days; $\tan\delta_7$ represents position of tan δ peak at 7 days at temperature

Table 5.10: Regression statistics and ANOVA table

Regression coefficient	% Crystallisation (DSC)				% Crystallisation (NIR)				Surface Area (cm2)				DMA
	40°C 75%	40°C 60%		25°C 60%	40°C 75%	40°C 60%		25°C 60%	40°C 75%	40°C 60%		25°C 60%	25°C 60%
	$*C_{14}$	$*C_{14}$	$*C_{21}$	$*C_{21}$	$*C_{14}$	$*C_{14}$	$*C_{21}$	$*C_{21}$	$*SA_{14}$	$*SA_{14}$	$*SA_{21}$	$*SA_{21}$	$*tan\delta_{7}$
βo	32.316	14.68	25.94	6.92	26.59	10.49	13.30	4.18	5.200	5.253	5.222	5.535	73.03
β1	**	0.428	2.830	**	**	**	**	**	0.027	0.023	0.030	0.041	0.633
β2	5.218	4.628	*	1.17	3.306	1.571	0.851	0.741	0.057	0.042	0.023	0.051	0.388
β11	**	**	**	**	**	**	**	**	**	**	0.024	**	**
β22	3.415	1.375	**	**	**	**	**	0.648	0.054	0.023	0.008	**	0.695
β12	**	0	-2.22	**	**	**	**	**	**	**	0.005	**	**
Significance F	0.002	0.00	0.037	0.23	0.042	0.050	0.049	0.023	0.004	0.002	0.00	0.031	0.0421
R2	0.993	0.997	0.945	0.80	0.971	0.937	0.937	0.962	0.988	0.992	0.998	0.977	0.944

*X1, X2 represents packing pressure and mould temperature; C_{14}, C_{21}, represents the crystallisation at 14 and 21 days SA_{14}, SA_{21}, represents the surface area at 14 and 21 days; $tan\delta_{7}$ represents position of tan δ peak at 7 days at temperature ; ** insignificant

The multiple regression equation was used to plot surface response curves where the significant parameters were selected based on regression statistics. The statistical data and ANOVA table is provided in the Table 5.10. The equation 5.5 was further modified based on the results obtained after regression analysis. For example, based on the regression analysis of % crystallisation data at 40°C 75%RH condition after 14 days showed that the factor X_1 and X_{22} were found to be statistically significant and the following equation was used to plot the surface response curve (equation 5.5)

$$y = \beta_0 + \beta_2 X_2 + \beta_{22} X_2^2 \qquad \text{(Equation 5.5)}$$

Where β_0, β_2, β_{22} are the regression coefficients, X_1, X_2 are the process variables i.e packing pressure,mould temperature respectively.

Similarly, all of the data mentioned in the Table 5.10 was processed and significant varibles were identified and used to generate the regression equation. The equations obtained was used to plot surface response curves.

For the batches kept at 40ºC 75%RH, the surface response curve suggested that there is a more significant effect of the mould temperature used for the part cooling during processing on % crystallisation compared to the mould packing pressures.
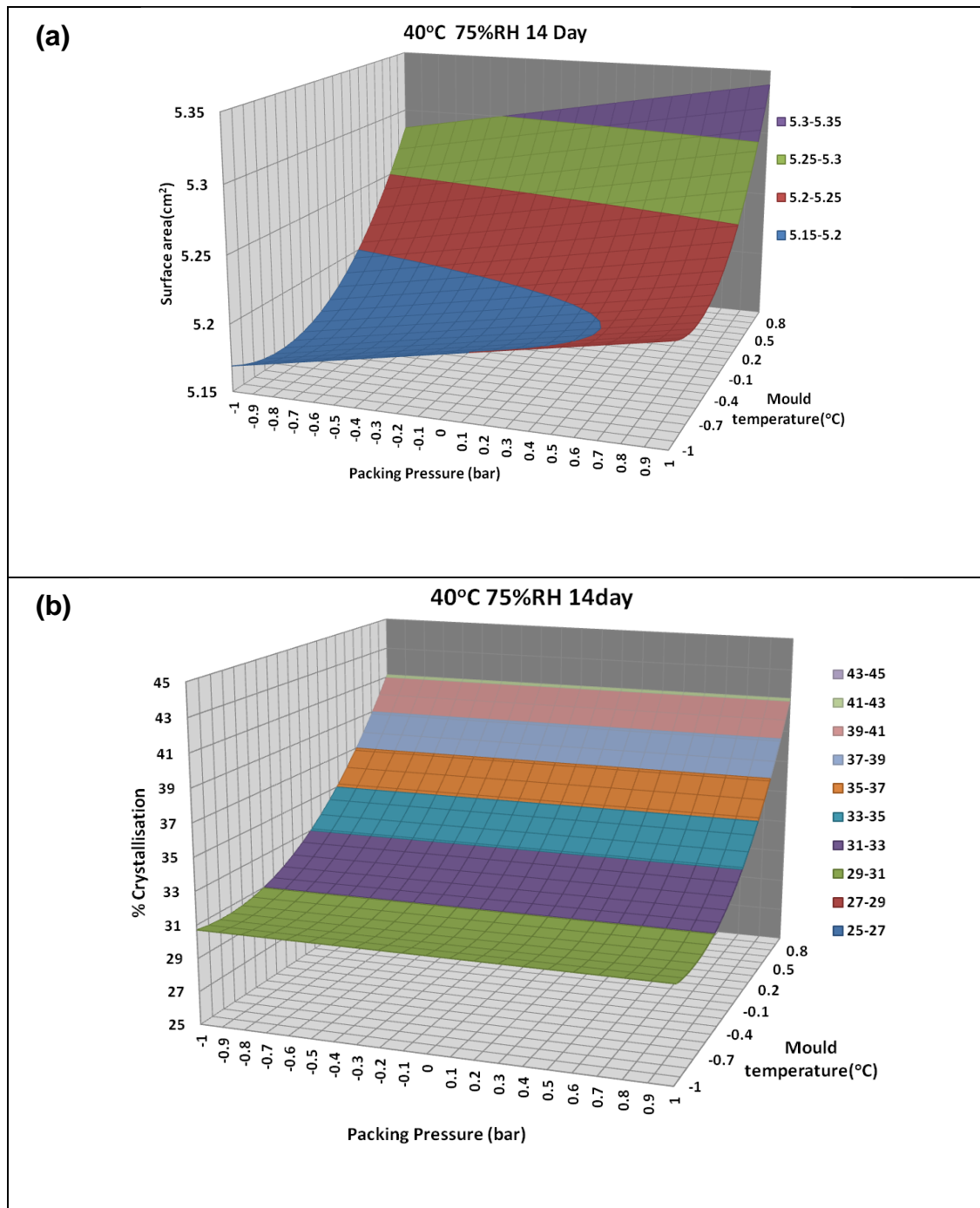
Figure 5.48 : Surface response curve for 40ºC 75%RH 14 days (a) surface area (b) %crystallisation

The surface response curve (Figure 5.48 a) also showed the higher surface area at the high packing pressures and mould temperatures. Hence, the influential parameter for the surface crystallisation of the ibuprofen was the mould temperature and the higher the mould temperature the faster was the rate of the crystallisation at $40^{\circ}C$ 75%RH. This confirmed that the cooling rate of the moulded part and high plasticisation effect due to moisture caused the faster crystallisation of batches stored at $40^{\circ}C$ 75%RH and relatively less effect on the surface area and shrinkage.

For the $40^{\circ}C$ 60%RH stress conditions, surface area and % crystallisation response curves also suggested similar behaviour as at $40^{\circ}C$ 75%RH. However the rate of crystallisation and shrinkage was slower compared to $40^{\circ}C$ 75%RH confirming the role of moisture on the crystallisation process where higher moisture favoured the crystallisation. Mould packing pressures also showed an effect on shrinkage and effective surface area. At higher packing pressure, the higher surface area of the moulded bar was observed, suggesting that packing pressure has an influential effect on shrinkage (Figure 5.49). Interestingly, batches packed at high pack pressure and high mould temperature ($30^{\circ}C$) exhibited a higher surface area which therefore provided greater area for surface crysallisation to occur under stress conditions. Similar response curves were also obtained for the NIR % crystallisation data (provided in Appendix I).
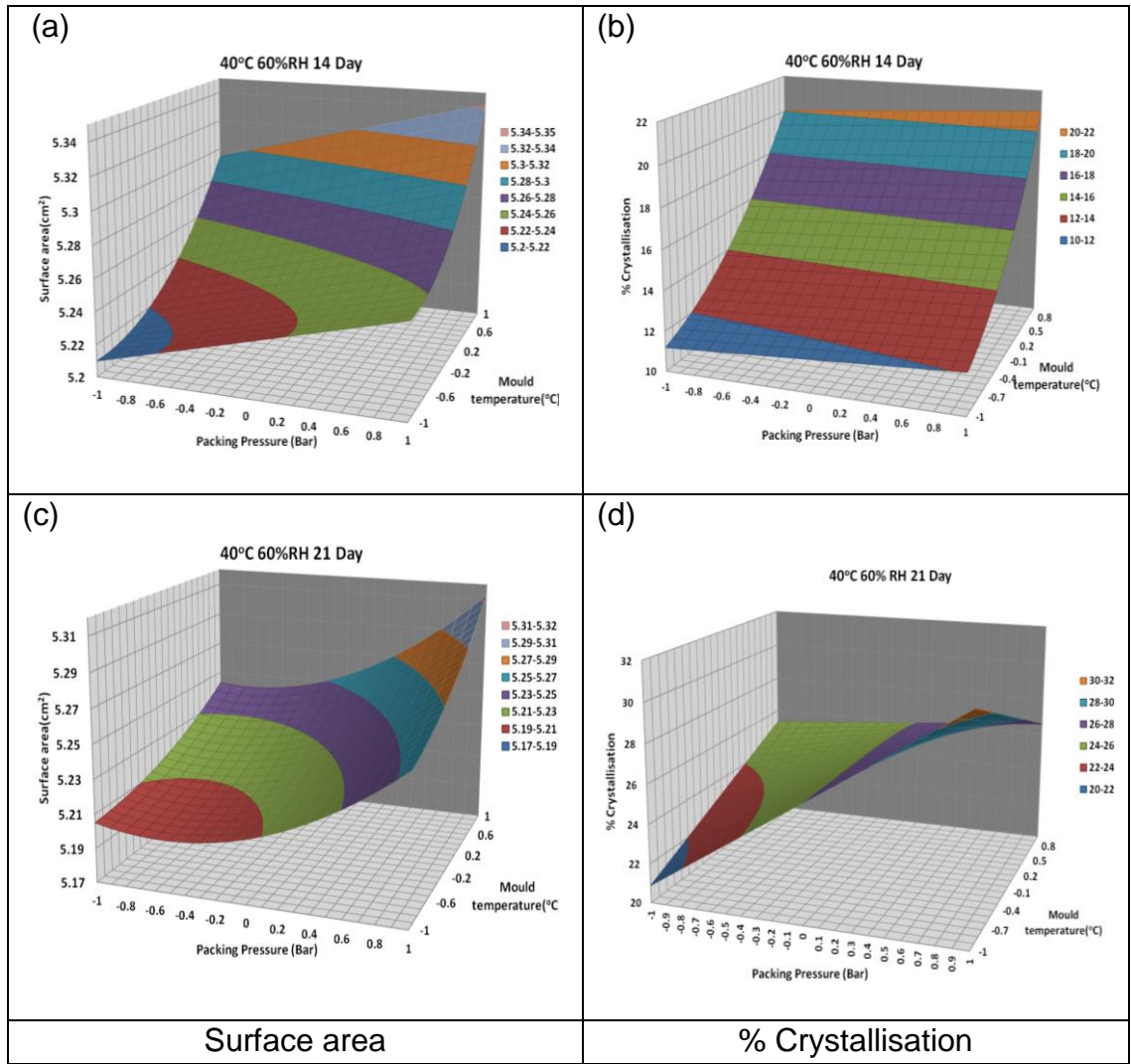
Figure 5.49: Surface response curve for 40°C 60%RH 14 and 21day (a, c) surface area; (b, d) %crystallisation
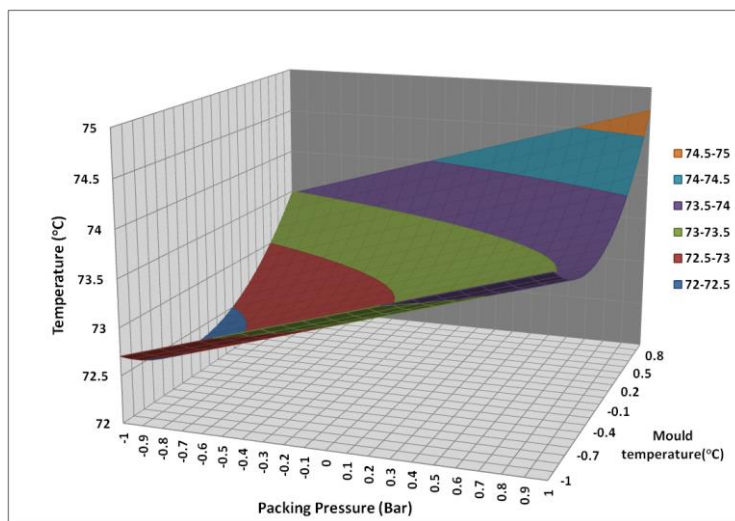
Figure 5.50: Surface response curve for tan δ temperature

The surface response curve of moulded samples obtained using DMA testing (second tan δ peak) suggested some correlation of the mould temperature and packing pressure with the temperature at which the tan δ peak was observed. At low packing pressures and low mould temperatures the tan δ peak was observed at lower temperature and increased at higher pack pressures and mould temperature (Figure 5.50). The position of tan δ peak temperature could be correlated with the melting point depression in the solid dispersion where a higher melting depression suggests the better interaction and miscibility between drug and polymer.

To summarise the discussion of crystallisation, at stress conditions, it was found that the surface response curve correlated with the surface area available for crystallisation. It was observed that as extreme stress conditions (40°C 75%RH) crystallisation was predominantly affected by the mould temperature and relatively less affected by packing pressure and shrinkage. On the other hand, at moderate stress condition (40°C 60%RH) the pack pressure, mould temperature combined to affect the surface area and thus influenced crystallisation.

To understand the morphology, crystal habits and surface crystallisation of ibuprofen; SEM, 3D laser microscopy and 2D Xray diffraction techniques were used. The results of these characterisation techniques are discussed in the foloowing sections.

5.1.3.6 SEM and 3D laser microscopy: Surface crystal orientation and roughness

The surface properties of I33 moulded bars were analysed at different positions. The representative positions of scanning are presented in the Figure 5.51. The scanning points were equidistant and distance between the points was 0.8 cm.
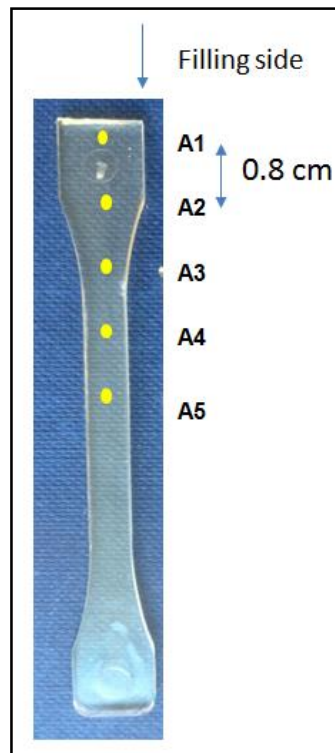
Figure 5.51: I33 mould and 3D laser scanning area

The scanning positions on the bar were chosen to observe the crystal habits and surface crystal orientation. The particular interest was to progressively monitor the crystal length, size, and the diameter after exposure to different stress conditions. The 2D Xrd results (provided in the later section) have shown the change in the relative intensity of 2θ peaks at various regions on the bar. Moreover the specific Xrd pattern was observed at specific stress conditions. Surface scanning of samples was performed at intervals of 24 hrs for 7 days. The

stress conditions i.e 40°C 75%RH, 25°C 60%RH and RT have shown the preferred orientation of crystals on the surface at different conditions (Figure 5.52). Moreover, from the point A1 (this is first point from mould filling side) to A5 different crystal habits of ibuprofen were observed on the surface.
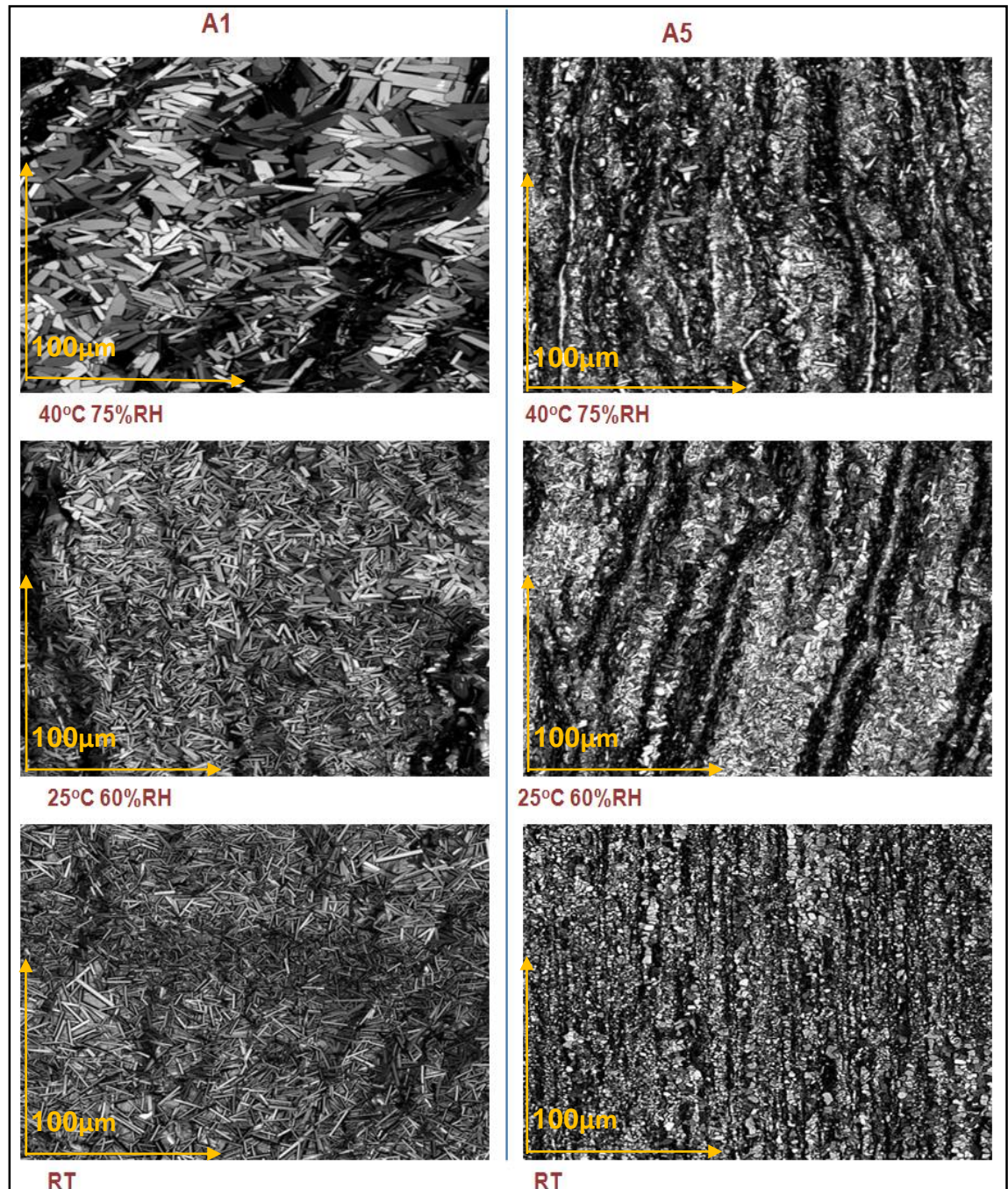
Figure 5.52: Crystal habit of ibuprofen on I33 moulded bar surface at A1 and A5 when exposed to 40°C 75%RH 25°C 60%RH and RT after 1day of exposure

The different regions on the moulded bar have promoted the different orientation of the crystals on the surface. Figure 5.52 shows that, at 40°C 75%RH (point A1, 1day) larger rectangular crystals while, at the same time 25°C 60% RH bar showed small rectangular crystals and at RT smaller (needle shaped) crystals. Interestingly, the A5 position (middle region) of the bar showed different crystal habit with small in size with marked shrinkage marks. This indicates that different crystal habits were present on the different surface regions of the moulded bar. Especially, after A3 region (necking region) the smaller crystals with a distinct habit were observed at all the conditions (Figure 5.53).
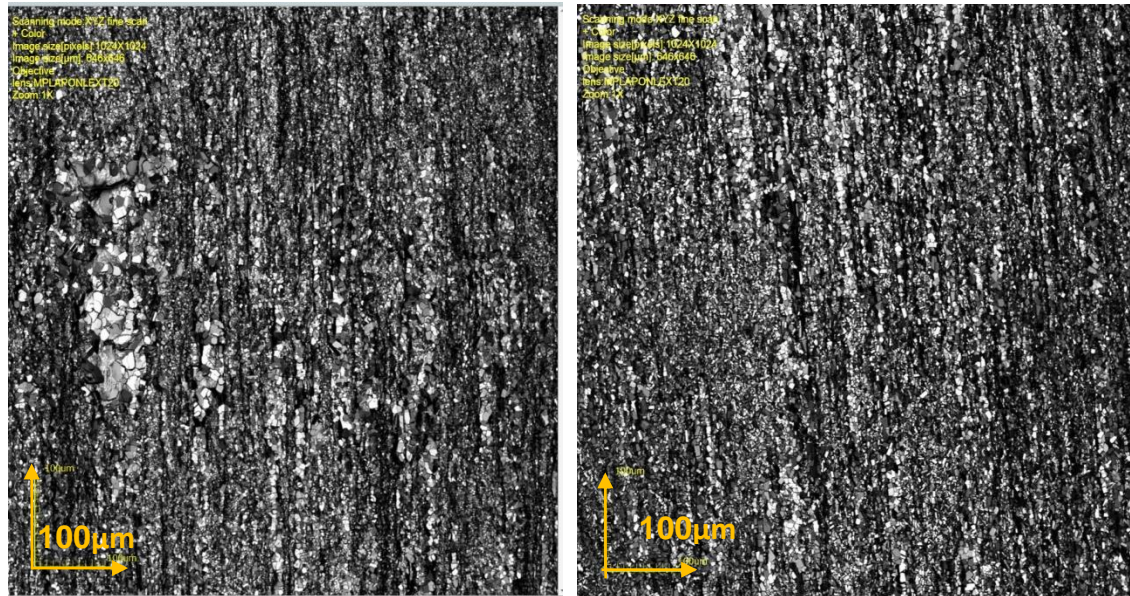
(A)   (B)

Figure 5.53: A3: Crystal habits after 7 days (A) 40°C 75%RH(B) 25° C 60%RH

The surface roughness of the representative moulded bars was calculated based on height parameters at evaluation area of 646 X 646 µm. The roughness of the surface was found to be depending on the surface crystal habit.

Surface after moulding

25°C 60%RH A5 surface : 7days

RT A5 surface: 7days
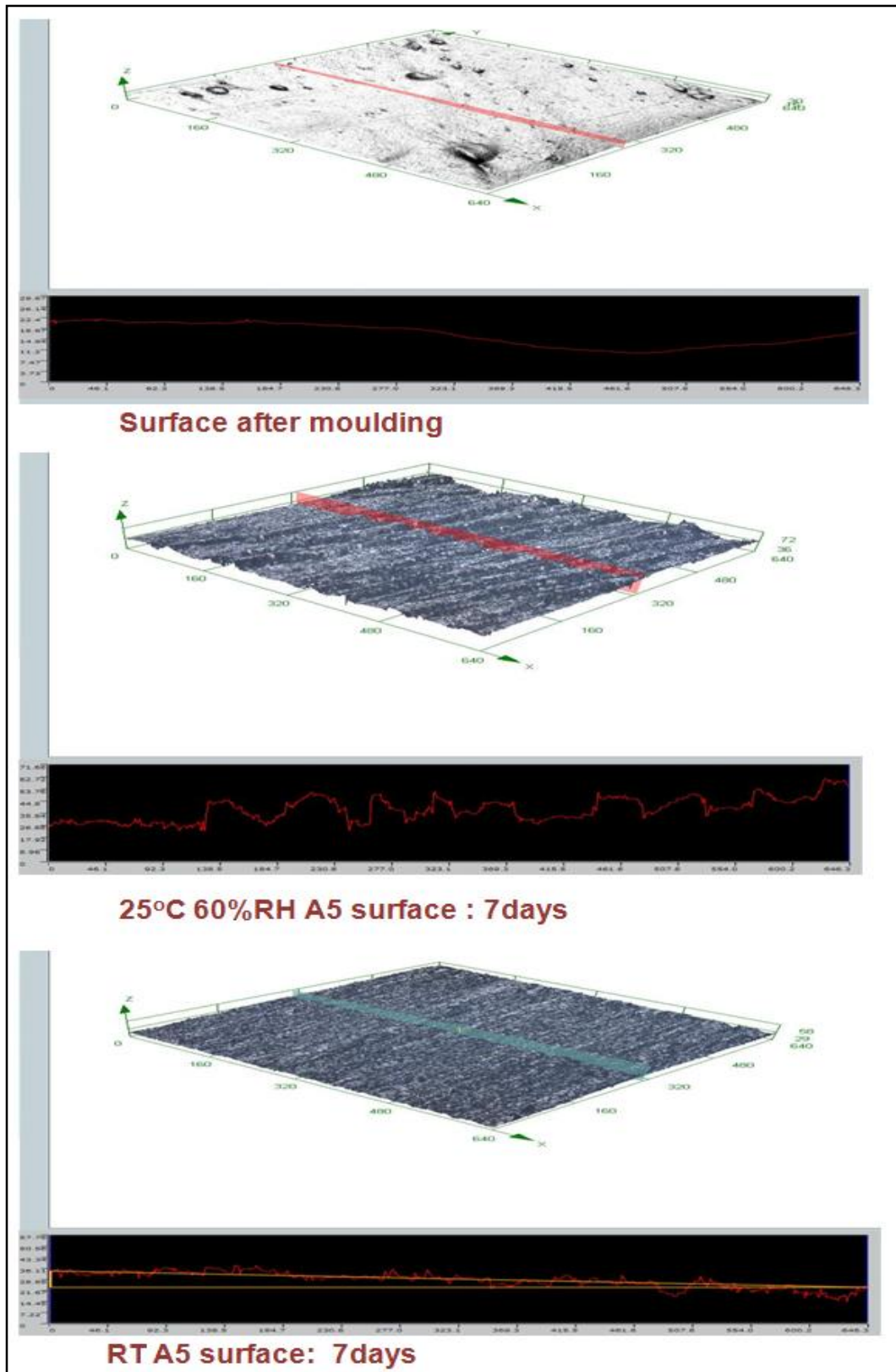
Figure 5.54: Line profiling of I33 moulded systems of the surface before and after storage

The line profiling of scanned 3D surfaces are presented in the Figure 5.54. The red line pattern shows the surface height in μm. A variation was seen at 25°C 60% and RT samples compared to surface scan of sample analysed immediately after moulding these differences could be attributed to the surface crystals of the ibuprofen. The representative 3D scan of 25°C 60%RH sample (A5 region) after 7days has shown in the Figure 5.55 and the wave-like patterns were observed due to shrinkage of the mould.
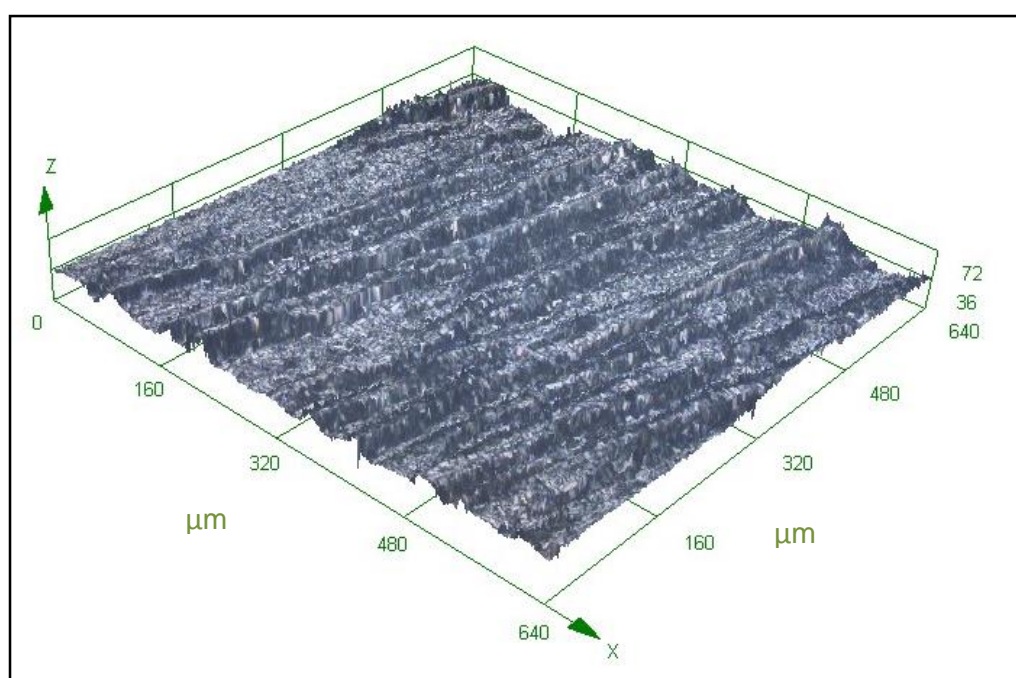
Figure 5.55: 3D Surface image of 25°C 60% A5 region after 7day

The surface roughness values after the 1st and 7th days of exposure to the storage conditions at different region on the bar are presented in the Figure 5.56. In general, higher surface roughness was observed at 40°C 75%RH condition where crystal growth on the surface and shrinkage rate was faster than the other conditions. Higher roughness values were observed on the 7th day as compared to 1st mainly due to the % crystallised ibuprofen on the surface. Moreover, from A3 downstream region higher shrinkage values were observed due to marked

shrinkage as shown in the Figure 5.55. The surface after moulding showed 0.25 µm surface roughness and after 24 hrs of exposure the roughness was increased to 3.1, 1.8, 1.3 µm at 40°C 75%RH, 25°C 60%RH, RT respectively (Figure 5.56). The least roughness was seen at RT due to small crystal size, crystal habit and less shrinkage.
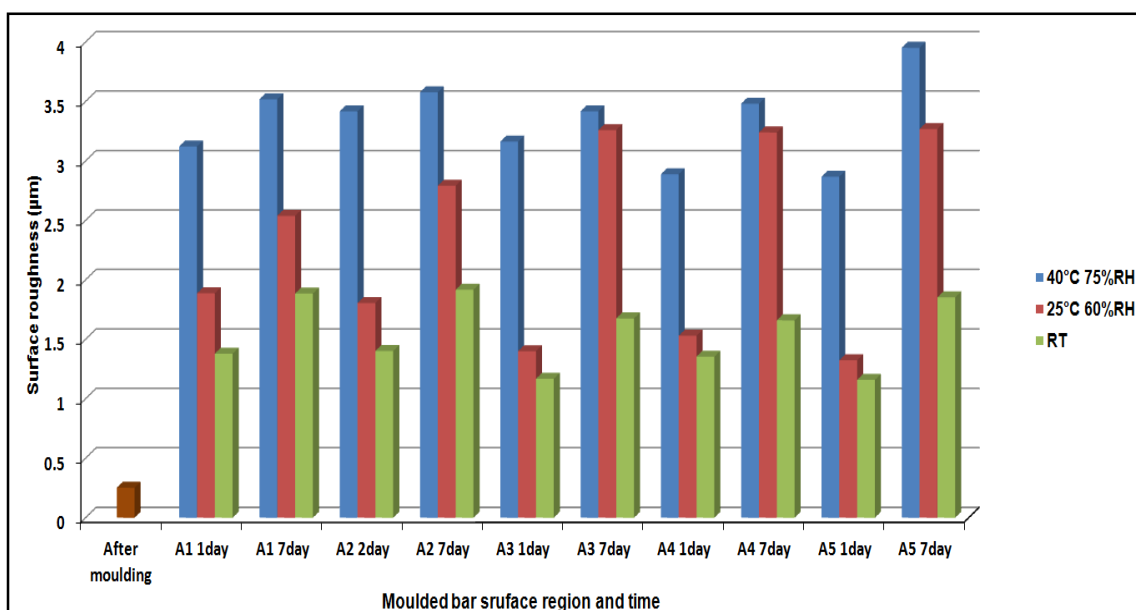
Figure 5.56: Surface roughness moulded bar at different region

Crystals at the A1 and A5 position were prominently different in their size and shape. Average crystal size for the 40°C 75%RH condition seen was 40 µm at A1 and 12 µm at A5 positions; which were doubled in size compared to those of RT (Table 5.11).

Table 5.11: Crystal size of ibuprofen on the surface after 7days of storage (n=3)

Stress Condition	Average Crystal size (µm)	
	A1	A5
40°C 75%RH	40.02 ± 0.5	12.2 ± 0.7
25°C 60%RH	25.01 ± 0.4	10.4 ± 0.7
RT	20.04 ± 0.6	8.78 ± 0.6

Ibuprofen was crystallised using organic solvents such as methanol, ethanol, isopropanol, hexane have shown different crystal habits such as polyhedral, elongated, needle etc (Garekani et al., 2001). The marked difference in crystal habits of ibuprofen was obtained due to the different solvent properties. In the I33 moulded systems the predominant effect of the humidity and temperature was observed, however the different regions of the bars at same stress conditions shown different crystal habit suggesting effect of the IM process and shrinkage on the surface crystallisation and crystal habit.

5.1.3.7 X-ray Diffraction

The crystalline nature of the pure ibuprofen was confirmed by XRD and it shows characteristic crystalline peaks at 2θ positions (6.09, 12.18, 16.78). The amorphous nature of HPMCAS was confirmed by the absence of crystalline peaks (Figure 5.57). Surface scanning of the moulded bars exposed to different stress conditions exhibited the preferred orientation of crystals. Moreover, changes in the relative intensity of XRD peaks were attributed to crystal habit and orientation. The 2D XRD pattern of moulded bars exposed to 40°C 75%RH and RT are shown in Figure 5.58.
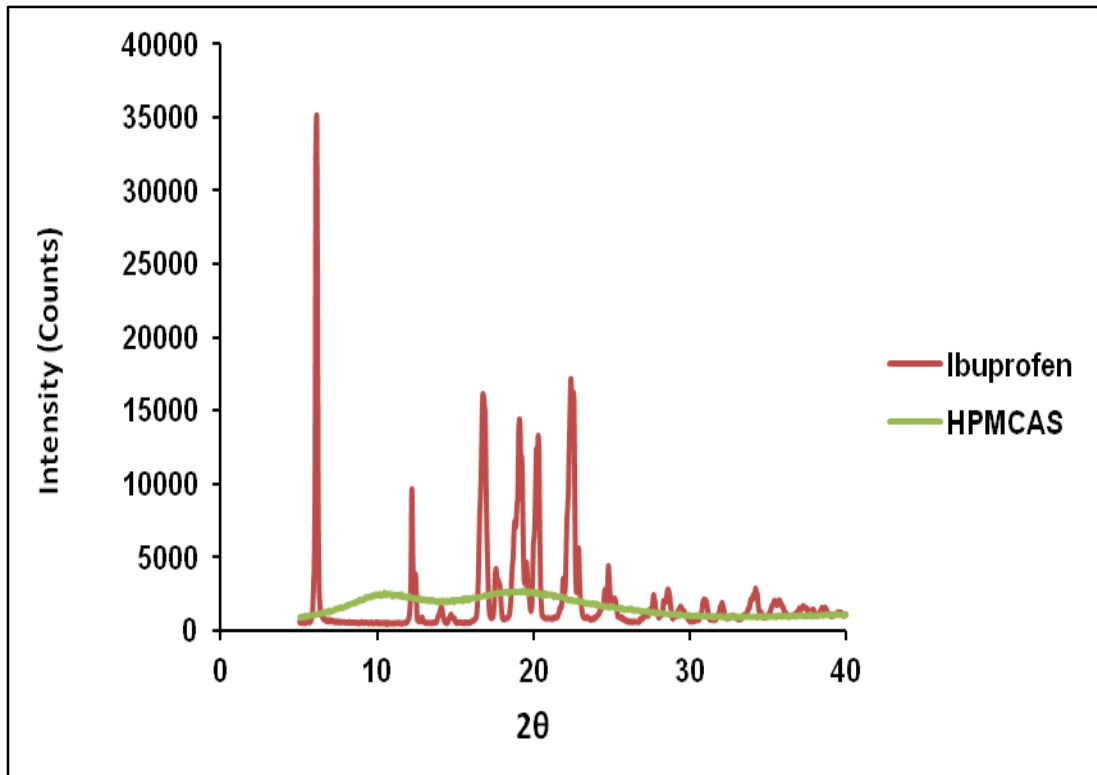
Figure 5.57: XRD pattern of pure ibuprofen and HPMCAS
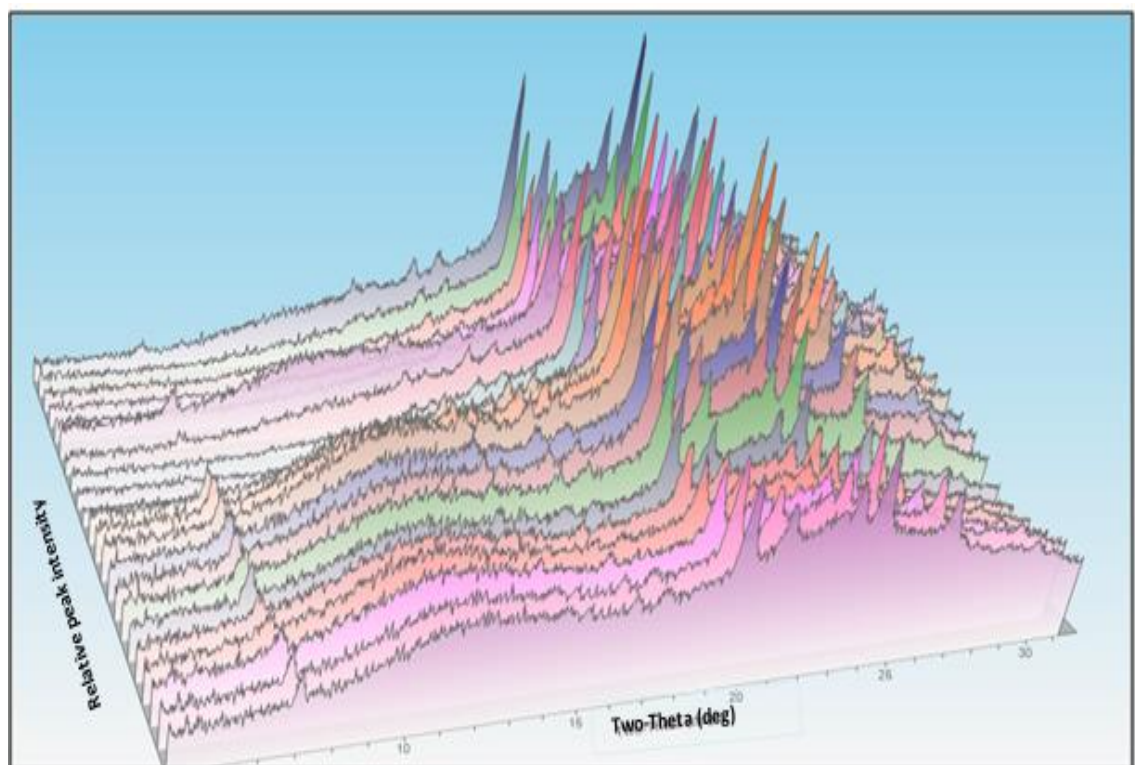
40ºC75%RH
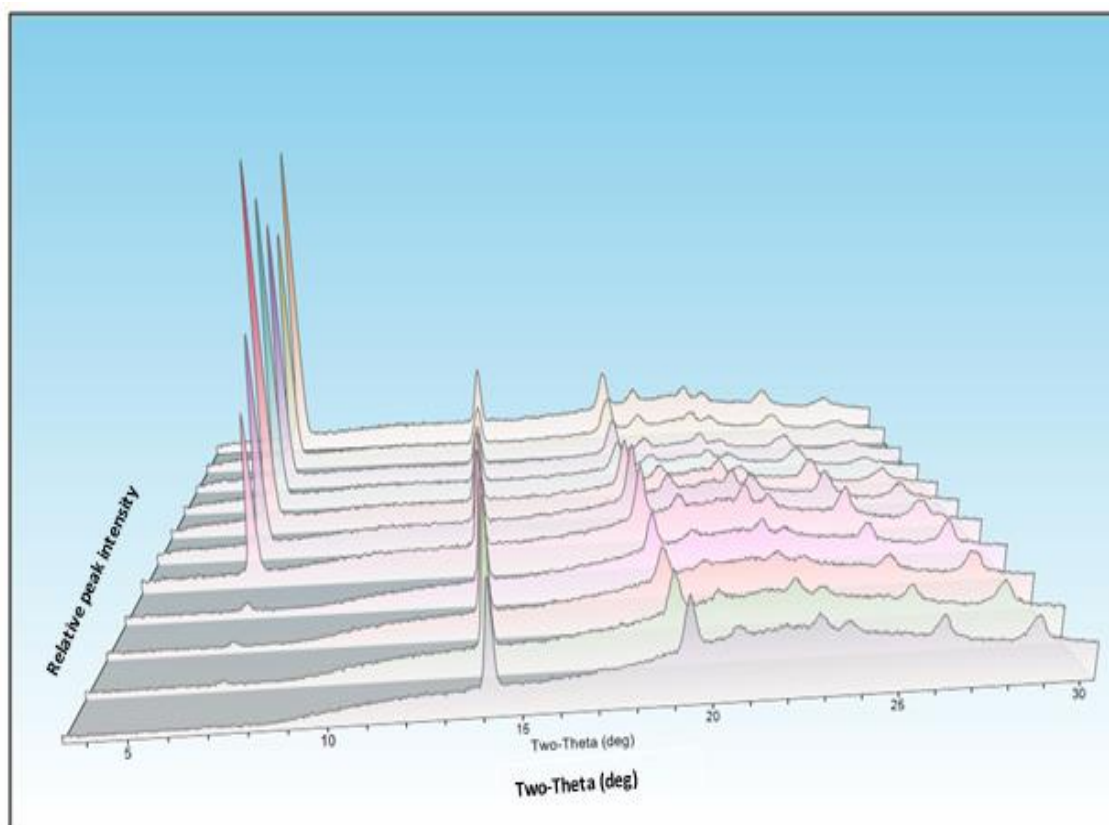
RT

Figure 5.58: XRD patterns of the surfaces of I33 moulded bar exposed to 40°C 75%RH and RT

Prominent peaks at 40°C 75%RH were 20, 22.32 and 24.76 whereas for RT samples 6.0, 14.70, 19 peaks were more dominant. The relative changes in the XRD patterns attributed to the crystal habits of ibuprofen. Pure ibuprofen (used for this study) shows the rectangular crystals with the average crystal size of approximately 150μm (ibuprofen in the physical mix). Figure 5.59 shows the SEM images of different crystal habits of the ibuprofen on the surface at different stress conditions resembles to the some of the reported crystals habits of ibuprofen obtained using the solution crystallisation as mentioned earlier. The relative peak intensity changes in 2D XRD presented merely due to the different crystal habits on the surface of the moulded bar.

216
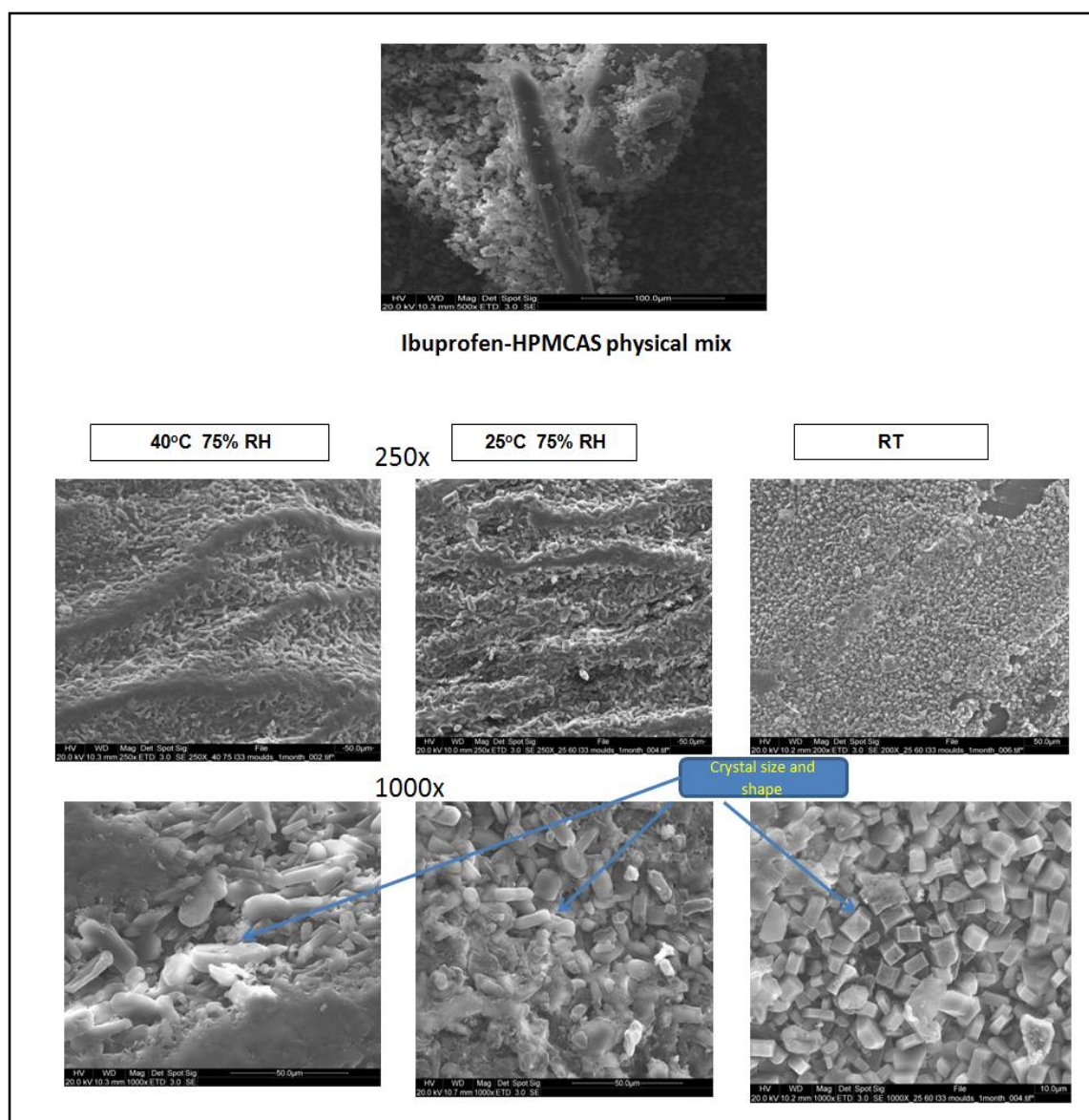
Figure 5.59: SEM of ibuprofen-HPMCAS physical mix and surface crystallised ibuprofen at different storage condition

5.1.3.7.1 Depth profiling

Depth profiling of injection moulded bars showed that sample stored at 40°C 75 %RH and 40°C 60%RH were crystallised throughout the cross-section of the sample. XRD patterns of the 40°C 75%RH samples analysed from top to the bottom and from right to left has shown in the Figure 5.60. XRD pattern provides a clear understanding of the re-crystallisation of amorphous ibuprofen on the surface as well as in the middle of the sample at extreme stress conditions.

Interestingly, the XRD patterns of 25°C 60%RH samples have given more insight on the surface crystallisation phenomenon. It was seen that the surface of the sample was crystallised but middle (core) of the system was still in an amorphous state. The absence of crystalline peaks of ibuprofen shows the ibuprofen-HPMCAS amorphous dispersion stable in middle of the bars even after 1 year at 25°C 60% (Figure 5.61).
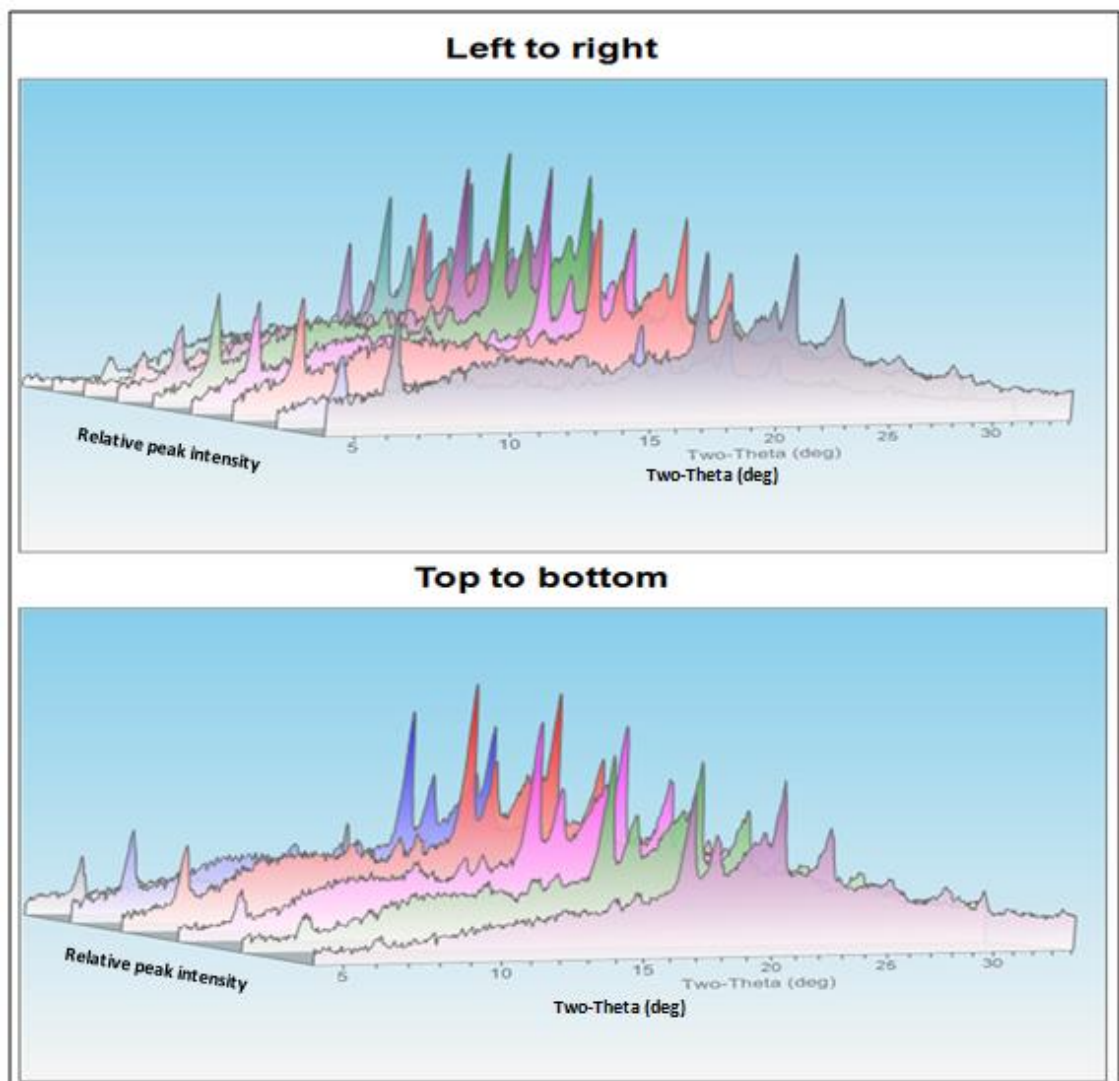
Figure 5.60: Depth profiling of I33 moulded bar after 1 year of storage bar at 40°C 75% RH
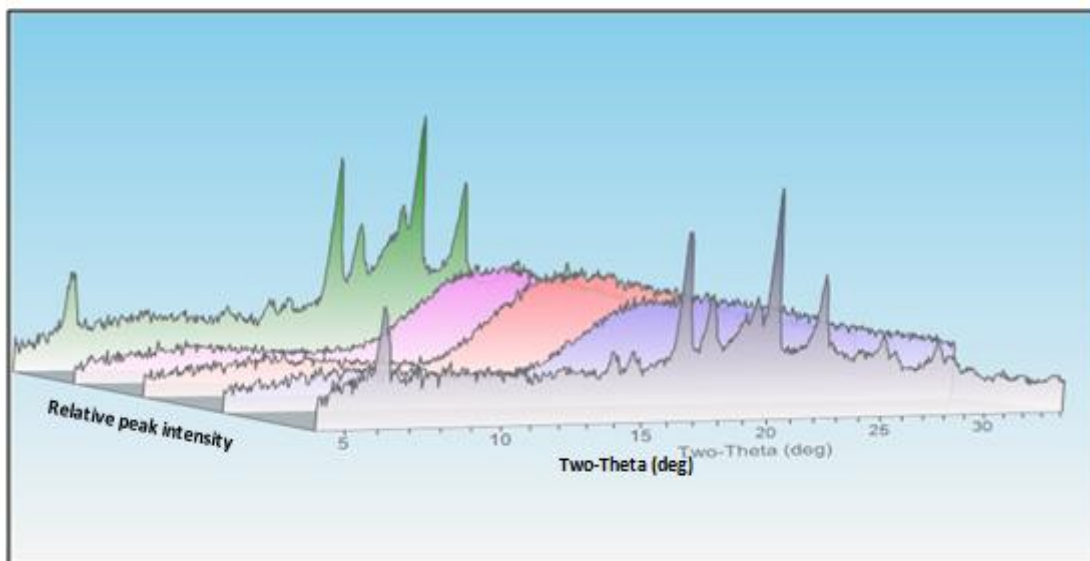
Figure 5.61: Depth profiling of I33 moulded bar after 1 year of storage bar at 25°C 60%RH

5.1.3.7.2 Calculation of degree of crystallinity

The XRD peaks obtained after analysis of physical mixture were used to calculate crystalline index of physical mixture (Figure 5.62). The crystalline index was calculated using following formula

$$\text{Crystalline index} = \frac{\text{Intensity of crystalline peak at } 2\theta \text{ peak}}{\text{Diffracted intensity}} \qquad \text{(Equation 5.6)}$$
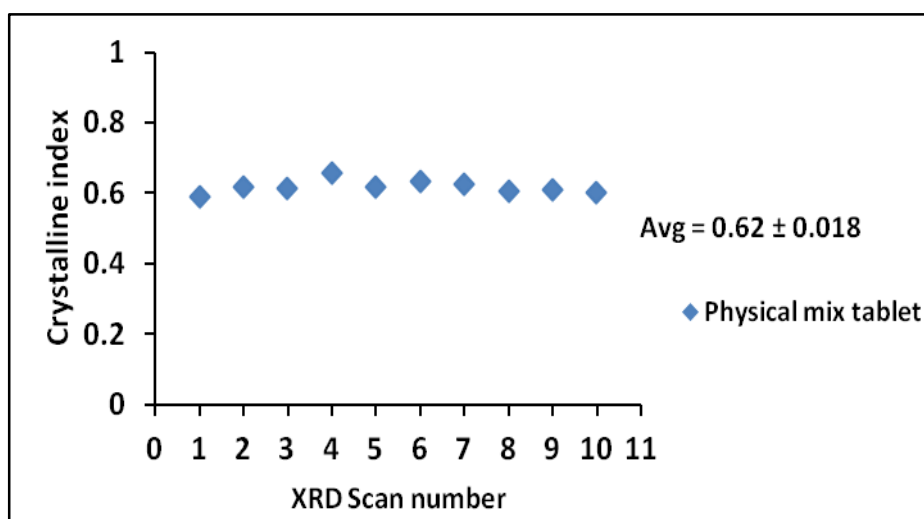
Figure 5.62: Crystalline index of I33 physical mixture

Depth profiling of 25°C 60%RH samples from the top crystalline surface region to the core of the system until it reaches the amorphous region provided good XRD patterns where the relative peak intensity decreased as it was progressing from the top surface to the middle of the system (Figure 5.63).
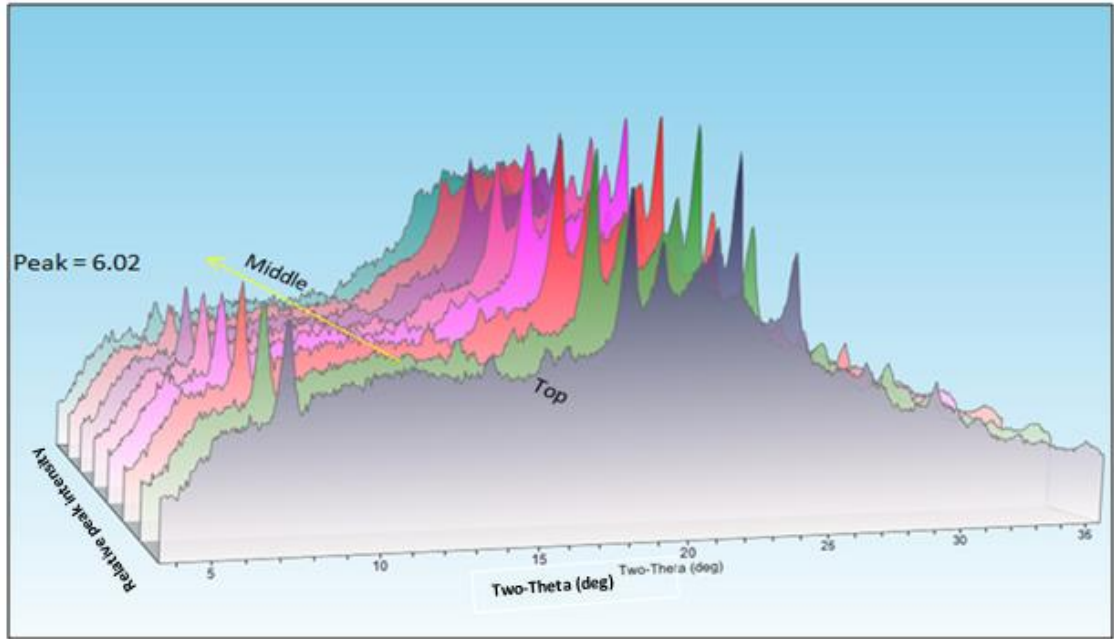
Figure 5.63: Depth profiling of I33 moulded bar 25°C 60%RH in crystalline region of ibuprofen

The crystalline index of the sample decreased from its top surface to the core which shows that the crystallinity was decreased across the sample (Figure 5.64).
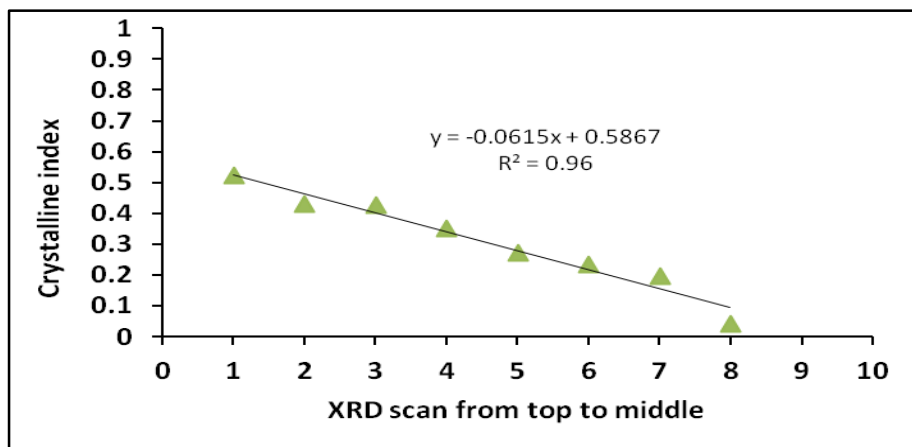
Figure 5.64: Crystalline index of I33 of moulded bar at 25°C 60%RH

The scanning area from T1 (top) to T8 (middle) was representative of the crystalline region and the distance between the each point was 0.085 mm (85 μm). Percentage crystallisation was calculated using the crystalline index of the sample and the crystalline index of reference. Table 5.12 shows that the topmost region (T1) of the moulded bar was crystallised approximately to 83% and the % crystallinity decreased to 6.9% at point T8. After this point the sample has shown the absence of any crystalline peaks indicating that an amorphous core was present. The depth profiling studies using 2D XRD complement the Raman data which show the samples are only crystallized onto the surface and middle portion was still in this amorphous phase. Hence, the phenomenon was a predominantly surface crystallization however, at extreme condition due to higher crystallization rate (2%/day), crystallinity was observed in the core.

Table 5.12: % Crystallisation of ibuprofen I33 bar of 25 °C 60%RH

Scanning area	Crystalline index of sample	Crystalline index of ref	CI of sample/CI of ref	% Crystallisation
T1	0.52	0.62	0.83	83.87
T2	0.43	0.62	0.69	69.35
T3	0.40	0.62	0.64	64.51
T4	0.35	0.62	0.56	56.45
T5	0.27	0.62	0.43	43.54
T7	0.24	0.62	0.38	38.70
T6	0.2	0.62	0.32	32.25
T8	0.043	0.62	0.069	06.93

The key findings of studies on the ibuprofen-HPMCAS moulded system where the firstly, phase separation; secondly, shrinkage; and thirdly surface crystallization. The phase separation at 33% drug loading was observed due to immiscibility of the two components at storage conditions. The system was completely miscible at processing conditions, however showed the immediate phase separation at stress conditions. Low Tg (38°C) of I33 extruded and IM systems decreased its stability as the higher glass transition temperature could have favoured amorphous phase stability. The rate of crystallisation was higher at extreme stress conditions; temperature and moisture played a significant the role in the crystallisation. The relationship between the crystallization and shrinkage was expected, however, no direct relationship was observed as the extruded systems crystallised at the same rate as that of moulded systems but it didn't show any sign of shrinkage. IM process variables showed an influential effect on the crystallisation where the effect of mould temperature was predominant.

5.2 Felodipine-PEO-HPMCAS (FDH) IM systems

Felodipine is a calcium channel blocker used in the treatment of hypertension. The daily dose of felodipine is 10 mg and being a BCS class II drug it has limited solubility and high permeability. Felodioine has high Tg (45°C) and high melting point (145°C) compared to ibuprofen (Figure 5.65). 33%w/w loading of felodipine in HPMCAS was achieved using HME however, IM was challenging due to melt flow of the system. The objective was to achieve a 10%w/w dispersion of felodipine in HPMCAS however; due to the high Tg of the mixture it becomes the necessary to add a plasticiser to the system. The final batch composition was the felodipine-PEON750-HPMCAS [FDH(10:20:70)]

5.2.1 Processability via HME and IM

The reversing heat flow curve of MDSC of physical mixture of FDH shows the melting point of semi-crystalline PEO at 66 °C, Tg of amorphous HPMCAS at 120°C±0.23 and melting point of felodipine at 145±0.22°C (Figure 5.66).
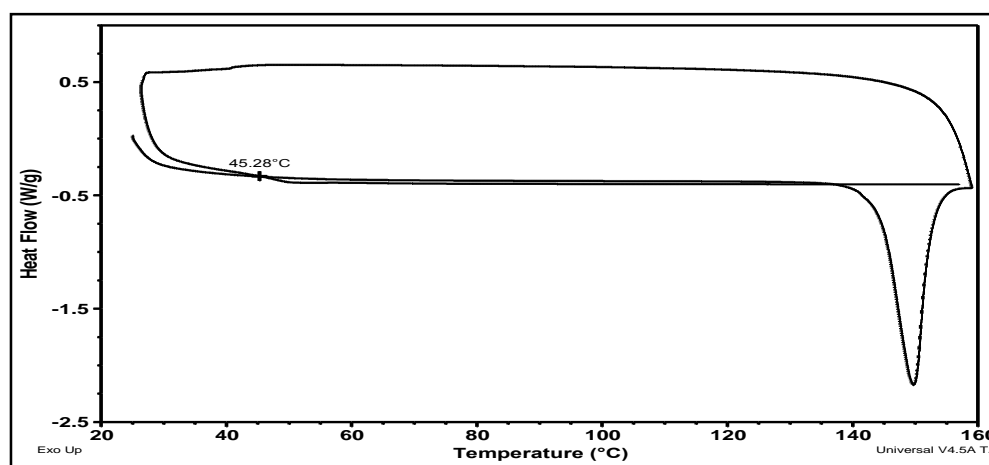
Figure 5.65: Heat cool heat DSC thermogram of pure felodipine (sample heating rate was 10°C/min and cooling rate 20°C/min)

223
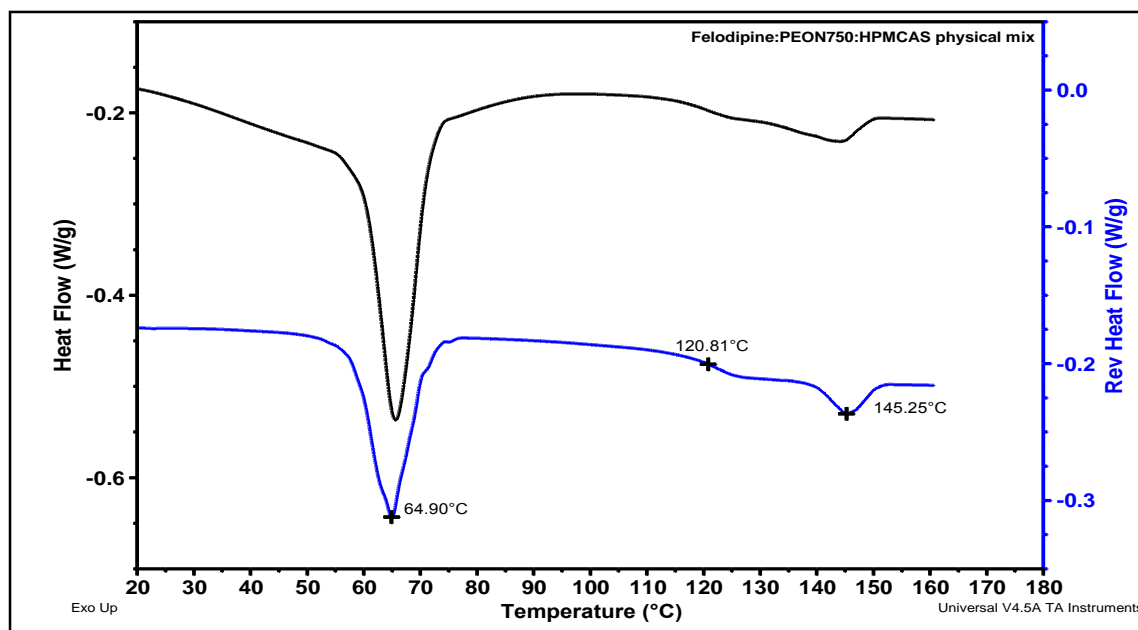
Figure 5.66: DSC thermogram of FDH physical mixture (modulated heating rate of 5°C/min)

HME of PEO-HPMCAS (20% PEO-HPMCAS) and FDH systems was carried out at 140°C. Details of the HME processing parameters were mentioned previously in chapter (table 3.12). PEON750-HPMCAS physical mixtures were initially processed to observe the miscibility of the polymer blends. Due to the very low Tg (-52°C) and melting at 66°C PEO acts as a good plasticiser for HPMCAS. The addition of 10%w/w felodipine further improves the processing; both torque and die pressures decreased indicating good mixing of drug with the PEO-HPMCAS mixture. Table 5.13 shows torque and die pressure during HME.

Table 5.13: Torque and die pressure associated with extrusion process

PEO-HPMCAS			Felodipine-PEON750-HPMCAS (FDH)		
Die pressure(bar)	Torque (%)	Motor power (kW)	Die pressure (bar)	Torque (%)	Motor power (kW)
35	35-40	0.88 -1.0	30	31-35	0.78-0.88
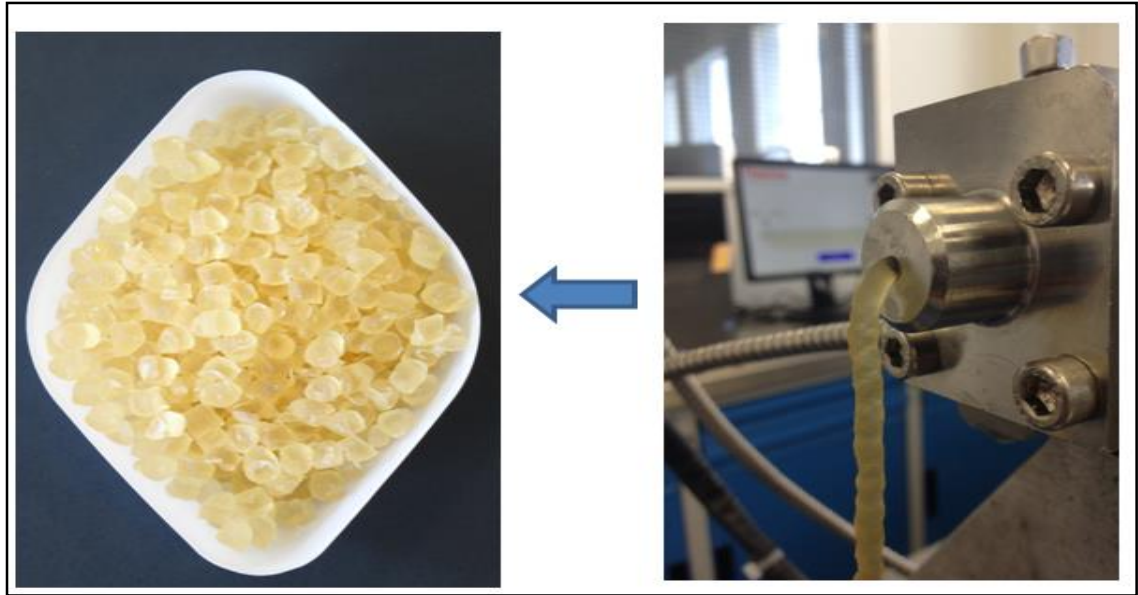
Figure 5.67: melt extruded strand of FDH system at the end of extrusion barrel (die) and product obtained after pelletisation

Approximately 2 mm diameter melt extruded pellets were obtained after cutting the extruded strand using a pelletiser (Figure 5.67). Pellets were used to produce the IM bar and IM tablets. At 140ºC, the melt viscosity of the system was optimum to get sufficient melt flow inside the runner system to achieve mould filling. For initial trials of moulded tablets, mould filling was achieved with injection velocity and shot size was increased from 10 mm to 14 mm. Figure 5.68 depicts short-shots of FDH tablets. When the mould cavity was approximately 95% filled, a packing pressure was applied to ensure 100% filling of the mould cavity. Packing pressure has significant effect on the filling of the mould cavity. Optimum quality parts were obtained when 900 bar of packing pressure was applied whereas in the case of I33 systems the optimum quality parts were made at 300 bar. To mould tensile bars a shot size of 23 mm was used.

shot size filling

(a)

(b)
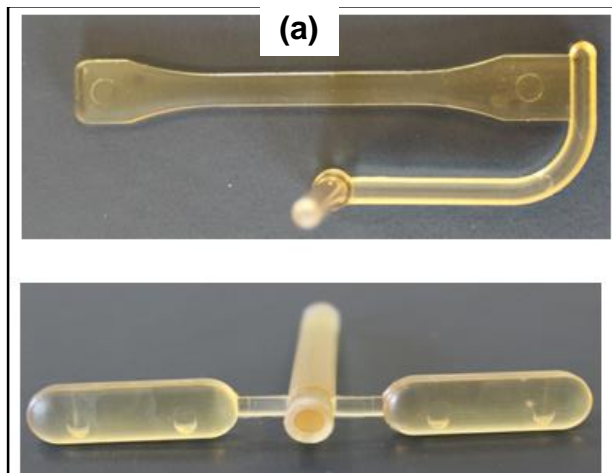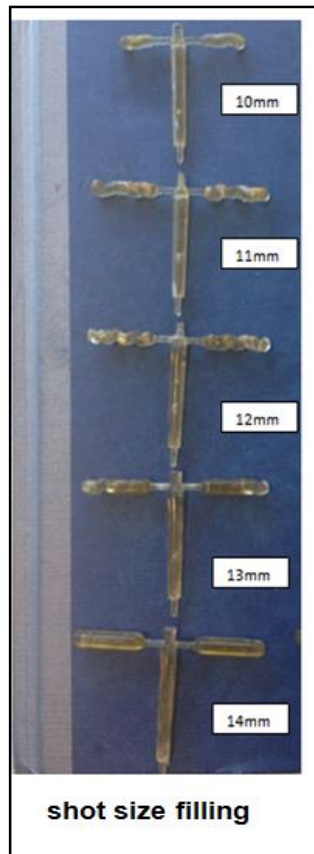
Figure 5.68: (a) short shots of FDH tablets (b) FDH moulded bar and IM tablets

5.2.2 Characterisation

Melt extruded pellets and injection moulded components were characterised to understand the nature of felodipine dispersion and the drug release behaviour of the melt processed system.

5.2.2.1 Thermal behaviour (MDSC)

Thermal analysis of melt extruded pellets and IM tablets using MDSC confirmed the absence of melting endotherm of the felodipine and the system exhibited a single Tg at 54.4±0.23°C (Figure 5.69) . Theoretically predicted Tg for FDH components using the Fox equation was 60.27oC which is closer to the practically estimated value. The single Tg of the system confirmed the formation of an amorphous molecular dispersion i.e solid solution (Caron et al., 2013). The Tg of the FDH systems was well separated on reversing heat flow curve of MDSC.
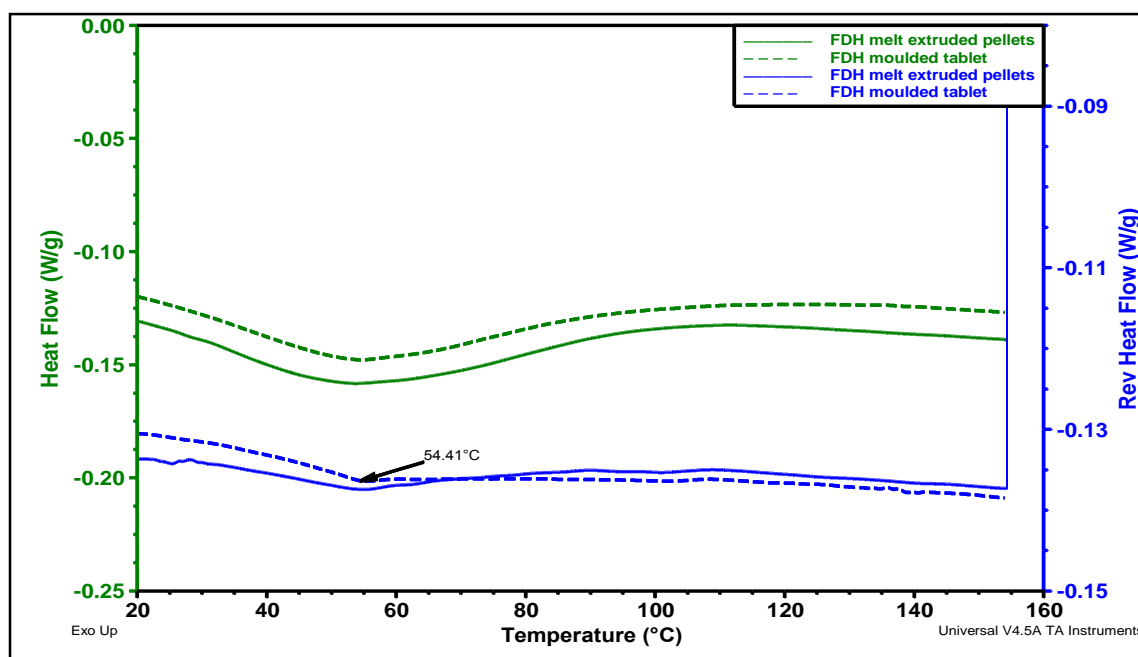
Figure 5.69: MDSC of FDH melt extruded pellets and IM tablet (modulated heating rate of 5oC/min)

It is known that the amorphous form is highly disordered and has a high-energy, therefore it is often associated with the risk of drug recrystallisation (Hancock and Zograf, 1997). The FDH system kept at stress conditions to observe the stability of the amorphous form in solid dispersion. At various stress conditions, the system has not shown any sign of re-crystallisation confirming the

good stability of FDH systems. The reversing heat flow curves for the sample kept at 40°C 75%RH and 25°C 60%RH (Figure 5.70 and Figure 5.71) did not show a significant change in the thermal behaviour of the system. Neither was there a change in the Tg of the system nor any sign of phase separation due to stress conditions, suggesting that the system had both good miscibility and stability.
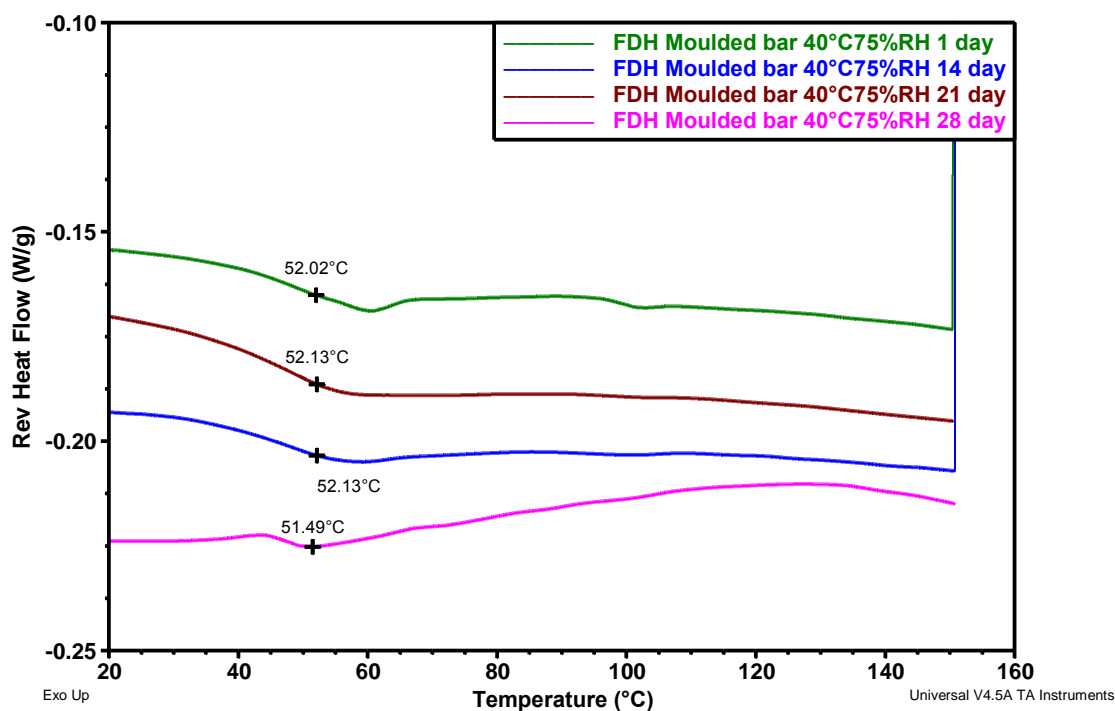
Figure 5.70: Reversing heat flow of FDH IM moulded bar kept at 40°C 75%RH (modulated heating rate of 5°C/min)
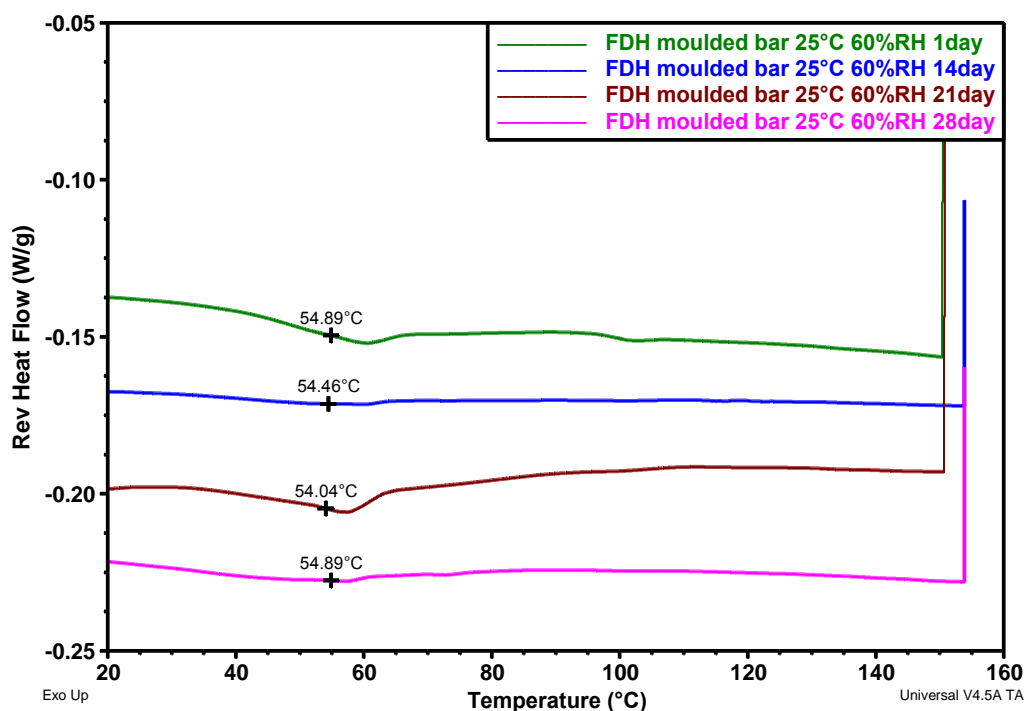
Figure 5.71: Reversing heat flow of FDH IM moulded bar kept at 25°C 60%RH (modulated heating rate of 5°C/min)

5.2.2.2 DMA

The dynamic mechanical behaviour of moulded bars was analysed using dual-cantilever mode DMA. PEO-HPMCAS moulded bars at 25°C exhibited a storage modulus of 52,743 MPa whereas the temperature near to the Tg (62°C) modulus decreased to 22,572 MPa. A drastic fall in storage modulus indicates the Tg of the system. Similarly, FDH moulded bars showed a fall in storage modulus at a temperature around 55°C (Figure 5.72). The comparative properties such as storage modulus, tan δ, and stiffness at 25°C and temperatures near Tg of the system are mentioned in Table 5.14. The comparison provided in the Table 5.14 suggested that the mechanical properties of the moulded bars (modulus and stiffness) decreased significantly near the Tg because of the higher molecular mobility and approximately half reduction in the modulus was observed.
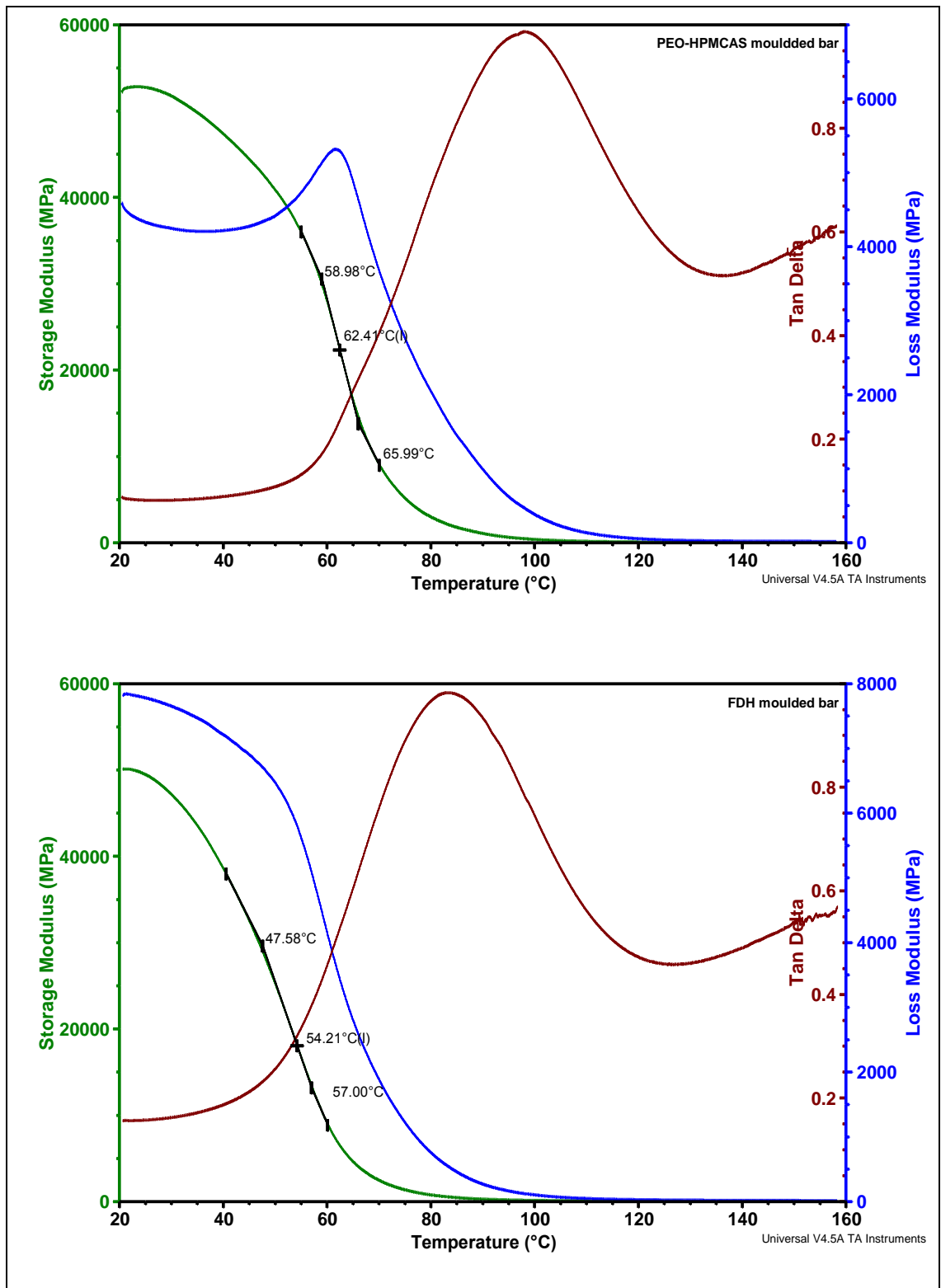
Figure 5.72: DMA of (a) PEO_HOMCAS and (b) felodipine-PEO-HPMCAS moulded bars

Table 5.14: Mechanical properties of injection moulded bars

Materials	Temperature (°C)	Storage Modulus (Mpa)	Loss Modulus (Mpa)	Tan Delta	Stiffness (N/m)
PEO-HPMCAS	25.08	52743	4329	0.08	755975
	62.31	22572	5298	0.23	323537
FDH	25.025	49446	7780	0.15	708718
	54.16	18132	5805	0.32	259898
33% Ibuprofen – HPMCAS (I33)	25.0	11345	4979	0.43	199456
	37.06	4825	3067	0.63	84826

The decrease in mechanical strength can be attributed to the higher molecular mobility at glass transition temperature which can be also explained by an increment in tan δ. Karavas et al. reported DMA studies on the felodipine nano-dispersions with PVP. The authors observed the two tan δ peaks; the first tan δ peak around 52 °C was attributed to the Tg of felodipine while the second tan δ peak at 165 °C was attributed to Tg of PVP. The presence of two tan δ peaks were considered as indication of incomplete miscibility of felodipine with PVP in other words, the system formed a single matrix but remained as a separate finely dispersed phases (Karavas et al., 2006). In the case of FDH systems the presence of a single tan δ confirms the complete miscibility of the system. FDH moulded system contains the 70%w/w of HPMCAS and 67% w/w of HPMCAS in the case of I33 moulded systems. However, it can seen that I33 systems have shown the least storage modulus as compared to FDH and PEO-HPMCAS systems where, the storage modulus exhibited by FDH systems was approximately 3.5 times higher than the I33 systems. This confirms the

plasticisation effect ibuprofen has decreased the mechanical strength of the moulded systems.

5.2.2.3 FTIR:

FTIR spectroscopy was used to investigate the intermolecular hydrogen bonding (H-bond) between the felodipine and the polymer in the solid dispersion. Felodipine has an –N-H functional group which is capable for forming H-bonds. Previous studies on felodipine have shown that the position of the –N-H peak is sensitive to the strength of H-bond formed (Tang et al., 2002). In the crystalline felodipine, a –N-H group is weakly bonded to the carbonyl function(-C=O) of another drug molecule i.e intermolecular H-bonding between two felodipine molecules (Fossheim, 1986). FTIR studies on felodipine have also shown that in the case of an amorphous felodipine, the H-bonding also occurs between the -N-H group and the carbonyl functional group, but average H-bonding in the amorphous phase are stronger than in the crystalline felodipine (Tang et al., 2002). Hence both - C=O and –N-H groups of the spectrum can be used to understand the H-bonding between the felodipine and the polymer.

Tang et al. have studied the hydrogen bonding pattern in crystalline and amorphous phases of the dihydropyridine series of the calcium channel blockers (felodipine, nimodipine, nifedipine nitrendipine etc). Crystalline and amorphous felodipine exhibit different spectra the –N-H stretch of crystalline felodipine observed at 3373 cm^{-1} and which was shifted by around 33cm^{-1} to a lower wave-number (3341cm^{-1}) in case of amorphous felodipine (Tang et al., 2002). Simultaneously, the -C=O stretching seen in crystalline sample at 1696 cm^{-1} splits into two peaks at 1701 cm^{-1} and 1682 cm^{-1} assigned to non-hydrogen bonded

and hydrogen bonded carbonyl, respectively. Figure 5.73 shows the FTIR spectra of the pure crystalline felodipine and the felodipine in physical mixture. This showed -C=O stretching at 1688 cm^{-1} and a small shoulder peak at 1698 cm^{-1} attributed to hydrogen and non hydrogen bonded peaks of felodipine, respectively. In the case of FDH extruded and injection moulded systems the height of the 1698cm^{-1} non-hydrogen bonded carbonyl peak increases relative to the hydrogen bonded peak at 1688cm^{-1}.
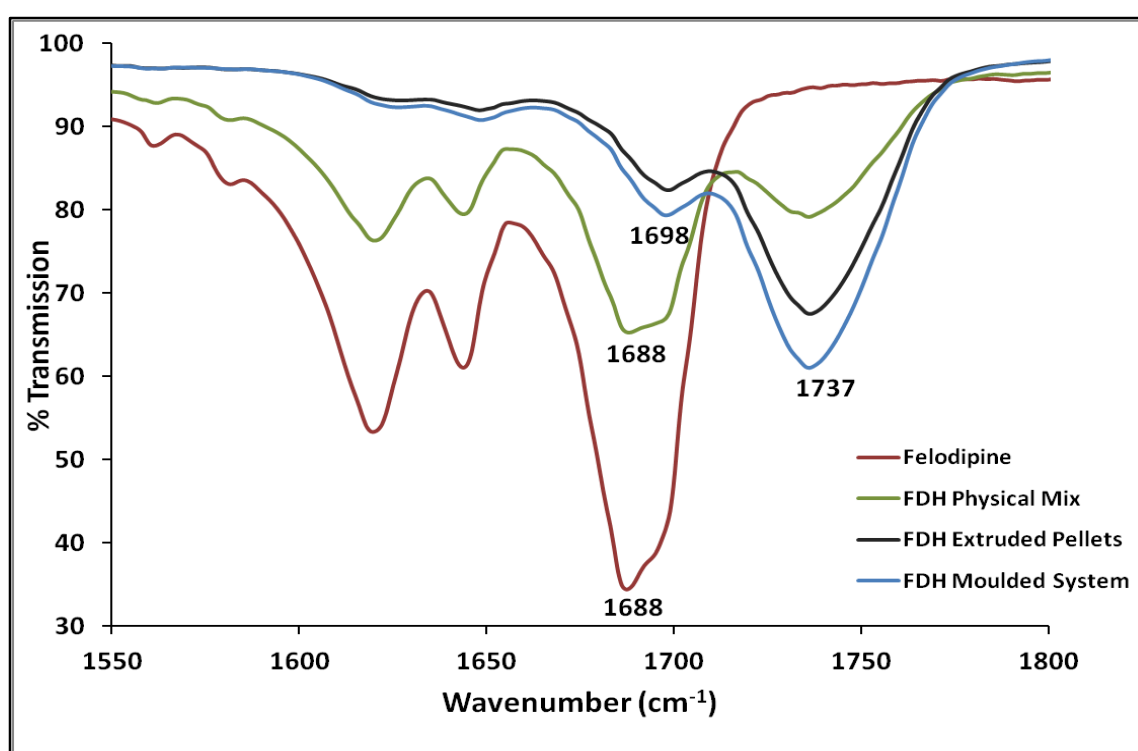
Figure 5.73: -C=O stretching of FDH systems

This increase in the relative intensity of the non-hydrogen bonded –C=O stretching peaks of the felodipine suggest an interaction between the two felodipine molecules was disturbed by a new interaction formed between the –N-H groups of felodipine and –C=O group in HPMCAS Figure 5.74) (Konno and Taylor, 2006). The -NH stretching of FDH extruded and moulded systems showed weak signals but a decrease in the wavenumber by 26

cm^{-1} confirmed the formation of H-bond with the HPMCAS ((Konno and Taylor, 2006).
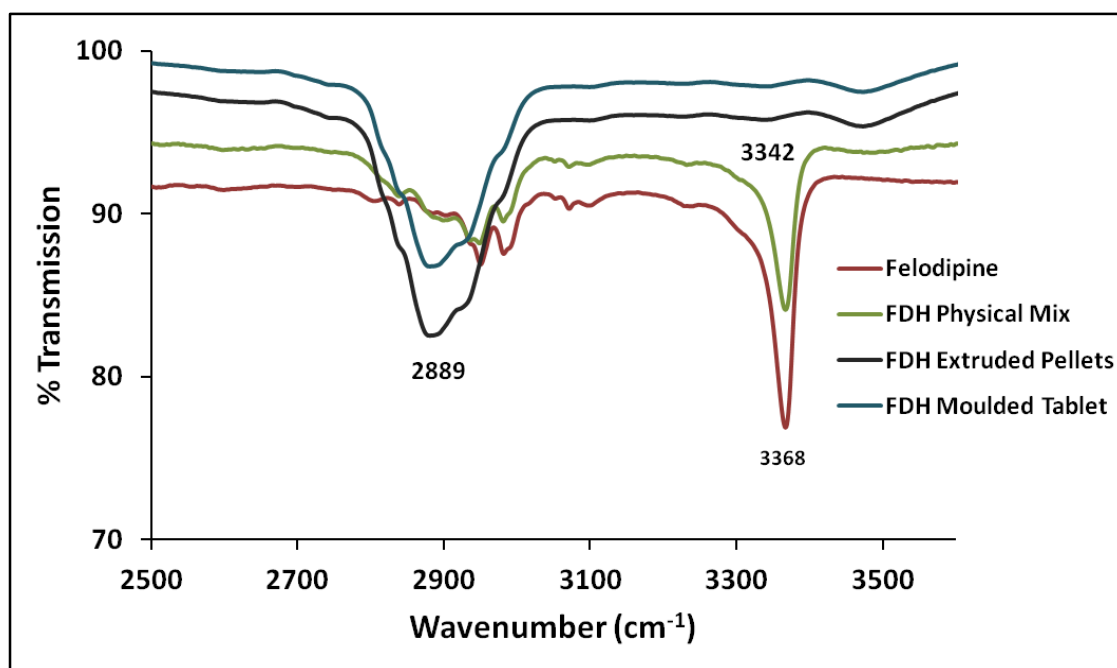
Figure 5.74: N-H stretching of FDH systems

5.2.2.4 Raman spectroscopy

The Raman peak of carbonyl stretching (–C=O) of crystalline felodipine in the physical mixture was observed at 1702 cm^{-1} and shifted to 1700 cm^{-1} in the case of FDH extruded pellets and moulded tablets. The opposite shift was observed at –C=C aryl stretching, where peaks shifts from 1643 cm^{-1} (physical mix) to 1649 cm^{-1} for extruded and moulded samples (Figure 5.75). The Raman spectrum of the pure crystalline and amorphous forms of felodipine have shown similar changes in the carbonyl and aryl –C=C stretching's (Tang et al., 2002). This shift in the Raman band confirms the formation of amorphous solid dispersion of felodipine in HPMCAS.
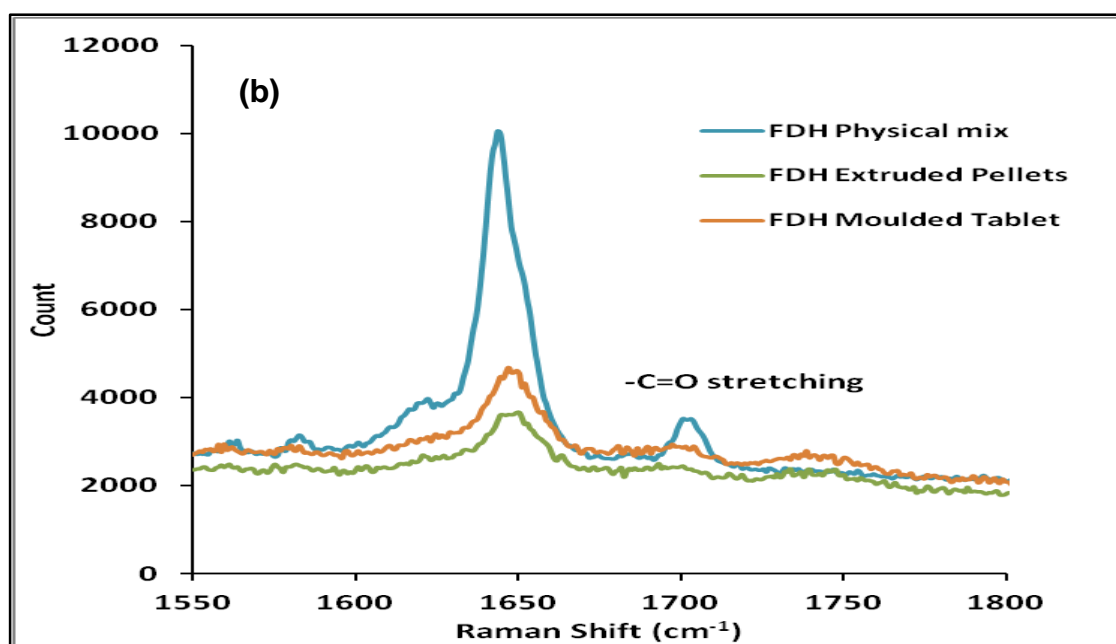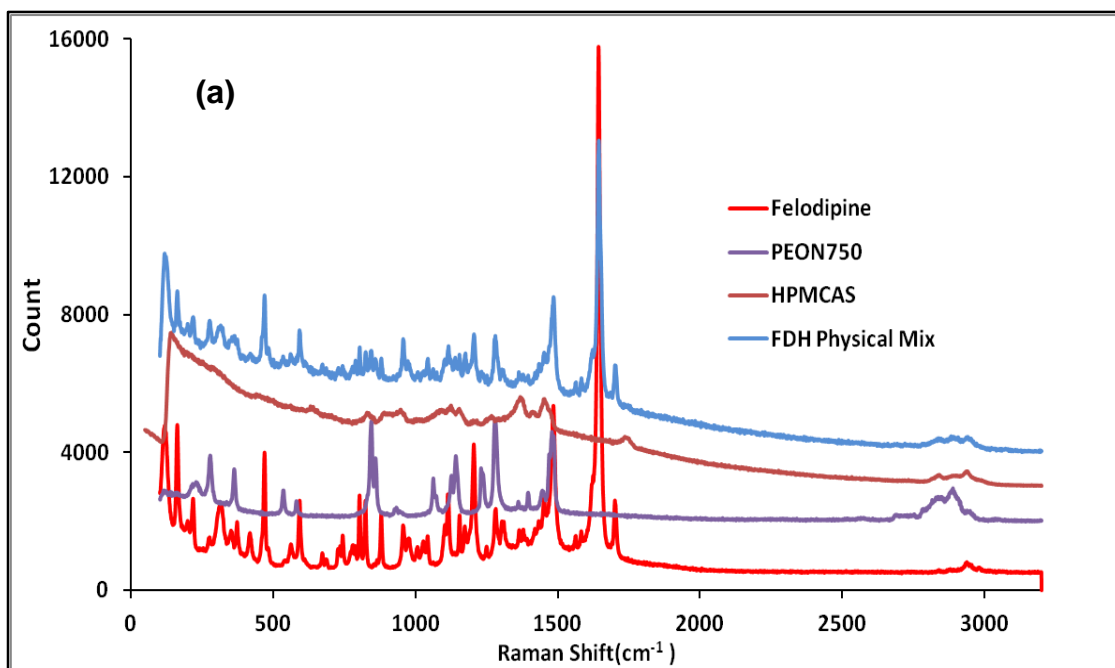
Figure 5.75: Raman spectra of (a) felodipine, PEO N750 FDH physical mixture and (b) processed samples

5.2.2.5 Shrinkage

The PEO-HPMCAS and FDH moulded bars kept at stress conditions have shown the different rate of shrinkage and the prominent effect of both the composition of moulded system and effect of the stress conditions was observed. PEO-HPMCAS systems containing PEO-HPMCAS (20:80 %w/w) showed comparatively lower shrinkage when to compared to FDH systems containing 20%PEO, 10% felodipine 70% HPMCAS.
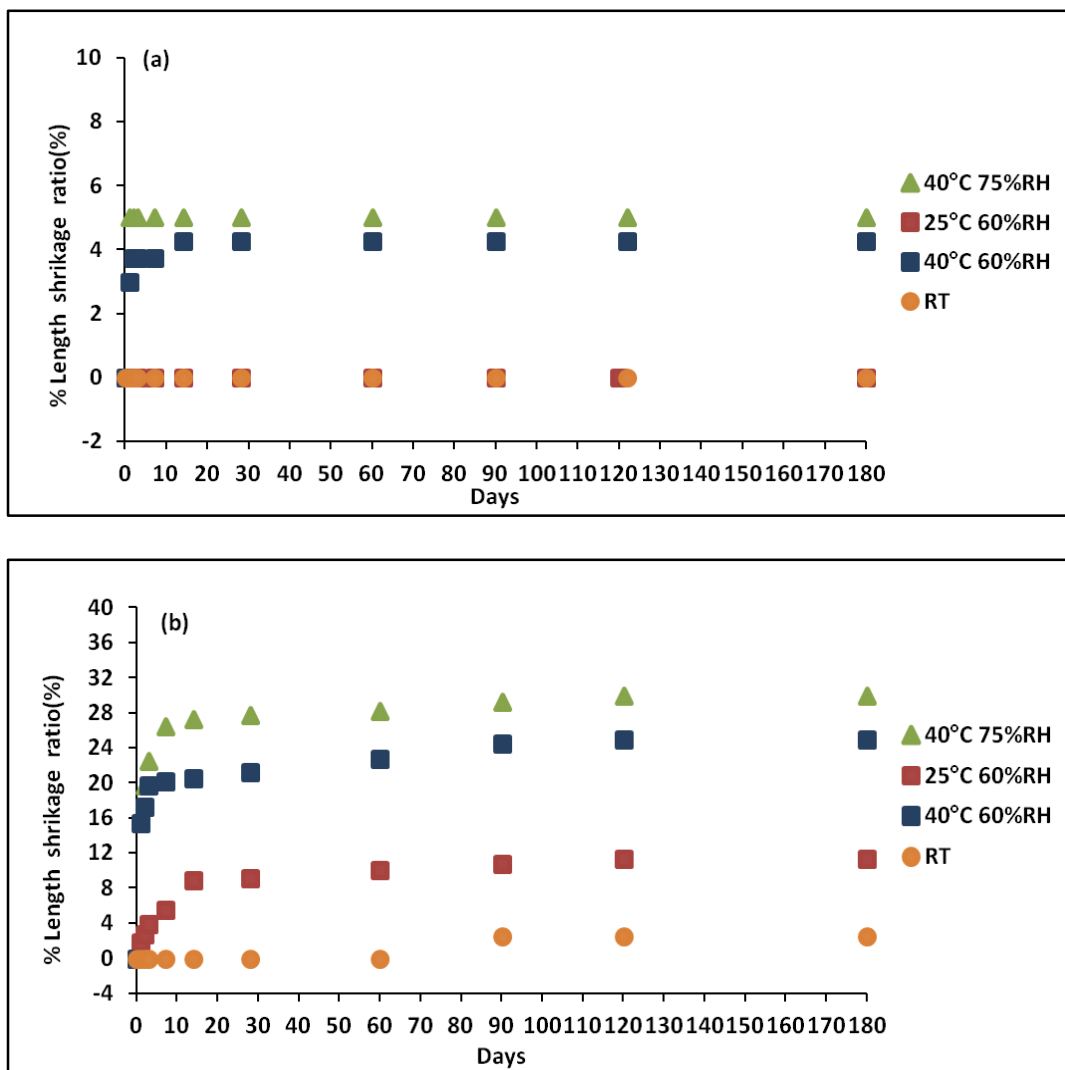
Figure 5.76: % length shrinkage ratio of (a) PEO-HPMCAS and (b) FDH systems

The FDH system was different from the PEO-HPMCAS system in two aspects first, 10% felodipine and second, the difference in the Tg. The Tg confirmed by MDSC of the FDH system was 54°C and Tg of PEO-HPMCAS system was 64°C. The higher molecular mobility could possibly leads to higher shrinkage rate for the FDH system than PEO-HPMCAS. At 40°C 75%RH, the PEO-HPMCAS system showed a maximum of 5% length shrinkage whereas the FDH system shrank by 30% of its original length (Figure 5.76). At RT conditions PEO-HPMCAS did not show any shrinkage and only 2.5% shrinkage for FDH was seen after 180 days. This suggests the temperature and humidity has major role in the shrinkage process as both have the strong influence on the molecular mobility of system. The least shrinkage was observed for the PEO-HPMCAS moulded bar suggesting PEO helps to retard the shrinkage of the HPMCAS. However, the 10% dispersion of the felodipine in the PEO - HPMCAS polymer matrix made a significant impact of the shrinkage.

5.2.3 In-vitro drug release using (USP IV)

The dissolution testing using an open loop configuration of flow through cell provides an infinite sink condition for dissolution by maintaining a continuous flow of fresh dissolution medium. The dissolution behaviour of I33 pellets, I33 moulded tablets, FDS pellets and FDS moulded tablets was studied drug release profiles are provided in figure 5.75. I33 pellets showed 50% release after 5 hrs of dissolution and complete release after 10 hrs of dissolution. In contrast the drug release from the I33 moulded tablets was erosion controlled hence the slower drug release was observed. From I33 tablets, 50 % release was observed after 11 hrs and 70 % release after 18 hrs of dissolution (Figure 5.77).
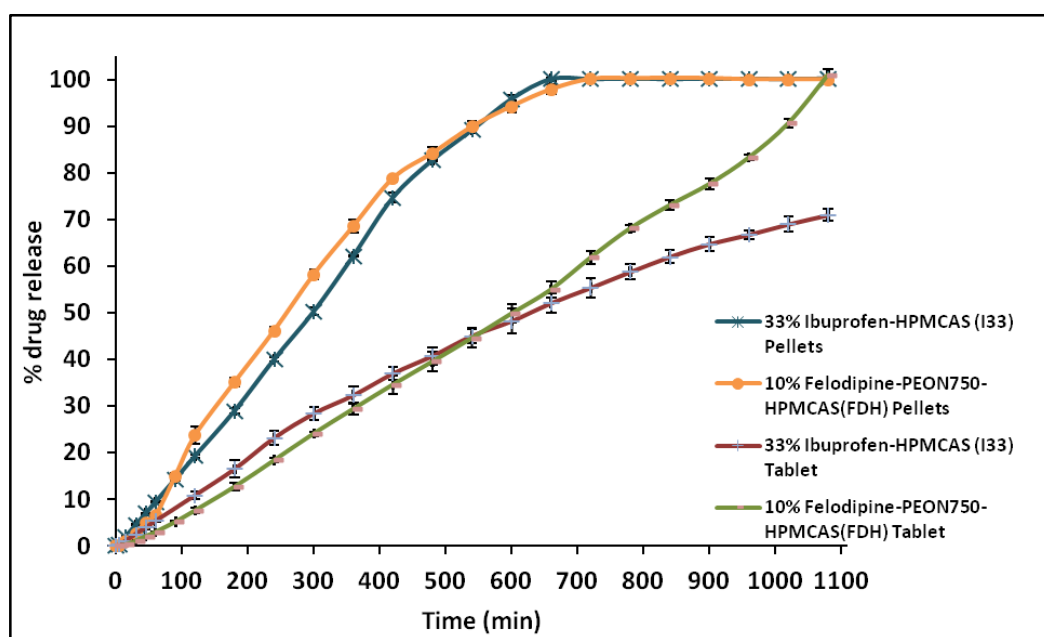
Figure 5.77: Dissolution profiles for extruded pellets and injection moulded tablets of ibuprofen and felodipine using flow through cell (USP IV) (n=3)

The drug release from the PEO-HPMCAS matrix would be diffusion and erosion based as PEO is a highly water soluble polymer and it swells and drug release is primarily controlled either by diffusion or erosion based on the molecular weight of PEO (Figure 5.79). Therefore, the controlled release of felodipine from the PEO-HPMCAS matrix was considered to be due to diffusion and erosion based mechanisms.

FDH pellets showed 50% release after 5 hrs and 100% release after 11hrs while in the case of FDH tablets 50% release was observed after 10 hrs and complete drug release was observed after 18hrs. The difference in the release profile from pellets and injection moulded tablet could be attributed to the surface area and densification during the injection moulding process. The extruded pellets were expected to give higher dissolution rate due to the higher surface area provided for the dissolution due to the particle size of the product i.e. pellets.

Figure 5.78: Dissolution images of I33 pellets and I33 moulded tablets (USP IV)
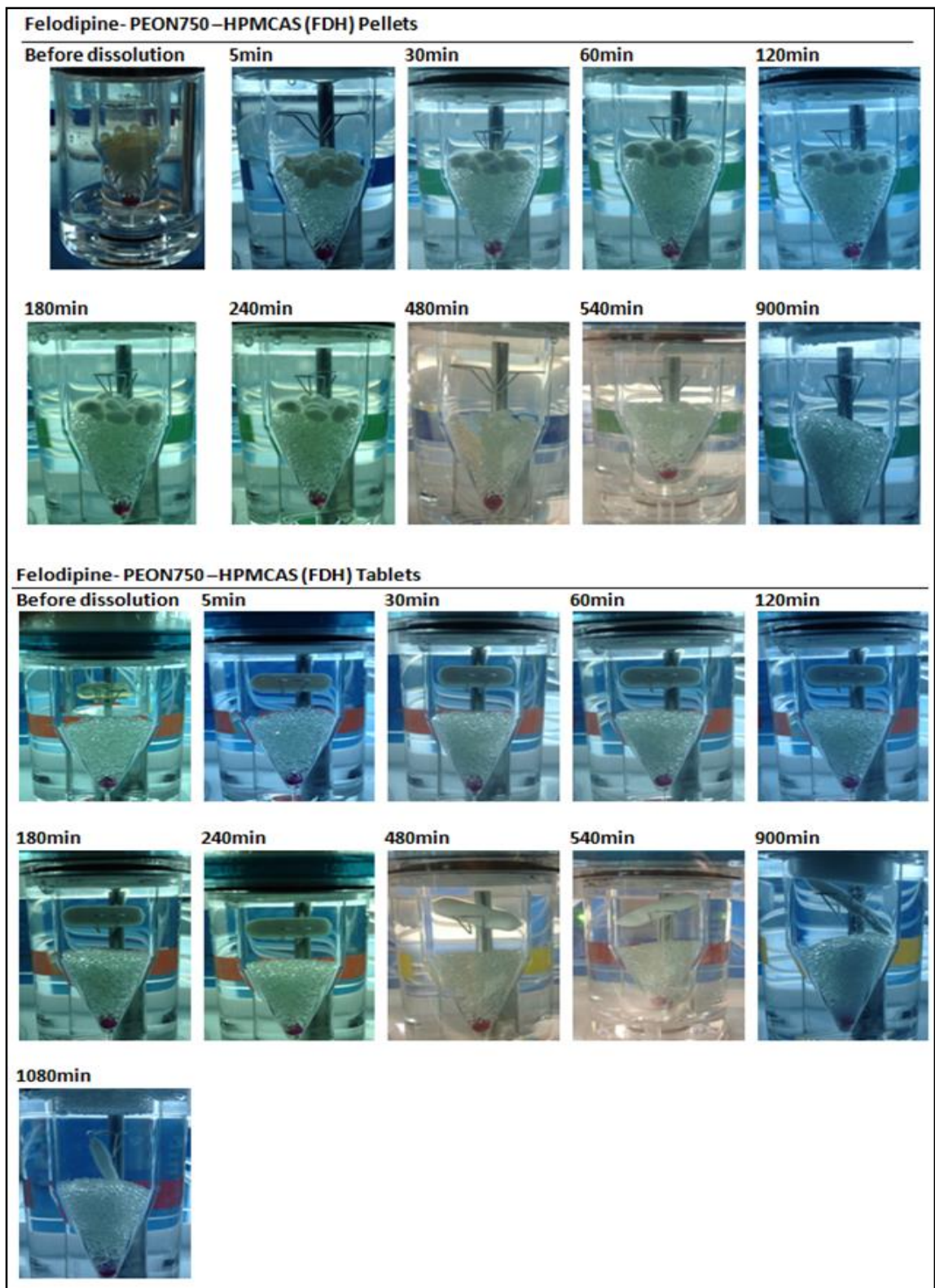
Figure 5.79: Dissolution images of FDS pellets and FDS moulded tablets (USP IV)

Chapter 6

Soluplus® IM systems

This chapter provides an insight into the processing of the Soluplus® IM systems using HME and injection moulding. The processing behaviour and the results of product characterisation using of thermal, spectroscopic and In-vitro drug release methods are discussed.

6.1 Processability using HME and IM

Soluplus® is designed for use with HME and it is mainly used to obtain solid solutions with APIs as it is good solubiliser and stabiliser. Although Soluplus® has low Tg (72 °C) compared to other pharmaceutical polymers it has a very high shear viscosity. The Soluplus® has been recommended for HME over wide temperature range (120-180ºC). When Soluplus® was alone extruded at 150ºC but generated a high torque (50-55%) which reduced to 20-25% with the 10%w/w addition of ibuprofen and allowed extrusion to be carried out 130ºC suggests the ibuprofen has a plasticisation effect on the Soluplus®. The addition of 10%w/w felodipine did not have a significant effect on the processing behaviour; however, it reduced the processing torque and the die pressure, indicating good miscibility with Soluplus®. The torque and die pressure associated with HME of the all three batches are listed in the Table 6.1.

Table 6.1: HME parameters of Soluplus®, IBS and FDS batches

Composition used for extrusion	Torque (%)	Motor power (kW)	Die pressure (bar)
Soluplus®	50-55	1.3-1.4	40
Ibuprofen-Soluplus®(IBS)	25-30	0.6-0.8	20
Felodipine Soluplus®(FDS)	40-42	1.0-1.1	33

Soluplus®, ibuprofen-Soluplus® (IBS) and felodipine-Soluplus® (FDS) pellets were injection moulded into the two shapes; the tensile bars and the tablets. In general, The IM of amorphous material is challenging as compared to semi-crystalline materials as an amorphous material softens upon heating and posses poor lubricity hence melt flow inside the mould cavity becomes challenging (Zema et al., 2012). The processing of Soluplus® alone was very challenging and filling inside the mould cavity was achieved with high injection speed of 120mm/s and with mould lubrication. The moulded parts obtained were very brittle in nature therefore the mould temperature was gradually increased to 70°C from 20°C and the mould ejection speed was reduced to 2mm/sec from the 5mm/s. This process modification helped to eject the parts without breaking as 70°C was close to the Tg of Soluplus®.

IBS pellets were injection moulded at 135°C and the mould temperature required for ejection of the moulded part was 50°C. Ejection was possible at 50°C mould temperature due to the Tg of the system being decreased to 54°C with addition of ibuprofen. Moulding of FDS systems was performed at a slightly higher temperature than IBS systems as the addition of 10%w/w felodipine did not significantly affect the Tg of the polymer. The processing parameters used for IM are described in Table 3.15.

6.2 Characterisation of extruded pellets and IM systems

Extruded pellets and injection moulded systems were characterised to understand the thermal, spectroscopic and drug release properties.

6.2.1 Modulated DSC

The reversing heat flow of pure Soluplus® and the products obtained using both HME and IM are presented in the Figure 6.1. The reversing heat flow of MDSC allows the separation of reversable phenomena such as Tg and melting on the reversing curve (Solarski et al., 2005). The Tg of Soluplus® was observed at 72.0±0.21°C. The absence of melting endotherms of ibuprofen at 76°C and felodipine at 145°C in the case of IBS and FDS systems, respectively, confirms the formation of amorphous solid dispersions.
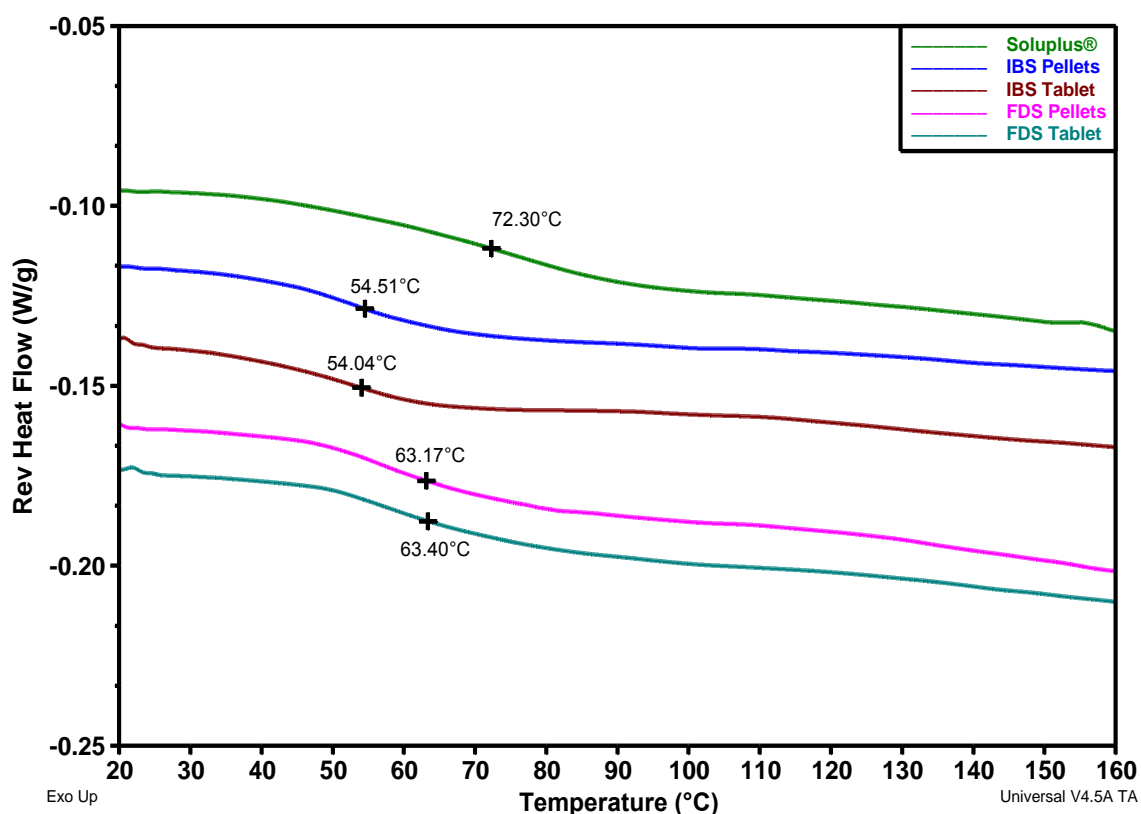
Figure 6.1: Reversing heat flow curve for Soluplus®, IBD and FDS systems

244
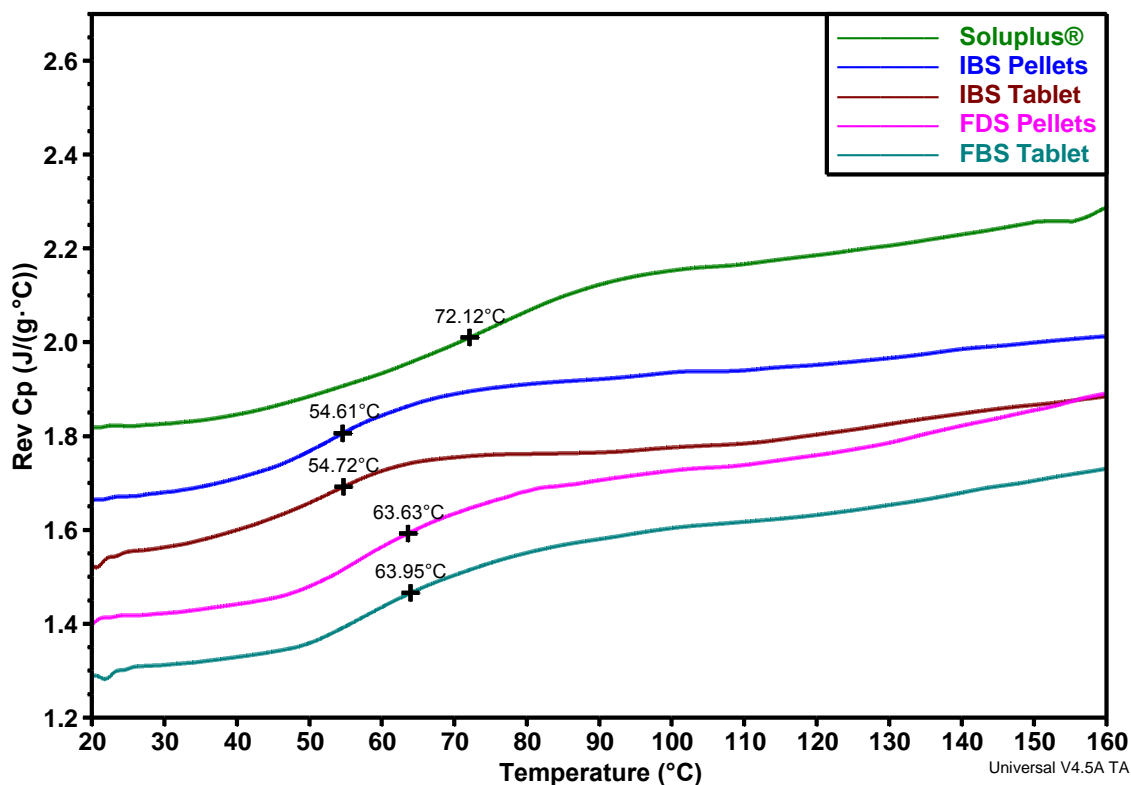
Figure 6.2: Reversing heat capacity curve for Soluplus®, IBS and FDS systems

The presence of a single Tg in the case of pellets and IM tablets of IBS and FDS confirms the formation of a solid solution (molecular level dispersion) Moreover, changes in heat capacity of samples could be seen in Figure 6.2. The heat capacity of material should increase at the Tg of the system due to increased molecular mobility. At the respective glass transition the heat capacity of each sample increased and resembled a mirror image of the Tg curve. The plasticisation effect of ibuprofen and felodipine was clearly observed on the Tg of Soluplus® and it decreased to 54°C±0.19 for IBS systems and 63°C±0.22 for FDS systems. The higher decrease in the Tg for the ibuprofen containing pellets and IM tablets could be attributed to the lower Tg of ibuprofen than felodipine. Theoretical calculations of Tg by the Fox equation estimated similar values for IBS and FDS mixtures (Reported in chapter 4, equation 4.3).

245

6.2.2 Dynamic Mechanical Analysis (DMA)

The moulded tensile bars were characterised using DMA to understand the dynamic mechanical properties as a function of temperature. A sharp decrease in the storage modulus of the Soluplus® moulded bar in the temperature region of 65 - 75°C and a small tan δ peak near 73°C (Figure 6.3, Figure 6.4) corresponds to the Tg of Soluplus® (Karavas et al., 2006). The mechanical behaviour of IBS and FDS moulded bars showed a similar behaviour where a decrease in the storage modulus was observed at 64°C and 72°C respectively.
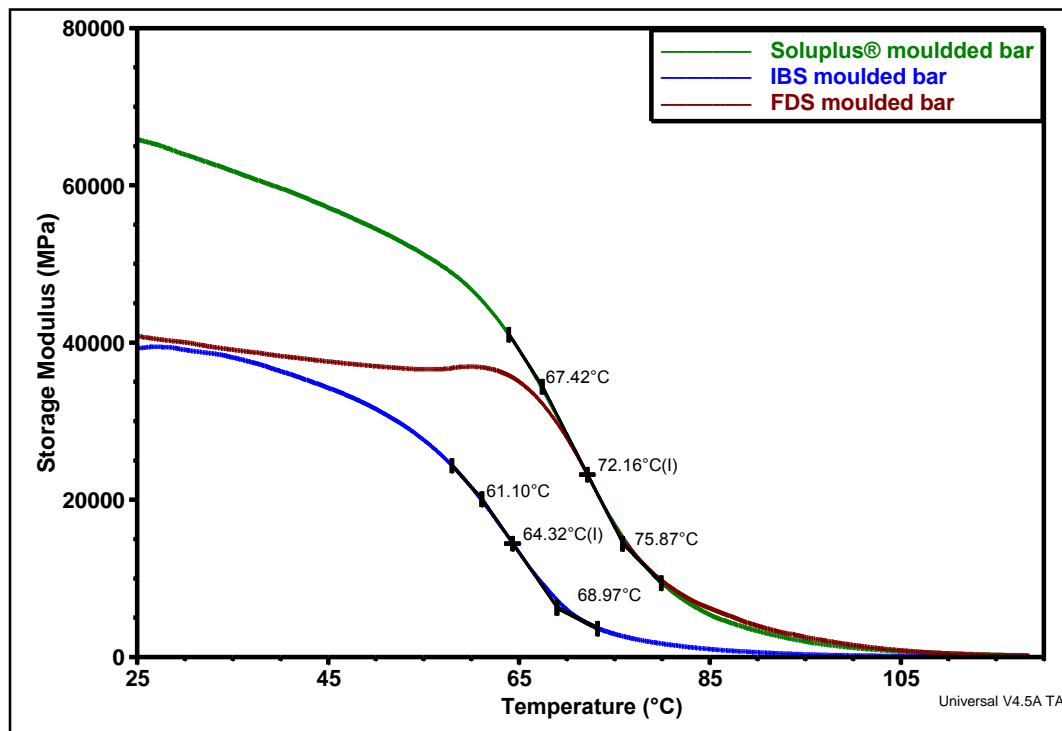
Figure 6.3: Storage modulus curves for Soluplus®, IBS and FDS systems
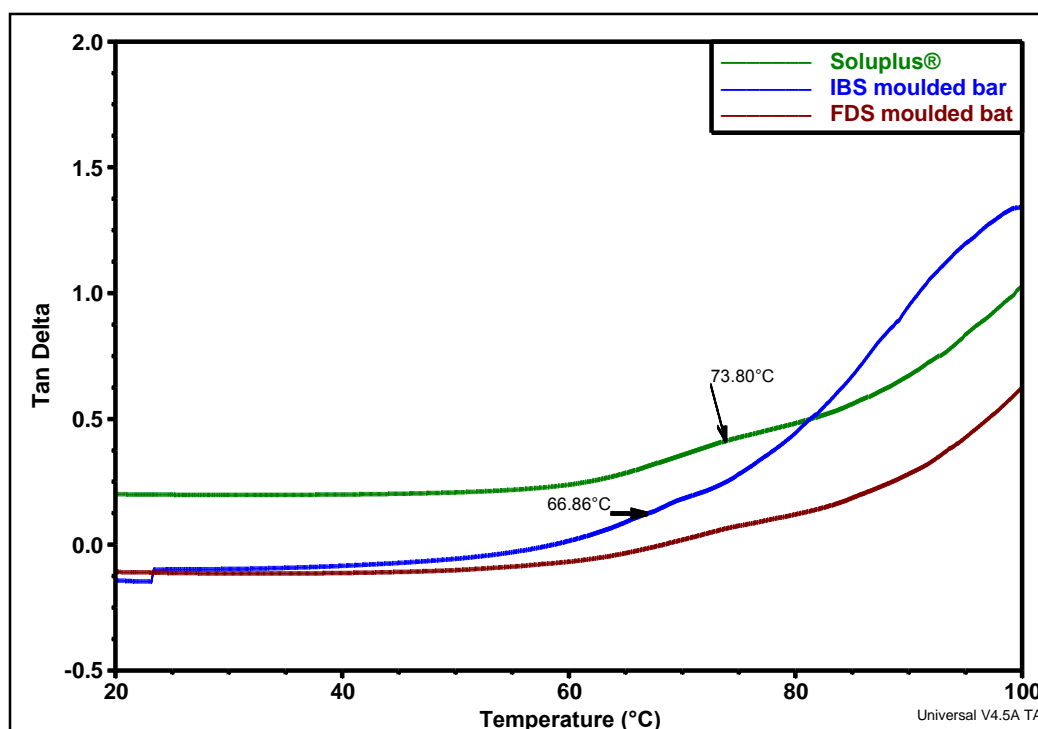
Figure 6.4: Tan δ curve of Soluplus® injection moulded systems

The comparative mechanical properties of the three moulded system are presented in the Table 6.2. When the storage modulus and stiffness of the moulded bars at 25°C were compared to values at temperatures close to the Tg of system approximately a 50% reduction was observed (Table 6.2).

Table 6.2 : Mechanical properties of Soluplus® injection moulded systems

Materials	Temperature (°C)	Storage Modulus (MPa)	Loss Modulus (MPa)	Tan Delta	Stiffness (N/m)
Soluplus®	25.07	65801	3724	0.05	943143
	72.25	22959	5726	0.25	329079
Ibuprofen-Soluplus® (IBS)	25.061	39298	6361	0.16	563271
	64.41	14235	4831	0.33	196475
Felodipine-Soluplus®(FDS)	25.06	40796	2844	0.07	584742
	72.91	21261	5012	0.26	304746

6.2.3 FTIR spectroscopy

The FTIR spectra's of pure drug, physical mixture and processed sample were compared to understand the interaction within functional groups of a drug and a polymer. In the case of the felodipine molecule the -N-H group acts as a hydrogen donor and is capable of forming a hydrogen bond (H-bond) with an appropriate acceptor molecule such as a carbonyl (-C=O) group. (Tang et al., 2002). The FTIR spectra of pure felodipine, Soluplus®, and its 10%w/w physical mixtures are shown in the Figure 6.5. The Soluplus® exhibits characteristic peaks at 1732 cm^{-1} due to -C=O stretching, 2925 cm^{-1} due to aliphatic C-H stretching and 3452 cm^{-1} due to the -O-H stretching. The FTIR spectra of FDS physical mixture appears as a summation of the peaks of the Soluplus® and the felodipine where -C=O stretching of the felodipine at 1688 cm^{-1} and 1699 cm^{-1} and -C=O stretching of the Soluplus® at 1732cm^{-1} was observed (Figure 6.5). Moreover, the physical mixture shows the -N-H stretching of felodipine at 3368cm^{-1} and free -O-H stretching of Soluplus® at 3452cm^{-1} (Figure 6.6). This suggests that there was no interaction between felodipine and Soluplus® when they were physically mixed with each other.

IR spectra of melt extruded pellets and IM tablets showed changes in the –N-H stretching vibrations where –N-H stretching was observed at 3288 cm^{-1}. This large downward shift suggests the involvement of the –N-H group of the felodipine for the H-bonding with Soluplus®. Felodipine is known to form a H-bond with the other felodipine molecules and IR spectra of the FDS pellets and moulded tablet have shown two peaks first at 3230cm^{-1} second at 3294cm^{-1} both are attributed to the N-H stretching. The frequency shift at –N-H stretching was

observed due to the involvement of N-H group for H-bonding with another felodipine molecule and/or with polymer as shown in fig (Figure 6.6).
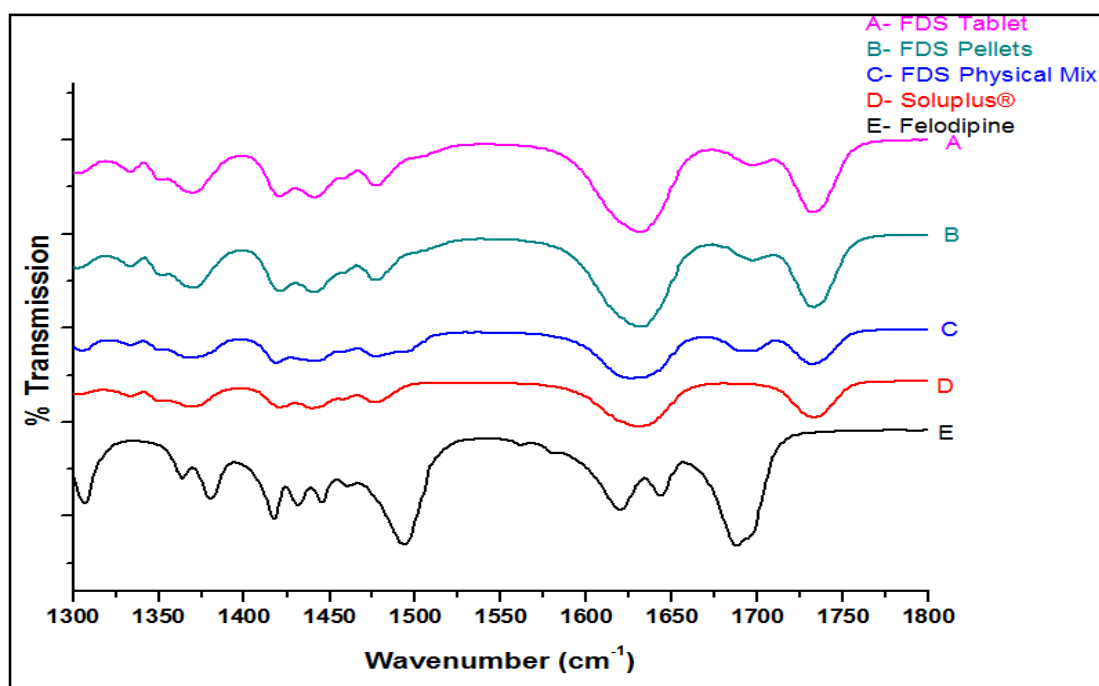
Figure 6.5:FTIR spectra of Felodipine-Soluplus® systems (1300-1800 Cm⁻¹)
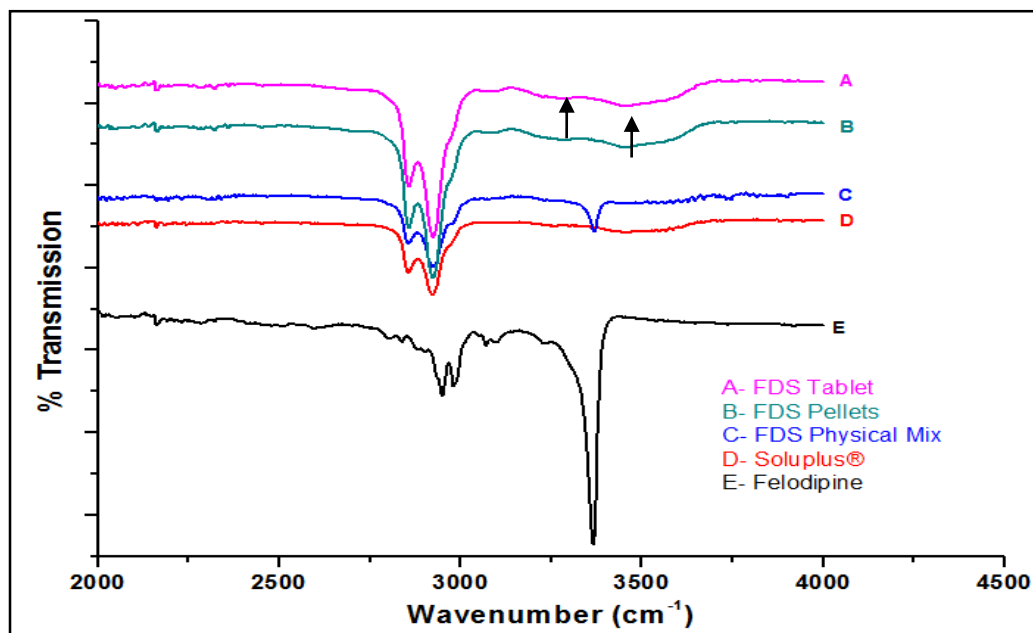
Figure 6.6: -N-H stretching of FDS systems

A similar observation was also reported when the felodipine has formed solid dispersions with other polymers such as HPMCAS, PVP Kollidon V64 (Song et al., 2013) (Tian et al., 2014b). The functional group peaks of the Soluplus® and FDS systems are presented in the Table 6.3.

Table 6.3: Funtional groups of Soluplus ® and FDS moulded systems

Sample	Wavenumber (cm^{-1})	Assignment
Amorphous felodipine	3339	N-H, H-bonded with other molecules
	1701	C=O, non-H-bonded
	1684	C=O, H-bonded
Soluplus®–FD	3452	free OH from Soluplus®
	3294	N-H, H-bonded with other drug molecule
	3230	N-H, strong H-bonding with Soluplus®
	1701	C=O of felodipine, non-H-bonded
	1732	Unbonded C=O from Soluplus®

In the case of IBS systems the pure crystalline ibuprofen and the ibuprofen present in the physical mixture has shown –C=O stretching at 1708 cm^{-1} whereas –C=O stretching of the Soluplus® was observed at 1732 cm^{-1} (Figure 6.7). Only the – C-H stretching vibrations were observed at 2954 cm^{-1} and no peaks in the region of 3000-3500 cm^{-1} due to the absence of –N-H functional groups and free –O-H functional groups in the ibuprofen (Figure 6.8). IBS pellets and IBS tablets showed the identical spectra to the Soluplus® with no change in the peak intensity or broadening of peaks, suggesting that ibuprofen was dispersed in the Soluplus® matrix in the amorphous state. However, this does not involve in any interactions with Soluplus® to form the intermolecular H-bonding.
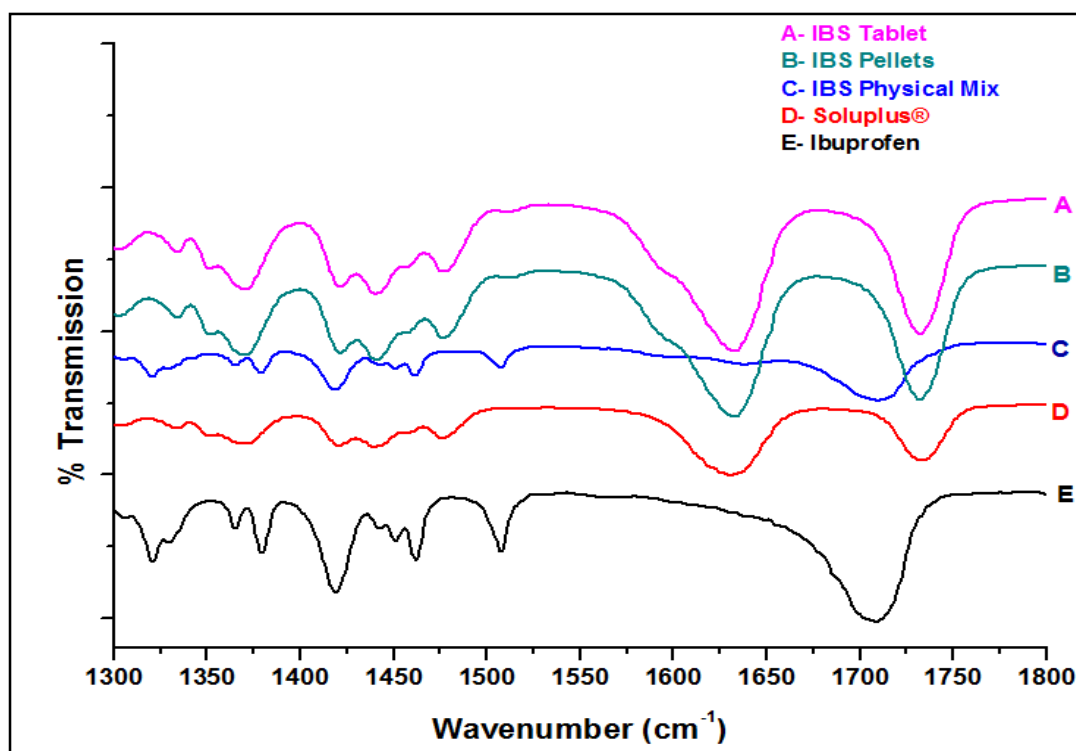
Figure 6.7: FTIR spectra of IBS systems (1300cm^{-1} – 1800 cm^{-1})
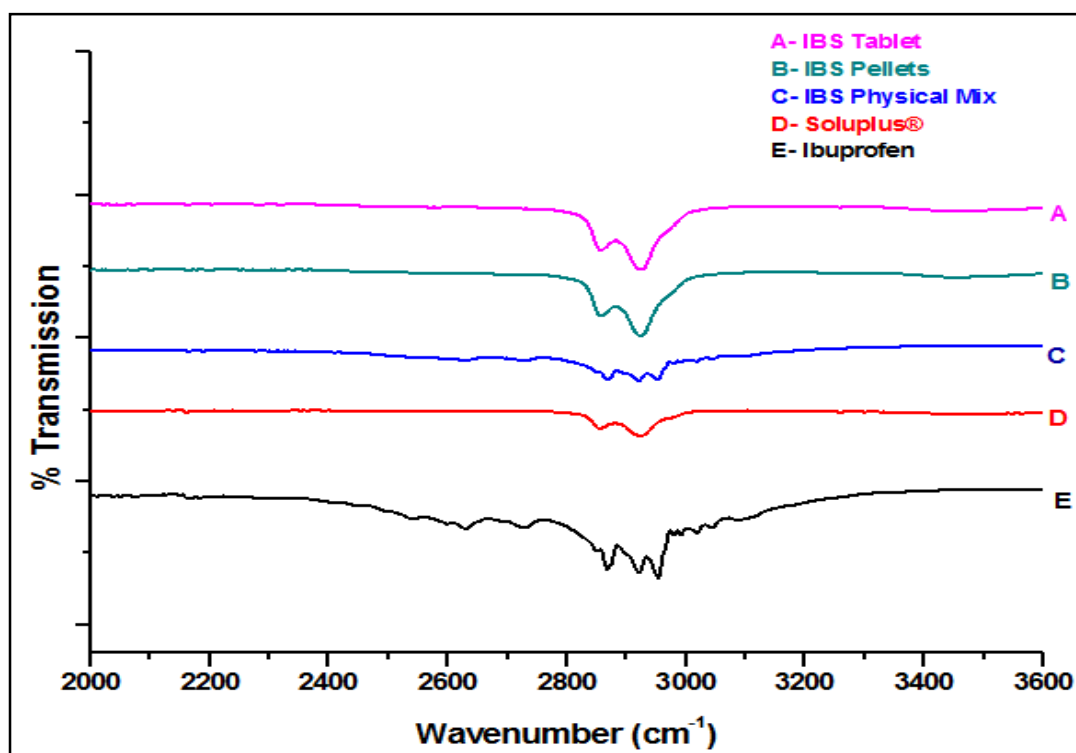
Figure 6.8: FTIR spectra of IBS systems (2200 cm^{-1} – 3600 cm^{-1})

251

6.2.4 Raman spectroscopy

The crystalline and amorphous forms of ibuprofen and the felodipine show distinct changes in their Raman spectra. Raman shifts are associated with the molecular arrangement and drug- polymer interactions. As described in the previous chapter (section 5.1.2.4) the ibuprofen shows characteristic peak changes when dispersed in the amorphous form and when it interacts with the polymer. The shift in the characteristic band at 1608 cm^{-1} to 1613 cm^{-1} confirms that ibuprofen has formed a molecular level dispersion with Soluplus® (Figure 6.9 and Figure 6.10)
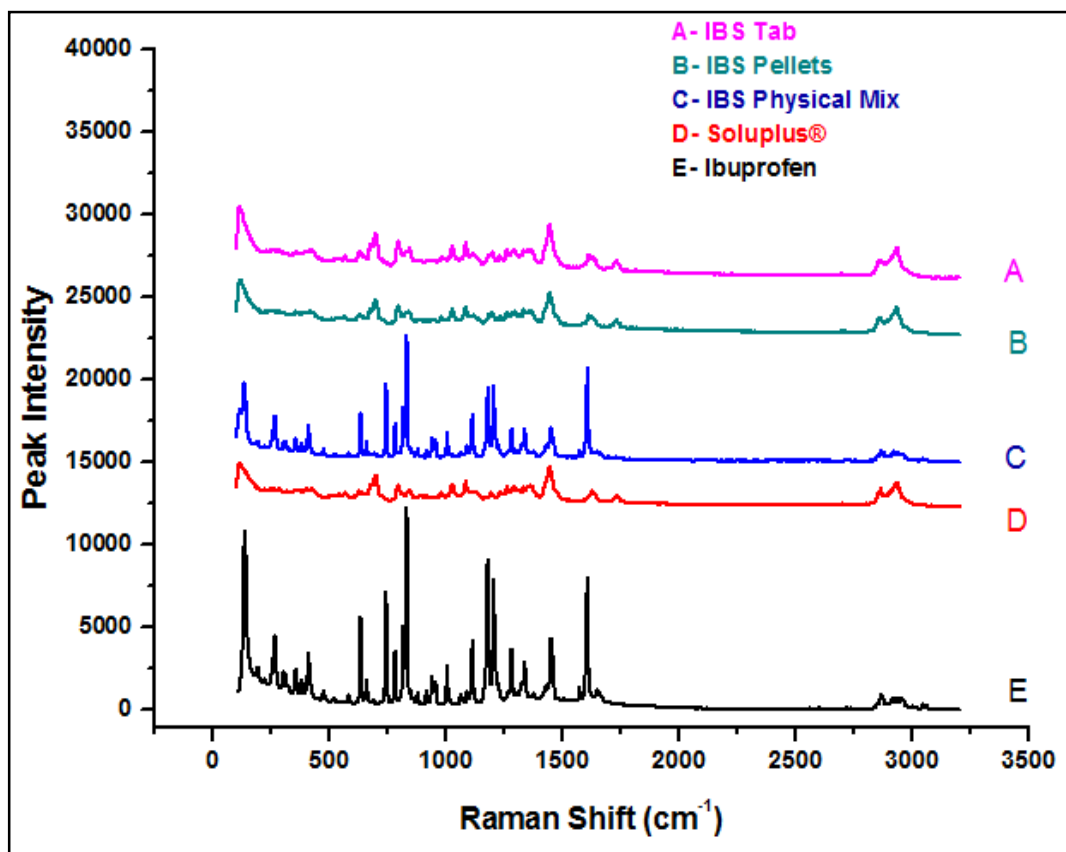
Figure 6.9: Raman Spectra of Ibuprofen-Soluplus® (IBS) systems
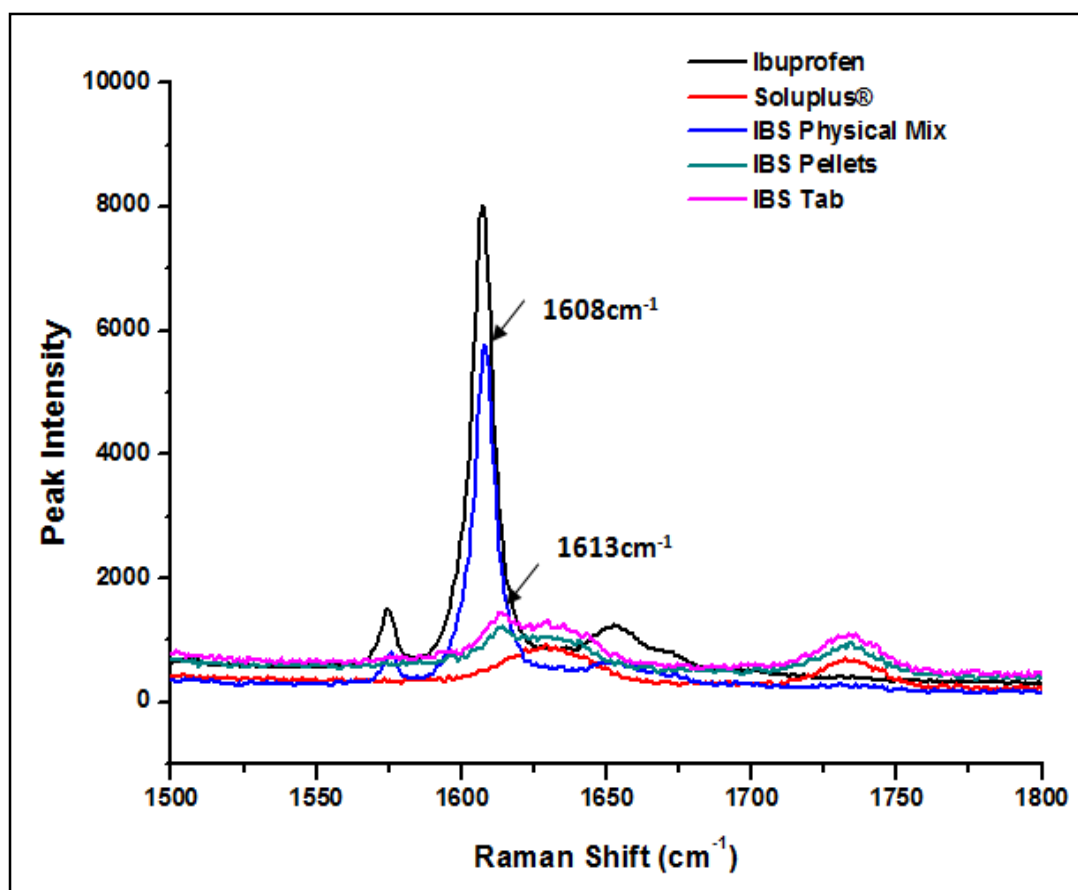
Figure 6.10: Raman Spectra of Ibuprofen-Soluplus® (IBS) systems (carbonyl stretching region: 1500 – 1800 cm^{-1})

The Figure 6.11 shows the full Raman spectra of pure felodipine, Soluplus®, FDS physical mixture and processed samples. –N-H stretching of felodipine was observed at 3370cm^{-1}. In general, when the felodipine converted into the amorphous form it showed a shift by approximately 33cm^{-1} to lower Raman shifts due to the presence of stronger H-bond in the amorphous form than the crystalline form (Tang et al., 2002). The aryl ring -C=C stretching at 1643cm^{-1} showed an upward shift to 1649 cm^{-1} and carbonyl stretching at 1702cm^{-1} was shifted to 1700cm^{-1} with a broad peak suggesting that a different molecular association was present in the pellets and moulded tablets (Figure 6.12). Similar changes were reported earlier (section 5.2.3) due to the amorphous form of the felodipine and due to the possibility of involvement with the Soluplus® for an H-

bond. Although a distinct change in the -N-H stretching was not observed, this may be because the peak intensity was too small to detect. However, conjugated -C-H stretching vibration in the moulded tablets suggested the strong molecular interaction between the felodipine and Soluplus® (Figure 6.13).
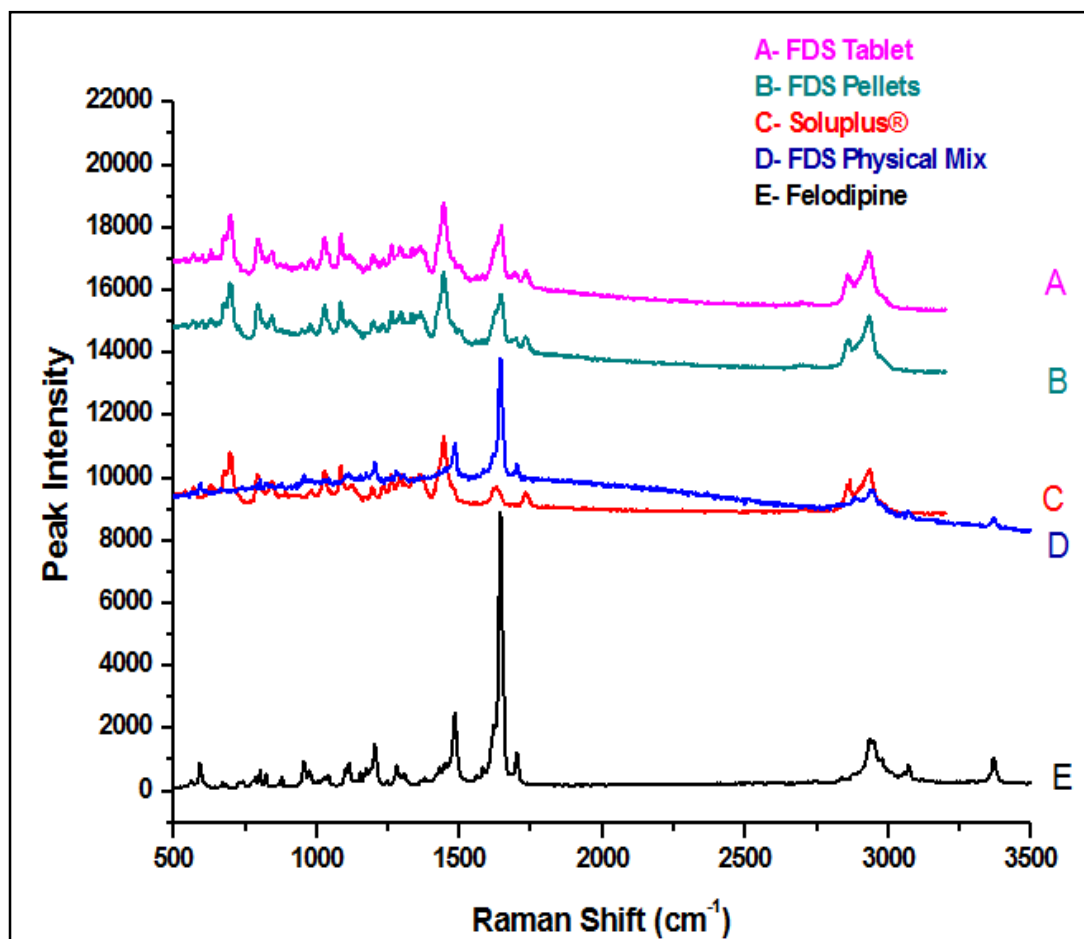
Figure 6.11: Raman Spectra of Felodipine-Soluplus® systems
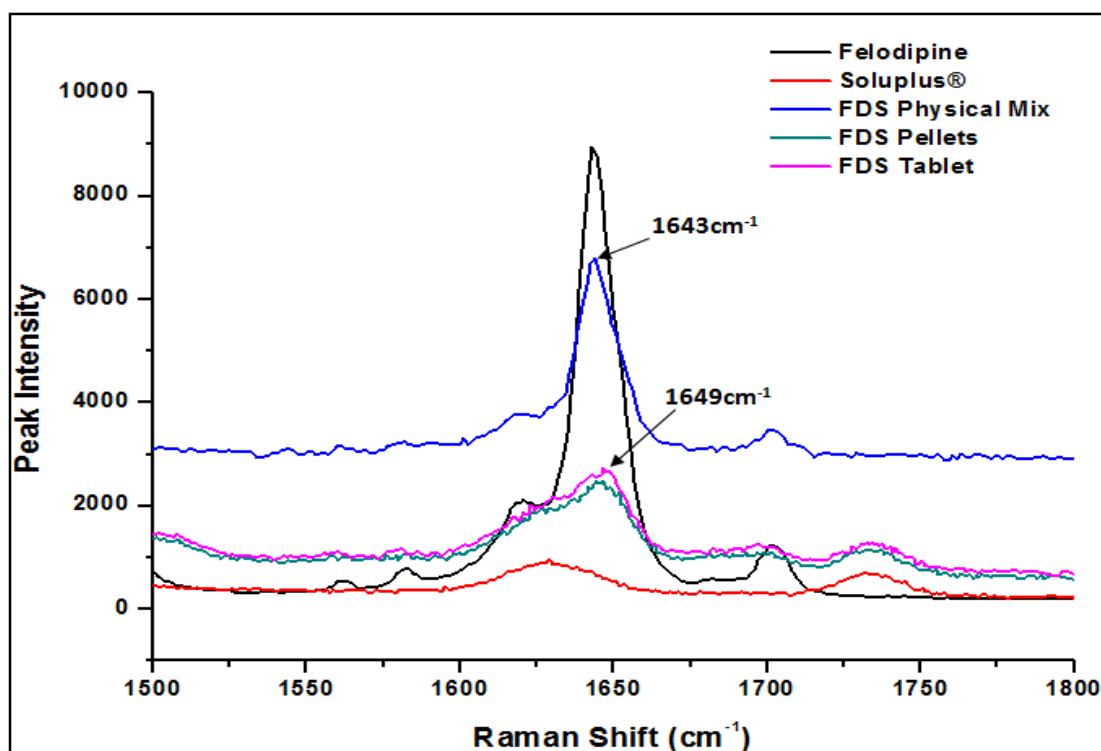
Figure 6.12 Raman Spectra of Felodipine-Soluplus® (FDS) systems (carbonyl stretching region: 1500 – 1800 cm^{-1})
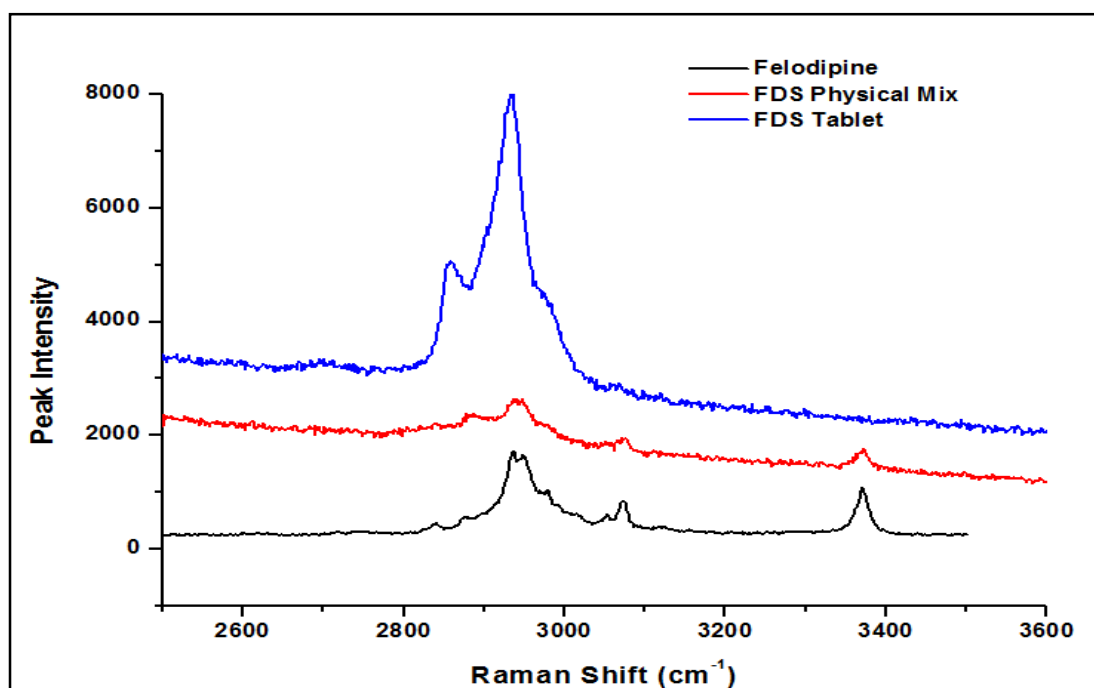
Figure 6.13 Raman Spectra of Felodipine-Soluplus® (FDS) systems (2600-3600cm^{-1})

6.2.5 In-vitro drug release

Drug release from pellets and moulded tablets was characterised using the flow through cell (USP IV). The melt extruded pellets and injection moulded tablets of IBS and FDS systems were subjected to dissolution testing to understand the drug release bheaviour. The drug-release profile for pellets and moulded tablets is shown the Figure 6.14.
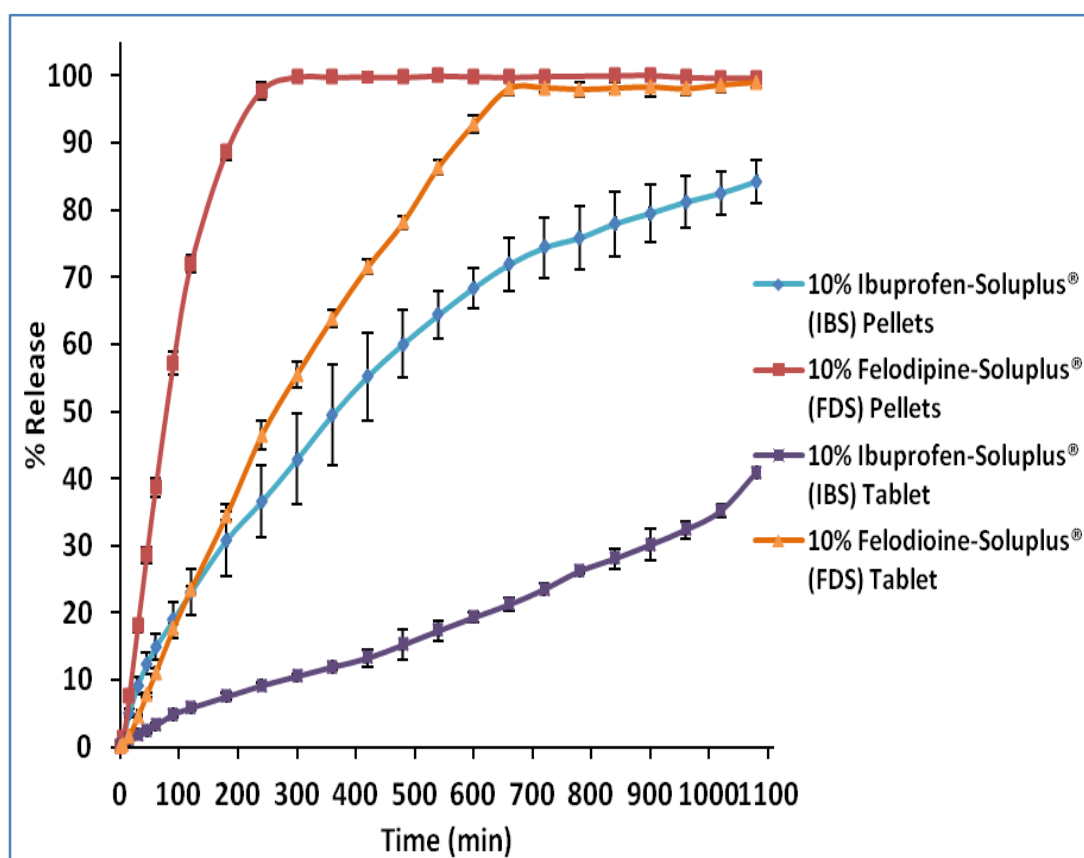
Figure 6.14: Dissolution profiles for IBS and FDS pellets and tablets using a flow-through method (USP 4) with an open-loop configuration (n = 3)

In general pellets showed a faster dissolution than the moulded tablets attributed to the higher surface area of the pellets for the dissolution. Felodipine release from the FDS systems was faster and complete compared to the release of the ibuprofen from the IBS systems. FDS pellets showed a faster drug release among all the products where 50% drug release was observed after 90 mins and

100% release within 240mins. The FDS moulded tablets showed the controlled release where approximately the 10% drug release was observed after every 60 mins Figure 6.14. Tablets showed a controlled drug release due to the constant surface erosion of the dosage form. The dissolution process of the FDS pellets and moulded tablet have shown in the Figure 6.15.
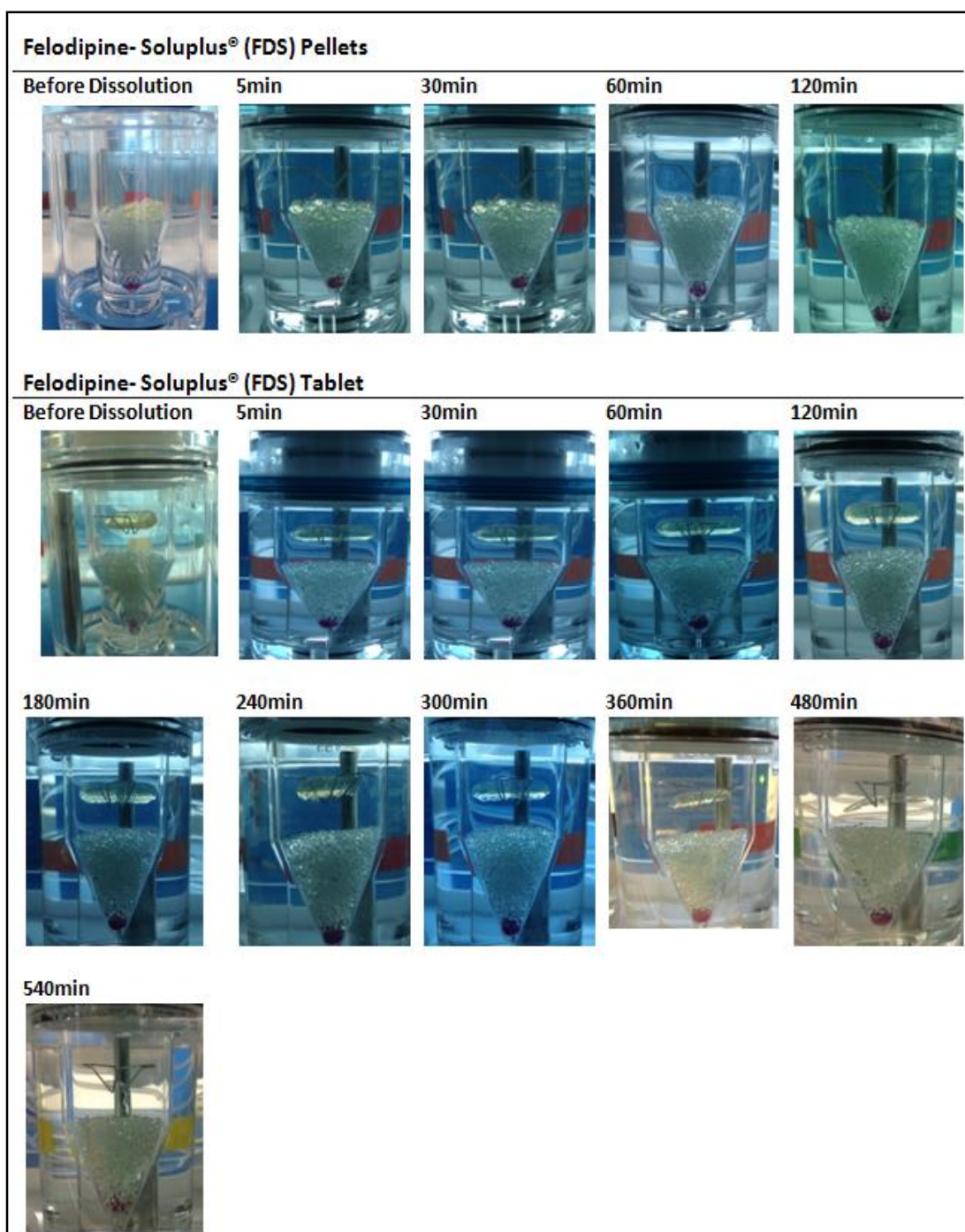
Figure 6.15: Dissolution images of FDS pellets and FDS moulded tablets

Neither the pellets nor the tablets showed the complete drug release from the IBS systems (Figure 6.14). Crystallisation of the amorphous drug during dissolution can adversely affect the dissolution rate and solution concentration required to maintain supersaturation. The dissolution advantage of amorphous solid dispersions can be negated either by crystallisation of the amorphous drug in contact with the dissolution media or rapid crystallisation of the supersaturated solution. In the case of IBS systems, crystallisation during dissolution should have decreased the dissolution rate of the ibuprofen and clear surface whitening was seen during the dissolution.

The Raman spectra confirmed the crystallisation at the pellets and a tablet surface during the dissolution. The surface Raman spectra taken after 3 hrs of dissolution showed the characteristic crystalline band of ibuprofen at 1608cm^{-1} which was at 1613cm^{-1} due to the amorphous molecular dispersion within the Soluplus® matrix (Figure 6.16)
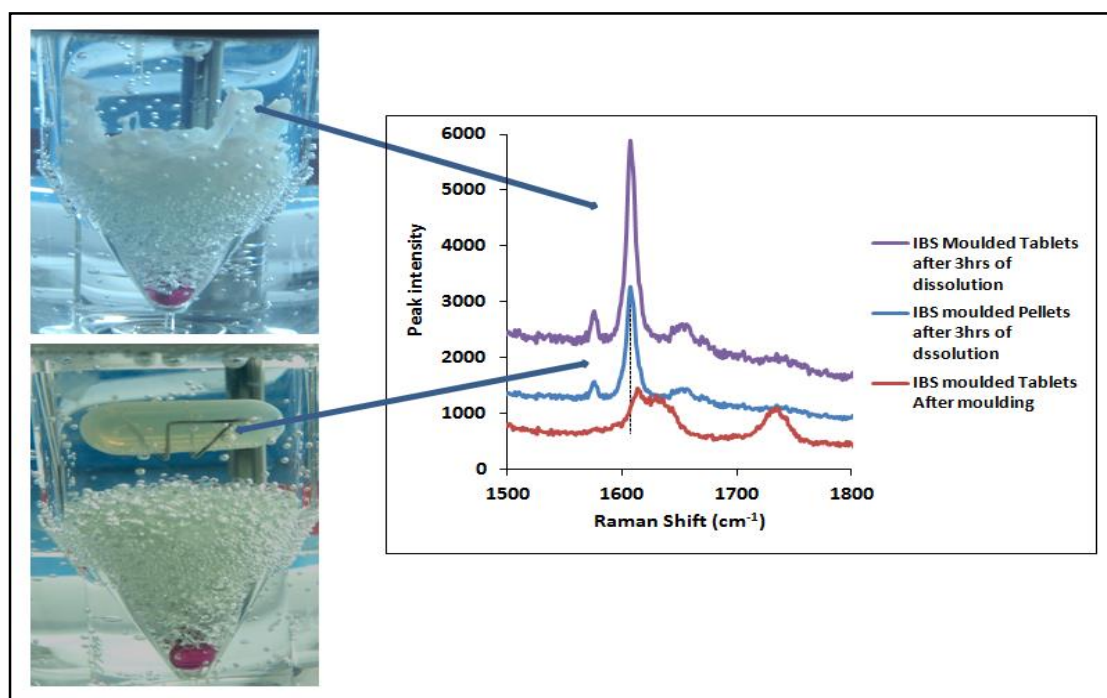
Figure 6.16: Raman spectra of surface of IBS pellets and tablets after 3hrs of dissolution

The 60 min and 180 min photographs in Figure 6.17 clearly shows the surface changes of samples and this suggests the ingress of the water in the dosage form could have decreased the Tg of the system and thus favoured crystallisation. Indomethacin pioglitazone and nifedipine are some of the drugs known to crystallise or phase transform during the dissolution process. (Alonzo et al., 2011; Alonzo et al., 2010; Raina et al., 2014; Shi et al., 2014)
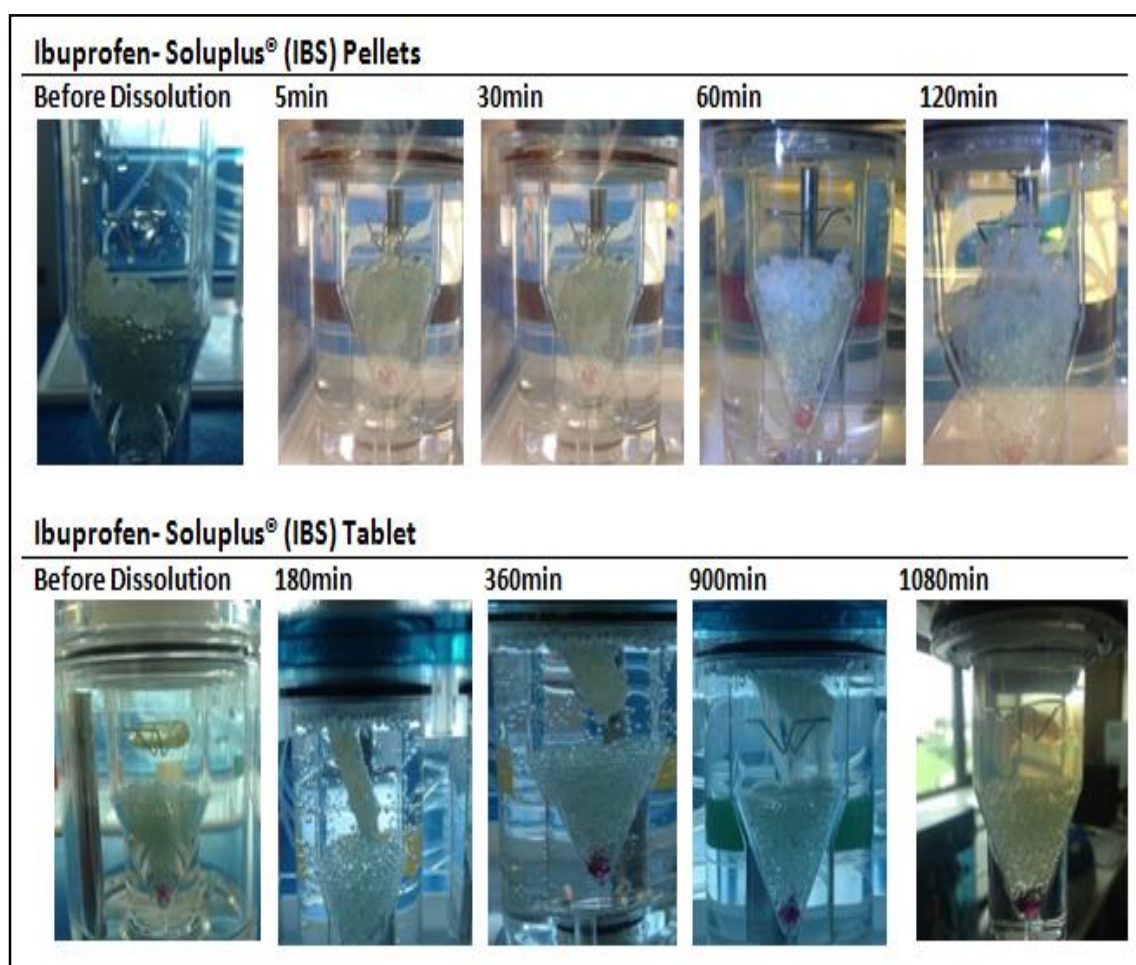
Figure 6.17: Dissolution images of IBS pellets and IBS moulded tablets

To summarise the results and discussion of this chapter, the injection moulded systems of the Soluplus® were achieved without the addition of processing aids. An addition of the low Tg drug (ibuprofen) and the medium Tg drug (felodipine) assisted the processing by HME and IM as a result of their plasticization effect. The molecular level dispersion of both the drugs was achieved within the Soluplus®matrix using the HME and IM processes. Thermal, mechanical and spectroscopic studies suggested that the FDS systems would be more stable compared to the IBS systems due to high Tg and H-bonding. These results can also be correlated with the good drug polymer miscibility which was predicted the higher miscibility of the felodipine with Soluplus® using van Krevelens group contribution and the F-H theory. The clear difference observed in the drug release performance of both IBS and FDS systems where, ibuprofen crystallized during the dissolution whereas felodipine released at a constant rate over the time and released 100% of the drug. Soluplus® IM systems are also discussed in the next global discussion chapter.

Chapter 7

Discussion: HPMCAS and Soluplus® moulded systems

A combined discussion of results presented in chapters 4, 5 and 6 is provided. In particular, the properties of HPMCAS and Soluplus® IM systems are discussed in relation to API and polymer properties, moulding and storage conditions. Global findings from this research work are highlighted.

7.1 Pre-formulation

Physicochemical properties of the materials and pre-formulation studies were used to predict the miscibility, solubility and stability of the selected drug-polymer pairs. The APIs (ibuprofen and felodipine) and polymers (HPMCAS and Soluplus®) have several distinguishing properties such as Tg, melting point, solubility parameter etc. The Tg of mixtures was calculated using the Fox equation and MDSC whereas rheological properties were measured using capillary rheometry. These indicated a high level of plasticisation by ibuprofen on the polymers compared to felodipine. Theoretically predicted Tg curves for IBH, IBS, FDH and FDS mixtures were shown in Figure 4.1 (Chapter 4)

The logarithmic relationship between apparent shear viscosity and wall shear rate for HPMCAS and Soluplus® with and without the addition of ibuprofen and felodipine was shown in Figure 7.1. The shear viscosity of HPMCAS at 170°C at low shear rate ($50s^{-1}$) was approximately 1300 Pa.s while FDH mixture (10% felodipine, 20% PEO) was similar. However, the addition of 33% ibuprofen significantly decreased the shear viscosity to 480 Pa.s at 120°C. This result suggests a higher plasticisation effect of ibuprofen on HPMCAS than felodipine and PEO. HPMCAS, IBH and FDH showed shear thinning behaviour where a linear decrease in the log shear viscosity with log shear rate was observed.

Figure 7.1b shows the shear viscosity of Soluplus®, IBS and FDS mixtures at 140°C in the low shear rate range 20- 100 s^{-1}. Soluplus® exhibited Newtonian behaviour followed by shear thinning behaviour at higher shear rates (> 500 s^{-1}). 10% addition of felodipine has shown similar behaviour while 10% ibuprofen addition showed a significant decrease in the shear viscosity with shear thinning

262

behaviour. However, at high shear rates (2000 s^{-1}) the Soluplus$^®$ and all the mixtures have shown the shear viscosity in the range of 150-400 Pa.s.
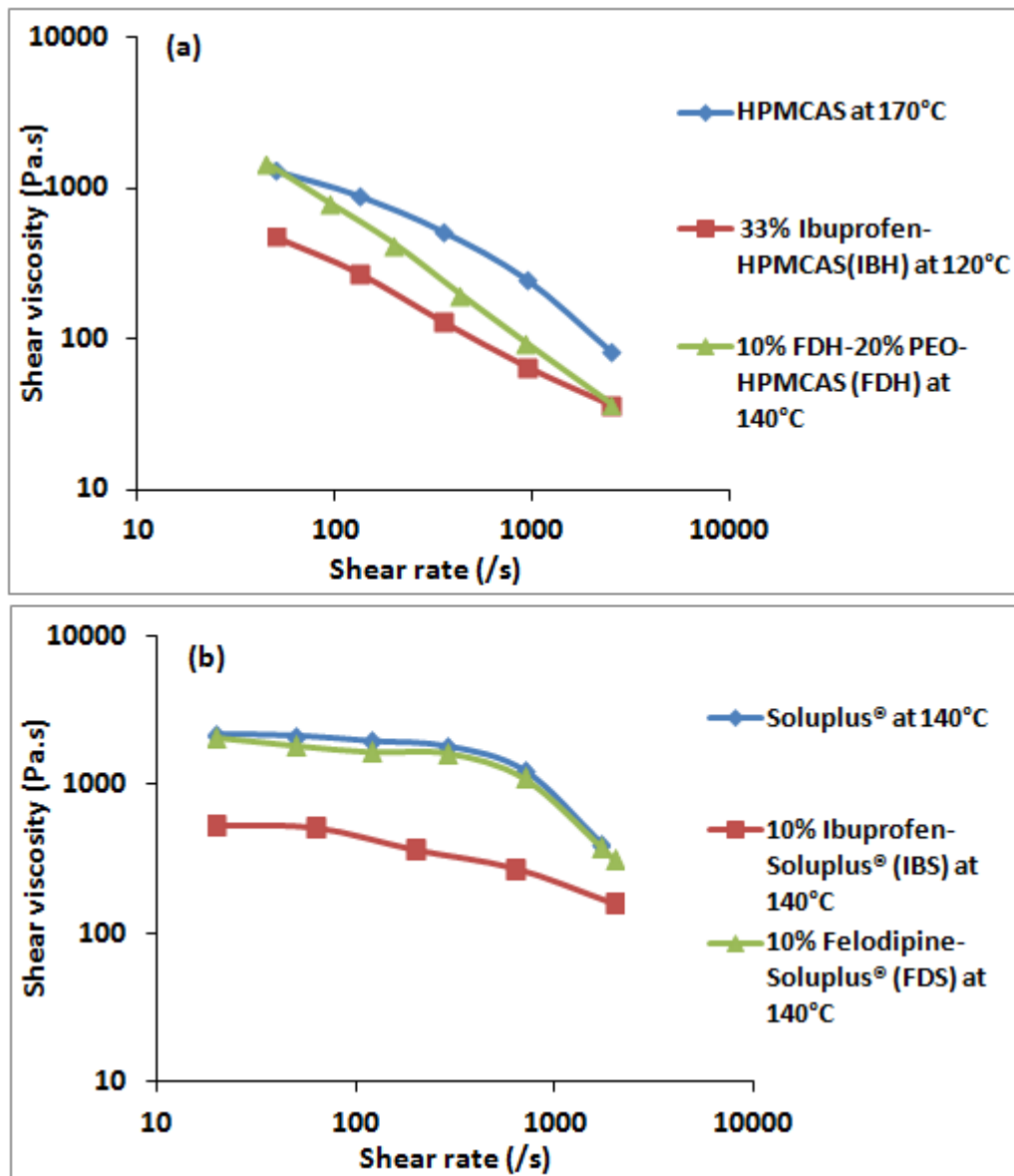
Figure 7.1: Shear viscosity of (a) HPMCAS with addition of ibuprofen and Felodipine (b) Soluplus$^®$ with addition of ibuprofen and felodipine

During the injection moulding process higher shear rates generated in the nozzle and gate during the injection will further decrease the viscosity and thus allow better filling of the mould cavity. The precise level of shear rate generated in a particular mould will depend upon mould tool geometry and injection velocity.

Melt rheology studies of both polymers suggested HPMCAS shows shear thinning behaviour of HPMCAS and Soluplus® needs high shear in order follow shear thinning behaviour. At a very high shear rate (2000 s^{-1}) however, both the polymers have shown the decrease in viscosity (50-200Pa. s) suggests the adaptability of polymer for IM. The plasticisation effect of APIs was also very prominent where a low Tg ibuprofen reduced polymer viscosity at least by order of 2 and thus suggesting better performance during IM.

7.1.1 Stability prediction using temperature-composition phase diagram

Using phase diagrams, the solubility and miscibility of APIs in both polymers were calculated with respect to temperature. The estimation of miscibility and solubility of drugs in different polymers was reported earlier by various groups using the melting point depression method combined with Flory-Huggins lattice based theory (Marsac et al., 2006) (Nishi and Wang, 1975) (Yang et al., 2015). The miscibility of felodipine was reported in various polymers such as polyvinyl pyrrolidone (PVP) (Marsac et al., 2006); Eudragit EPO (Yang et al., 2015), HPMCAS and Soluplus® (Tian et al., 2013), Poly acrylic acid (PAA) (Lin and Huang, 2010). Tian et al. reported at room temperature (25°C) 7% wt miscibility of felodipine in HPMCAS compared to 12% wt miscibility in Soluplus®. In this research, the ibuprofen miscibility and solubility in HPMCAS and Soluplus® was obtained.

The phase diagram based on the F-H theory provides an interesting platform to understand the drug-polymer system performance and stability of the amorphous form of the drug within the polymer matrix. The liquid-solid phase transition curve represents the equilibrium solubility of drug crystals within the

polymer matrices with respect to temperature (Figure 7.2; blue line). Above this curve the drug is dissolved in the polymer and forms an unsaturated solution while below this curve the solid dispersion is above the equilibrium solubility. The region between the solubility and miscibility curves is called the meta-stable region (Lin and Huang, 2010).
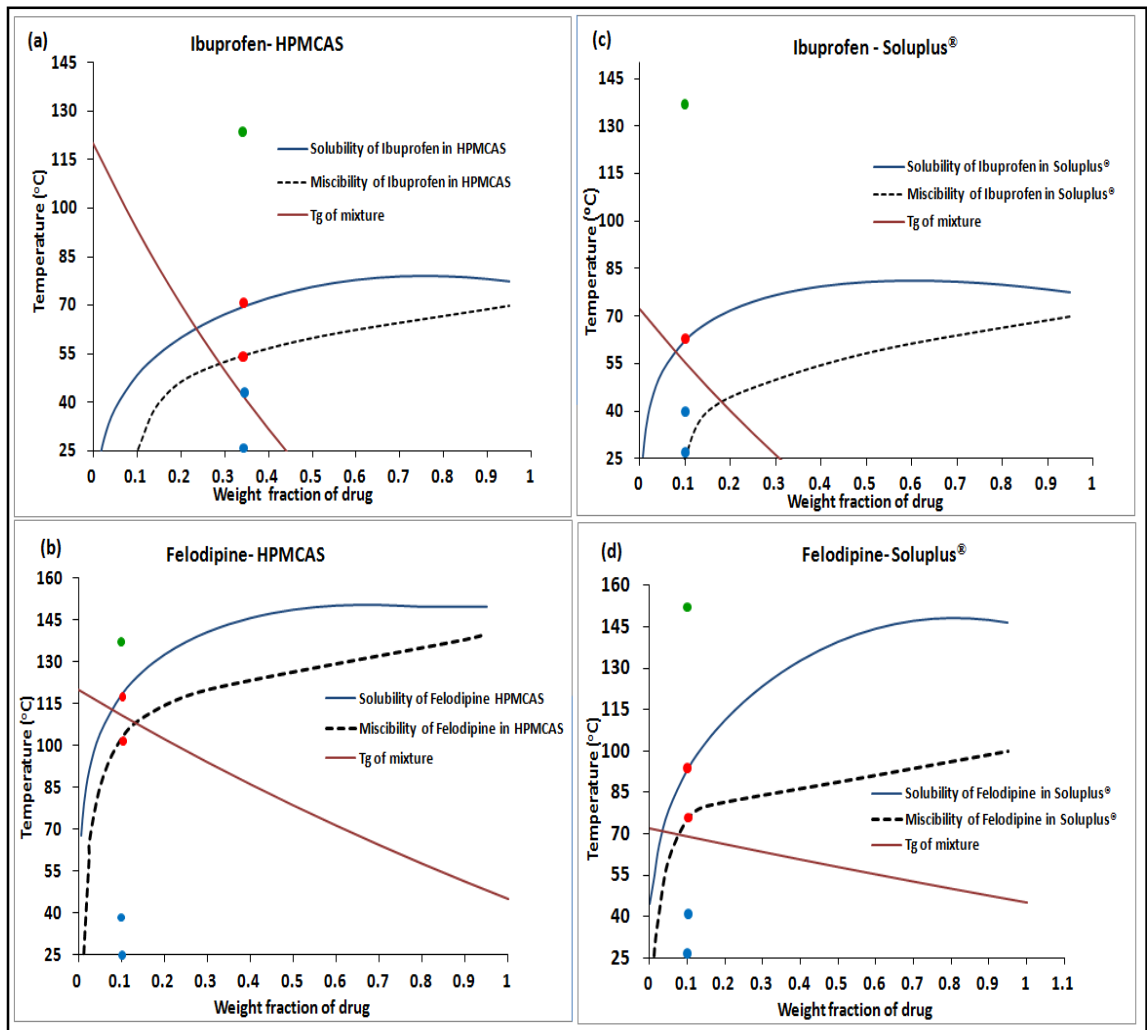
Figure 7.2 Temperature composition phase diagram (a) ibuprofen-HPMCAS; (b) felodipine-HPMCAS (c) Ibuprofen-HPMCAS (d) felodipine-Soluplus® , IM processing temperature (●), Stress temperatures (●);and Miscibility and solubility temperature (●)

The phase diagram shown in the Figure 7.2 provides information about the processing temperatures used for the injection moulding of all four systems

(green dot). All systems were processed above the thermodymically established solubility curve (blue line) indicating that the systems formed a homogenous dispersion as processed above the solid-liquid transition temperature and which also suggests the strong possibility of the formation of amorphous molecular dispersions. The miscibility and solubility temperatures of both the ibuprofen and felodipine in the HPMCAS and Soluplus® are provided in the Figure 7.2 (red dots). It was seen that, at the same weight fraction ibuprofen becomes miscible and soluble in both polymers at lower temperatures than felodipine. For example 10%wt ibuprofen shows miscibility with HPMCAS and Soluplus® at 25°C. However 10%wt felodipine shows miscibility with HPMCAS at 100°C and miscibility with Soluplus® at 74°C.

The solubility of an API in a polymer will be a function of its melting temperature and heat of fusion as well as a sign of mixing enthalpy as reflected in the interaction parameter (Marsac et al., 2006). It is reported that APIs with a high heat or temperature of fusion will therefore be less soluble in a polymer. This is apparent from comparing data for ibuprofen and felodipine where it can be seen that the lower melting and lower heat of fusion of ibuprofen is predicted to have a greater solubility in the polymers (HPMCAS and Soluplus®) than felodipine. The effect of fusion properties on the solubility of small molecule in conventional solvents has been discussed in detail previously (Yalkowsky, 1999). Therefore, high melting point/ high enthalpy of fusion compounds which do not have substantial interaction with the polymer will display less solubility. Conversely, a negative enthalpy of mixing (and FH interaction parameter χ) will display higher solubility (Marsac et al., 2006). Similarly, the calculated FH interaction parameters for ibuprofen and felodipine in HPMCAS at 25°C were

1.29 and 5.26 respectively, which suggest higher solubility of low melting ibuprofen than felodipine (details are provided in Table 4.4).

According to the phase diagrams provided in the Figure 7.2, if the felodipine (10%wt) containing injection moulded systems formed with HPMCAS and kept at stress temperature, it will show higher stability due to broad supersaturated glassy state (zone V). Moreover, practically and theoretically predicted Tg (brown curve) of the felodipine-HPMCAS system is very high compared to stress temperatures hence system stability would be higher due to the kinetic barrier offered by Tg. In general, the thermodynamic stability of the system predicted using the binary phase diagram shows a Tg curve which defines the kinetic boundary of molecular mobility and defines the glass and the equilibrium liquid below and above the Tg curve, respectively. For comparing data between felodipine-HPMCAS (FDH) and felodipine-Soluplus® (FDS) the miscibility and solubility curve suggest the felodipine-Soluplus® systems would be thermodynamically more stable than felodipine-HPMCAS however the broad glassy region of the felodipine-HPMCAS will offer greater kinetic stability.

In the case of the ibuprofen containing system the miscibility and solubility curves for ibuprofen-Soluplus® and ibuprofen-HPMCAS systems were almost identical. However, the broad supersaturated glass region (Zone V) of ibuprofen-HPMCAS suggests it would be a more stable system than the ibuprofen-Soluplus®. In this research, 33% ibuprofen dispersion was obtained with HPMCAS (I 33) and theoretically predicted Tg of the system was 38°C. I33 systems kept at stress condition (25° and 40°C) showed spontaneous crystallisation. The reason for crystallization can be explained based on the

phase diagram (Figure 7.2a). When I 33 moulded systems were stored at 40°C, the system was stored above the Tg and behaved like a supersaturated immiscible liquid (Zone VI of phase diagram). Hence the driving forces for crystallisation were amorphous phase separation and crystallisation of the supersaturated drug (Qian et al., 2010). Moreover the kinetic effect for stability was negligible as the stress temperature > Tg. At the lower stress condition (25°C) I33 moulded systems were practically stored below the Tg therefore it was behaving like a supersaturated immiscible glass (zone v). I33 moulded systems should crystallise at a slower rate at 25°C compared to 40°C and this crystallisation behaviour was confirmed by MDSC and NIR crystallisation studies.

7.2 Formulation and chracterisation

Processing considerations and a combined discussion on the properties of the four injection moulded systems is provided in this section

7.2.1 HME and IM Processing

Melt processing of HPMCAS alone was not possible below 160°C using HME and the addition of ibuprofen allowed the extrusion to be carried out at 100-120°C with a reduction in measured torque and die pressure highlighting the plasticisation effect of ibuprofen. The medium Tg drug (felodipine) was not an effective plasticiser for HPMCAS hence the low Tg polymer (PEO) was incorporated with 20% concentration. This allowed melt processing to be carried out at 140°C.

HME and IM of HPMCAS required the addition a low Tg drug and/or polymer. Conversely, Soluplus® was developed for HME processing and its feasibility for IM was explored at 140°C. Mould filling was performed at high

injection speed and a higher set mould temperature (70°C) allowed better ejection from the mould. Soluplus® showed Newtonian behaviour in low shear rate and shear thinning behaviour at high shear rate. Better mould filling at higher injection speed was attributed to a decrease in the shear viscosity. 10% addition of ibuprofen and felodipine decreased the Tg of the systems to 54°C and 63°C respectively, which favoured melt processing.

7.2.2 Characterisation

Moulded ibuprofen-HPMCAS systems were produced with different drug loadings of ibuprofen and with/without a hydrophilic additive (mannitol). Mannitiol containing systems slightly increased the ibuprofen release from the moulded tablets due to the formation of pores. However, the tablet surface was eroding at constant rate and the limited surface area was available for the dissolution. It might be possible that the small pores formed due to the dissolution of mannitol at the tablet surface could have promoted the ibuprofen release to only small extent. 33% ibuprofen-HPMCAS (I33) systems were studied in detail using 3^2 factorial designs for the IM process. When kept at stress conditions moulded samples exhibited a surface crystallisation phenomenon. Crystallisation kinetics were quantified using the NIR and MDSC; results suggested that the 40°C 75%RH condition produced a crystallisation rate of $\cong$ 2%/day approximately 10 times higher than compared to the 25°C 60%RH condition ($\cong$0.2%/day). FTIR and Raman spectroscopy confirmed molecular association and formation of H-bonds between the drug and the polymer. Amorphous and crystalline phase separation was observed using DMA which complimented the MDSC results.

Earlier reports showed that Ibuprofen and felodipine can form intermolecular hydrogen bonding (Kestur and Taylor, 2010; Konno and Taylor, 2006) (Bras et al., 2008). Ibuprofen is known to form a dimer by involvement of two -C=O functional of groups whereas the –N-H functional group of felodipine form H-bonding with –C=O of other felodipine molecule (Figure 7.3). The HPMCAS and Soluplus® used in these studies are proton acceptors hence they can possibly form H-bonds with a proton donor of APIs. Felodipine formed a strong H-bond with both polymers through involvement of -N-H functional groups of felodipine and –C=O functional groups of HPMCAS and Soluplus® (details of IR shift provided in sections 5.2.2.5 and 6.2.3). Similarly, Ibuprofen formed an H - bond with HPMCAS however, no changes in –C=O stretching's were seen when ibuprofen formed an amorphous solid dispersion with Soluplus®.
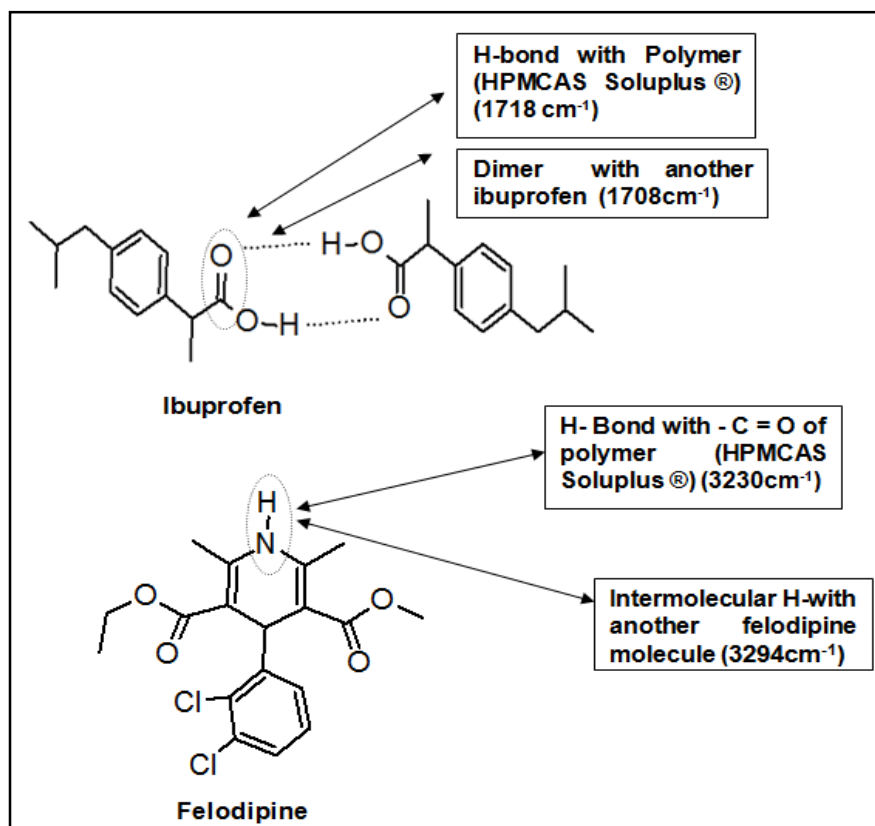
Figure 7.3: H-bondings of ibuprofen and felodipine

The stability of an amorphous solid dispersion can be correlated with the nature of H-bonding between the drug and a polymer. Solubility parameters (δ) calculated using Van Krevelen and Hoftyzer's group contribution method by measuring their cohesive energy density (CED) also considered a contribution from hydrogen bonding (equation 4.2). The calculated solubility parameter difference ($\Delta\delta$) for ibuprofen-Soluplus® was 12.41. The higher difference in $\Delta\delta$ indicated immiscibility and unlikeness to a form H-bonding. Solubility parameter difference ($\Delta\delta$) (MPa$^{1/2}$) of the four systems predicted the order of miscibility as follows; felodipine-HPMCAS > felodipine-Soluplus® > ibuprofen-HPMCAS > ibuprofen-Soluplus®. The observed stability of IM systems was in accordance with the H-bonding measured by FTIR and calculated from solubility parameters.

The solubility parameters, glass transition temperature, drug-polymer miscibility and solubility, H-bonding and concentration of the drug all played important role in understanding stability of the injection moulded amorphous molecular dispersions.

7.2.3 Drug release

Release profiles for ibuprofen and felodipine were obtained from the HPMCAS and Soluplus® matrices. Although the release was primarily governed by the nature of the polymer matrix, the product properties and processing history also affected the dissolution rate. As per the Noyes-Whitney equation (equation 2.1) the surface area is one of the prominent factors governing dissolution rate. Therefore, the product particle size and the densification during processing have a significant influence on the surface area and consequently the dissolution rate.

For example, extruded pellets will provide higher surface area for dissolution than the moulded tablet due to the smaller particle size.

HPMCAS has a pH dependent solubility and amphiphilic nature whereas Soluplus® has amphiphilic nature, water soluble and also known to form micelles above certain concentrations. PEO is a highly water soluble polymer and has swelling properties, thus exhibits drug release either by swelling followed by diffusion or erosion depending on the molecular weight (Apicella et al., 1993).

Ibuprofen release from I33 pellets and tablets were observed to be controlled release. Extruded pellets showed the faster release where (100% within 6 hrs) whereas moulded tablets showed only 50 % release in 6hrs indicating the controlled release behaviour of the tablets (Figure 7.4). IBS pellets and IBS tablets showed erratic and incomplete drug release due to the crystallisation of ibuprofen during dissolution (Figure 7.4). The decrease in Tg of the product upon contact with dissolution media led to crystallisation and thus affected the dissolution. The Raman spectroscopy confirmed the crystallisation of ibuprofen after 3hrs of dissolution.

For the felodipine-HPMCAS systems two different polymer matrices dictate the drug release. PEO polymer matrix governs the release by and diffusion whereas HPMCAS exhibit release by surface erosion. Figure 7.4 shows the drug release profile of HPMCAS and Soluplus® IM systems. FDH pellets have showed faster release where the 50% release was observed within 5 hrs whereas; FDH tablets have shown only 25% drug release within 5 hrs of dissolution and 50% release after 10 hrs.
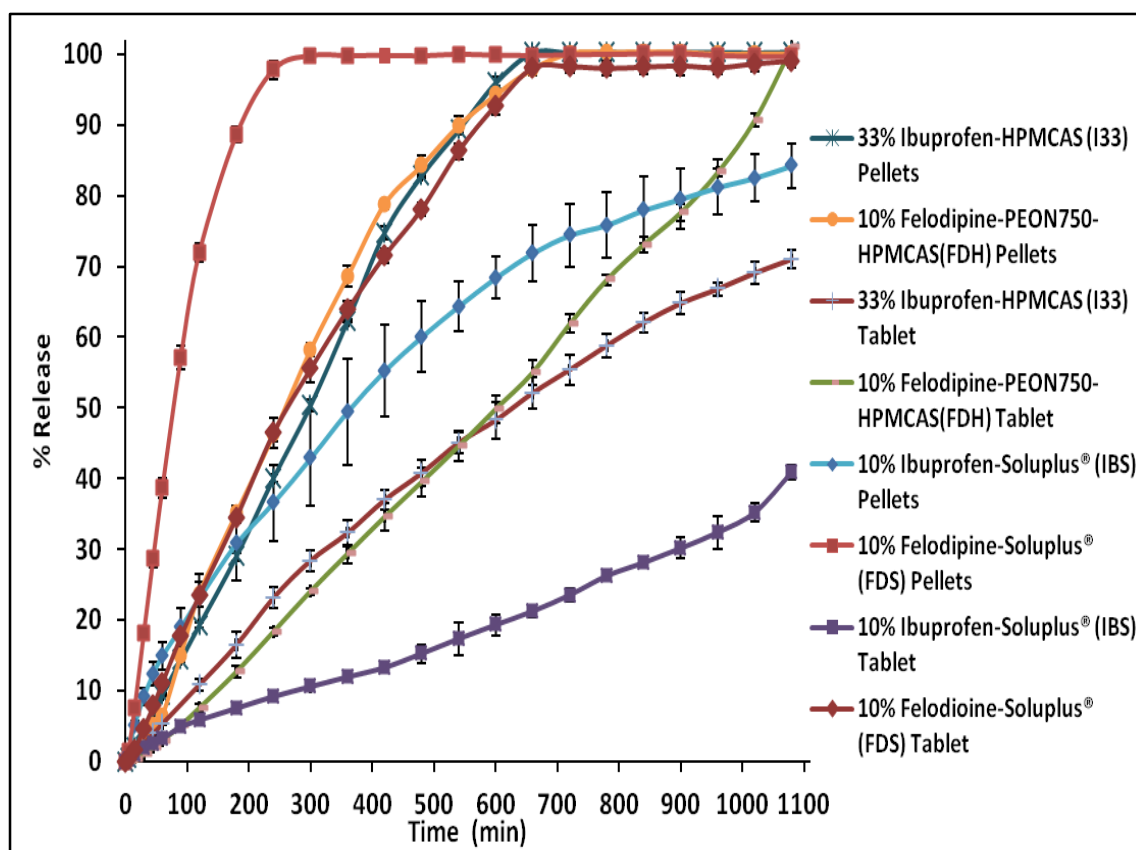
Figure 7.4: dissolution profiles of extruded pellets and moulded tablets studied using flow-through cell (USP IV): I33 and IBS systems in Phosphate buffer pH 7.2; FDH and FDS systems in Phosphate buffer pH 6.5 (n=3)

The release from FDH pellets and FDH tablet completed within 11hrs and 18hrs of the dissolution, respectively. When compared to the release of the felodipine from the Soluplus®, it was comparatively faster and the dissolution rate was almost twice that of FDH. FDS pellets and tablets showed 50% release in 1.5 hrs and 4 hrs respectively. The complete drug release was seen after 4 hrs and 11 hrs of dissolution of FDS pellets and tablets respectively. The drug release from Soluplus® matrix was faster than the HPMCAS matrix which could be attributed to the pH dependent solubility of HPMCAS.

7.2.3.1 Dissolution model fitting

The % drug release data obtained was used for dissolution model fitting. The representative model fitting profile of I33 pellets is shown in Figure 7.5.
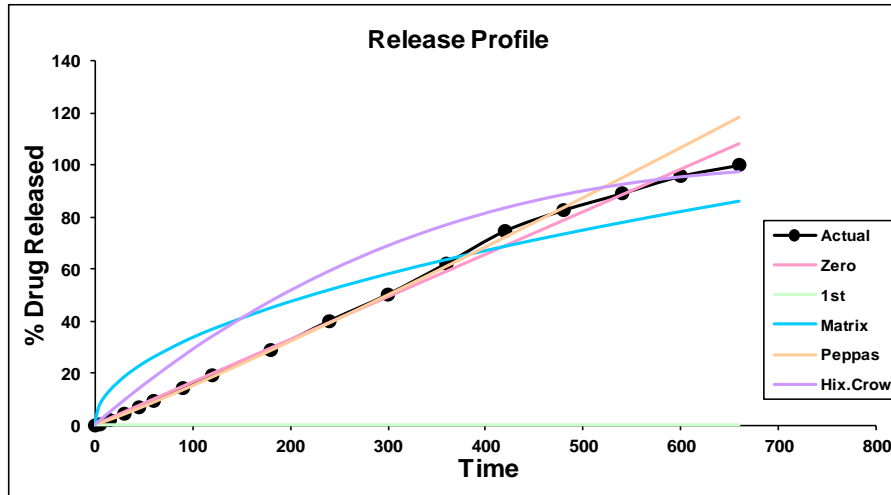
Figure 7.5 Dissolution model fitting for I33 pellets

The Peppas developed the equation to analyze both Fickian and non-Fickian release of drug from swelling as well as non- swelling polymeric drug delivery systems (Peppas, 1985).

$$\frac{M_t}{M_\infty} = kt^n$$ (Equation 7.1)

Where, M_t/M_∞ is the fraction of drug released at time t, n is diffusion exponent indicative of the mechanism of transport of drug through the polymer; K is a kinetic constant incorporating structural and geometric characteristics of the drug delivery systems. The value of n provided in the Table 7.1 suggests that, for the cylindrical sample when n < 0.5 the drug release mechanism follows a fickian diffusion whereas n > 0.89 suggests anomalous transport.

Table 7.1: Interpretation of diffusional release mechanisms from controlled release polymeric systems (Costa and Sousa Lobo, 2001)

Release exponent (Films) (n)	Release exponent (Cylindrical) (n)	Drug transport mechanism	Rate as a function of time
0.5	0.45	Fickian diffusion	$t^{-0.5}$
$0.5<n<1.0$	$0.45<n<0.89$	Anomalous transport	t^{n-1}
1.0	0.89	Case-II transport	Zero order release

Drug release from the injection molded tablets, followed the Korsmeyer-Peppas model. The release mechanism obtained from I33, FDH, FDS pellets and moulded (cylindrical) tablets showed n values higher than 0.89 or equal to 1 suggesting that the drug release follows zero order except for IBS tablets which showed an anomalous transport mechanism (Table 7.2).

The zero order release from moulded systems confirmed that drug dissolution from the tablets that do not disaggregate released the drug slowly assuming that no equilibrium condition is obtained (Costa and Sousa Lobo, 2001). These release profiles also suggests that the release of the same amount of drug by unit of time was achieved, which is an ideal method of drug release to achieve prolonged pharmacological action. The densification during injection moulding leads to dissolution of dosage forms at constant rate, providing a constant surface area for drug diffusion and the amount of drug released was independent of initial drug concentration. For IBS systems crystallisation during dissolution caused erratic behaviour and anomalous drug release.

Table 7.2: The model fitting and mechanism of release from HMPCAS and Soluplus® pellets and moulded systems

Drug-polymer system	Model fitting					Release mechanism
	Zero order	1st Order	Matrix	Hix. Crow	Pappas	
33%Ibuprofen-HPMCAS (I33) Pellets	0.9969	*	0.9392	0.9303	0.9974 n = 1.09 k = 0.096	Peppas, zero order release
33%Ibuprofen-HPMCAS (I33) Tablet	0.9865	0.9451	0.9910	0.940	0.999 n = 1.023 k = 0.069	Peppas, zero order release
10%Felodipine-PEO-HPMCAS (FDH) pellets	0.9142	*	0.9654	0.9725	0.9780 n = 1.165 K = 0.056	Peppas, zero order release
10%Felodipine-PEO-HPMCAS (FDH) Tablet	0.9923	*	0.9180	0.8462	0.9971 n = 1.384 k = 0.007	Peppas, zero order release
10% Ibuprofen-Soluplus® (IBS) Pellets	0.9283	.9801	.9872	0.9785	0.9878 n= 0.727 k = .656	Peppas Anomalous
10% Ibuprofen-Soluplus® (IBS) Tablet	0.9925	0.9847	0.9319	0.9882	0.9944 n = 0.842 K = 0.090	Peppas, Anomalous;
10% Felodipine - Soluplus® (FDS) Pellets	0.9298	*	0.9678	0.9752	0.9893 n= 1.04 k= 0.410	Peppas, zero order release
10% Felodipine - Soluplus® (FDS) Tablet	0.9929	*	0.9566	0.9539	0.9878 n= 1.152 k= 0.743	Peppas, zero order release

* Insignificant

The preformulation, processing, stability and drug release studies performed here on the four injection moulded systems suggested that Felodine-PEO-HPMCAS (FDH) and feloddipien-Soluplus® (FDS) were the most stable systems in term of stability of amorphous solid dispersion. Moreover, the controlled drug release from these systems was achieved with 100% release within 18 hrs.

Ibuprofen formed a homogenous amorphous solid dispersion with polymer matrices and provided a good plasticisation effect during HME and IM compared to felodipine. However, higher drug loadings (33%) with HPMCAS formed a supersaturated dispersion which leads to crystallsation. Stable amorphous solid dispersion was achieved with Soluplus®, however crystallisation of ibuprofen was observed during dissolution.

These studies have provided a sound understanding of the material properties, processability and performance of injection moulded dosage forms containing an amorphous solid dispersion. The significant factors affecting the performance and stability of injection moulded drug delivery systems consist of the solubility parameter difference ($\Delta\delta$), glass transition temperature of the drug and polymer (Tg), drug-polymer miscibility and solubility (χ, ΔG), and processing variables such pack pressure and mould temperature during IM.

Chapter 8

Conclusion

This work provides a detailed study of formulation development of pharmaceutical dosage forms using the injection moulding process. Four API-polymer formulations were successfully developed using IM. The findings of present work suggest that IM may have extensive applications in pharmaceuticals either as a downstream manufacturing process for melt extruded formulation or as an independent single unit operation. From the current research, the following conclusions could be drawn:

❖ Material behaviour during melt processing was found to be heavily dependent upon physicochemical properties. The combination of a low Tg, low melting temperature drug (ibuprofen); with a low Tg polymer (Soluplus®) was found to be most suitable combination for processing by injection moulding.

❖ IM of pharmaceutical grade amorphous polymers was successfully performed; however in order to mould HPMCAS, the addition of low Tg plasticisers was required to lower the processing temperature and viscosity. Soluplus® was found to be suitable for injection moulding and could be moulded alone or in combination with model APIs.

❖ Low and medium Tg APIs, ibuprofen and felodipine, respectively were found to act as sufficient plasticisers for HPMCAS and Soluplus® to be moulded. Amorphous polymers soften above the Tg and exhibit higher heat capacity and molecular mobility. Based on this study it can be

concluded that for injection moulding of amorphous materials the most important consideration is the glass transition temperature of the total system.

❖ Each API - polymer formulation studied formed a solid solution after extrusion. IM was also found to be suitable for manufacturing a final dosage form from these solid solutions.

❖ Although the drug was molecularly dispersed in both the cases extruded pellets and moulded tablets, the rate of drug release from pellets was faster compared to moulded tablets suggesting an effect of processing history on the product properties. This was attributed to the effect of particle size and densification during injection moulding on the drug release rate.

❖ All of the moulded systems studied were stable after processing and when held at stress conditions. However, surface crystallisation under stress conditions was observed for one drug-polymer pair (ibuprofen-HPMCAS) where supersaturated drug dispersion led to drug crystallisation. Crystallization on the surface and stability in the bulk (amorphous phase) suggested that phase separation of the moulded system was a time dependent process. Stress condition also had a significant influence on the crystallisation rate. Moulding parameters such as pack pressure and mould temperature were identified as important process variables affecting product properties and stability.

❖ Shrinkage of moulded drug delivery systems was observed, and results suggest that shrinkage could be used as a quality control parameter for

injection moulded systems. A higher shrinkage tendency of HPMCAS mouldings was observed compared to Soluplus® mouldings. Shrinkage rate was quantified at various stress conditions and temperature and moisture were found to affect the rate and extent of shrinkage.

❖ All injection moulded tablets, except IBS, showed a controlled release of drug and the release mechanism primarily followed the Peppas model of zero order release, suggesting diffusion of drug molecule at a constant rate with drug release being independent of concentration.

❖ Overall, this study presents a successful attempt to develop and understand controlled release from amorphous solid dispersions using injection moulding

The currently developed injection moulded systems (tablets) were specifically designed with the objective of obtaining the oral drug delivery systems. IM has commonly been used for making pharmaceutical packaging materials and recently for the production of biomedical devices such as scaffolds, microneedles, microfluidic devices, implants. Only a limited number of studies have been performed to investigate the applications of injection moulding for the oral drug delivery. Moreover, the polymers used were semi-crystalline in nature, e.g. Polylactic acid, polycaprolactone etc. These polymmers are relatively suitable for injection moulding compared to the currently investigated amorphous polymers i.e HPMCAS and Soluplus®. The main challenges associated with the current product development was the material suitability for the injection moulding. The pre-compounding of drug-polymers mixtures using the HME and use of plasticisers for amorphous polymers became the necessity prior to the

injection moulding. This investigation has helped to the identify some of the important material attributes (e.g Tg, miscibility and solubility) and critical process parameters (e.g., pack pressure, mold temperature) for the pharmaceutical product development using IM.

The drug delivery systems developed in this research have limitation in term of the dissolution and drug release from the dosage forms. In general, drug delivery products developed using injection moulding are highly dense, non-disintegrating and potentially challenging for oral drug delivery. However, the potential application of IM technique was seen for the development of the controlled release oral dosage forms. All of the moulded systems studied have shown the shrinkage at various stress conditions, therefore this study recommends that the shrinkage should be used as a quality assessment parameter for the injection moulded pharmaceutical products.

Injection moulding offers many advantages over the current pharmaceutical product manufacturing; especially tabletting. The pharmaceutical industries are currently using solvent assisted, batch processing which often involves use of organic solvents and number of unit operations. Injection moulding could be a viable technology for the continuous manufacturing as it can be transferred to the industrial scale and it has an ability to produce components with excellent dimensional accuracy. The versatility of IM technique can be exploited for the production of novel drug delivery systems with defined shape and/or dimension characteristics.

Chapter 9

Suggested further work

❖ To develop immediate release injection moulded oral drug delivery systems. Due to densification during injection moulding, tablets do not readily disintegrate and the use of suitable material properties and process parameters to develop disintegrating dosage forms is suggested.

❖ Development of two component injection moulded systems using co-injection moulding

❖ To understand the micromoulding process.

❖ Surface structuring of injection moulded tablets to understand the effect of surface roughness and surface area on drug dissolution.

❖ To develop ultrasound assisted injection moulding method for pharmaceutical dosage forms to reduce the effect of exposure to high temperature and understand the effect process on the properties.

❖ To understand the behaviour of a range of pharmaceutical polymers such cellulose, polyacrylates, vinyl polymers, Poly(ethylene oxide) & their derivatives.

❖ To study the effect of injection moulding process variables on to shrinkage of moulded system and to optimise process parameters to control shrinkage.

❖ To develop different intermediate compounding processes such high shear granulation or direction compaction to prepare drug-polymer mixtures for injection moulding. To characterise material properties to understand the effect of IM on polymer molecular weight distribution using GPC.

References

ASTM D955 Standard Test Method of Measuring Shrinkage from Mold Dimensions of Thermoplastics STM Volume 08.01 Plastics (I): C1147 D315http://www.astm.org/Standards/D955.htm cited on 17/12/2014

Aaltonen, J., Rantanen, J., Siiria, S., Karjalainen, M., Jorgensen, A., Laitinen, N., Savolainen, M., Seitavuopio, P., Louhi-Kultanen, M. and Yliruusi, J. (2003) Polymorph screening using near-infrared spectroscopy. *Analytical Chemistry,* 75 (19)**,** 5267-5273.

Adamska, K. and Voelkel, A. (2005) Inverse gas chromatographic determination of solubility parameters of excipients. *International Journal of Pharmaceutics,* 304 (1-2)**,** 11-17.

Aitken, D., Burkinshaw, S. M., Cox, R., Catherall, J., Litchfield, R. E., Price, D. M. and Todd, N. G. (1991) Determination of the Tg of wet acrylic fibers using DMA. *Journal of Applied Polymer Science :Applied Polymer Symposium* 47**,** 263-269.

Al Omari, M. A., Zughul, M. B., Davies, J. E. D. and Badwan, A. A. (2006) Sildenafil/cyclodextrin complexation: Stability constants, thermodynamics, and guest-host interactions probed by H-1 NMR and molecular modeling studies. *Journal of Pharmaceutical and Biomedical Analysis,* 41 (3)**,** 857-865.

Alonzo, D. E., Gao, Y., Zhou, D., Mo, H., Zhang, G. G. Z. and Taylor, L. S. (2011) Dissolution and Precipitation Behavior of Amorphous Solid Dispersions. *Journal of Pharmaceutical Sciences,* 100 (8)**,** 3316-3331.

Alonzo, D. E., Zhang, G. G. Z., Zhou, D., Gao, Y. and Taylor, L. S. (2010) Understanding the Behavior of Amorphous Pharmaceutical Systems during Dissolution. *Pharmaceutical Research,* 27 (4)**,** 608-618.

Angell, C. A., Macfarlane, D. R. and Oguni, M. (1986) The Kauzmann Paradox, Metastable Liquids, and Ideal Glasses: A Summary. *Annals of the New York Academy of Sciences,* 484 (1)**,** 241-247.

Apicella, A., Cappello, B., Delnobile, M. A., Larotonda, M. I., Mensitieri, G. and Nicolai, L. (1993) Poly(ethylene oxide) (peo) and different molecular-weight peo blends monolithic devices for drug release. *Biomaterials,* 14 (2)**,** 83-90.

Atkinson, R. M., Bedford, C., Child, K. J. and Tomich, E. G. (1962) Effect of particle size on blood griseofulvin-levels in man. *Nature,* 193**,** 588-9.

Babu, N. J. and Nangia, A. (2011) Solubility Advantage of Amorphous Drugs and Pharmaceutical Cocrystals. *Crystal Growth & Design,* 11 (7)**,** 2662-2679.

Bak, A., Gore, A., Yanez, E., Stanton, M., Tufekcic, S., Syed, R., Akrami, A., Rose, M., Surapaneni, S., Bostick, T., King, A., Neervannan, S., Ostovic, D. and Koparkar, A. (2008) The co-crystal approach to improve the exposure of a water-insoluble compound: AMG 517 sorbic acid co-crystal characterization and pharmacokinetics. *Journal of Pharmaceutical Sciences,* 97 (9)**,** 3942-3956.

Barshalom, D., Bukh, N. and Larsen, T. K. (1991) Egalet, a novel controlled-release system. *Annals of the New York Academy of Sciences,* 618**,** 578-580.

Basavoju, S., Bostrom, D. and Velaga, S. P. (2006) Pharmaceutical cocrystal and salts of norfloxacin. *Crystal Growth & Design,* 6 (12)**,** 2699-2708.

Bayer, R. K., ELIA, A. E. and SEFERIS, J. C. (1984) Structural Characterization of Polyethylene Injection Molded by Elongational Flow. *Journal of Polymer Engineering,* 4 (3)**,** 201-220.

Blagden, N., de Matas, M., Gavan, P. T. and York, P. (2007) Crystal engineering of active pharmaceutical ingredients to improve solubility and dissolution rates. *Advanced Drug Delivery Reviews,* 59 (7)**,** 617-630.

Bras, A. R., Noronha, J. P., Antunes, A. M. M., Cardoso, M. M., Schoenhals, A., Affouard, F., Dionisio, M. and Correia, N. T. (2008) Molecular motions in amorphous ibuprofen as studied by broadband dielectric spectroscopy. *Journal of Physical Chemistry B,* 112 (35)**,** 11087-11099.

Breitenbach, J. (2002) Melt extrusion: from process to drug delivery technology. *European Journal of Pharmaceutics and Biopharmaceutics,* 54 (2)**,** 107-117.

Breitenbach, J., Schrof, W. and Neumann, J. (1999) Confocal Raman-spectroscopy: Analytical approach to solid dispersions and mapping of drugs. *Pharmaceutical Research,* 16 (7).

Bryce, D. M. (1996) Plastic Injection Molding, Volume I - Manufacturing Process Fundamentals. Michigan, Society of Manufacturing Engineers (SME).

Cappello, B., De Rosa, G., Giannini, L., La Rotonda, M. I., Mensitieri, G., Miro, A., Quaglia, F. and Russo, R. (2006) Cyclodextrin-containing poly(ethyleneoxide) tablets for the delivery of poorly soluble drugs: Potential as buccal delivery system. *International Journal of Pharmaceutics,* 319 (1-2)**,** 63-70.

Caron, V., Hu, Y., Tajber, L., Erxleben, A., Corrigan, O. I., McArdle, P. and Healy, A. M. (2013) Amorphous Solid Dispersions of Sulfonamide/Soluplus (R) and Sulfonamide/PVP Prepared by Ball Milling. *Aaps Pharmscitech,* 14 (1)**,** 464-474.

Caron, V., Tajber, L., Corrigan, O. I. and Healy, A. M. (2011) A Comparison of Spray Drying and Milling in the Production of Amorphous Dispersions of Sulfathiazole/Polyvinylpyrrolidone and Sulfadimidine/Polyvinylpyrrolidone. *Molecular Pharmaceutics,* 8 (2)**,** 532-542.

Carrasco, F., Pages, P., Gamez-Perez, J., Santana, O. O. and Maspoch, M. L. (2010) Processing of poly(lactic acid): Characterization of chemical structure, thermal stability and mechanical properties. *Polymer Degradation and Stability,* 95 (2)**,** 116-125.

Chan, K. L. A. and Kazarian, S. G. (2006) High-throughput study of poly(ethylene glycol)/ibuprofen formulations under controlled environment using FTIR imaging. *Journal of Combinatorial Chemistry,* 8 (1)**,** 26-31.

Chauhan, H., Hui-Gu, C. and Atef, E. (2013) Correlating the behavior of polymers in solution as precipitation inhibitor to its amorphous stabilization ability in solid dispersions. *Journal of Pharmaceutical Sciences,* 102 (6)**,** 1924-1935.

Chen, M.-L. and Yu, L. (2009) The Use of Drug Metabolism for Prediction of Intestinal Permeability†. *Molecular Pharmaceutics,* 6 (1)**,** 74-81.

Childs, S. L., Stahly, G. P. and Park, A. (2007) The salt-cocrystal continuum: The influence of crystal structure on ionization state. *Molecular Pharmaceutics,* 4 (3)**,** 323-338.

Chiou, W. L. and Riegelman, S. (1969) Preparation and dissolution characteristics of several fast-release solid dispersions of griseofulvin. *Journal of pharmaceutical sciences,* 58 (12)**,** 1505-1510.

Chiou, W. L. and Riegelman, S. (1971) Pharmaceutical applications of solid dispersion systems. *Journal of Pharmaceutical Sciences,* 60 (9)**,** 1281-1302.

Cirri, M., Maestrelli, F., Orlandini, S., Furlanetto, S., Pinzauti, S. and Mura, P. (2005) Determination of stability constant values of flurbiprofen-cyclodextrin complexes using different techniques. *Journal of Pharmaceutical and Biomedical Analysis,* 37 (5)**,** 995-1002.

Coleman, N. J. and Craig, D. Q. M. (1996) Modulated temperature differential scanning calorimetry: A novel approach to pharmaceutical thermal analysis. *International Journal of Pharmaceutics,* 135 (1-2)**,** 13-29.

Costa, P. and Sousa Lobo, J. M. (2001) Modeling and comparison of dissolution profiles. *European Journal of Pharmaceutical Sciences,* 13 (2)**,** 123-133.

Crowley, M. M., Zhang, F., Repka, M. A., Thumma, S., Upadhye, S. B., Battu, S. K., McGinity, J. W. and Martin, C. (2007) Pharmaceutical applications of hot-melt extrusion: part I. *Drug Dev Ind Pharm,* 33 (9)**,** 909-26.

Cuff, G. and Raouf, F. (1998) A preliminary evaluation of injection moulding as a technology to produce tablets. *Pharm. Technol.,* 22**,** 96-106.

Cui, F. D., Yang, M. S., Jiang, Y. Y., Cun, D. M., Lin, W. H., Fan, Y. L. and Kawashima, Y. (2003) Design of sustained-release nitrendipine microspheres having solid dispersion structure by quasi-emulsion solvent diffusion method. *Journal of Controlled Release,* 91 (3)**,** 375-384.

De Beer, T., Burggraeve, A., Fonteyne, M., Saerens, L., Remon, J. P. and Vervaet, C. (2011) Near infrared and Raman spectroscopy for the in-process monitoring of pharmaceutical production processes. *International Journal of Pharmaceutics,* 417 (1-2)**,** 32-47.

Desai, J., Alexander, K. and Riga, A. (2006) Characterization of polymeric dispersions of dimenhydrinate in ethyl cellulose for controlled release. *International Journal of Pharmaceutics,* 308 (1-2)**,** 115-123.

Di Colo, G., Burgalassi, S., Chetoni, P., Fiaschi, M. P., Zambito, Y. and Saettone, M. F. (2001) Gel-forming erodible inserts for ocular controlled delivery of ofloxacin. *International Journal of Pharmaceutics,* 215 (1-2)**,** 101-111.

Dimitrov, M. and Lambov, N. (1999) Study of Verapamil hydrochloride release from compressed hydrophilic Polyox-Wsr tablets. *International Journal of Pharmaceutics,* 189 (1)**,** 105-111.

Dressman, J. B. and Reppas, C. (2000) In vitro-in vivo correlations for lipophilic, poorly water-soluble drugs. *European Journal of Pharmaceutical Sciences,* 11**,** S73-S80.

Dudognon, E., Danede, F., Descamps, M. and Correia, N. T. (2008) Evidence for a New Crystalline Phase of Racemic Ibuprofen. *Pharmaceutical Research,* 25 (12).

Ediger, M. D., Angell, C. A. and Nagel, S. R. (1996) Supercooled Liquids and Glasses. *The Journal of Physical Chemistry,* 100 (31)**,** 13200-13212.

Eith, L., Stepto, R. F. T., Tomka, I. and Wittwer, F. (1986) The injection-molded capsule. *Drug Development and Industrial Pharmacy,* 12 (11-13)**,** 2113-2126.

Fei, G., Tuinea-Bobe, C., Li, D., Li, G., Whiteside, B., Coates, P. and Xia, H. (2013) Electro-activated surface micropattern tuning for microinjection molded electrically conductive shape memory polyurethane composites. *Rsc Advances,* 3 (46)**,** 24132-24139.

Ferguson, L. N. (1964) *The Modern Structural Theory of Organic Chemistry.* New Jersey: Prentice-Hall, Englewood Cliffs.

Figueiras, A., Sarraguca, J. M. G., Carvalho, R. A., Pais, A. A. C. C. and Veiga, F. J. B. (2007) Interaction of omeprazole with a methylated derivative of beta-cyclodextrin: Phase solubility, NMR spectroscopy and molecular simulation. *Pharmaceutical Research,* 24 (2)**,** 377-389.

Fischer, J. M. (2003) 2 - Shrinkage and Warpage. In: Fischer, J. M. (Ed.) *Handbook of Molded Part Shrinkage and Warpage.* Norwich, NY: William Andrew Publishing, pp. 9-16.

Flory, P. J. (1953) *Principles of Polymer Chemistry.* Ithaca: Cornell University Press.

Forster, A., Hempenstall, J. and Rades, T. (2001a) Characterization of glass solutions of poorly water-soluble drugs produced by melt extrusion with hydrophilic amorphous polymers. *Journal of Pharmacy and Pharmacology,* 53 (3)**,** 303-315.

Forster, A., Hempenstall, J., Tucker, I. and Rades, T. (2001b) Selection of excipients for melt extrusion with two poorly water-soluble drugs by solubility parameter calculation and thermal analysis. *International Journal of Pharmaceutics,* 226 (1-2)**,** 147-161.

Fossheim, R. (1986) Crystal-structure of the dihydropyridine ca-2+ antagonist felodipine - dihydropyridine binding prerequisites assessed from crystallographic data. *Journal of Medicinal Chemistry,* 29 (2)**,** 305-307.

Fox, T. G. and Flory, P. J. (1950) Second-Order Transition Temperatures and Related Properties of Polystyrene. I. Influence of Molecular Weight. *Journal of Applied Physics,* 21 (6)**,** 581-591.

Friesen, D. T., Shanker, R., Crew, M., Smithey, D. T., Curatolo, W. J. and Nightingale, J. A. S. (2008) Hydroxypropyl Methylcellulose Acetate Succinate-Based Spray-Dried Dispersions: An Overview. *Molecular Pharmaceutics,* 5 (6)**,** 1003-1019.

Fukuoka, E., Makita, M. and Yamamura, S. (1989) Glassy state of pharmaceuticals .3. thermal-properties and stability of glassy pharmaceuticals and their binary glass systems. *Chemical & Pharmaceutical Bulletin,* 37 (4)**,** 1047-1050.

Garekani, H. A., Sadeghi, F., Badiee, A., Mostafa, S. A. and Rajabi-Siahboomi, A. R. (2001) Crystal habit modifications of ibuprofen and their physicomechanical characteristics. *Drug Development and Industrial Pharmacy,* 27 (8)**,** 803-809.

Ghebremeskel, A. N., Vernavarapu, C. and Lodaya, M. (2007) Use of surfactants as plasticizers in preparing solid dispersions of poorly soluble API: Selection of polymer-surfactant combinations using solubility parameters and testing the processability. *International Journal of Pharmaceutics,* 328 (2)**,** 119-129.

Goldberg, A. H., Gibaldi, M. and Kanig, J. L. (1965) Increasing dissolution rates and gastrointestinal absorption of drugs via solid solutions and eutectic mixtures I. Theoretical considerations and discussion of the literature. *Journal of Pharmaceutical Sciences,* 54 (8)**,** 1145-1148.

Goldberg, A. H., Gibaldi, M., Kanig, J. L. and Mayersohn, M. (1966) Increasing dissolution rates and gastrointestinal absorption of drugs via solid solutions and eutectic mixtures IV: Chloramphenicol—urea system. *Journal of Pharmaceutical Sciences,* 55 (6)**,** 581-583.

Gomes, M. E., Ribeiro, A. S., Malafaya, P. B., Reis, R. L. and Cunha, A. M. (2001) A new approach based on injection moulding to produce biodegradable

starch-based polymeric scaffolds: morphology, mechanical and degradation behaviour. *Biomaterials,* 22 (9)**,** 883-889.

Greenhalgh, D. J., Williams, A. C., Timmins, P. and York, P. (1999) Solubility parameters as predictors of miscibility in solid dispersions. *Journal of Pharmaceutical Sciences,* 88 (11)**,** 1182-1190.

Gupta, J., Nunes, C., Vyas, S. and Jonnalagadda, S. (2011) Prediction of Solubility Parameters and Miscibility of Pharmaceutical Compounds by Molecular Dynamics Simulations. *Journal of Physical Chemistry B,* 115 (9)**,** 2014-2023.

Hancock, B. C. and Parks, M. (2000) What is the true solubility advantage for amorphous pharmaceuticals? *Pharmaceutical Research,* 17 (4)**,** 397-404.

Hancock, B. C., York, P. and Rowe, R. C. (1997) The use of solubility parameters in pharmaceutical dosage form design. *International Journal of Pharmaceutics,* 148 (1)**,** 1-21.

Hancock, B. C. and Zograf, G. (1997) Characteristics and significance of the amorphous state in pharmaceutical systems. *Journal of Pharmaceutical Sciences,* 86 (1)**,** 1-12.

Haugen, H., Will, J., Fuchs, W. and Wintermantel, E. (2006) A novel processing method for injection-molded polyether-urethane scaffolds. Part 1: Processing. *Journal of Biomedical Materials Research Part B-Applied Biomaterials,* 77B (1)**,** 65-72.

Hedoux, A., Guinet, Y., Derollez, P., Dudognon, E. and Correia, N. T. (2011) Raman spectroscopy of racemic ibuprofen: Evidence of molecular disorder in phase II. *International Journal of Pharmaceutics,* 421 (1)**,** 45-52.

Hemmingsen, P. H., Haahr, A.-M., Gunnergaard, C. and Cardot, J.-M. (2011) Development of a new type of prolonged release hydrocodone formulation based on Egalet® ADPREM technology using *in vivo-in vitro* correlation. *Pharmaceutics,* 3 (1)**,** 73-87.

Hilton, J. E. and Summers, M. P. (1986) The effect of wetting agents on the dissolution of indomethacin solid dispersion-systems. *International Journal of Pharmaceutics,* 31 (1-2)**,** 157-164.

Horter, D. and Dressman, J. B. (2001) Influence of physicochemical properties on dissolution of drugs in the gastrointestinal tract. *Advanced Drug Delivery Reviews,* 46 (1-3)**,** 75-87.

Isayev, A. I. and Hariharan, T. (1985) Volumetric effects in the injection-molding of polymers. *Polymer Engineering and Science,* 25 (5)**,** 271-278.

Jansen, K. M. B., Van Dijk, D. J. and Husselman, M. H. (1998) Effect of processing conditions on shrinkage in injection molding. *Polymer Engineering and Science,* 38 (5)**,** 838-846.

Jeffrey, G. A. (1997) *An Introduction to Hydrogen Bonding.* New York: Oxford University Press.

Jones, W., Motherwell, S. and Trask, A. V. (2006) Pharmaceutical cocrystals: An emerging approach to physical property enhancement. *Mrs Bulletin,* 31 (11)**,** 875-879.

Jounela, A. J., Pentikainen, P. J. and Sothmann, A. (1975) Effect of particle-size on bioavailability of digoxin. *European Journal of Clinical Pharmacology,* 8 (5)**,** 365-370.

Jung, M.-S., Kim, J.-S., Kim, M.-S., Alhalaweh, A., Cho, W., Hwang, S.-J. and Velaga, S. P. (2010) Bioavailability of indomethacin-saccharin cocrystals. *Journal of Pharmacy and Pharmacology,* 62 (11)**,** 1560-1568.

Kanaujia, P., Lau, G., Ng, W. K., Widjaja, E., Schreyer, M., Hanefeld, A., Fischbach, M., Saal, C., Maio, M. and Tan, R. B. H. (2011) Investigating the effect of moisture protection on solid-state stability and dissolution of fenofibrate and ketoconazole solid dispersions using PXRD, HSDSC and Raman microscopy. *Drug Development and Industrial Pharmacy,* 37 (9)**,** 1026-1035.

Kanig, J. L. (1964) Properties of fused mannitol in compressed tablets. *Journal of Pharmaceutical Sciences,* 53 (2)**,** 188-192.

Karavas, E., Georgarakis, E. and Bikiaris, D. (2006) Felodipine nanodispersions as active core for predictable pulsatile chronotherapeutics using PVP/HPMC blends as coating layer. *International Journal of Pharmaceutics,* 313 (1–2)**,** 189-197.

Keller, R. A. and Breen, D. E. (1965) Formation of Crystallites of Benzophenone in Hydrocarbon Glass. *The Journal of Chemical Physics,* 43 (7)**,** 2562-2564**.**

Kelly, A. L., Gough, T., Dhumal, R. S., Halsey, S. A. and Paradkar, A. (2012) Monitoring ibuprofen-nicotinamide cocrystal formation during solvent free continuous cocrystallization (SFCC) using near infrared spectroscopy as a PAT tool. *International Journal of Pharmaceutics,* 426 (1-2)**,** 15-20.

Kelton, K. F. (1998) A new model for nucleation in bulk metallic glasses. *Philosophical Magazine Letters,* 77 (6)**,** 337-343.

Kestur, U. S. and Taylor, L. S. (2010) Role of polymer chemistry in influencing crystal growth rates from amorphous felodipine. *Crystengcomm,* 12 (8)**,** 2390-2397.

Kestur, U. S., Van Eerdenbrugh, B. and Taylor, L. S. (2011) Influence of polymer chemistry on crystal growth inhibition of two chemically diverse organic molecules. *Crystengcomm,* 13 (22)**,** 6712-6718.

Kim, C. J. (1998) Effects of drug solubility, drug loading, and polymer molecular weight on drug release from polyox (R) tablets. *Drug Development and Industrial Pharmacy,* 24 (7)**,** 645-651.

Kinoshita, M., Baba, K., Nagayasu, A., Yamabe, K., Shimooka, T., Takeichi, Y., Azuma, M., Houchi, H. and Minakuchi, K. (2002) Improvement of solubility and oral bioavailability of a poorly water-soluble drug, TAS-301, by its melt-adsorption on a porous calcium silicate. *Journal of Pharmaceutical Sciences,* 91 (2)**,** 362-370.

Kolter, K., Karl, M. and Gryczke, A. (2012) *Hot-melt extrusion with BASF pharma polymers.* Extrusion compandium 2nd Revised and Enlarged edition ed*.* BASF SEPharma ingredients and services67056 Ludwigshafen, Germany

Konno, H. and Taylor, L. S. (2006) Influence of different polymers on the crystallization tendency of molecularly dispersed amorphous felodipine. *Journal of Pharmaceutical Sciences,* 95 (12)**,** 2692-2705.

Langkilde, F. W., Sjoblom, J., TekenbergsHjelte, L. and Mrak, J. (1997) Quantitative FT-Raman analysis of two crystal forms of a pharmaceutical compound. *Journal of Pharmaceutical and Biomedical Analysis,* 15 (6)**,** 687-696.

Larregieu, C. A. and Benet, L. Z. (2014) Distinguishing between the permeability relationships with absorption and metabolism to improve BCS and BDDCS predictions in early drug discovery. *Mol Pharm,* 11 (4)**,** 1335-44.

Leuner, C. and Dressman, J. (2000) Improving drug solubility for oral delivery using solid dispersions. *European Journal of Pharmaceutics and Biopharmaceutics,* 50 (1), 47-60.

Li, W. Y., Worosila, G. D., Wang, W. and Mascaro, T. (2005) Determination of polymorph conversion of an active pharmaceutical ingredient in wet granulation using NIR calibration models generated from the premix blends. *Journal of Pharmaceutical Sciences,* 94 (12), 2800-2806.

Li, Y. M., Wei, G. X. and Sue, H. J. (2002) Morphology and toughening mechanisms in clay-modified styrene-butadiene-styrene rubber-toughened polypropylene. *Journal of Materials Science,* 37 (12), 2447-2459.

Lin, D. and Huang, Y. (2010) A thermal analysis method to predict the complete phase diagram of drug-polymer solid dispersions. *International Journal of Pharmaceutics,* 399 (1-2), 109-115.

Linn, M., Collnot, E.-M., Djuric, D., Hempel, K., Fabian, E., Kolter, K. and Lehr, C.-M. (2012) Soluplus (R) as an effective absorption enhancer of poorly soluble drugs in vitro and in vivo. *European Journal of Pharmaceutical Sciences,* 45 (3), 336-343.

Lipinski, C. A. (2000) Drug-like properties and the causes of poor solubility and poor permeability. *Journal of Pharmacological and Toxicological Methods,* 44 (1), 235-249.

Marsac, P., Shamblin, S. and Taylor, L. (2006) Theoretical and Practical Approaches for Prediction of Drug–Polymer Miscibility and Solubility. *Pharmaceutical Research,* 23 (10), 2417-2426.

Marsac, P. J., Konno, H., Rumondor, A. C. F. and Taylor, L. S. (2008) Recrystallization of nifedipine and felodipine from amorphous molecular level solid dispersions containing poly(vinylpyrrolidone) and sorbed water. *Pharmaceutical Research,* 25 (3), 647-656.

Marsac, P. J., Li, T. and Taylor, L. S. (2009) Estimation of Drug-Polymer Miscibility and Solubility in Amorphous Solid Dispersions Using Experimentally Determined Interaction Parameters. *Pharmaceutical Research,* 26 (1), 139-151.

Marsac, P. J., Rumondor, A. C. F., Nivens, D. E., Kestur, U. S., Stanciu, L. and Taylor, L. S. (2010) Effect of Temperature and Moisture on the Miscibility

of Amorphous Dispersions of Felodipine and Poly(vinyl pyrrolidone). *Journal of Pharmaceutical Sciences,* 99 (1)**,** 169-185.

McNamara, D. P., Childs, S. L., Giordano, J., Iarriccio, A., Cassidy, J., Shet, M. S., Mannion, R., O'Donnell, E. and Park, A. (2006) Use of a glutaric acid cocrystal to improve oral bioavailability of a low solubility API. *Pharmaceutical Research,* 23 (8)**,** 1888-1897.

Mehuys, E., Remon, J. P. and Vervaet, C. (2005) Production of enteric capsules by means of hot-melt extrusion. *European Journal of Pharmaceutical Sciences,* 24 (2-3).

Menard, K. P. (2008) *Dynamic Mechanical Analysis.* 2 ed*.* New York: CRC Press Taylor and Francis Group.

Meza, C., Santos, M. and Romañach, R. (2006) Quantitation of drug content in a low dosage formulation by transmission near infrared spectroscopy. *AAPS PharmSciTech,* 7 (1)**,** E206-E214.

Miyazaki, T., Yoshioka, S., Aso, Y. and Kojima, S. (2004) Ability of polyvinylpyrrolidone and polyacrylic acid to inhibit the crystallization of amorphous acetaminophen. *Journal of Pharmaceutical Sciences,* 93 (11)**,** 2710-2717.

Moffat, J. G., Qi, S. and Craig, D. Q. M. (2014) Spatial Characterization of Hot Melt Extruded Dispersion Systems Using Thermal Atomic Force Microscopy Methods: The Effects of Processing Parameters on Phase Separation. *Pharmaceutical Research,* 31 (7)**,** 1744-1752.

Moneghini, M., Kikic, I., Voinovich, D., Perissutti, B. and Filipović-Grčić, J. (2001) Processing of carbamazepine–PEG 4000 solid dispersions with supercritical carbon dioxide: preparation, characterisation, and in vitro dissolution. *International Journal of Pharmaceutics,* 222 (1)**,** 129-138.

Mosharraf, M. and Nystrom, C. (1995) The effect of particle-size and shape on the surface specific dissolution rate of microsized practically insoluble drugs. *International Journal of Pharmaceutics,* 122 (1-2)**,** 35-47.

Muller, R. H. and Peters, K. (1998) Nanosuspensions for the formulation of poorly soluble drugs - I. Preparation by a size-reduction technique. *International Journal of Pharmaceutics,* 160 (2)**,** 229-237.

Murthy, A. S. N. and Rao, C. N. R. (1968) Spectroscopic studies of hydrogen bond. *Applied Spectroscopy Reviews,* 2 (1)**,** 69-&.

Nakamichi, K., Yasuura, H., Fukui, H., Oka, M. and Izumi, S. (2001) Evaluation of a floating dosage form of nicardipine hydrochloride and hydroxypropylmethylcellulose acetate succinate prepared using a twin-screw extruder. *International Journal of Pharmaceutics,* 218 (1-2), 103-112.

Nishi, T. and Wang, T. T. (1975) Melting-point depression and kinetic effects of cooling on crystallization in poly(vinylidene fluoride) poly(methyl methacrylate) mixtures. *Macromolecules,* 8 (6), 909-915.

Paudel, A., Worku, Z. A., Meeus, J., Guns, S. and Van den Mooter, G. (2013) Manufacturing of solid dispersions of poorly water soluble drugs by spray drying: Formulation and process considerations. *International Journal of Pharmaceutics,* 453 (1), 253-284.

Peppas, N. A. (1985) Analysis of Fickian and non-Fickian drug release from polymers. *Pharm Acta Helv,* 60 (4), 110-1.

Pikal, M. J., Lukes, A. L., Lang, J. E. and Gaines, K. (1978) Quantitative crystallinity determinations for beta-lactam antibiotics by solution calorimetry - correlations with stability. *Journal of Pharmaceutical Sciences,* 67 (6), 767-772.

Price, D. M. (2002) Thermomechanical, Dynamic Mechanical and Dielectric Methods. In: Haines, P. J. (Ed.) *Principles of Thermal Analysis and Calorimetry.* 1 ed. Great Britain: Royal Society of Chemistry pp. 94-125.

Prodduturi, S., Urman, K. L., Otaigbe, J. U. and Repka, M. A. (2007) Stabilization of hot-melt extrusion formulations containing solid solutions using polymer blends. *Aaps Pharmscitech,* 8 (2).

Qi, S. and Craig, D. Q. M. (2012) The Development of Modulated, Quasi-Isothermal and Ultraslow Thermal Methods as a Means of Characterizing the alpha to gamma Indomethacin Polymorphic Transformation. *Molecular Pharmaceutics,* 9 (5), 1087-1099.

Qian, F., Huang, J. and Hussain, M. A. (2010) Drug-Polymer Solubility and Miscibility: Stability Consideration and Practical Challenges in Amorphous Solid Dispersion Development. *Journal of Pharmaceutical Sciences,* 99 (7), 2941-2947.

Quinten, T., De Beer, T., Vervaet, C. and Remon, J. P. (2009) Evaluation of injection moulding as a pharmaceutical technology to produce matrix

tablets. *European Journal of Pharmaceutics and Biopharmaceutics,* 71 (1)**,** 145-154.

Raina, S. A., Alonzo, D. E., Zhang, G. G. Z., Gao, Y. and Taylor, L. S. (2014) Impact of Polymers on the Crystallization and Phase Transition Kinetics of Amorphous Nifedipine during Dissolution in Aqueous Media. *Molecular Pharmaceutics,* 11 (10)**,** 3565-3576.

Rathbone, M. J., Bunt, C. R., Ogle, C. R., Burggraaf, S., Macmillan, K. L. and Pickering, K. (2002) Development of an injection molded poly(epsilon-caprolactone) intravaginal insert for the delivery of progesterone to cattle. *Journal of Controlled Release,* 85 (1-3).

Rautio, J., Kumpulainen, H., Heimbach, T., Oliyai, R., Oh, D., Jarvinen, T. and Savolainen, J. (2008) Prodrugs: design and clinical applications. *Nature Reviews Drug Discovery,* 7 (3)**,** 255-270.

Reed-Hill, R. E. (1964) *Physical metallurgy principles.* New York: Van Nostrand.

Repka, M. A., Battu, S. K., Upadhye, S. B., Thumma, S., Crowley, M. M., Zhang, F., Martin, C. and McGinity, J. W. (2007) Pharmaceutical applications of hot-melt extrusion: Part II. *Drug Development and Industrial Pharmacy,* 33 (10)**,** 1043-1057.

Rodriguez-Spong, B., Price, C. P., Jayasankar, A., Matzger, A. J. and Rodriguez-Hornedo, N. (2004) General principles of pharmaceutical solid polymorphism: a supramolecular perspective. *Advanced Drug Delivery Reviews,* 56 (3)**,** 241-274.

Rosato, D. V., Rosato, D. V. and Rosato, M., G (2000) *Injection moulding handbook.* Massachuseets: Kluwer Academic Publisher.

Rossi, B., Verrocchio, P., Viliani, G., Mancini, I., Guella, G., Rigo, E., Scarduelli, G. and Mariotto, G. (2009) Vibrational properties of ibuprofen-cyclodextrin inclusion complexes investigated by Raman scattering and numerical simulation. *Journal of Raman Spectroscopy,* 40 (4)**,** 453-458.

Rothen-Weinhold, A., Besseghir, K., Vuaridel, E., Sublet, E., Oudry, N., Kubel, F. and Gurny, R. (1999) Injection-molding versus extrusion as manufacturing technique for the preparation of biodegradable implants. *European Journal of Pharmaceutics and Biopharmaceutics,* 48 (2).

Royall, P. G., Craig, D. Q. M. and Doherty, C. (1998) Characterisation of the glass transition of an amorphous drug using modulated DSC. *Pharmaceutical Research,* 15 (7)**,** 1117-1121.

Rubinstein, M. and Colby, R. H. (2003) Thermodynamics of blends and solutions. In: *Polymer physics.* New York: Oxford University Press Inc, pp. 137– 170.

Rutland plastic Limited Plastic Injection Moulding http://www.rutlandplastics.co.uk/injection_moulding/moulding.html Cited on 280614

Saerens, L., Dierickx, L., Lenain, B., Vervaet, C., Remon, J. P. and De Beer, T. (2011) Raman spectroscopy for the in-line polymer-drug quantification and solid state characterization during a pharmaceutical hot-melt extrusion process. European Journal of Pharmaceutics and Biopharmaceutics, 77 (1).

Sahoo, N. G., Kakran, M., Li, L., Judeh, Z. and Mueller, R. H. (2011) Dissolution enhancement of a poorly water-soluble antimalarial drug by means of a modified multi-fluid nozzle pilot spray drier. Materials Science & *Engineering C-Materials for Biological Applications,* 31 (2)**,** 391-399.

Sangalli, M. E., Maroni, A., Foppoli, A., Zema, L., Giordano, F. and Gazzaniga, A. (2004) Different HPMC viscosity grades as coating agents for an oral time and/or site-controlled delivery system: a study on process parameters and in vitro performances. *European Journal of Pharmaceutical Sciences,* 22 (5).

Scholz, A., Abrahamsson, B., Diebold, S. M., Kostewicz, E., Polentarutti, B. I., Ungell, A. L. and Dressman, J. B. (2002) Influence of hydrodynamics and particle size on the absorption of felodipine in labradors. *Pharmaceutical Research,* 19 (1)**,** 42-46.

Schultheiss, N. and Newman, A. (2009) Pharmaceutical Cocrystals and Their Physicochemical Properties. *Crystal Growth & Design,* 9 (6)**,** 2950-2967.

Sekiguchi, K. and Obi, N. (1961) Studies on Absorption of Eutectic Mixture. I. A Comparison of the Behavior of Eutectic Mixture of Sulfathiazole and that of Ordinary Sulfathiazole in Man. *CHEMICAL & PHARMACEUTICAL BULLETIN,* 9 (11)**,** 866-872.

Serajuddin, A. T. M. (2007) Salt formation to improve drug solubility. *Advanced Drug Delivery Reviews,* 59 (7)**,** 603-616.

Shah, S., Maddineni, S., Lu, J. and Repka, M. A. (2013) Melt extrusion with poorly soluble drugs. *International Journal of Pharmaceutics,* 453 (1)**,** 233-252.

Shegokar, R. and Mueller, R. H. (2010) Nanocrystals: Industrially feasible multifunctional formulation technology for poorly soluble actives. *International Journal of Pharmaceutics,* 399 (1-2)**,** 129-139.

Shi, N. Q., Yao, J. and Wang, X. L. (2014) Effect of polymers and media type on extending the dissolution of amorphous pioglitazone and inhibiting the recrystallization from a supersaturated state. *Drug Development and Industrial Pharmacy,* 40 (8)**,** 1112-1122.

Silverstein, R. M., Bassler, G. C. and Terence, C. M. (1981) *Spectrometric Identification of Organic Compounds.* 4 ed*.* New York: Wiley.

Simonelli, A. P., Mehta, S. C. and Higuchi, W. I. (1976) Dissolution rates of high-energy sulfathiazole-povidone coprecipitates .2. characterization of form of drug controlling its dissolution rate via solubility studies. *Journal of Pharmaceutical Sciences,* 65 (3)**,** 355-361.

Solarski, S., Ferreira, M. and Devaux, E. (2005) Characterization of the thermal properties of PLA fibers by modulated differential scanning calorimetry. *Polymer,* 46 (25)**,** 11187-11192.

Song, Y. J., Wang, L. Y., Yang, P., Wenslow, R. M., Tan, B., Zhang, H. L. and Deng, Z. W. (2013) Physicochemical characterization of felodipine-kollidon VA64 amorphous solid dispersions prepared by hot-melt extrusion. *Journal of Pharmaceutical Sciences,* 102 (6)**,** 1915-1923.

Speiser, P. (1969) Injection-moulded oral medicament in solid form. Google Patents.

Stegemann, S., Leveiller, F., Franchi, D., de Jong, H. and Linden, H. (2007) When poor solubility becomes an issue: From early stage to proof of concept. *European Journal of Pharmaceutical Sciences,* 31 (5)**,** 249-261.

Sun, Y., Tao, J., Zhang, G. G. Z. and Yu, L. (2010) Solubilities of Crystalline Drugs in Polymers: An Improved Analytical Method and Comparison of Solubilities of Indomethacin and Nifedipine in PVP, PVP/VA, and PVAc. *Journal of Pharmaceutical Sciences,* 99 (9)**,** 4023-4031.

Takagi, T., Ramachandran, C., Bermejo, M., Yamashita, S., Yu, L. X. and Amidon, G. L. (2006) A provisional biopharmaceutical classification of the top 200 oral drug products in the United States, Great Britain, Spain, and Japan. *Molecular Pharmaceutics,* 3 (6)**,** 631-643.

Tanaka, N., Imai, K., Okimoto, K., Ueda, S., Tokunaga, Y., Ibuki, R., Higaki, K. and Kimura, T. (2006) Development of novel sustained-release system, disintegration-controlled matrix tablet (DCMT) with solid dispersion granules of nilvadipine (II): In vivo evaluation. *Journal of Controlled Release,* 112 (1)**,** 51-56.

Tang, X. L. C., Pikal, M. J. and Taylor, L. S. (2002) A spectroscopic investigation of hydrogen bond patterns in crystalline and amorphous phases in dihydropyridine calcium channel blockers. *Pharmaceutical Research,* 19 (4)**,** 477-483.

Tanno, F., Nishiyama, Y., Kokubo, H. and Obara, S. (2004) Evaluation of hypromellose acetate succinate (HPMCAS) as a carrier in solid dispersions. *Drug Development and Industrial Pharmacy,* 30 (1)**,** 9-17.

Tao, J., Sun, Y., Zhang, G. G. Z. and Yu, L. (2009) Solubility of Small-Molecule Crystals in Polymers: d-Mannitol in PVP, Indomethacin in PVP/VA, and Nifedipine in PVP/VA. *Pharmaceutical Research,* 26 (4)**,** 855-864.

Taylor, L. S. and Zografi, G. (1997) Spectroscopic characterization of interactions between PVP and indomethacin in amorphous molecular dispersions. *Pharmaceutical Research,* 14 (12)**,** 1691-1698.

Taylor, L. S. and Zografi, G. (1998) The quantitative analysis of crystallinity using FT-Raman spectroscopy. *Pharmaceutical Research,* 15 (5)**,** 755-761.

Tian, B., Zhang, L., Pan, Z., Gou, J., Zhang, Y. and Tang, X. (2014a) A comparison of the effect of temperature and moisture on the solid dispersions: Aging and crystallization. *International Journal of Pharmaceutics,* 475 (1-2)**,** 385-392.

Tian, Y., Booth, J., Meehan, E., Jones, D. S., Li, S. and Andrews, G. P. (2013) Construction of Drug-Polymer Thermodynamic Phase Diagrams Using Flory-Huggins Interaction Theory: Identifying the Relevance of Temperature and Drug Weight Fraction to Phase Separation within Solid Dispersions. *Molecular Pharmaceutics,* 10 (1)**,** 236-248.

Tian, Y. W., Caron, V., Jones, D. S., Healy, A. M. and Andrews, G. P. (2014b) Using Flory-Huggins phase diagrams as a pre-formulation tool for the production of amorphous solid dispersions: a comparison between hot-melt extrusion and spray drying. *Journal of Pharmacy and Pharmacology,* 66 (2)**,** 256-274.

Tjong, S. C., Shen, J. S. and Liu, S. L. (1996) Structural properties and impact fracture behavior of injection molded blends of liquid crystalline copolyester and modified poly(phenylene oxide). *Polymer Engineering and Science,* 36 (6)**,** 797-806.

Tran, T. T.-D., Tran, P. H.-L., Lim, J., Park, J. B., Choi, S.-K. and Lee, B.-J. (2010) Physicochemical principles of controlled release solid dispersion containing a poorly water-soluble drug. *Therapeutic delivery,* 1 (1)**,** 51-62.

Urbanetz, N. A. (2006) Stabilization of solid dispersions of nimodipine and polyethylene glycol 2000. *European Journal of Pharmaceutical Sciences,* 28 (1-2)**,** 67-76.

van Drooge, D. J., Hinrichs, W. L. J., Wegman, K. A. M., Visser, M. R., Eissens, A. C. and Frijlink, H. W. (2004) Solid dispersions based on inulin for the stabilisation and formulation of Δ9-tetrahydrocannabinol. *European Journal of Pharmaceutical Sciences,* 21 (4)**,** 511-518.

Van Krevelen, D. W. and Te Nijenhuis, K. (2009) Chapter 7 - Cohesive Properties and Solubility. In: By, D. W. V. K. andNijenhuis, K. T. (Eds.) *Properties of Polymers (Fourth Edition).* Amsterdam: Elsevier, pp. 189-227.

van Laarhoven, J. A. H., Kruft, M. A. B. and Vromans, H. (2002) In vitro release properties of etonogestrel and ethinyl estradiol from a contraceptive vaginal ring. *International Journal of Pharmaceutics,* 232 (1-2)**,** 163-173.

Vaz, C. M., van Doeveren, P., Reis, R. L. and Cunha, A. M. (2003) Development and design of double-layer co-injection moulded soy protein based drug delivery devices. *Polymer,* 44 (19)**,** 5983-5992.

Verheyen, S., Augustijns, P., Kinget, R. and Van den Mooter, G. (2001) Determination of partial solubility parameters of five benzodiazepines in individual solvents. *International Journal of Pharmaceutics,* 228 (1-2)**,** 199-207.

Vervaet, C., Verhoeven, E., Quinten, T. and Remon, J. P. (2008) Hot melt extrusion and injection moulding as manufacturing tools for controlled release formulations. *DOSIS,* 24 (2)**,** 119-123.

Vishweshwar, P., McMahon, J. A., Bis, J. A. and Zaworotko, M. J. (2006) Pharmaceutical co-crystal. *Journal of Pharmaceutical Sciences,* 95 (3)**,** 499-516.

Vo, C. L.-N., Park, C. and Lee, B.-J. (2013) Current trends and future perspectives of solid dispersions containing poorly water-soluble drugs. *European Journal of Pharmaceutics and Biopharmaceutics,* 85 (3)**,** 799-813.

Vueba, M. L., Pina, M. E. and De Carvalho, L. A. E. B. (2008) Conformational stability of ibuprofen: Assessed by DFT calculations and optical vibrational spectroscopy. *Journal of Pharmaceutical Sciences,* 97 (2)**,** 845-859.

Wacker, S., Soliva, M. and Speiser, P. (1991) Injection molding as a suitable process for manufacturing solid dispersions or solutions. *Pharmazeutische Industrie,* 53 (9)**,** 853-856.

Weuts, I., Kempen, D., Decorte, A., Verreck, G., Peeters, J., Brewster, M. and Van den Mooter, G. (2005) Physical stability of the amorphous state of loperamide and two fragment molecules in solid dispersions with the polymers PVP-K30 and PVP-VA64. *European Journal of Pharmaceutical Sciences,* 25 (2-3)**,** 313-320.

Weuts, I., Van Dycke, F., Voorspoels, J., De Cort, S., Stokbroekx, S., Leemans, R., Brewster, M. E., Xu, D., Segmuller, B., Turner, Y. T. A., Roberts, C. J., Davies, M. C., Qi, S., Craig, D. Q. M. and Reading, M. (2011) Physicochemical properties of the amorphous drug, cast films, and spray dried powders to predict formulation probability of success for solid dispersions: Etravirine. *Journal of Pharmaceutical Sciences,* 100 (1)**,** 260-274.

Wikstrom, H., Marsac, P. J. and Taylor, L. S. (2005) In-line monitoring of hydrate formation during wet granulation using Raman spectroscopy. *Journal of Pharmaceutical Sciences,* 94 (1)**,** 209-219.

Wu, C. Y. and Benet, L. Z. (2005) Predicting drug disposition via application of BCS: transport/absorption/ elimination interplay and development of a

biopharmaceutics drug disposition classification system. *Pharm Res,* 22 (1)**,** 11-23.

Yalkowsky, S. H. (1999) *Solubility and Solubilization in Aqueous Media.* American Chemical Society and Oxford University Press.

Yang, J., Grey, K. and Doney, J. (2010) An improved kinetics approach to describe the physical stability of amorphous solid dispersions. *International Journal of Pharmaceutics,* 384 (1-2)**,** 24-31.

Yang, Z., Nollenberger, K., Albers, J., Craig, D. and Qi, S. (2015) Molecular Indicators of Surface and Bulk Instability of Hot Melt Extruded Amorphous Solid Dispersions. *Pharmaceutical Research,* 32 (4)**,** 1210-1228.

Yoshinari, T., Forbes, R. T., York, P. and Kawashima, Y. (2003) Crystallisation of amorphous mannitol is retarded using boric acid. *International Journal of Pharmaceutics,* 258 (1-2)**,** 109-120.

Yoshioka, M., Hancock, B. C. and Zografi, G. (1994) Crystallization of indomethacin from the amorphous state below and above its glass-transition temperature. *Journal of Pharmaceutical Sciences,* 83 (12)**,** 1700-1705.

Yu, L. (2001) Amorphous pharmaceutical solids: preparation, characterization and stabilization. *Advanced Drug Delivery Reviews,* 48 (1)**,** 27-42.

Zema, L., Loreti, G., Melocchi, A., Maroni, A. and Gazzaniga, A. (2012) Injection Molding and its application to drug delivery. *Journal of Controlled Release,* 159 (3)**,** 324-331.

Zhao, Y., Inbar, P., Chokshi, H. P., Malick, A. W. and Choi, D. S. (2011) Prediction of the Thermal Phase Diagram of Amorphous Solid Dispersions by Flory-Huggins Theory. *Journal of Pharmaceutical Sciences,* 100 (8)**,** 3196-3207.

Zhou, D., Zhang, G. G. Z., Law, D., Grant, D. J. W. and Schmitt, E. A. (2008) Thermodynamics, Molecular Mobility and Crystallization Kinetics of Amorphous Griseofulvin. *Molecular Pharmaceutics,* 5 (6)**,** 927-936.

Zidan, A. S., Rahman, Z., Sayeed, V., Raw, A., Yu, L. and Khan, M. A. (2012) Crystallinity evaluation of tacrolimus solid dispersions by chemometric analysis. *International Journal of Pharmaceutics,* 423 (2)**,** 341-350.
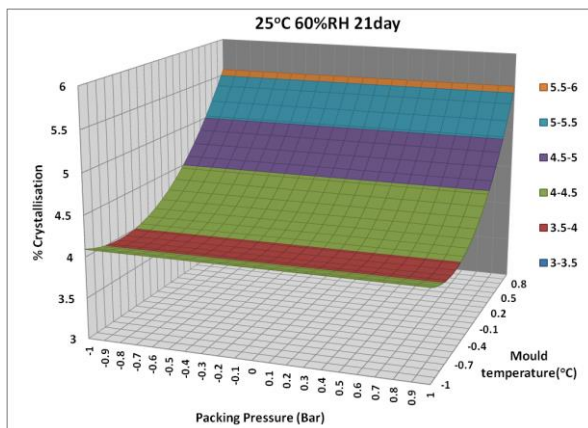
Appendix 1

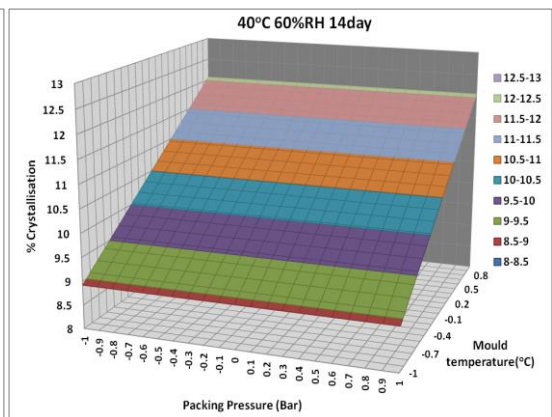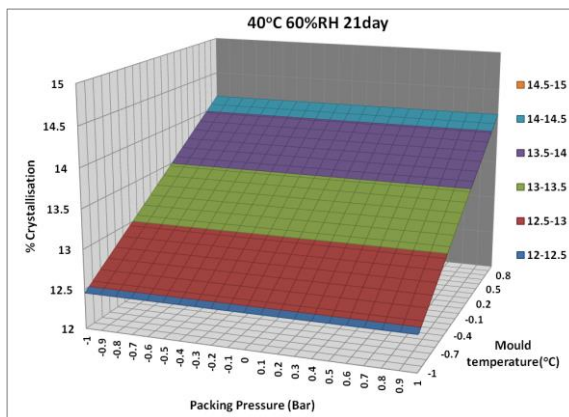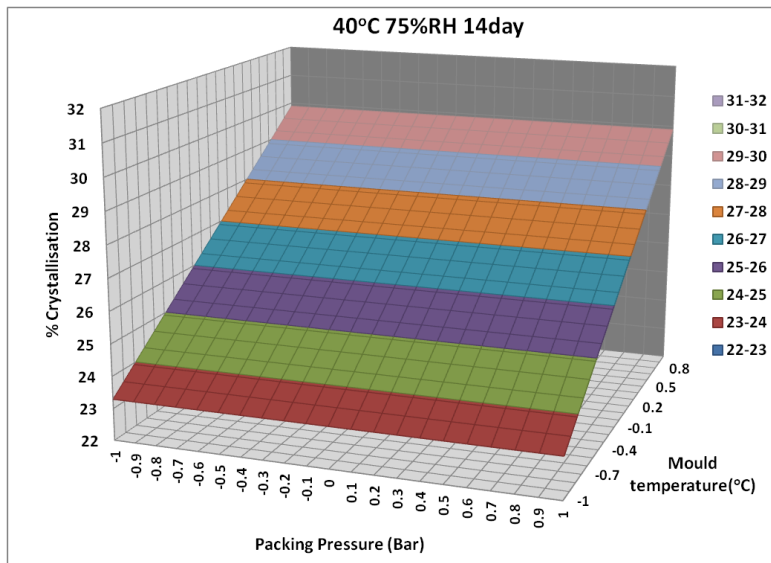## NIR surface response curves

Figure: Surface response curves for % crystallisation of ibuprofen-HPMCAS moulded system at different stress conditions

Appendix 2

Preface

This research work was carried out at the Centre for Pharmaceutical Engineering Science and Interdesciplinary Research Centre at the University of Bradford, Bradford, UK, between July 2011 and June 2014 under the supervison of Dr. Adrian Kelly and Professor Anant Paradkar a. The contents are original and reference has made to others work mentioned in this dissertation.

Presentation of research work in conferences

A) Poster presentation

1. "Investigation of Mechanical Properties of Injection Moulded Poly (Lactic Acid)"; 2012, APS PharmSCi,Nottingham, UK

2. "Moisture-induced surface crystallisation of injection moulded pharmaceutical system"; 2013, British Association for Crystal Growth (BACG), Manchester, UK

3. "Development of injection moulded systems for oral drug delivery"; 2013, APS UK PharmSci, Edinburgh, UK

4. "Crystallisation from injection moulded systems"; 2014, British Association for Crystal Growth (BACG), Leeds, UK

5. "Surface crystallisation from injection moulded amorphous systems"; 2014APS Amorphous By Design, University of Bradford, UK

B) Oral presentation

1. "Development of injection moulded systems for oral drug delivery"; UK PharmSCi 2013, Edinburgh, UK

2. "Development of the injection moulding process for pharmaceutical dosage forms"; 2014, UKIERI Seminar, University of Bradford, UK

3. "Injection moulding process for development of novel drug delivery systems, Hot Melt Extrusion"; 2014, ShinEtsu conference, University of Bradford, UK

Manuscripts under preparation

1. Processing, Stability and Performance of Injection Moulded Novel Drug Delivery Systems, *Pharmaceutical Research*

2. Injection moulded novel drug delivery systems: Investigation of ibuprofen-HPMCAS; *Molecular Pharmaceutics*